1996

Conducting polymer electrodes for electrochemical detection of amino acids and haloacetic acids

Parveen Akhtar
University of Wollongong

CONDUCTING POLYMER ELECTRODES FOR ELECTROCHEMICAL DETECTION OF AMINO ACIDS AND HALOACETIC ACIDS

A thesis submitted in fulfilment of the requirement

for the award of the degree

DOCTOR OF PHILOSOPHY

from

The University of Wollongong

by

PARVEEN AKHTAR, M.Sc, M.Phil

Department of Chemistry

May 1996

Acknowledgment

Sincere thanks are given to Professor Gordon G. Wallace and Professor Leon Kane-Maguire for their guidance and encouragement throughout this work. I greatly appreciate the guidance and support of Dr Chee On Too during the preparation of this manuscript.

Many thanks are also due to Ms Kerry Gilmore, Dr Norman Barisci, Dr Huijun Zhao, Mr Trevor Lewis and Miss Daniela Ongarato for their technical help and support during this work. I also acknowledge the assistance of the Australian International Development Assistance Bureau for financial support in the form of an Equity and Merit Scholarship (EMSS).

I am deeply indebted to my family for their continued loving support and encouragement.

Abstract

There is a growing interest in the utilisation of various kinds of conducting polymers to modify the physico-chemical properties of electrodes for use in flow injection analysis (FIA) and liquid chromatography. Conducting electroactive polymers such as polypyrrole, polythiophene and polyaniline represent a new class of organic polymers that are capable of a range of interactions enabling them to interact with the species of interest.

The discovery of new electrode materials has greatly expanded the range of detectable compounds using electrochemical methods. Conducting polymers have successfully been applied for the detection of electroinactive ions and proteins in flowing solutions. This work has sought to investigate the capability of conducting polymers for detection of organic compounds which includes amino acids and haloacetic acids.

The platinum surface was modified by depositing conducting polymers electrochemically. Two different approaches were employed. Firstly, a range of counterions were incorporated as dopant. It was observed that the polymer electroactivity was affected by the nature of the counterions incorporated. The polymer was anion, cation or both anion/cation-exchanging depending upon the nature of dopant. Derivatised monomers with cation exchange groups were also synthesised, and the resultant polymer possessed both anion and cation-exchange properties. Chiral polymers were also prepared using both chiral dopant and derivatised chiral monomers. The anion exchange properties of these polymers were confirmed by mass changes monitored by use of the electrochemical quartz crystal microbalance (EQCM).

It has been found that conducting electroactive polymers can be used for the detection of amino acids. The responses for four amino acids belonging to each group are characteristic. Based on these observations, amino acid to polymer interaction can be characterised as neutral, anionic and cationic. The extent of interaction can be altered by careful selection of the polymers, the potential applied, current sample points and pulse width. For aspartic acid, linearity of sensor response was obtained over the concentration range of 7.5×10^{-6}M to 6×10^{-5}M with a correlation coefficient of 0.979. This corresponds to a 99% confidence level. The limit of detection (LOD) for aspartic acid was 7.5×10^{-6}M (1ppm).

The effect of rapid electrochemical interaction at polymer coated microelectrodes with amino acids, which can enhance the sensitivity/selectivity of the electrodes for analytes, has also been studied. With microelectrodes a background eluent of low concentration could be used which minimises interferences in FIA. Polymers were deposited with ease on microelectrodes and their FIA responses to amino acid solutions were similar to those observed at macroelectrodes. The selectivity and limit of detection for amino acids were improved at microelectrodes when compared with those at macroelectrodes. A linear calibration curve was obtained between 7.5×10^{-6}M and 1×10^{-4}M amino acid. The correlation coefficients were 0.992 and 0.982 for aspartic acid and glutamic acid respectively. These correspond to a 99.9% confidence level. The LOD for both aspartic acid and glutamic acid was 3×10^{-6}M (0.4ppm).

The detection of haloacids at conducting polymers was carried out with pulsed integrated amperometry in suppressed eluent after separation of the mixture of organic acids by anion exchange chromatography. The selectivity factors (ratio of peak heights) can be manipulated either by changing the

applied potential or polymer electrode composition. Linear calibration curves were obtained between 0.001mg/l to 30mg/l, with correlation coefficients > 0.992. This corresponds to a 99.9% confidence level. The responses were maximum at PPy/SBA. The LODs were 1.0µg/l and 10µg/l for monochloroacetic acid and dichloroacetic acid respectively. These limits of detection were an improvement over those obtained by conductivity detection and UV method.

Publications

1. P. Akhtar, F. Chen, L. A. P. Kane-Maguire and G. G. Wallace, "Synthesis and electropolymerisation of new chiral polymers based on polypyrrole", Abstracts, 3rd Pacific Polymer Conference, Gold Coast, Australia, Dec, 1993, 363-364.

2. Synthesis and characterisation of chiral conducting polymers based on polypyrrole., Submitted.

3. P. Akhtar, M. D. Imisides and G. G. Wallace, "Electrochemical detection of amino acids at conducting polymer electrodes", Abstracts, Royal Australian Chemical Institute Analytical Chemistry Group Research and Development Topics, University of Canberra, Australia, Dec, 1994.

4. Detection of amino acids at conducting electroactive polymer modified electrodes using flow injection analysis - I. Macroelectrodes., Submitted.

5. Detection of amino acids at conducting electroactive polymer modified electrodes using flow injection analysis - II. Microelectrodes., In preparation.

6. Detection of haloacetic acids at conducting electroactive polymer modified microelectrodes., In preparation

Abbreviations and Symbols

Ag/AgCl	Silver/Silver Chloride
ADI	Analog-Digital Instruments
AR	Analytical Reagent
A/A'	Anions
BAS	Bioanalytical Systems
B/B'	Cations
°C	Degrees Celcius
CA	Chronoamperometry
CD	Circular Dichroism
CEP	Conducting Electroactive Polymer
cm	Centimetre
Conc.	Concentration
CV	Cyclic Voltammetry
DC	Direct Current
e-	Electron(s)
EC	Electrochemical
E_f	Final Potential
E_i	Initial Potential
E^o	Standard Electrode Potential
E_{pa}	Anodic Peak Potential
E_{pc}	Cathodic Peak Potential
EQCM	Electrochemical Quartz Crystal Microbalance
FIA	Flow Injection Analysis
g	Gram(s)
GC	Gas Chromatography
HDV	Hydrodynamic Voltammogram
HPLC	High Pressure Liquid Chromatography

i	Current
IC	Ion Chromatography
i_{pa}	Anodic Peak Current
i_{pc}	Cathodic Peak Current
iR	Ohmic drop
ITO	Indium Tin Oxide
LC	Liquid Chromatography
LOD	Limit of Detection
mA	Milliampere(s)
nA	Nanoampere(s)
μA	Microampere(s)
min	Minute(s)
ml	Millilitre(s)
msec	Millisecond(s)
mV	Millivolt(s)
M	Molar
mM	Millimolar
mm	Millimetre
n	Nano
nC	NanoCoulomb
NPV	Normal Pulse Voltammetry
p	Pico
pC	Pico Coulomb
PCD	Pulsed Coulometric Detection
PED	Pulsed Electrochemical Detection
pI	Isoelectric Point
PPy	Polypyrrole
PS	Potential Sweep

R_f	The ratio of the distance moved by a particular solute to that moved by the solvent
RPHPLC	Reverse Phase High Pressure Liquid Chromatography
RVC	Reticulated Vitreous Carbon
s	Second(s)
S	Siemen(s)
SCE	Standard Calomel Electrode
t	Time
TLC	Thin Layer Chromatography
UV	Ultraviolet
V	Volts
α	alpha
β	beta
μ	Micro

Table of Contents

CHAPTER 4

DETECTION OF AMINO ACIDS AT CONDUCTING POLYMER MODIFIED MICROELECTRODES USING FLOW INJECTION ANALYSIS

CHAPTER 1

GENERAL INTRODUCTION

1.1 INTRODUCTION

Modified electrodes are designed and implemented in the fields of electroanalytical detection to improve the sensitivity and selectivity of the system. In this respect the electrode material is tailored specifically in such a way as to promote the desired electrochemical reaction [1,2]. Soon after the first systematic demonstration of modified electrodes in the early 1970's, by Lane and Hubbard [3], modified electrodes became an important domain in electrochemistry.

In modified electrodes, specific chemical groups are produced on the otherwise conventional or classical electrodes. These electrodes offer easy variation of redox properties as well as the physical and chemical properties such as charge, porosity, chirality, and permeability [4]. Therefore, modified electrodes offer greater selectivity compared to unmodified electrodes towards the target molecule. A range of chemically modified electrodes are being applied in both flow-injection and liquid chromatography (LC) to enhance the electrode performance. Such electrodes include those which are perm-selective (enhanced selectivity) or those which can prevent electrode fouling. An example is the use of cellulose acetate to block adsorption of large molecules in the sample while passing the analyte over the electrode surface; as for the selective flow injection analysis (FIA) detection of H_2O_2 [5]. Other examples include: (i) electrodes modified with electron transfer mediator to catalyse the reaction, such as the use of cobalt pthalocyanine (CoPC) incorporated into a carbon paste electrode for FIA oxidation detection of hydrazine [6]; (ii) enzyme modified electrodes for specific biological activity, like glucose oxidase [7]; (iii) ion-exchange coatings for detection of electroinactive ions (ions that do not undergo redox reaction

at the electrode) [8]; and (iv) the use of osmium-containing redox active metallo polymers to determine nitrite amperometrically [9].

1.2 Electrode Modification

The immobilisation of different species on various electrode materials can be achieved by the following techniques:

(i) Adsorption of electrode modifier on the bare electrode surface;

(ii) Covalent bonding of the modifier on the electrode surface;

(iii) Physical coating of the preformed polymer on the electrode surface ;

(iv) Direct deposition of polymer on the bare electrode surface.

The ideal chemically modified electrode for analytical applications in flow systems for continuous long term operation should possess the following characteristics: good mechanical and chemical stability, good reproducibility and long term stability of the electrodes towards the analytes, wide linear dynamic range, low and stable background current over the applied potential range, and easy, simple and reproducible fabrication of electrodes. Among the above mentioned methods of electrode fabrication, electrode modification by polymer layers can be simpler, more effective and versatile than derivatisation methods [10,11,12]. Polymer films have fundamental advantages over covalently bonded or adsorbed groups as the latter methods offer only a monolayer of the groups attached [13,14]. Direct deposition of polymers (conducting polymers) on the electrode surface offers some advantages over deposition as preformed polymers. In the former method, polymerisation and electrode modification steps can be conveniently combined in a single electropolymerisation process. The resultant modified electrodes have much greater chemical and mechanical stability [15, 16], and are compatible with a much wider range of aqueous and organic matrices.

The easy control over the thickness of the polymer layer allows one to maintain the loading of active sites [17]. Thus these materials can have wide application as non-metallic electrode materials.

1.2.1 Conducting Polymers

Conducting polymers with conjugated π-electron backbones, constitute a new class of materials that have electronic conductivity. Polyacetylene was the first polymer that could be made electronically conductive and the conductivities range upto 10^3 S/cm for an iodine doped polymer [18]. This discovery unexpectedly started a great deal of research activity in conducting polymers [19,20]. Since then a large number of conducting polymers have been synthesised. The most important polymers are polyacetylene (1977) [18,21,22], polypyrrole (1979) [23], polyphenylene (1979) [24], polythiophene (1981) [25], polyaniline (1980) [26], and poly(phenylene vinylidene) (1979) [27]. Among these, three polymer systems that have been studied extensively since the early 1980s are polypyrrole, polythiophene and polyaniline. The structure of these polymers are shown in Table 1.1

Of these three materials, polypyrrole modified electrodes are preferred as electrochemical detectors or sensors due to the following reasons: (i) polypyrrole can be polymerised from aqueous solutions, and (ii) they can be prepared at low anodic potentials. These characteristics allow the incorporation of a variety of species (counterions) into the polymer which is advantageous in molecular recognition systems [28,29], as will be discussed later. On the other hand polyaniline could only be prepared from acidic solutions, although some active molecules have been incorporated into the polymer [30,31,32]. To avoid the denaturing of enzymes it is desirable to perform electropolymerisation in neutral media [33]. Thiophene requires

high electropolymerisation potentials (1.65-1.7 V (vs SSCE)) [34] and organic solvent (acetonitrile) [35]. This can limit the range of active species that can be incorporated into the polymer [30].

Table 1.1 *Characteristic properties of polypyrrole, polythiophene and polyaniline*

Polymer	Structure	Doping material	Approximate conductivity (S/cm)
Polypyrrole	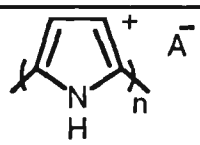	BF_4^-, ClO_4^-, tosylate	500-7500
Polythiophene	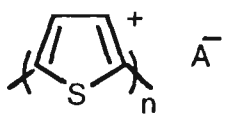	BF_4^-, ClO_4^-, tosylate, $FeCl_4^-$	10-1000
Polyaniline	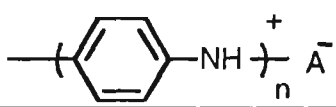	HCl	30-200

A^-= Counterion
Reference=36

1.2.1.1 Electrochemical Polymerisation

Conducting polymers can be synthesised either by chemical or electrochemical polymerisation from a monomer solution containing an electrolyte salt like $LiBF_4$ [17]. Polypyrroles are generally synthesised electrochemically [15, 37-40], because electrochemical methods allow the oxidation potential of polymerisation to be controlled and thus the quality of the polymer can be optimised. Electrochemically synthesised polymer films also possess adequate mechanical properties compared to chemical methods. A. F. Diaz [23] reported (in 1979) that polypyrrole could be obtained as a film, by electrochemical oxidation of pyrrole in acetonitrile, with 100 S/cm conductivity. A flexible, relatively dense, shiny blue-black

free standing film was prepared by this method. The insolubility and conductive nature of the film is important because it allows one to control the polymer thickness by controlling the charge density. The electrochemical polymerisation can be performed in an electrochemical cell with a three electrode system. The working electrode is usually made of platinum [38,41], glassy carbon [42,43], or ITO (indium-tin-oxide) glass [44]. The auxiliary electrode can be made of platinum gauze or reticulated vitreous carbon [45,46]. The selection of reference electrode is dependent on the solvent. In aqueous media Ag/AgCl or SCE reference electrodes are suitable, while in organic solvent the Ag/Ag^{+} reference electrode is commonly employed [45,47,48].

Electrochemical polymerisation can be done by different methods of which the following three are most common. (i) In the galvanostatic method a controlled anodic current is applied to the working electrode of the electrochemical cell to oxidise the monomer. As a result of this, polymer film is produced on the electrode surface. The rate of polymer synthesis can be controlled by the oxidation current density. The major advantage of the galvanostatic technique is that large surface area films can be synthesised on a batch or continuous basis. (ii) In the potentiostatic method the potential of the electrode is maintained at a certain value where the polymerisation reaction occurs. The potentiostatic technique has the major advantage of being able to selectively oxidise the monomer at a given potential. (iii) The third method is potentiodynamic, where the potential is scanned over the range at which polymerisation takes place. This technique has been employed for initial studies to obtain the optimum monomer oxidation potential for potentiostatic synthesis.

The oxidation of monomers and oligomers creates cation radicals which combine to form the polymer backbone. This polymer backbone is positively charged and the charge compensation is achieved by the incorporation of a dopant anion. The amount of anion is related to the level of oxidation of the polymer backbone and is characteristic of each polymer film. Generally, one dopant anion is incorporated for every two to three monomer units [49]. Properties like morphology, electroactivity and conductivity of the polymer are very much dependent on the conditions of polymerisation such as the electrolyte, solvent, monomer concentration, temperature, current, and potential applied [45,49,50-68].

Aprotic solvents have commonly been used because the polymerisation reaction is sensitive to the nucleophilicity of the solvent. It has been reported that the best polymerisation films were produced in acetonitrile, methylene chloride, butane and propylene carbonate [49,69,70]. Pletcher et al. [35,62] have shown that small amounts of water in acetonitrile can affect the rate of deposition and properties of the film. With the increase in the water content from 0.01 M to 0.1 M, the rate of the reaction increased by a factor of 10 to 100. The increase in the water content from 1 to 33%, however, resulted in a decrease in the films conductivity from 100 down to 0.5 S/cm. Good quality films were also prepared in aqueous solutions irrespective of its aprotic nature [38,71,72]. Park et al. [56] have given a very interesting comparison of the polypyrrole films prepared from aqueous and nonaqueous (acetonitrile) solvents by electrochemical techniques. It was observed that pyrrole oxidised at less positive potentials in water than in acetonitrile (by 200 mV). The reason given was that pyrrole molecules are better solvated in acetonitrile, while radical cations produced are better solvated in water. The electrochemical reversibility during potentiodynamic polymerisation was higher for polymer films prepared in

acetonitrile. The poor electrochemical reversibility in water was explained as due to the oxidised forms of polymer undergoing slow irreversible chemical reaction in more nucleophilic environments or simply that the electron transfer is slow. The coulombic efficiencies were not significantly different in these two media as evidenced by the formation of equal amounts of polymer in both cases. The post-polymerisation cyclic voltammograms recorded in 0.1 M TEAP in acetonitrile showed larger ΔE_p (difference between anodic peak potential and cathodic peak potential) for films prepared in water. In addition the conductivities recorded for the films were found to be higher for films prepared in acetonitrile (60-100S/cm) than water (5-6 S/cm). As far as the surface characteristics are concerned the films formed in aqueous media were more porous than in acetonitrile.

The working electrode material is an important consideration, because the films are produced anodically and the electrode material should not oxidise concurrently [49]. Platinum [38,41], glassy carbon [42,43] and gold electrodes [73] are most commonly employed in polymerisation. To obtain reproducible results it is essential to clean and polish the electrode surface before every experiment [38].

With the same electrolyte conditions, the nature of the polymer film can be changed by changing the potential applied. For example, films prepared from aqueous solution containing 0.25 M pyrrole and 0.08 M PTS had conductivities 150, 500 and 100 S/cm with applied potentials of 0.6, 0.75 and 1.0 V vs SCE [63]. In constant potential polymerisation at higher anodic potentials, the nucleation of the new phase is faster and the current rises to higher rates, and a progressive decrease occurs later, which relates to the passivation of the process when the conductive phase becomes more and more resistive, thus hindering the current flow. This passivation process

occurs more quickly at higher potentials because there is a tendency to overoxidise the polymer and cause deterioration in conductivity and electroactivity [45].

The temperature at which electropolymerisation is performed has also been reported to affect the conductivity of the polymer [63, 64]. In general, more conductive polymers are produced at lower temperatures. For example, polypyrrole films prepared at -20°C in propylene carbonate are more conductive (300 S/cm) than the films prepared at 20 °C (97 S/cm) [64].

The concentration of the monomer also affects the morphology of the film. Patchy and brittle polypyrrole films were obtained from lower pyrrole concentration (0.015 M) [70].

1.2.1.2 Mechanism of Electropolymerisation

The anodic oxidative polymerisation reaction consists of several steps that lead to aromatic polypyrrole with primarily 2,5-coupled pyrrole monomers [49]. The initial step consists of the oxidation of the pyrrole monomer to produce radical cations. The anodic oxidative polymerisation has an electrochemical stoichiometry of 2.20-2.40 Faraday/mol of reacting monomer [23]. Since the film forming process needs only 2 Faraday/mol, i.e. 2 electrons/molecule, the additional charge is utilised in partial reversible oxidation (doping) of the polymer film [74-76]. The polymerisation reaction proceeds when the applied electrode potential is sufficiently high to oxidise the monomer (Figure 1.1-a). Thus, the concentration of radical cationic monomer and oligomer is high at the electrode surface compared to neutral species. These conditions lead to the dimerisation of radical cations forming the dication of the dihydrodimer.

Diaz et al. [37,74] suggested that the subsequent deprotonation of the radical dimer forms an aromatic dimer (Figure 1.1-b). Furthermore, this mechanism is consistent with the decrease in the pH of the electrolyte solution during film growth [77,78]. As the oxidation of dimer is more favourable compared with monomer, the dimer immediately reoxidises to form a cation [Figure 1.1-c]. This is followed by coupling with another radical cation and deprotonation, and oxidation of the propagated oligomer unit to a cation to produce a higher homologue (Figure 1.1-d, e). Finally, the incorporation of counterion results in the doped polymer films (Figure 1.1-f). Since the potential needed for monomer oxidation is higher than the oxidation of the existing polymer, the film formation and its oxidation occur simultaneously. A detailed work of the mechanism and efficiency of electropolymerisation of pyrrole, in different electrolytes and pyrrole concentrations, showed that the polymerisation is affected by the solubilisation of oligomers in the initial stages but ultimate efficiency is dependent on the electrolyte employed [79,80].

(a) Oxidation

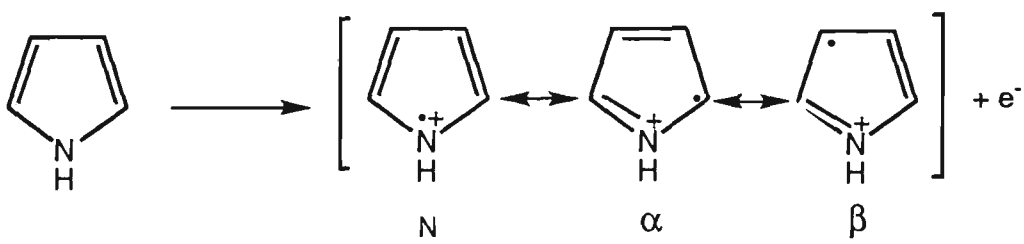

possible resonance forms of radical cation

(b) Radical Coupling /Deprotonation

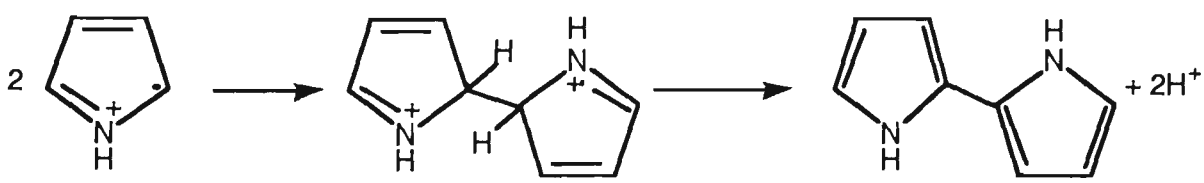

(c) Oxidation

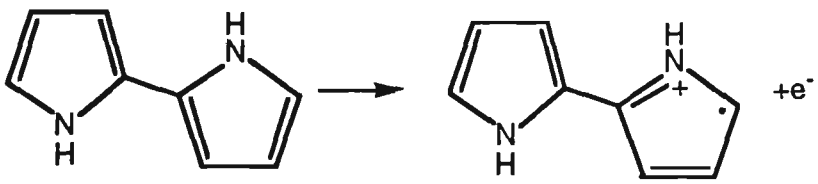

(d) Coupling/Oxidation

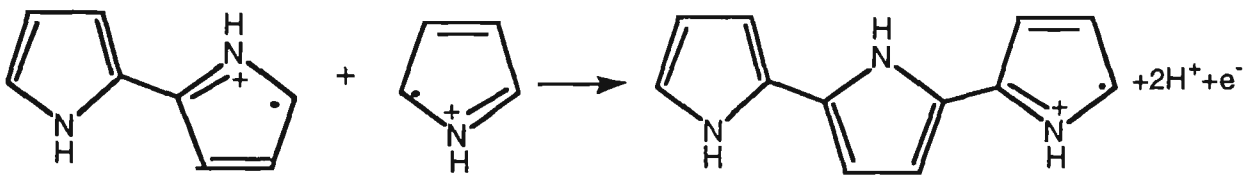

(e) Chain propagation

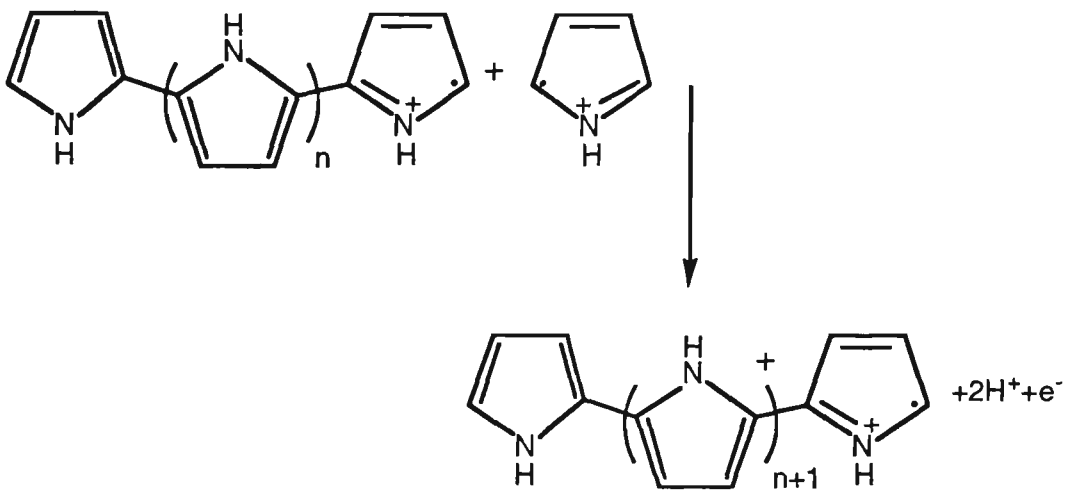

(f) Doping

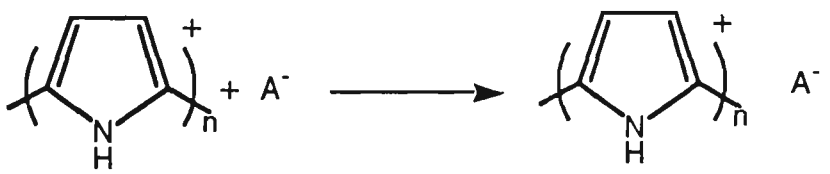

Figure 1.1: *Mechanism of polypyrrole formation upon oxidative electropolymerisation.*

The mechanism through dimer formation by coupling of radical cations has been challenged on the basis that the coulombic repulsion between small cation radicals hinder the dimerisation process [38,81-83]. The alternative route proposed was an electrophilic attack by the radical cations

on the neutral monomer to produce the single charged dihydro derivative, and this is followed by further charge transfer and proton elimination leading to dimer formation (Figure 1.2). But this alternative route is not compatible with experimental observations because polymer growth only proceeds when the oxidation of the monomer occurs along with the oxidation of the film [84,85].

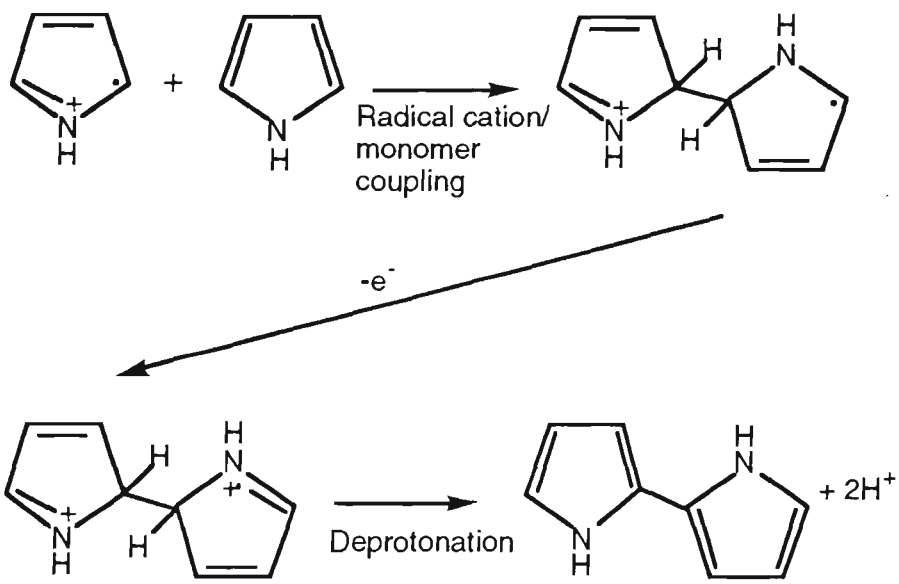

Figure 1.2: *An alternative route to dimerisation.*

The fact that the monomeric units in the pyrrole chains are α,α'-linked is further supported by electropolymerisation studies on α-substituted monomers. It was observed that α-substituted monomers did not polymerise [86]. Therefore during polymerisation of unsubstituted monomer a linear polymer chain is expected, which is bonded at α,α' positions, with the elimination of α-hydrogen [87]. The 2,5-coupling is desirable from a theoretical point of view (resonance structure is stable), but the less desirable 2,3-coupling may also take place. In addition, hydrogenation of polymer backbone also occurs. The hydrogenation of double bond decreases the degree of conjugation which therefore lowers the

conductivity [88]. A disordered structure of polypyrrole results and is shown in Figure 1.3.

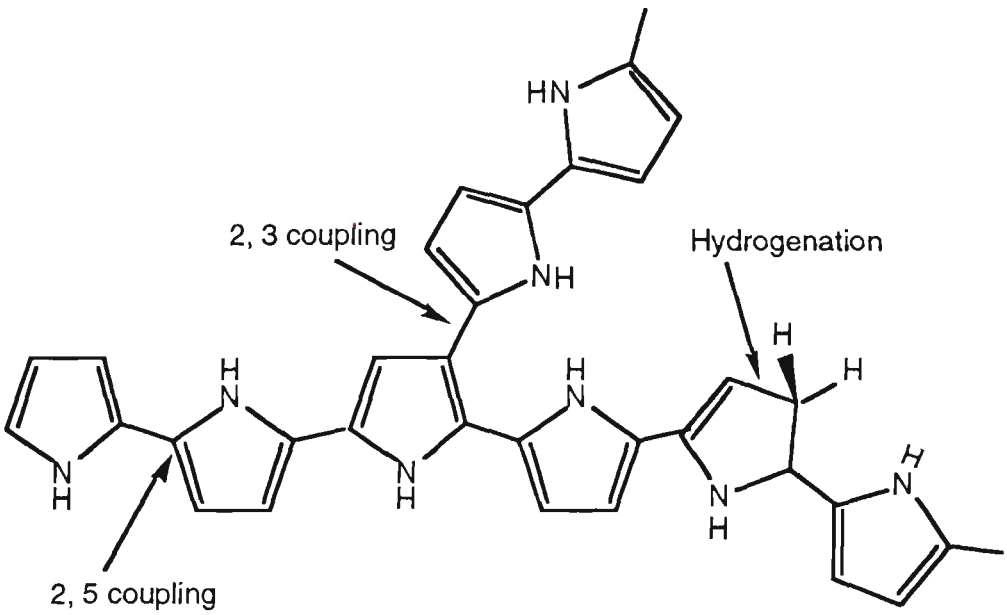

Figure 1.3: *Structure of polypyrrole with 2,3-coupled chain and hydrogenated backbone.*

1.2.2 Types of Doping Agents and their Influence on Properties of Conducting Polymers

The concept of doping/dedoping in conducting polymers is the central and unique theme. For conducting polymers, doping refers to the process associated with polymer oxidation where charge neutrality of the polymer backbone is maintained by incorporation of counterion (dopant anion). Dedoping, however, involves polymer reduction which results in the expulsion of these counterions. These processes distinguish conducting polymers from all other types of polymers. Doping agents or dopants are classified as (i) ionic dopant, (ii) organic dopant, (iii) polymeric dopant (Table 1.2). Ionic dopants constitute the anions derived from the dissociation of the dopant molecule, that neutralises the positive charge of the polymer during the electrochemical doping process. Organic dopants are

also anionic, and they are generally incorporated from the aqueous solution of the electrolyte during polymerisation. Polymeric dopants are functionalised polymers with ampiphilic anions.

Table 1.2 *Dopants for conducting polymers*

Dopant	Active species for dopant	Polymer	Reference
Ionic dopant			
$LiClO_4$	ClO_4^-	PPy, PTh	73,75,89,90
KNO_3	NO_3^-	PPy	91
$LiBF_4$, Bu_4NBF_4	BF_4^-	PPy, PTh	35,89,92,93,73
$(CH_3)_4\ NPF_6$	PF_6^-	PPy, PTh, P3MT	73,89,93
HCl	Cl^-	PAn	94
Organic dopant			
$CH_3CH_2C_6H_4SO_3Na$	$-SO_3^-$	PPy	48
CF_3SO_3Li	$-SO_3^-$	PPy,PTh	73,89,93
p-$CH_3C_6H_4SO_3Na$	$-SO_3^-$	PPy	48,95
Polymeric dopant			
PVS	$-SO_3^-$	PPy	96
PSS	$-SO_3^-$	PPy	96

PPy=Polypyrrole, PTh=polythiophene, 3PTh=Poly(3-methyl thiophene), PAn=Polyaniline, PVS=polyvinyl sulfonate, PSS=Polystyrene sulfonate

Doping/dedoping is reversible and the original polymer can be reproduced without any degradation. Both chemical and electrochemical processes can be utilised to dope and dedope the polymer. Since the nature of the anion in the polymer film is critical in determining the intrinsic properties of the polymer film, the film properties can be changed simply by changing the electrolyte salt used in polymerisation. For example, the incorporation of

inorganic anions [97], large organic anions [49,77,98], enzymes [31,99,100], proteins [101,102] and electroactive anions (ferrocyanide [103] and iron phthalocyanine tetrasulphate [104]) have been reported. The unique property of conducting polymers, in that anions can be incorporated, makes it possible to create surface modifications. Bio-recognition sites such as enzyme glucose oxidase (GOx) [105,106] or urease [107] have been incorporated as counterions. Polynucleotides [108] and macromolecules such as antibodies have also been incorporated directly.

The counterions incorporated also have a marked effect on the polymer morphology. For example, polymer morphologies are dramatically different for perchlorate, sulfonate and trifluoroacetate [93]. The presence of small amounts of polystyrenesulfonate (PSS^-) in the monomer solution was found to affect the morphology of the polymer film. Thus smooth and continuous films were obtained with small amounts of PSS^- as counterions in monomer solution containing perchlorate ions as well (1M ClO_4^- and 0.1M PSS^-) [72]. Wegner et al. [109,110] have also reported on smooth and continuous films prepared from PSS^-. The mechanical properties are reported to be better for films containing toluenesulfonate anions. These films are stronger; tensile strength is 30-40 % higher than other films [95]. The films with aromatic sulfonate counteranions show conductivities as high as 50-100 S/cm [93]. Mitchell et al. [111,112] have prepared polypyrrole films with an anisotropic molecular organisation by incorporating 10-camphor sulfonate. In these polymers the pyrrole rings are preferentially aligned parallel to the electrode surface while camphor sulfonate intercalates these pyrrole layers.

The dopant species also affects the switching potential of the polymer. For example, polypyrrole containing small inorganic anions such as BF_4^-, ClO_4^-,

and PF_6^- shows broad reduction waves at +200 mV which are associated with anion expulsion. In contrast, polypyrrole with large anions such as DS^-, PSS^-, and PTS^- shows large reduction peaks at -500 mV but only a small reduction current at +200 mV. In addition a cathodic shift was observed in both reduction and oxidation potentials [70]. These properties are important because potential applications are based on them.

The switching rates from neutral (non-conductive) to oxidised (conductive) states [23,74] are limited by the rate of diffusion of anion in and out of the polymer film. For polymers with small inorganic anions, the electrochemistry of the polymers require influx of anion during oxidation and expulsion of anions during reduction [74,113]. EQCM studies reveal that even with these mobile anions some cation movement occurs [47,114].

For polypyrroles doped with high molecular weight organic anions, the mobility of the anion is considerably reduced [115]. For example, reduced mobility of polystyrenesulfonate (PSS^-) and dodecylsulfate electrolytes [71,116] practically creates fixed sulfonate negative charges. In the oxidised state of the polymer (PPy^+) the cationic sites are compensated by anionic sulfonate groups, while in the reduced state anionic sites of sulfonate groups are neutralised by the influx of electrolyte cation. The polymer acts predominantly as a cation exchanger and this behaviour has been confirmed by different analytical methods [109,110,117-122]. However, some possibility of leakage of large anionic dopant has also been reported by Zhong and Doblhofer [121], at least for the polypyrrole-dodecylsulfate system.

In short, the ease with which the desired counterion can be incorporated and its affect on the resultant properties of the polymer provide a facile way of preparing tailor made surfaces.

1.2.3 Derivatised Monomers for Electrode Modification

Another way to modify the properties of the polymers is to introduce substituents on the nitrogen [123-125] and/or the 3-position [42,93,126-128] of the pyrrole ring. For alkyl N-substituted pyrrole (methyl, ethyl, butyl, iso-butyl) both electrochemical and physical properties were affected. The degree of oxidation and conductivity were decreased. The oxidation potential of polypyrrole also changed due to the presence of N-alkyl substituents. Polypyrrole oxidizes at -0.2 V, while the oxidation potentials for N-alkyl substituted pyrrole lies in the region 0.45-0.64 V. For pyrrole with larger alkyl groups (propyl, butyl) the quality of the film was also affected in that rough and wrinkled films were obtained [123]. Deronzier et al. [129,130] have synthesised N-substituted polypyrrole with doner/acceptor moieties. A large alkyl group at the C3 on the pyrrole ring will produce a polymer (I) with strong hydrophobic character [125].

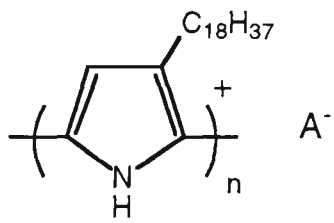

(I)

The ion exchange properties of polypyrrole can be modified by introducing ionic substituents on the pyrrole ring at C3. Tabba and Smith obtained a yellow soluble polymer from the electrochemical polymerisation of 3-methylpyrrole-4-carboxylic acid (MPC) in acetonitrile [131]. The pH dependence of the electroactivity of the polymer deposited on platinum and the reversible electrostatic binding of $Co(bpy)_3^{2+}$ and methyl viologen by PMPC has also been shown [132].

Cation exchange groups covalently bound to the monomer contain fixed negative charges and, upon polymerisation, act as polymer dopant. Such polymers are known as "self-doped" polymers (II). The resultant polymers are cation exchangers [133].

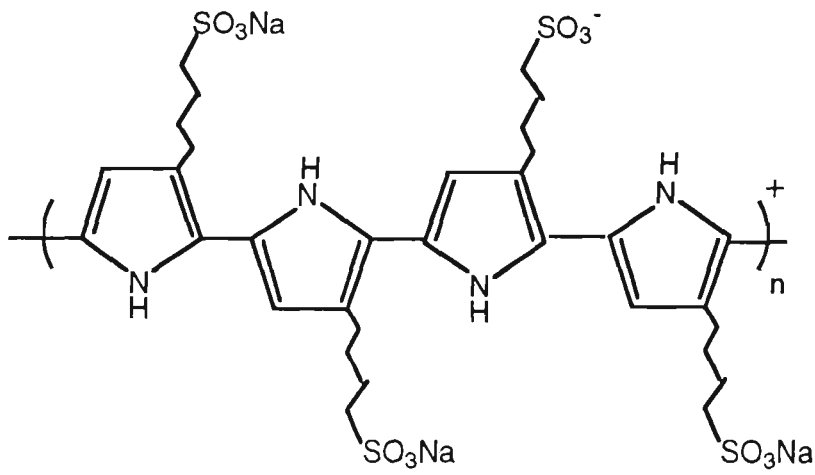

(II)

A sketch of self-doped conducting polymer [133]

A permanent negative fixed charge can also be created by copolymerisation of long chain aliphatic sulfate substituted pyrrole monomer with pyrrole. For example, pyrrole/N-sulfopropyl-pyrrole copolymer (III), from co-polymerisation of pyrrole and 3-(pyrrole-1yl-)-propane sulfonate has been produced. The resultant product has cation exchange behaviour [47,48,134-136]. The main advantage of such substituents is the creation of permanent anionic sites in the polymer.

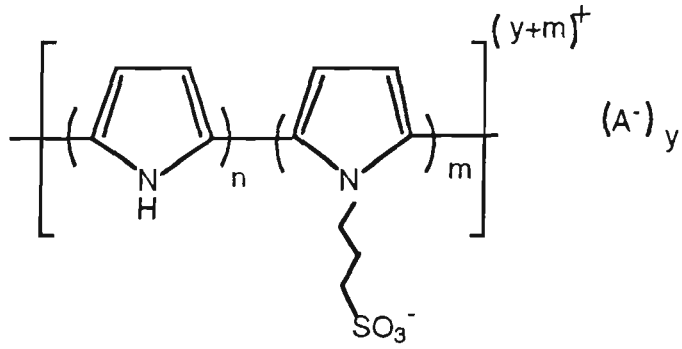

(III)

Poly{pyrrole-co-[3-(pyrrol-1-yl)propanesulfonate]} [134]

The easy functionalisation of the pyrrole ring, as well as copolymerisation of pyrrole with functionalised monomer, widens the opportunity to prepare surfaces with desired properties.

1.2.4 Chiral Conducting Polymer Modified Electrodes

The preparation of inherently chiral conducting polymer modified electrodes has been of considerable recent interest because of their potential applications in areas such as electrochemical asymmetric synthesis [137,138]. Most approaches to such chiral polymers have involved the covalent attachment of chiral groups to pyrrole [44,139-141] or thiophene rings [142-144] prior to polymerisation so that the existence of chirality in the resulting polymer is well established.

Chiral polypyrroles were prepared either from N-substituted or from C_3-substituted pyrroles. Some of these chiral N-alkyl substituted polypyrroles are shown below (IV to VI). Unfortunately, these polymers suffered from poor conductivity (10^{-6} S/cm) and mechanical property [145].

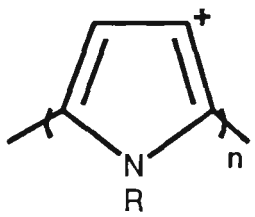

R= IV, V, VI

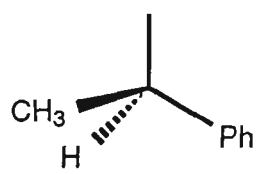

(IV)

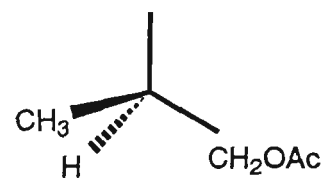

(V)

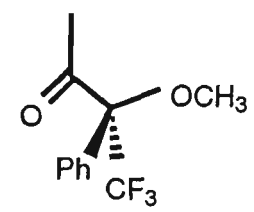

(VI)

Salmon and Bidon [44] reported on N-substituted pyrrole (VII) and (VIII). These chiral monomers contained (+) camphor-10-sulfonate ester as the chiral group. The resulting polypyrroles were mechanically and electrochemically stable with reversible redox electrochemistry.

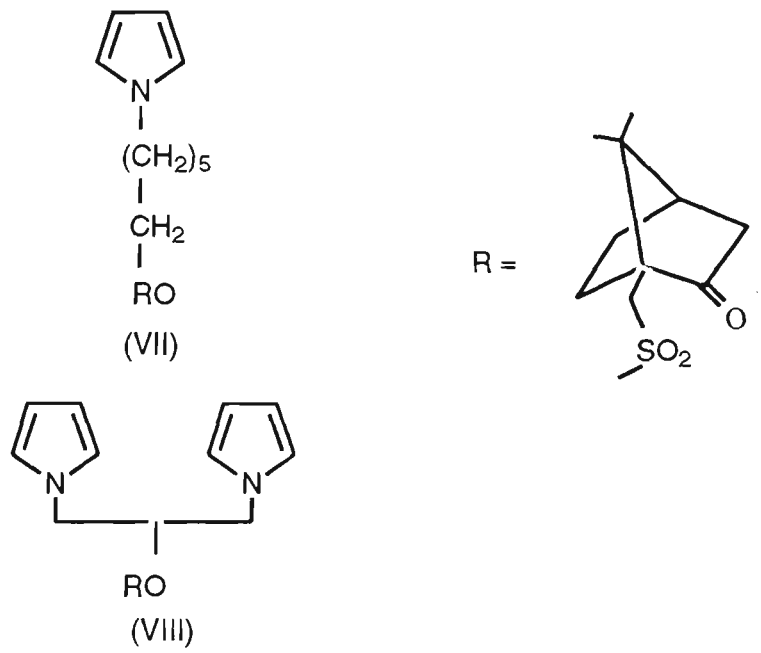

N-alkyl pyrrole (+) camphor-10-sulfonate ester derivatives

Garnier et al. [141] reported that the C_3-substituted pyrrole, with chiral amino acid, upon polymerisation produced polypyrroles with helices in the polymer chain. It was claimed that the chiral substituents (amino acids) induced helical chains in the polymer. The electroactivity of these amino acid substituted polymers decreased from (IX) to (XI) due to the increasing size of the hydrocarbon part in the R- group [140].

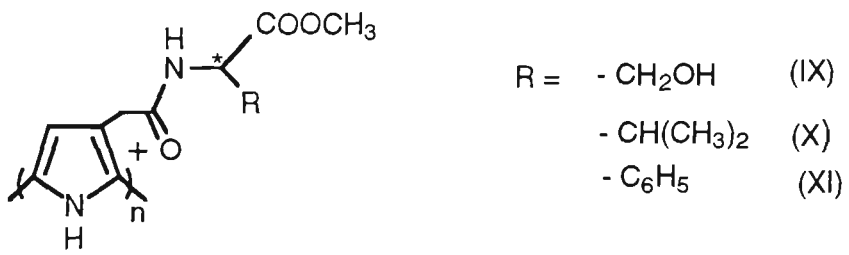

Structure of three Pyrroles substituted with small peptidic fragments

Chiral poly(thiophenes) are prepared by substituting chiral groups on C_3-of thiophene monomers. The polymer (XII) has low conductivity due to the low doping level (one counterion for nine monomeric units). The doping level was believed to be affected by the close proximity of the substituent to the thiophene ring [143].

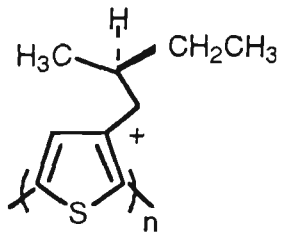

(XII) *(s)(+)-3-(2-methyl-butyl) thiophene*

With the introduction of the spacer between the substituent and the thiophene unit the polymers (XIII) and (XIV) were obtained as free standing films with ~ 1S/cm conductivity. The polymers possess high electrochemical stability and good electroactivity [142].

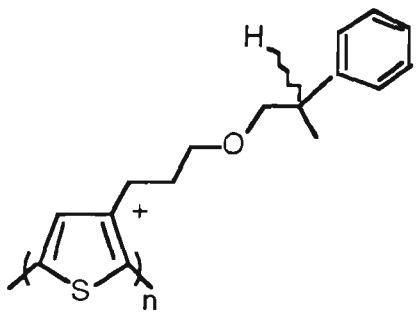

(XIII) *(2S)-(+)- 3-(3'-thienyl) propyl 2-phenyl butyl ether*
(XIV) *(2R)-(-) 3-(3'-thienyl) propyl 2-phenyl butyl ether*

Some other C-3 substituted poly(thiophenes) [144,146] with spacer between the thiophene ring and chiral substituent was reported to have polymer chain helix structures.

Recently a more facile route to the production of chiral polyaniline has been reported by doping with chiral camphorsulfonic acid [147,148]. These polymers also possess helical structures in the polymer chain and have good electroactivity.

In a few cases such polymers have been shown to exhibit enantioselective recognition of chiral anions used as electrolyte and doping agents during

redox cycles. For example, polypyrrole bearing a β-D-glucose substituent covalently attached to the N atom of pyrrole, showed stereoselective recognition towards optically active 10-camphor sulfonic acid [139]. For chiral poly(thiophenes), the doping level of (+) hand of the polymer (IX) was 50% higher in (+)-10-camphorsulfonic acid compared with the doping level in (-)-10-camphorsulfonic acid [142]. The stereoselectivity of chiral polymers might have specific applications which include enantioselective membrane separations, and electrodes for enantioselective electrochemical (EC) detection.

1.3 *In-situ* Electrochemical Characterisation of Conducting Polymer Modified Electrodes

For the *in situ* characterisation of conducting polymer modified electrodes, the preferred method is cyclic voltammetry (CV). The cyclic voltammetric technique has been used widely to investigate the electronic and electrochemical properties of the polypyrrole films because this technique can better describe the characteristics of the electrochemical switching [38,41,74,97,149].

The redox process in conducting polymers is, in most circumstances controlled by electronic and ionic charge transport. So far several models have been put forward to explain the origin of the current and shape of the voltammogram, quasi-reversible nature of the electron transfer reaction, and associated large capacitive current [150-154] during electrochemical switching of polypyrrole between its reduced and oxidised states. During redox cycling the switching of the polymer from its conductive to neutral state and vice versa, as well as associated ion movement, are affected by several factors such as solvent, potential applied, and polymer thickness.

The dominant factor, however, is the nature of the anion incorporated during electropolymerisation. We will consider here the electrochemical behaviour observed through cyclic voltammetry in terms of diffusion of ions. In the polymer chain, the backbone has positive charges which are balanced for charge neutrality by dopant anions. For polymers incorporated with small anions (Cl^-, ClO_4^-) [155], the anions are expelled from the polymer film (dedoping) when the film is reduced to the neutral state by an applied negative potential. Conversely, when a positive potential is applied to oxidise the neutral film, anions are taken up (doping). A reversible redox reaction is shown below (1.1):

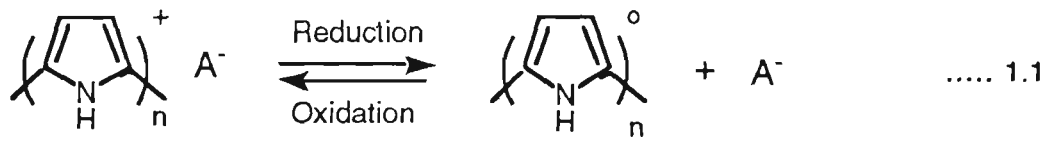

..... 1.1

For polymers incorporated with immobile anions such as PSS^- [114,115,155], when a negative potential is applied, the polymer backbone is reduced to neutral charge but because the counterion is immobile a net negative charge will result in the polymer. Thus cations are incorporated from the electrolyte solution to maintain charge balance in the polymer. On reversing the scan to positive potentials, the polymer backbone is reoxidised to a positive charge thus displacing the incorporated cations from the polymer. Such a reversible reaction is shown below (1.2):

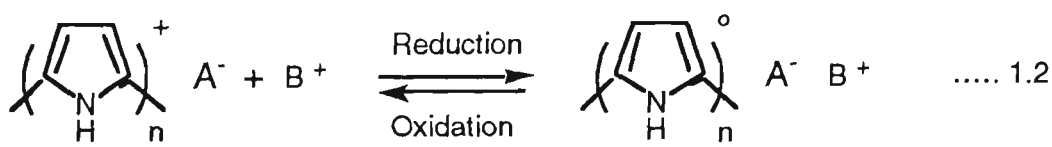

..... 1.2

However, a third possibility also exists, in that, a combination of anion and cation exchange can occur during redox processes when medium sized

counteranions (tosylate and trifalate [155]) have been incorporated during electropolymerisation.

To analyse the effect of applied potential on the whole redox process influenced by the nature of the anion incorporated, the schematic of the contribution from anions and cations during CV are shown in Figure 1.4.

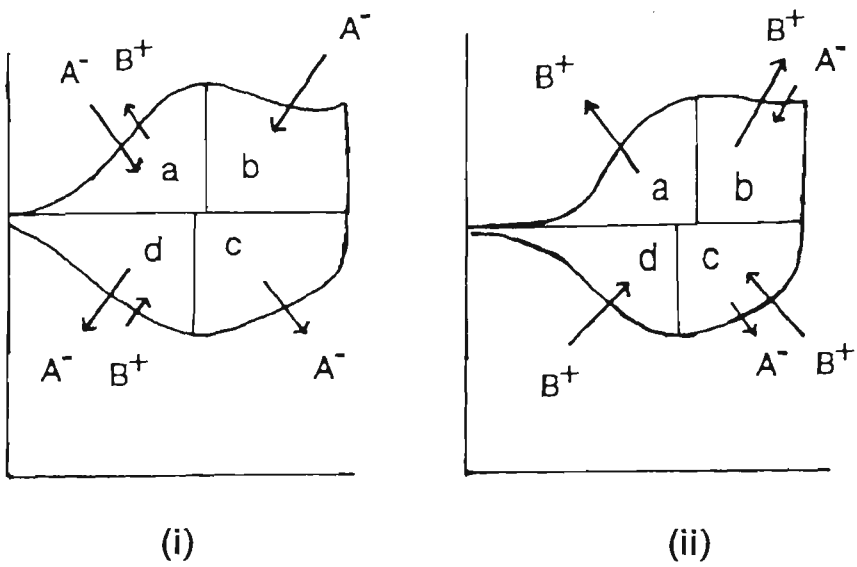

Figure 1.4: *A schematic diagram showing the potential dependent ion-exchange processes. (i) PPy with mobile anion, (ii) PPy with immobile anion.*

For polypyrrole incorporated with mobile anions, at potentials anodic of the peak potential (b, c regions, Figure 1.4-i) only the movement of anions occurs while at potentials cathodic of the peak potential (a, d regions, Figure 1.4-i) the exchange involves the participation of anions and cations simultaneously. For polymers incorporated with immobile anion, at potentials cathodic of the peak potential (a, d regions, Figure 1.4-ii) cation exchange occurs, but at potentials anodic of the peak potential (b, c, regions, Figure 1.4-ii) the exchange requires simultaneous participation of anions and cations. This type of description is supported by energy dispersive X-ray studies, volta-potential measurements [121] and optical beam deflection measurements [47,122,156].

The redox reaction is fast with thin films and the oxidation state of the film can be changed in milliseconds. The redox process in polypyrrole is also associated with a colour change from pale yellow for the neutral film to brown-black for the oxidised films [23,74].

Since the discovery of conducting polymers, several methods including the electrochemical quartz crystal microbalance (EQCM) technique. have been employed for *in situ* characterisation. The unique feature of the EQCM is its ability to provide information regarding mass changes associated with redox processes. Such information is useful in designing strategies to improve the electronic and morphological properties of these materials.

Kaufman and coworkers [157] were the first to describe the use of EQCM for transport studies in polypyrrole films during redox switching. It was observed that lithium ions were incorporated during reduction of PPy/ClO_4 instead of perchlorate ion expulsion. The ion exchange property of polypyrrole has also been studied by others [158-160,115,116-120]. For example, in the case of PPy/PSS electrodes [118], in $LiClO_4$, $NaClO_4$ and $Mg(ClO_4)_2$, only ClO_4^- was incorporated in the region -0.3 to 0.3 V vs SCE as indicated by mass increase during oxidation. Cations were incorporated in the region -0.7 to -0.3 V vs SCE as indicated by the mass increase during reduction. Similar studies have also been reported for copolymers of pyrrole where the copolymer was perm-selective to potassium ions [161], while in self-doped polymers [162], cations of the supporting electrolyte are the main ion transport species.

Orata and Buttry [163] first studied aniline by EQCM. Potentiodynamic and potentiostatic polymerisation efficiency was compared by measuring the charge and mass measurement. It was found that the potentiodynamic

polymerisation was more efficient. Effect of pH and electrolyte on protonation of the insulating and conducting form of polyaniline have also been considered. Polyaniline/Nafion composites [164] showed that the cation transport is dominant in such films due to fixed anionic sites of the nafion matrix. EQCM combined with other techniques have been used to study the kinetics of ion movement in redox processes [119,161]. The proton transport is dominant in the beginning of oxidation/reduction while anion transport is more important in thicker films [165]. The EQCM is an excellent tool for electrochemical characterisation, because mass changes of the polymer films, resulting from electrochemical treatment like CV and pulse potentials can be observed simultaneously in situ.

1.4 Stability and Degradation of Conducting Polymers in Electrochemical Systems

Degradation processes were also observed at anodic potentials for polypyrroles [74]. In literature the opinion on this subject varies; concerning the region of potentials where PPy is chemically stable. The application of potentials positive of this value causes degradation of the polymer properties and loss of electroactivity. This has been attributed to an irreversible oxidation of the polymer. This phenomenon is known as overoxidation [166-170].

Christensen and Hamnett [171] have reported that in 1.0 M $NaClO_4$ over-oxidation of polypyrrole starts at potentials higher than 0.7 V (vs SCE). Pletcher et al. [38] reported deterioration in the polypyrrole film properties, such as decrease in conductivity and decrease in adhesion to electrode substrate in 1.0 M KNO_3 solutions, at 0.8V (vs SCE). Furthermore, irreversible oxidation of polypyrrole films in aqueous solutions of acids [172]

was observed at potentials higher than 1.0 V. Irreversible electrochemical oxidation and simultaneous film break down of polypyrrole in acidic and neutral media occurred at potentials 1.24, 1.13, 1.07, 0.99, and 0.96 V in $HClO_4$, TsOH, H_2SO_4, TsONa, and Na_2SO_4 respectively [173]. Kras'ko et al. [174] have reported for polypyrrole that the anodic peak observed in 0.1 M $NaClO_4$ at about 1.0 V did not manifest a counterpart in the reverse scan. On repetitive cycling, the anodic peak decreased both in current value and size. As a result of this potential cycling the polypyrrole conductivity dropped.

According to Beck et al. [166] PPy/BF_4 overoxidation (in the presence of nucleophiles: H_2O, OH^-, CH_3OH, CH_3O^-, Br^- and CN^-) is related to the interaction of charged polymer chains with nucleophiles. Even though the radical cation (polarons) are not sufficiently reactive for electro-organic reaction, the slow addition of strong nucleophiles is not ruled out (Equation 1.3) [166]:

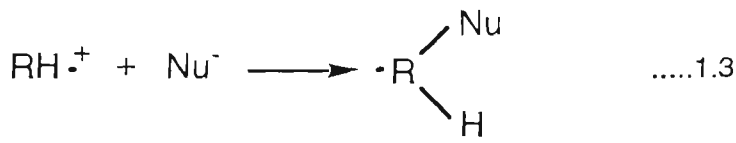

.....1.3

In most cases, however, the radical cation is oxidised to the dication (bipolaron), which then reacts with the corresponding nucleophiles (Equation 1.4):

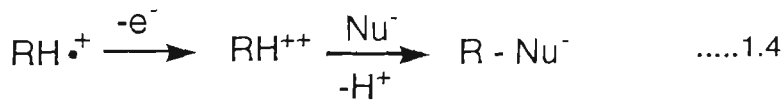

.....1.4

It was also suggested that polypyrrole overoxidised to the dication at potentials of about 1.0 V versus SSCE or +236 mV versus SCE in neutral and acidic solutions and is followed by formation of (XV) [166]. Pyrrolinone (XV) may furthur oxidise to the 4-hydroxylation product (XVI):

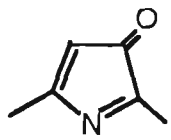

(XV)

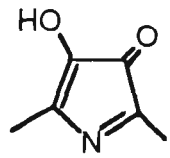

(XVI)

In the IR reflectance spectroscopy of overoxidised polypyrrole, the formation of (XVI) is in accordance with the presence of the carbonyl band at 1720 cm^{-1}, and a new band at 775 cm^{-1} which is supposedly related to the change in the pyrrole ring vibrations due to the substitution process.

1.5 Application of Conducting Polymer Modified Electrodes as Sensors

Conducting electroactive polymers with their dynamic properties such as electrical conductivity (100 S/cm for polypyrrole) with good mechanical properties and environmental stability [49] have potential applications in electrochromic displays [175], batteries [176], electrocatalysis [177], corrosion protection [178], and in particular sensor applications [179]. Conducting electroactive polymers are attractive materials for sensor applications because of the following properties [180]:-

- Deposition on the substrate electrode by electrochemical oxidation of the monomer is direct and facile. Electrode modification is easy with the liberty to incorporate a range of counterions capable of analyte recognition, and/or use of functionalised of the monomer.

- Conductive electroactive polymers in their oxidised form conduct ionically and electronically. Sensor response is based on properties such as resistance, current or electrochemical potential change. In short their

electronic conductivity and electroactivity provides a means by which the sensing capability can be fine tuned.

Conducting polymer sensors can be classified as:

- Chemical Sensors.
- Biosensors.
- Gas Sensors.

1.5.1 Chemical Sensors

The electrochemical sensor based on current (amperometric) or potential (potentiometric) response to the analysed species constitute one of the main classes of sensors. "A chemical sensor is a device that transforms chemical information, ranging from the concentration of a specific sample component to total composition analysis, into an analytically useful signal. The chemical information mentioned above, may originate from a chemical reaction of the analyte or from a physical property of the system investigated."[181]

Conducting polymers due to their ion-exchange properties have been used in the development of potentiometric sensors. The detection of electroinactive ions was also reported to be influenced by the 'ion-sieving' or memory effect. This property was produced and controlled during electrochemical growth by the size of the anion used during polymerisation. The polypyrrole film prevented anions of larger size from penetrating the film. For example, Dong et al. [182,183] described a potentiometric sensor for chloride and perchlorate prepared using 0.1 M LiCl and 0.1 M $LiClO_4$ respectively. The selectivity of the electrodes for Cl^- or ClO_4^- was attributed to the size of the incorporated ion. The linear response range for both the

chloride and perchlorate electrodes was from about 0.1 mM to 0.1 M. A similar potentiometric sensor was reported [184] with PPy incorporated separately with different counterions; Cl^-, ClO_4^-, NO_3^-, and Br^-. The polymers were more selective towards the incorporated anions, and the detection limits were $4.5x10^{-5}$ M, $4.5x10^{-5}$ M, $3.2x10^{-5}$ M, $7.0x10^{-5}$ M respectively.

The doping/dedoping property of PPy was utilised by Ikariyama and Heineman [8] in FIA for amperometric detection of electroinactive anions. The detector was a thin layer flow through cell with the working electrode coated with polypyrrole. The detection scheme is based on the doping of the polymer film with the anion to be determined at the doping potentials and thus cause an electron flow. The electrode was held at -0.3 V for dedoping and then stepped to 0.9 V to detect injected analyte anions by the doping process. The anions studied were carbonate, phosphate, and acetate. The eluent used here was a zwitterion (0.1 M glycine) which does not incorporate into the polymer matrix and hence the selectivity of the system was improved. A linear response over the range of 10^{-5} M to 10^{-3} M was observed for the anions studied.

Ikariyama et al. [185] also reported the detection of the halide ions fluoride, chloride, bromide, and iodide. The effect of the composition of the carrier stream was also investigated. It was observed that the background currents were much higher for N-2-hydroxyethylpiperazine-N'-2-ethanesulfonic acid and polyacrylate than when glycine was used in the carrier stream. For chloride the linear response was 1 μM to 1 mM.

Ye and Baldwin [186] described a similar FIA method but used polyaniline as the working electrode. They found that polyaniline was chemically more

stable than polypyrrole and the doping/dedoping process was faster and more reproducible than with the polypyrrole electrode. They studied the response of nitrate, chloride, and sulfate using either 0.2 M acetate buffer (pH 5.45), 0.2 M acetate buffer (pH 5.45) containing also 0.1 M perchlorate, or 0.2 M glycine (pH 6.0) as the carrier stream. The responses were highest with glycine. They also reported that the responses observed could also be due to some changes in viscosity and carrier stream concentrations rather than to the actual doping of the polyaniline film with the anion injected. Following this, E. Wang et al. [187] then reported the use of the polyaniline modified electrode for the detection of I^-, Br^-, SCN^-, $S_2O_3^{2-}$, ClO_4^-, and NO_3^- in FIA and ion chromatography (IC). The selectivity was varied by varying the background eluent. Similarly Ward and Smyth [188] reported a PPy-based electrode in FIA and ion-chromatography. Cl^-, NO_3^-, NO_2^-, ClO_4^-, Br^-, CO_3^2, SO_4^{2-}, and PO_4^{3-} were detected reproducibly over the 1-100μg/ml concentration range.

The PPy/DS electrode was applied in the detection of the cations Li^+, Na^+, and K^+ [189]. To detect the cations the current was measured at reduction potentials. The cation exchange property of incorporated DS^- was reported to be the active species in the detection mechanism.

The signal obtained in amperometric detection is reported to be composed of more than one factor [186,190,191]. The signal may not just be composed of the current arising from doping/dedoping of the polymer. The several components contributing to the signal could be: (i) current due to the change in the polymer conductivity as ion exchange takes place, (ii) from doping/dedoping, (iii) due to a change in solution conductivity, and (iv) electrode charging current. However the contribution from each component is dependent on the nature of the polymer, electrolyte, potential

applied and analyte detected. The sensitivity and limit of detection (LOD) of a polymer based sensor will also depend on the background current exhibited by the polymer sensor. The background current, to a great extent, can be a function of the morphology of the polymer which in turn will depend on the electropolymerisation conditions and on the nature of the dopant counterion.

1.5.2 Biosensors

"A biosensor [192] is an analytical device incorporating a biological or biologically derived material, either intimately associated or integrated within a physio-chemical transducer." The main advantage of the biosensor is its ability to exploit the biological specificity. So it is possible to detect low analyte concentrations in complex media.

A polypyrrole based amperometric biosensor was reported by Umana and Waller [28]. The enzyme glucose oxidase was immobilised into and onto the polypyrrole film during electrochemical polymerisation on the substrate electrode surface. The trapped enzyme was active within the polymer film. In the presence of glucose oxidase, the glucose reacts with oxygen to produce gluconic acid, and hydrogen peroxide which was amperometrically detected.

Iwakura et al. [193] incorporated the enzyme glucose oxidase and the mediator ferrocene carboxylic acid simultaneously during polymerisation of pyrrole. The hydrogen peroxide produced was determined amperometrically at 0.4 V. The thickness of the sensor film was important as the responses increased with increased film thickness. This is because the amount of enzyme and mediator incorporated into the film increases as

well. The response decreased after a certain thickness as a result of slow diffusion of glucose into the film.

The polyaniline based sensors were prepared by the physical entrapment of the corresponding enzyme to detect glucose [194]. The polymer acts as an immobilisation medium and transducer to convert a biological signal to an electronic signal. The sensor response is due to the change in the micro-environment occurring as a result of enzyme reaction. For example, the conductivity of polyaniline is influenced by pH and potential [195]. The conductivity tends to decrease with the increase in pH at a given potential. Similarly at a given pH the polymer conductivity is a function of applied potential.

In a polyaniline-glucose oxidase system [194], the sensor responded as a change in resistance caused by the change in the concentration of glucose (upto 10 mM). The resistance of the polymer decreased with increase in concentration of glucose. This change in resistance was reversible and reproducible. The sensor was shown to be stable for more than 14 independent measurements with a standard deviation of less than 10%. Conducting polymers have been widely applied in developing the glucose sensor; some of these examples are given in Table 1.3.

Microelectrodes have also been used to prepare biosensors. A penicillin sensor [99] has been reported, where a microarray electrode was coated with polypyrrole. The electrical conductivity of the polymer membrane increased as a result of enzyme reaction, which acidifies the polypyrrole membrane. The conductivity changes were detected by the increase in the current between the arrays at constant applied voltage.

A microarray electrode coated with pyrrole-N-methyl pyrrole co-polymer containing diaphrose showed an on/off response upon addition of NADH, because diaphrose catalyses the reduction of polymer by NADH from a conductive to an insulating state [196].

Table 1.3 *Conducting polymer based amperometric glucose sensor*

Polymer	Mode of immobilisation	Analyte	Linear range/ (LOD)	Reference
PPy	GOx adsorbed after polymerisation	glucose	2.5-30 mM	198
PPy	incorporated during electropolymerisation	glucose	10^{-3} to $1x10^{-1}$ M	199
PPy	GOx immobilised via post-polymerisation functionalisation	glucose	(5 µM)	200
PPy	GOx adsorbed on PPy tubules	glucose	0.1-250 mM	201
PPy	GOx functionalised on amino substituted pyrrole	glucose	(5 mM)	202
PPy	GOx immobilised by physical ion exchange	glucose	(5 mM)	203
PAn	GOx incorporated during polymerisation	glucose	10^{-4} to $5x10^{-3}$ M	30
PAn	GOx incorporated during polymerisation	glucose	0.1 mM to 1 mM	204

PPy=polypyrrole, PAn=Polyaniline, GOx=glucose oxidase

An enzyme switch responsive to glucose was prepared by immobilising glucose oxidase in an electropolymerised film of poly(1,2-diaminobenzene) grown on top of a polyaniline film. Tetrathiofulvalene (TTF) was used as a redox mediator to shuttle the charge between the enzyme and the conducting polymer. On the addition of glucose the current increased rapidly [197].

These sensor concepts can be utilised to prepare inexpensive chips for sensing a range of biomolecules.

1.5.3 Gas Sensors

The electronic conductivity of conducting polymers is dependent on their electrochemical state [205]. The variation of doping level results in conductivity change, and this property of conducting polymers has been utilised to develop gas sensors.

Polypyrrole sensors for ammonia and hydrazine have been reported [206]. The polymer sensor was prepared by dipping a non-conducting material (acrylic strips) in a colloidal suspension of polypyrrole. The resistance of the thin polymer film increased reversibly upon exposure to hydrazine or ammonia vapours (0.1 $\mu g\ cm^{-3}$ of ammonia can be detected with $1cm^2$ area of sensor).

Miasik et al. [207] have prepared gas sensors by covering interdigitated electrodes with polypyrrole for the detection of NH_3, NO_2 and H_2S gases. The resistance of the PPy increased upon exposure to ammonia; an electron donating gas, which reduces the carrier density in oxidised polymer. In contrast, NO_2 withdraws electrons and increases conductivity. Yoneyama et al. [208-210] have reported that the prior reduction of the PPy film can improve gas sensitivity to electron-acceptor gases such as PCl_3, SO_2 and NO_2 at room temperature. The FT-IR spectral analysis has revealed that the NO_2-sensing mechanism is based on the chemical doping by NO_2 to give dopant anion NO_2^- (Equation 1.5):

$$PPy + NO_2\ (gas) \rightleftharpoons PPy^+ /NO_2^- \qquad .....1.5$$

where PPy symbolises the dedoped polypyrrole and PPy^+ the oxidised polypyrrole.

Bartlett and Ling-Chung [211] have employed polypyrrole, poly-N-methyl pyrrole, poly-5-carboxyindole and polyaniline as sensors for vapours of methanol, ethanol, toluene, acetone and ether. Sensor electrodes were prepared by the electrochemical deposition of a particular polymer between a gap of 12μm between two gold electrodes [212]. Upon exposure to the vapours, the oxidised polymer showed rapid and reversible conductivity changes. The polymer conductivity decreases reversibly upon exposure to the organic vapours. This could be due to the reduction as well as the change in the moisture content of the polymer film. The most stable and reproducible response was reported for poly-5-carboxyindole. A gas sensor composed of polythiophene film [213] when exposed to NO showed an increase in conductivity by more than two orders of magnitude, while conductivity was little affected by CO and N_2O.

Wrighton et al. [214] modified microelectrode arrays by coating electrodes with platinised poly(3-methylthiophene) to build up micro electrochemical 'transistors' that operated in solution according to electrochemical redox reactions. Poly(3-methylthiophene) was impregnated with metallic Pt in order to make conducting polymer responsive to H_2 and O_2, the oxidising and reducing species. The conducting polymers acted as electrical conductors and in this way H_2 and O_2 can be detected. To detect water vapours [215] polyaniline based microelectrochemical transistors were developed that can operate in the solid state by using a poly(vinyl alcohol)/phosphoric acid solid-state electrolyte.

The nature of interactions in gas sensors is not fully known; redox processes, acid-base reaction, solvation or aromatic charge-transfer complexes could contribute simultaneously. However, the specificity of the sensor can be improved by introducing specific interacting groups, for example, bromo-substituted thiophene has been reported to be specific to bromine vapours [216,217].

1.6 Electrochemical Techniques

1.6.1 Cyclic voltammetry

Cyclic voltammetry is a versatile electrochemical technique. It is often the first technique used in electrochemical characterisation. It provides initial information about the heterogeneous redox reactions.

In cyclic voltammetry the potential is scanned linearly from an initial potential (E_i) to a final potential (E_f) and then back to the initial value, the resulting current is measured. The triangular potential waveform is shown in Figure 1.5.

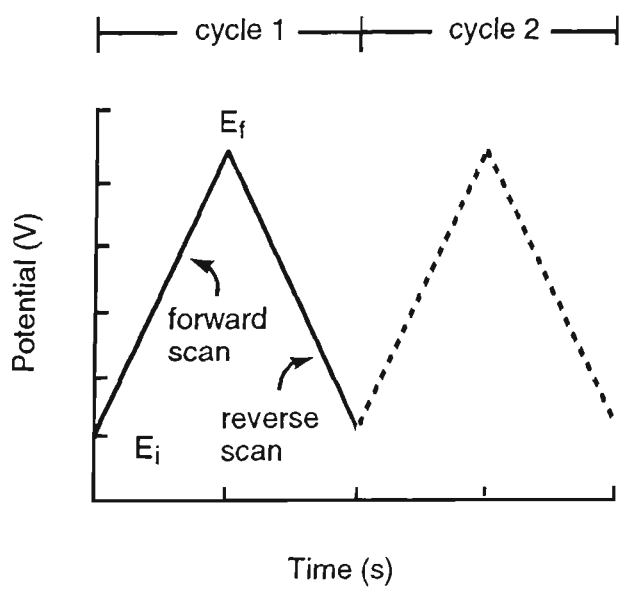

***Figure 1.5**: A triangular potential waveform for cyclic voltammetry.*

The resultant voltammogram is the display of the resulting current (vertical axis) versus applied potential (horizontal axis). The main parameters of a cyclic voltammogram are:

i) the anodic peak current (i_{pa}),

ii) the cathodic peak current (i_{pc}),

iii) the anodic peak potential (E_{pa}), and

iv) the cathodic peak potential (E_{pc}),

A typical voltammogram is shown in Figure 1.6. The voltammogram obtained at a Pt working electrode was recorded in a solution containing 6.0mM $K_3Fe(CN)_6$ in 1.0M KNO_3 [218]. The redox couple involved here is $[Fe^{III}(CN)_6]^{3-}/[Fe^{II}(CN)_6]^{4-}$. A redox couple where both redox species are stable and rapidly exchange electrons with the electrode is termed as an electrochemically reversible couple.

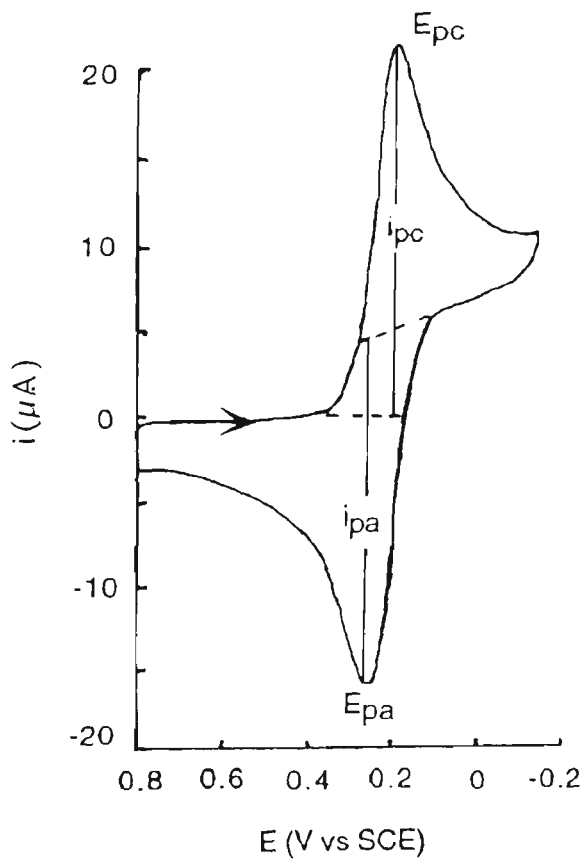

Figure1.6: *Cyclic voltammogram of 6 mM $K_3Fe(CN)_6$ in 1 M KNO_3. Scan rate=50 mV/s. Platinum electrode area=2.554 mm^2 [218].*

E_i is selected where no electrolysis of electroactive species occurs. When the potential is scanned negatively, $[Fe^{III}(CN)_6]^{3-}$ is reduced (Equation 1.6) and a cathodic current (ipc) is produced. On reversing the scan anodically $[Fe^{II}(CN)_6]^{4-}$ is oxidised producing an anodic current (ipa).

$$[Fe^{III}(CN)_6]^{3-} + e^- \rightleftharpoons [Fe^{II}(CN)_6]^{4-} \qquad \text{..... 1.6}$$

The ip can be measured by extrapolating the base line current as given in Figure 1.6. The formal reduction potential E^o is the mean value of E_{pa} and E_{pc} (Equation 1.7):

$$E^o = \frac{E_{pa} + E_{pc}}{2} \qquad \text{..... 1.7}$$

The number of electrons (n) transferred in the electrode reaction for a reversible couple can be determined from the separation between the peak potentials (Equation 1.8):

$$\Delta E_p = E_{pa} - E_{pc} = \frac{0.058}{n} \qquad \text{.....1.8}$$

Therefore a one electron process, such as the oxidation of Fe^{II} to Fe^{III}, ΔE_p should be 0.058V.

The peak current for a reversible system is described by the Randles-Sevcik Equation (Equation 1.9) for the forward sweep of the first cycle:

At 25 °C, $ip = 2.69 \times 10^5 \, n^{3/2} \, AD^{1/2} \, C \, v^{1/2}$ 1.9

where ip= peak current (amperes)

n=electron stoichiometry

A= electrode area (cm^2)

C= concentration (mol/cm^3)

v= scan rate (V/s)

D= diffusion coefficient (cm^2/s)

According to this equation, i_p increases with $v^{1/2}$ and is directly proportional to concentration.

With microelectrodes the cyclic voltammogram obtained differ significantly from those obtained on conventional size electrodes (Figure 1.7).

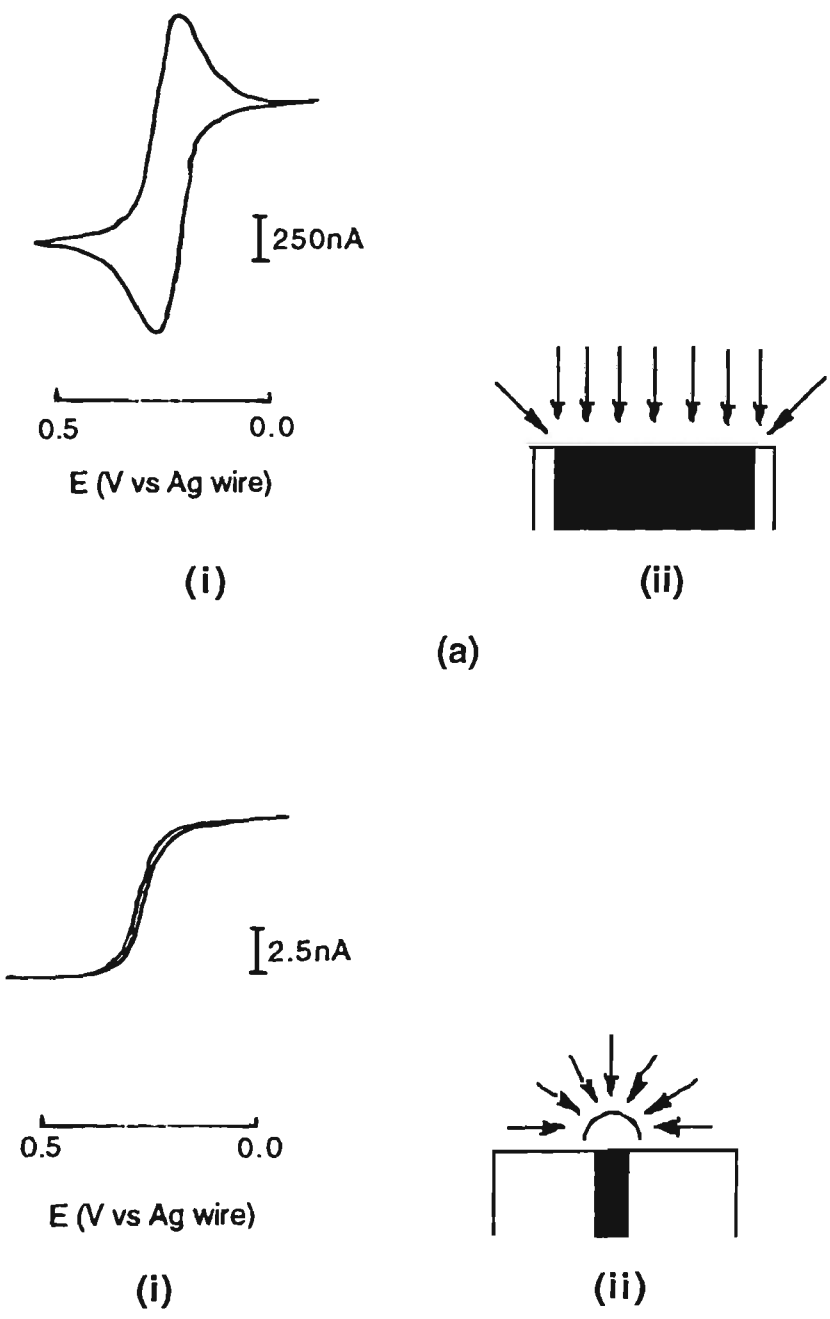

Figure 1.7 : *Cyclic voltammograms and diffusion layer profiles (a) at a conventionally-sized electrode (2 mm) (i) CV, (ii) planar diffusion and (b) at an ultramicroelectrode (10 µm) (i) CV, (ii) radial diffusion . Solution : 1mM ferrocene in 0.1 M $TBAPF_6/CH_3CN$. Scan rate =50 mV/s [219].*

This difference in cyclic voltammograms is due to the difference in the rate of mass transport by diffusion. At macroelectrodes the planar diffusion layer is due to the mass transport perpendicular to the electrode. This results in a peak shape voltammogram and for a reversible redox process, the peak current follows the Randles-Sevcik Equation. On the other hand for microelectrodes the mass transport is rapid, follows a radial diffusion and becomes diffusion limited. This produces a steady state voltammogram. In microelectrodes the limiting current is given by Equation 1.10.

$$i_{lim} = 4n\,FrDC \qquad \text{.....1.10}$$

where i_{lim} is the limiting current (A), F is the Faraday constant, and r is the electrode radius (cm). Unlike conventional size electrodes, currents obtained at microelectrodes are not geometry dependent.

As a result of radial diffusion the mass transport is greatly enhanced to and from the electrode surface. Therefore, the current density at a microelectrode is much higher compared to a conventionally sized electrode. In addition, background currents are smaller on microelectrodes under steady state conditions, which improves the ratio of Faradaic to non-Faradaic current; where Faradaic current is dependent on analyte concentration.

1.6.2 Chronopotentiometry

Chronopotentiometry consists of applying a constant current and monitoring the potential of the electrode with time (Figure 1.8). The constant current applied to the electrode causes the oxidation/reduction of the electroactive species at constant rate. The potential of the system

changes accordingly to maintain the rate of reaction. In chronopotentiometry the amount of charge applied can be controlled by maintaining the current for the required time. The amount of charge is obtained by the relationship: Q=it.

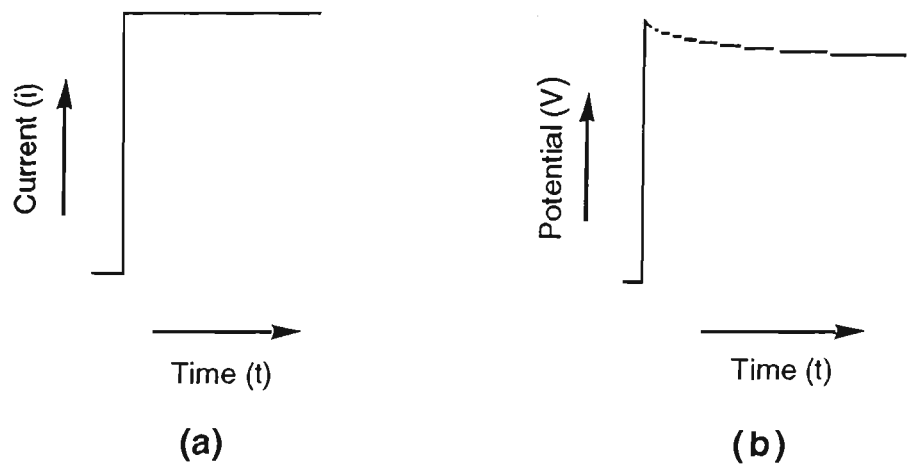

Figure 1.8: *(a) Current waveform, (b) Chronopotentiograms (potential vs time response).*

1.6.3 Chronoamperometry

Chronoamperometry consists of stepping the potential from an initial value (E_i) to the final value(E_f) instantaneously. The resultant current is recorded as a function of time. A typical potential step waveform and a typical current response are shown in Figure 1.9.

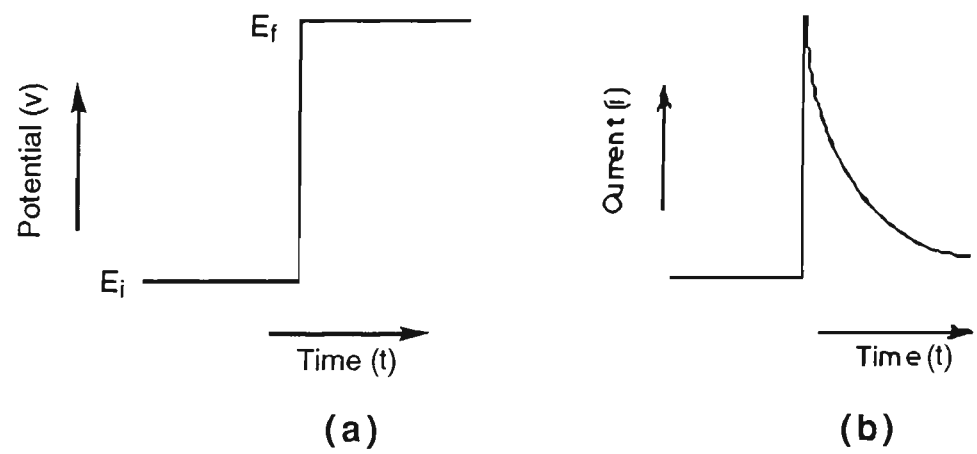

Figure 1.9: *(a) A typical potential step waveform for chronoamperometry. (b) Chronoamperogram (current vs time response).*

E_i is selected as the potential where no redox process takes place at the electrode surface (i=0). E_f is a potential where diffusion-controlled oxidation/reduction takes place. As a result of stepping the potential from E_i to E_f a large current flow takes place which decays as the depletion of electroactive species at the electrode takes place due to electrolysis. For a planar electrode the current response is described by the Cottrell equation (Equation 1.11):

$$i = (nFAD^{1/2} C)/ (\pi^{1/2} t^{1/2}) \qquad .....1.11$$

where, i is current (amperes), n is number of electrons per molecule (eq/mol), F is Faraday's constant (96,485 C/eq), A is electrode area (cm^2), C is the concentration (mol/cm^3), D is diffusion coefficient (cm^2/s) and t is time.

1.6.4 Normal Pulse Voltammetry

Normal pulse voltammetry (NPV) consists of applying a pulse waveform and measuring a current at the end of the pulse. The pulse waveform consists of a sequence of pulses with increasing pulse potentials. The response is the plot of sampled current versus pulse potential. A part of the normal pulse excitation waveform and response signal is shown in Figure 1.10.

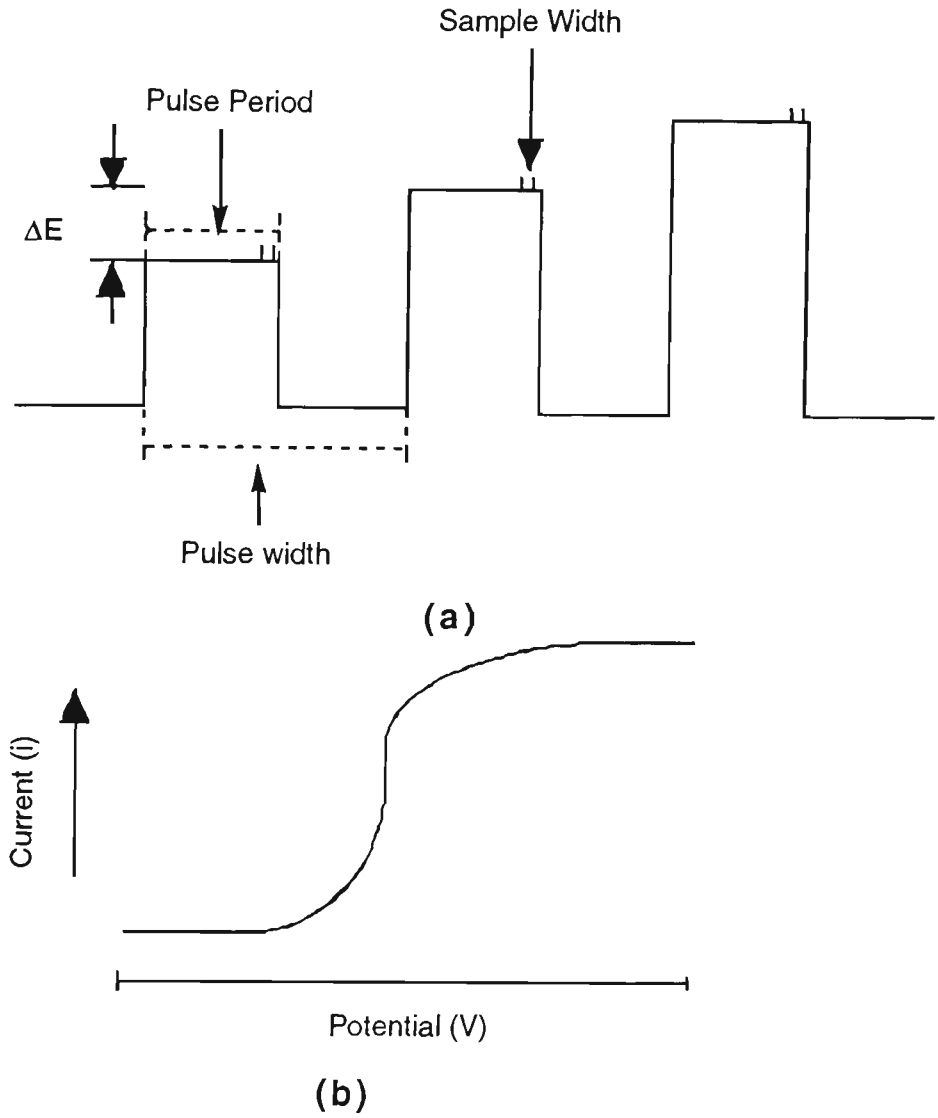

Figure 1.10 *: (a) A part of pulse waveform for NPV. (b) Typical response for NPV.*

1.6.5 Electrochemical Quartz Crystal Microbalance

The electrochemical quartz crystal microbalance (EQCM) is a very sensitive technique. It can probe the mass changes at the nanogram level. EQCM has been used to monitor the mass changes during polymerisation and subsequently mass changes during electrochemical studies of polypyrroles.

The EQCM consists of a thin quartz crystal disc sandwiched between two metal electrodes (gold, platinum, aluminium). These electrodes maintain an alternating electric field across the crystal, which causes a vibrational

motion of the crystal at its resonant frequency. This resonant frequency of the crystal is sensitive to mass changes of the crystal. The ability to sense minute mass changes has proven to be very useful in examining the electrochemical processes involving thin films [220].

The mass changes on thin rigid metallic films in vacuum can be monitored by measuring the changes in the resonant frequency (f) of an oscillating quartz crystal by using the Sauerbrey equation (Equation 1.12) [221]:

$$\Delta f = -f_o^2 \, \Delta m / A \, (\rho_q \, \mu_q)^{1/2} \qquad \text{..... 1.12}$$

where f_o=resonant frequency of the unloaded quartz crystal sandwiched between two metallic electrodes, Δm= change in mass in grams, A=surface area of electrode or film, ρ_q = density of the quartz =2.648 g cm^{-3}, μ_q =shear modulus of quartz = 2.947 x 10^{11} dynes cm^{-2}.

In liquid the resonant frequency of the quartz shifts by a constant frequency shift determined by the viscoelastic properties of the liquid overlayer given by Equation 1.13 [222]:

$$\Delta f = -f_0^{3/2} \, (\rho_1 \, \eta_1 / \pi \, \rho_q \, \mu_q)^{1/2} \qquad \text{.....1.13}$$

where ρ_1 and η_1 are the density and absolute viscosity of the overlayer, respectively. This permits one face of the quartz crystal to be used as the working electrode to monitor the mass changes associated with the electrochemical processes.

1.7 Detection in Flowing Solutions

The technique used to gather the information on conducting polymers is Flow Injection Analysis (FIA) or High Pressure Liquid Chromatography (HPLC). In the FIA technique, a small sample (25-50 μL) is injected into a carrier solution continuously flowing through the system. The sample plug is transported to the detector by the carrier solution where the analytical signal is generated. Technically, the HPLC system is similar to FIA except a column is introduced between injector and detector to separate the components of the analyte mixture. In FIA the signal is a sharp asymmetric peak [223]. The peak height is the analytical measurement and is proportional to the concentration of the test species. FIA is considered to be a simpler technique than batch methods. The advantages of the flow method over the batch experiment include improved reproducibility, lower cost and easy sample handling. The flow parameters studied to evaluate the detector efficiency in flowing solutions are:

(1) **Sensitivity** (S). The ratio of the change in the detector signal (ΔR) to the change in sample concentration (Δc) at a given point in the range of sample concentrations is given by Equation 1.14:

$$S = \frac{\Delta R}{\Delta c} \qquad \text{.....1.14}$$

or sensitivity is the slope of the calibration plot .

(2) **Noise.** In electrochemical flow systems, noise comes from chemical, electronic, hydrodynamic and environmental sources. Noise is an undesirable part of the signal. Most types of noise are directly proportional to the surface area of the working electrode. The S/N (signal-to-noise ratio)

increases by decreasing the electrode area. For electrochemical detection it is required to have S/N as high as possible.

(3) **Limit of detection** (LOD). The limit of detection is related to the sensitivity and noise for a given concentration. The detection limit can be defined in terms of the multiple (k) of an estimate of the standard deviation (s) of the noise [223]. The detection limit improves with increasing signal-to-noise ratio (Equation 1.15).

$$C_{lim.det.} = \frac{ks}{S} \qquad \text{..... 1.15}$$

where S is sensitivity

(4) **Selectivity** is defined as the ability of the sensor to respond to a particular substance without responding to the interferents present in the test system.

5) The **linear dynamic range** should be broad with sufficient sensitivity and precision at both extremes.

(6) Frequent calibration is undesirable with invasive sensors. However, when a sensor is used in FIA, calibration can easily be done at any time.

7) Miniaturisation of the sensor is desirable for portable sensors, where the sensor could be battery operated and have little power consumption.

8) Low sensor cost is also important from the marketing point of view.

1.7.1 Mode of Detection in Flowing Solutions

1.7.1.1 Amperometry

Amperometric detection is based on applying a constant potential (DC) to the working electrode and measuring the resultant current as the compound undergoes oxidation or reduction. Analyte concentration is determined by measuring the electronic current produced from the analyte during electron transfer. In amperometry the electrodes are in stirred or in flowing solutions.

If the applied potential is gradually increased and the resultant current is measured. The current obtained from the electrochemical reaction is plotted as a function of applied potential to produce a hydrodynamic voltammogram (HDV). For analysis the potential is held at the limiting current region of the species. In the limiting current region the reaction is diffusion controlled. The potential applied and the hydrodynamic voltammogram are shown in Figure 1.11.

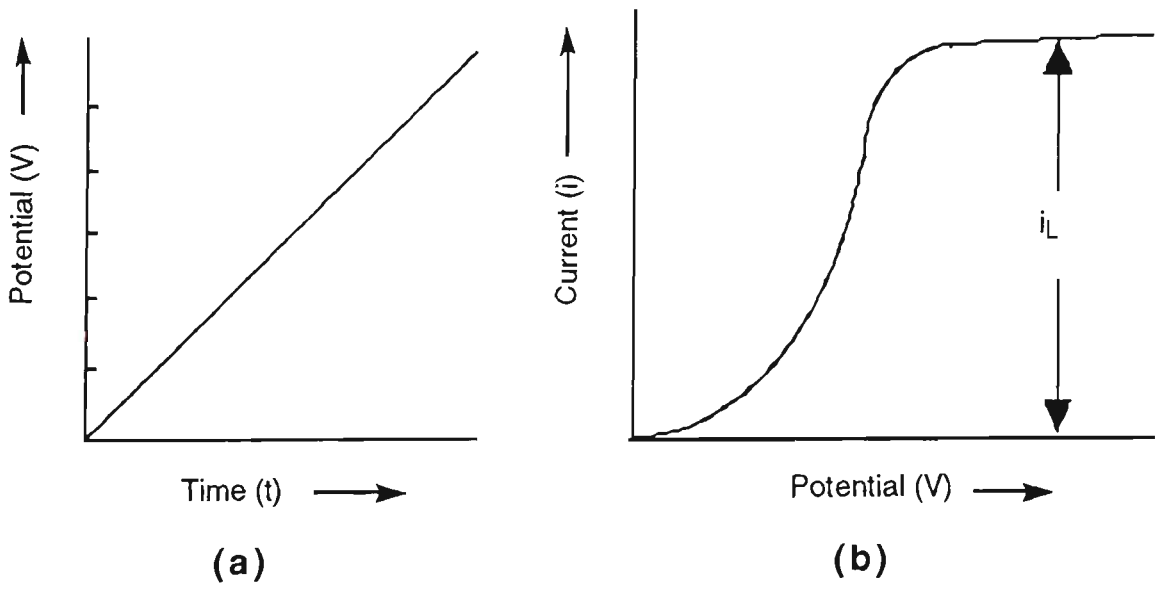

Figure 1.11: *(a) Potential applied with time and (b) hydrodynamic voltammogram showing limiting current* i_L.

The selection of E_{app} is very important, so that the species of interest are detected with optimum selectivity and sensitivity. The E_{app} can be obtained from the HDV. Amperometry is commonly used for easily oxidised species such as phenols, catecholamines, cyanide and sulfide.

1.7.1.2 Pulsed Integrated Amperometry

Integrated amperometry is a more advanced technique. Integrated amperometry consists of applying a multi-potential waveform to the working electrode. The potential waveform consists of a pulse or a scanned potential. The current can be integrated anywhere along the potential pulse or scan. The two types of waveforms are shown in Figure 1.12.

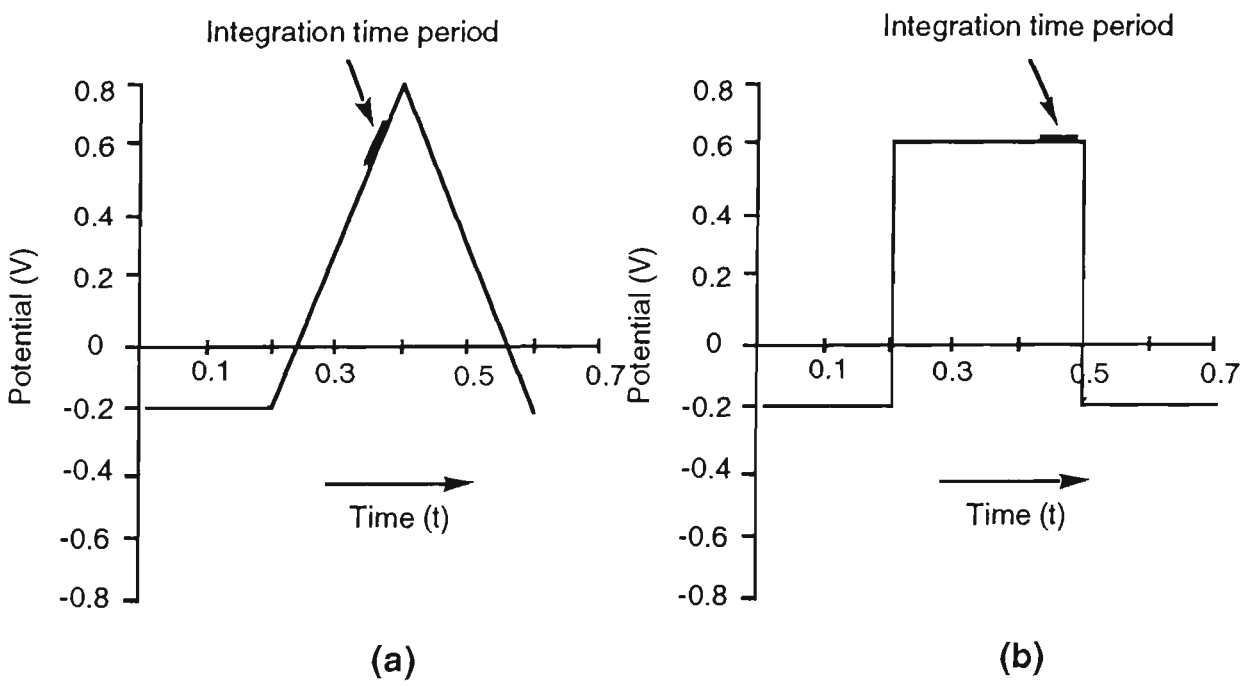

Figure 1.12: *(a) Scanned potential waveform and (b) pulsed potential waveform for integrated amperometry.*

1.8 Aims and Approach of the Project

The ease with which the conducting polymers can modify the metal electrode surfaces and the electrochemical properties associated with these polymers makes them suitable and attractive candidates for application in an electroanalytical detection system. The work presented in this thesis covers several aspects of electrochemical detection in flowing solutions. The order of presentation is given below.

The synthesis of conducting polymer modified electrodes is described in Chapter Two. Here, two approaches were applied to modify the electrode system. Firstly, the synthesis of polymers with a range of counterions. Secondly, derivatised monomers were used to prepare polymers on platinum substrates. The electrochemical characterisation of these electrodes was carried out by cyclic voltammetry. The chiral polymers prepared by both of the above mentioned approaches were characterised by the use of the electrochemical quartz crystal microbalance (EQCM) in order to investigate the mass changes associated with the electrochemical processes.

The work in Chapter Three addresses the detection of amino acids on conducting polymer electrodes, without any prior derivatisation of amino acids, using electrochemical detection in flow injection analysis. The work was aimed at developing simple, selective and sensitive electrochemical detection system as compared with existing methods. The effect of the electrochemical parameters for DC amperometry and pulsed potential analysis were investigated. The effect of polymer composition on the selectivity was determined by varying the counterions incorporated.

In Chapter Four the detection of amino acids was extended to conducting polymer coated microelectrodes in FIA. Here we focus on further improving the selectivity and LOD for amino acids. Microelectrodes are advantageous because they provide an increase in the faradaic-to-charging current ratio which results in an improvement in the limit of detection. In addition to that, with microelectrodes a background eluent of low electrolyte concentration could be used which minimises the interferences in FIA.

Chapter Five focuses on the development of conducting polymer sensors for detection of halogenated organic acids. Haloacetic acids are carcinogenic and health hazards even at low concentration levels. The work in this section concentrated on developing a method which is simple, does not require derivatisation, and also have low detection levels. To achieve this objective, polymer coated microelectrodes were applied. The electrochemical detection was carried out in suppressed mode subsequent to anion exchange separation of organic acids. The response of the conducting polymers was optimised by considering the polymer composition, effect of applied potential, and current sample point. The results obtained were compared with those obtained with conductimetric detection.

The overall conclusion is presented in Chapter Six.

CHAPTER 2

SYNTHESIS AND CHARACTERISATION OF SELECTED CONDUCTING POLYMER SENSORS

2.1 INTRODUCTION

The development of chemically modified electrodes (CMEs) has created a powerful detection method in FIA and liquid chromatography (LC). The development of new materials to modify electrode surfaces can greatly expand electrochemical detection. Conducting polymers are such materials, as tailor made surfaces can be prepared by incorporating desired species during electropolymerisation [15].

The electrochemical approach for making electroactive/conductive films is very versatile and it provides a facile way to vary the properties of the polymer films [16]. The controlled electrochemical conditions can produce polypyrroles with good electroactivity, adhesion to the electrode surface and stability both mechanical and chemical [15]. Polymer properties including conductivity, electroactivity and stability can be manipulated by choosing appropriate electrolyte, solvent, monomer concentration, temperature, current and potential applied during synthesis [45,49,123,50-67].

Synthesis methods are designed and implemented to improve the properties of the polymer for specific technological applications. For example, the potentiometric sensors for chlorate prepared from 0.05-0.1 M pyrrole and 0.1 M chlorate were found to exhibit better film electrode response. Incomplete electrode surface coverage resulted from lower pyrrole or chlorate concentrations. A decrease in the slope of the Nernstian potentiometric response was observed for such electrodes compared with the electrodes prepared using the above monomer solution.

Ward and Smyth [188] deposited the polymer (at Pt wire) in a flow cell using 0.5M pyrrole and 1.0M sodium chloride. The potential was cycled at 20mV/s

between -1.0 mV and 0.9 mV, for three complete cycles. The higher scan rates, 100 and 50 mV/s, deteriorated the films produced. Under these higher scan rates, thin, patchy and less stable polymer films were obtained.

For polypyrrole dodecylsulfate sensor, the best conditions were 0.25 M pyrrole and 0.05 M dodecylsulfate in acetonitrile-water (80+20, v/v) at Pt; potential applied was 1.4 V for 5 minutes followed by potential sweep between 0.7 V and -1.3 V. The film formation was completed by applying 0.7V for 5 minutes. The films prepared from aqueous solution did not give reproducible response in cyclic voltammetry. The variation of the acetonitrile-water solution composition indicated that more reproducible responses were obtained when the polymer was prepared in solution containing more than 70% acetonitrile [189].

The examples given above as well as others [28,200,224-226] show that the properties of the resulting polymer are dependent on the polymerisation conditions. These properties can be manipulated by varying any of the polymerisation parameters.

A detailed description of the dependence of the chemical and electrochemical properties of conducting polymers on the polymerisation parameters have also been outlined in Chapter 1.

2.1.1 Aims and Approach of this Chapter

This Chapter describes the synthesis and characterisation of some conductive/electroactive polymers. The work is divided into two sections. The first part covers the synthesis of conducting polymer modified electrodes with a range of counterions and monomers on platinum

substrates and electrochemical characterisation of these electrodes by cyclic voltammetry. The second part comprises the deposition and characterisation of polymers with chiral additives, with special attention paid to the use of the electrochemical quartz crystal microbalance (EQCM) to investigate the mass changes associated with oxidation/reduction of the polymer. Since extensive literature is available on EQCM of polymers with achiral dopants [79,157,159,160,227], our aim was to characterise new types of chiral polymers with EQCM. To our knowledge such studies have not been carried out before.

For the first part of this work, pyrrole (Py) and 3-methylpyrrole-4-carboxylic acid (MPC) were selected to represent non-functionalised and functionalised monomers respectively. Pyrrole can be polymerised from aqueous electrolytes which means that the choice of counterions is enormous, and also polypyrrole is one of the most stable conducting polymers [228]. The counterions to be incorporated in polypyrrole belong to several categories:
(i) small univalent inorganic anions such as chloride (Cl^-).
(ii) organic sulfonated anions of different sizes, and molecular functionality such as *p*-toluene sulfonate (PTS^-), (1S)-(+)-10-camphorsulfonate ($(+)\text{-}CSA^-$), 4-hydroxybenzene sulfonate ($HBSA^-$), 3-sulfobenzoic acid (SBA^-), and dodecyl sulfate (DS^-).
(iii) polyelectrolytes including polyvinylsulfonate (PVS^-).

The functionalised monomer (I) with carboxylic acid group substitution on the pyrrole ring is expected to give an electronically conducting cation-exchange polymer with increased polarity and hydrogen bonding capabilities.

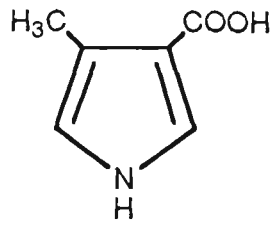

(I)

Therefore the polymer derived from 3-methylpyrrole-4-carboxylic acid is expected to have cation exchange as well as anion exchange properties due to incorporation of electrolyte anions during polymerisation. This polymer is expected to have some degree of self doping by $-COO^-$ [229]. Cation exchange properties of the polymer have also been shown by incorporation of a range of counterions [230]. PMPC cannot be electropolymerised from aqueous solutions as the monomer is insoluble in water [229,231], which restricts the choice of counterions that can be incorporated into the polymer. Here the dopant anions are also categorised into two groups:

(i) small inorganic anions such as perchlorate (ClO_4^-) and hexafluorophosphate (PF_6^-).

(ii) organic sulfonated anions including *p*-toluene sulfonate (PTS^-) and (1S)-(+)-10-camphorsulfonate, ((+) CSA^-).

A constant current approach was used to prepare the polymer film, and the polymer was characterised by cyclic voltammetry in a conventional cell.

For the second part of this work, EQCM analysis, chiral conducting polymers were prepared by the following two approaches:-

(i) incorporating a chiral dopant ion into polypyrrole during electrosynthesis. The counterions include (+) CSA^- (II) and (-) CSA^- (III).

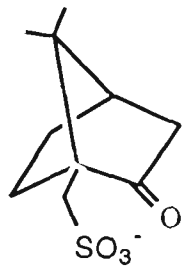

(II)

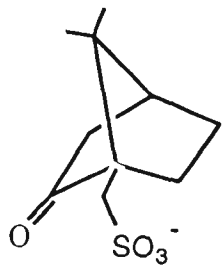

(III)

(ii) from chiral monomers N-[(1S)-(+)-1-phenylethyl] pyrrole (IV) and N-[(1R)-(-)-1-phenylethyl] pyrrole (V). The chiral centre* in (IV) and (V) is directly attached to the N of the pyrrole ring.

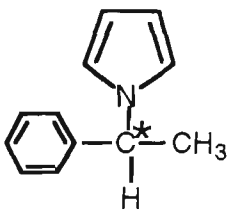

(IV)

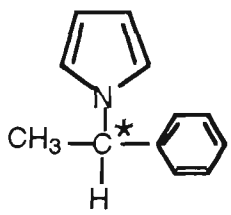

(V)

EQCM has been used to study mass changes during polymerisation and during oxidation/reduction of the polymer after synthesis.

2.2 EXPERIMENTAL

2.2.1 Reagents and Solutions

All reagents used were analytical reagent (AR) grade unless otherwise stated. Laboratory reagent (LR) grade pyrrole was obtained from Sigma. Pyrrole was distilled and kept in a cool dry place under nitrogen. MPC was synthesised in our laboratory by a method described previously [232,233]. N-[(1S)-(+)-1-phenylethyl] pyrrole; $[\alpha]_D$ = 22.5 (1% in acetonitrile), and N-[(1R)-(-)-1-phenylethyl] pyrrole; $[\alpha]_D$ = -23.0 (1% in acetonitrile), were prepared by the reaction of (S)-(+)-α-methyl benzylamine or (R)-(-)-α-methyl benzylamine with 2,5-dimethoxytetrahydrofuran in glacial acetic acid, respectively.

(1S)-(+)-10-camphorsulfonic acid, (1R)-(-)-10-camphorsulfonic acid, tetrabutylammonium hexafluorophosphate ($TBAPF_6$), tetrabutylammonium perchlorate (TBAP), 3-sulfobenzoic acid sodium salt (SBA) and 4-hydroxybenzenesulfonic acid sodium salt (HBSA) obtained from Aldrich, sodium chloride (NaCl) obtained from BDH; sodium dodecyl sulfate (SDS), *p*-toluene sulfonic acid (PTSH), and polyvinylsulfonic acid (PVS, Mr 900 - 1000) sodium salt (25% (w/v) in water) obtained from Sigma; and *p*-toluene sulfonic acid sodium salt (PTSNa) obtained from Merck were all used as received. All solutions were prepared using AR grade acetonitrile (Malinckrodt) or deionised Milli-Q water.

2.2.2 Instrumentation

An in-house built galvanostat was used for constant current work, a CV-27 Voltammograph (Bioanalytical Systems (BAS)) and Princeton Applied Research (PAR) model 363 galvanostat/potentiostat with home made pulse generator were used for cyclic voltammetric and pulsed potential analysis. Data were recorded using a MacLab (Analog Digital Instruments-ADI) with Chart v3.2.8 software system and Macintosh computer. Data manipulation was also carried out using the Igor software package (Wavemetrics).

The working electrode was a platinum disc (3mm diameter) which was polished on 0.3μm and 0.05μm alumina (Leco) respectively and ultrasonicated for 1 minute in Milli-Q water prior to electropolymerisation. A platinum plate (2.5 cm x 1.3 cm) working electrode was used to prepare samples for elemental analysis, and polymer films were prepared on ITO glass (4.2cm x 1.2cm) for spectroscopic analysis. A platinum wire or RVC (Reticulated Vitreous Carbon) was the auxiliary electrode and the reference electrode was a BAS Ag/AgCl or Ag/Ag^+ with an in-house built salt bridge.

The Electrochemical Quartz Crystal Microbalance (EQCM) was home made. The schematic of the EQCM circuit is shown in Figure 2.1. The electronic circuitry employed for the home made EQCM has been described [234]. A gold coated quartz crystal was employed as working electrode. 10 MHz AT-cut quartz crystals were obtained from International Crystal MFG.CO.,OK.,U.S.A. The surface area of the crystal was 0.24 ± 0.01 cm^2. The crystal was mounted in the electrochemical cell with silicone sealant as shown in Figure 2.2. The auxiliary electrode was kept parallel to the working electrode for even and reproducible mass collection on the crystal. The EQCM system was enclosed in a Faraday cage.

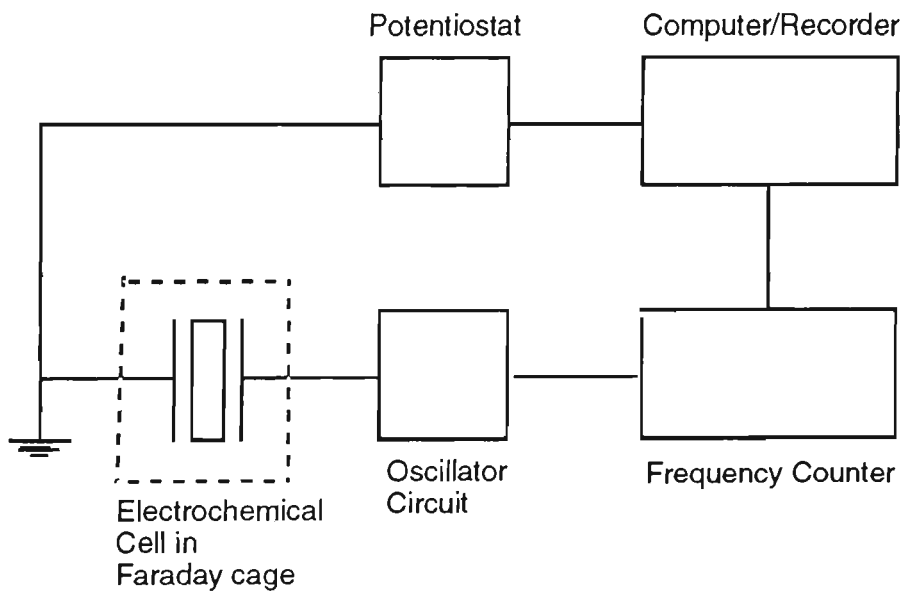

Figure 2.1: *Block diagram of EQCM Apparatus.*

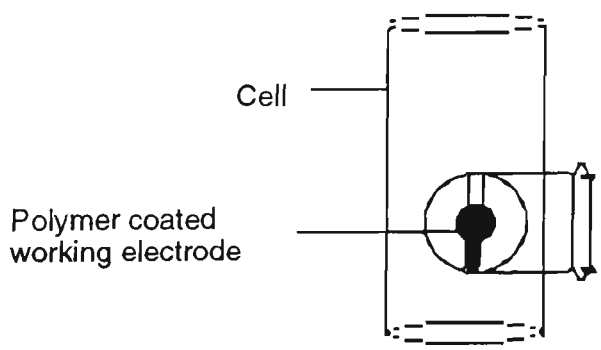

Figure 2.2: *EQCM cell with crystal.*

Circular dichroism (CD) spectra were measured using a Jasco-500C spectropolarimeter.

Elemental analysis of the films was carried out by the Microanalytical Service at the University of Queensland.

2.2.3 Polymerisation Procedure

The monomer solution consisted of 0.2 M pyrrole and 0.05 M electrolyte, except for chloride (0.5 M) and PVS (0.13%, w/w). All solutions were purged with nitrogen for 5 minutes before polymerisation.

The polymerisation solution for MPC consisted of 0.1 M MPC and 0.1 M TBAP in acetonitrile. Polymerisation was carried out galvanostatically.

2.2.4 Electrochemical Characterisation by Cyclic Voltammetry

After polymerisation, the polymer electrodes were rinsed with copious amounts of water before analysis, and redox scans were performed with the same cell and electrode configuration for all polymer electrodes characterised. The electrolyte medium was deoxygenated with nitrogen for 5 minutes. All scans were at the speed of 50 mV/s and started from a positive potential in negative direction.

2.2.5 Electrochemical Quartz Crystal Microbalance Analysis

For EQCM analysis of chiral polypyrrole film formation, monomer solution containing 0.2 M pyrrole and 0.05 M CSA((+) or(-)) was employed. The

polymerisation solution of phenylethyl pyrrole contained 0.1 M monomer and 0.1 M TBAP prepared in acetonitrile. The electrochemical analysis was carried out in 0.1 M $NaNO_3$ as well as in the corresponding dopant ion solutions.

Mass changes (Δm, in μg) were determined from observed resonance frequency shifts (Δf, in kHz). For our EQCM apparatus an average mass sensitivity of 0.97 Hz ng^{-1} was obtained (determined by calibration using the silver deposition method [235]). A crystal having a projected area of 0.24 cm^2 should have a mass sensitivity of 0.23 Hz ng^{-1} cm^{-2} (proportionality factor K) in the Saurebery Eqn. (2.1) shown below.

$$\Delta f = K\Delta m \qquad \text{.....(2.1)}$$

2.3 RESULTS AND DISCUSSION

2.3.1 Preparation of Polypyrrole

The polymerisation conditions were investigated using 0.20 M pyrrole with 0.05 M CSA^- counterion. Polymer electrodes were prepared using the constant current method to ensure the maximum control on the polymerisation process. The current densities applied were 0.50-5.0 mA/cm^2. The polymerisation process resulted in the deposition of a black film on the electrode surface which was adherent to the electrode. The polymerisation process can be represented by the following equation:

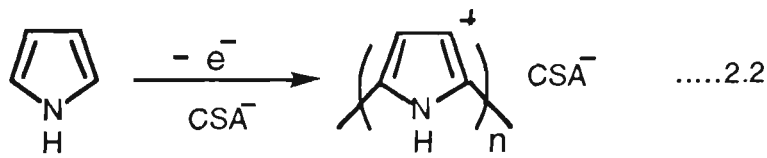

.....2.2

n=no.of monomer units

The deposition process was monitored by recording chronopotentiograms. Figure 2.3 shows the chronopotentiograms recorded at different current densities. The observed monomer oxidation potential was between 0.60-0.75V for different current densities applied and the potential settled to a constant value after an initial sharp rise. The polymerisation potential is an indication of the conductive nature of the polymer formed. If the potential attained during polymer growth remains constant or reduces throughout the polymerisation process, it indicates that such polymers are conductive.

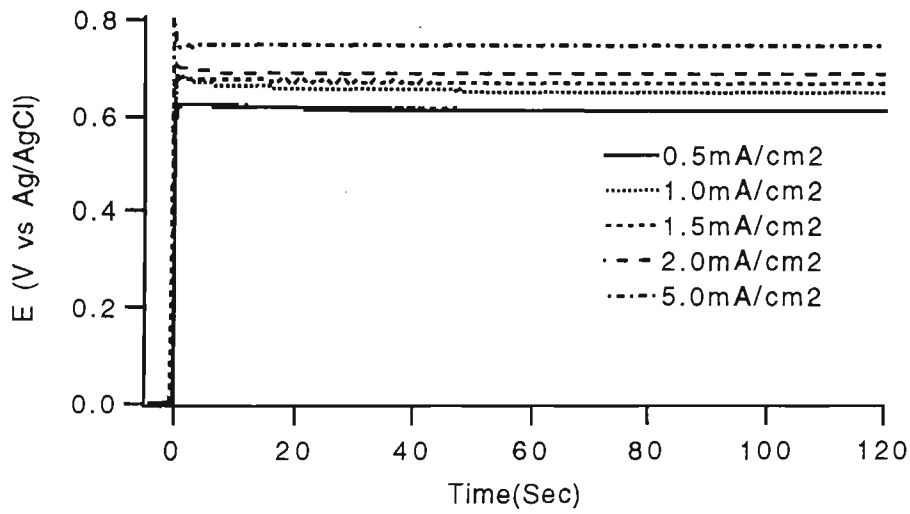

***Figure 2.3**: Chronopotentiograms for polymerisation of PPy/(+)CSA. Py=0.2 M, (+)CSA=0.05 M, time=2min. Platinum working electrode.*

At lower current densities (0.5-1.0 mA/cm^2) the potential levels off at a lower value than at higher current densities (5.0 mA/cm^2). The increase in the current density causes an increase in the potential drawn at the working electrode due to the need to drive the electrode reaction at a greater rate in order to maintain the required current density.

The polymer grown with 1 mA/cm^2 current density was selected for further studies on ion exchange properties. For consistency, incorporation of Cl^-, DS^-, PTS^-, SBA^-, $HBSA^-$, and PVS^- were carried out using a constant current

density of 1 mA/cm^2 for 2 minutes. In all cases black adherent films deposited on the electrode surface. The polymerisation potential (E_p) remained below 0.7 V for all electrodes considered here and remained constant during polymerisation; showing that conducting polymers were formed. The Eps are given in Table 2.1. The thickness of the PPy films deposited is estimated to be 0.5 μm, assuming that 24 mC/cm^2 gives a 0.1μm thick polymer [23].

Table 2.1 *Polymerisation potentials attained during growth of PPy with different counterions*

Polymer	$E_{p(V)}$
PPy/Cl	0.60
PPy/DS	0.55
PPy/PTS	0.65
PPy/SBA	0.65
PPy/HBSA	0.65
PPy/PVS	0.55

Conditions: Py=0.2 M, electrolyte=0.05--0.5 M of Cl^-, DS^-, PTS^-, SBA^-, $HBSA^-$, while PVS=0.13% (w/w).
Current density=1 mA/cm^2, time=2 min.
Electrode= 3 mm diameter Pt
E_p: polymerisation potential after 1 minute of polymerisation, where E_p levelled out.

2.3.1.1 Ion Exchange Properties of Polypyrrole

The ion exchange properties of PPy/(+)CSA have also been investigated in electrolyte solutions containing different electroinactive anions and cations. The redox properties of the polymer have been reported to be influenced by the electrolyte [74]. The anions and cations were varied from monovalent to divalent.

To study the effect of anions on the redox process, the nature of the anions was varied Cl^-, NO_3^-, SO_4^{2-}, and CO_3^{2-} while the cation (Na^+) was kept constant. The PPy/(+)CSA electrode when cycled in sodium chloride and sodium nitrate showed the wave shape typical of polypyrrole with a broad reduction peak having a peak potential value of -0.2 V and a sharp oxidation peak having a peak potential of -0.2 V (Figure 2.4(a-b)). This common behaviour was reported for PPy cycled in electrolytes containing small anions such as NO_3^- and Cl^- [231]. The broadness of the reduction peak is due to slow diffusion of electrolyte anion out of the polymer film [37]. The redox potential of the anion dedoping process cannot be precisely determined from the voltammogram of PPy electrode [37]. These cyclic voltammograms (CVs) can be repeated several times without any apparent loss of electrochemical activity.

The redox process could be represented by the following equations where (2.3) is the initial scan and (2.4) for subsequent scans in Cl^- containing supporting electrolyte.

$$PPy^+ . CSA_{(f)} + e^- \rightleftharpoons PPy^0{}_{(f)} + CSA^-{}_{(s)} \quad .... 2.3$$

$$PPy^0{}_{(f)} + Cl^-{}_{(s)} \rightleftharpoons PPy^+ . Cl^-{}_{(f)} + e^- \quad .... 2.4$$

where subscripts (s) and (f) represent solution and film phase, respectively.

Upon first reduction of PPy/CSA, CSA^- was released from the PPy matrix, and on subsequent oxidation, Cl^- in the electrolyte penetrated into the PPy matrix. Cl^- was incorporated instead of CSA^-, because the concentration of Cl^- in the electrolyte was much higher than that of CSA^-.

In solutions containing di-anions, such as SO_4^{2-} and CO_3^{2-}, the redox couples are shifted to more negative potentials (reduction at -0.5V and oxidation at -0.4V) indicating dominant charge compensation by cations of the electrolytes [191] (Figure 2.4 (c-d)). For di-anions the current at potentials positive to the oxidation peak potential has also been reduced, indicating that the current in this region is dependent on anion movement. These observations are similar to those reported before [236] for polypyrrole, previously formed in solutions of pyrrole and tetrabutylammonium perchlorate.

The chemical and electrochemical effects due to the nature of the cation on the oxidation and reduction of PPy/(+)CSA have also been studied. The cations include Na^+, Li^+, Ba^{2+}, Mg^{2+} while the anion (Cl^-) was kept constant. The cyclic voltammograms are shown in Figure 2.5 (a-d).

The voltammograms are typical for monovalent anions with a broad reduction peak at -0.2V for NaCl and LiCl, and at -0.35V for $BaCl_2$ and $MgCl_2$ with peak current approximately 50μA; suggesting that anions are the dominant charge compensating species. However, the current at the more negative potential (-0.8V) is different for Na^+ and Li^+, indicating the influence as well of the size of the alkali metal. In the case of Ba^{2+} and Mg^{2+}, however, current at -0.8V is unaffected by the nature of the cations [191]. The current in the capacitive region (potentials positive of oxidation peak potential) remains unaffected, showing that the charge compensation is dominated by anions of the electrolyte.

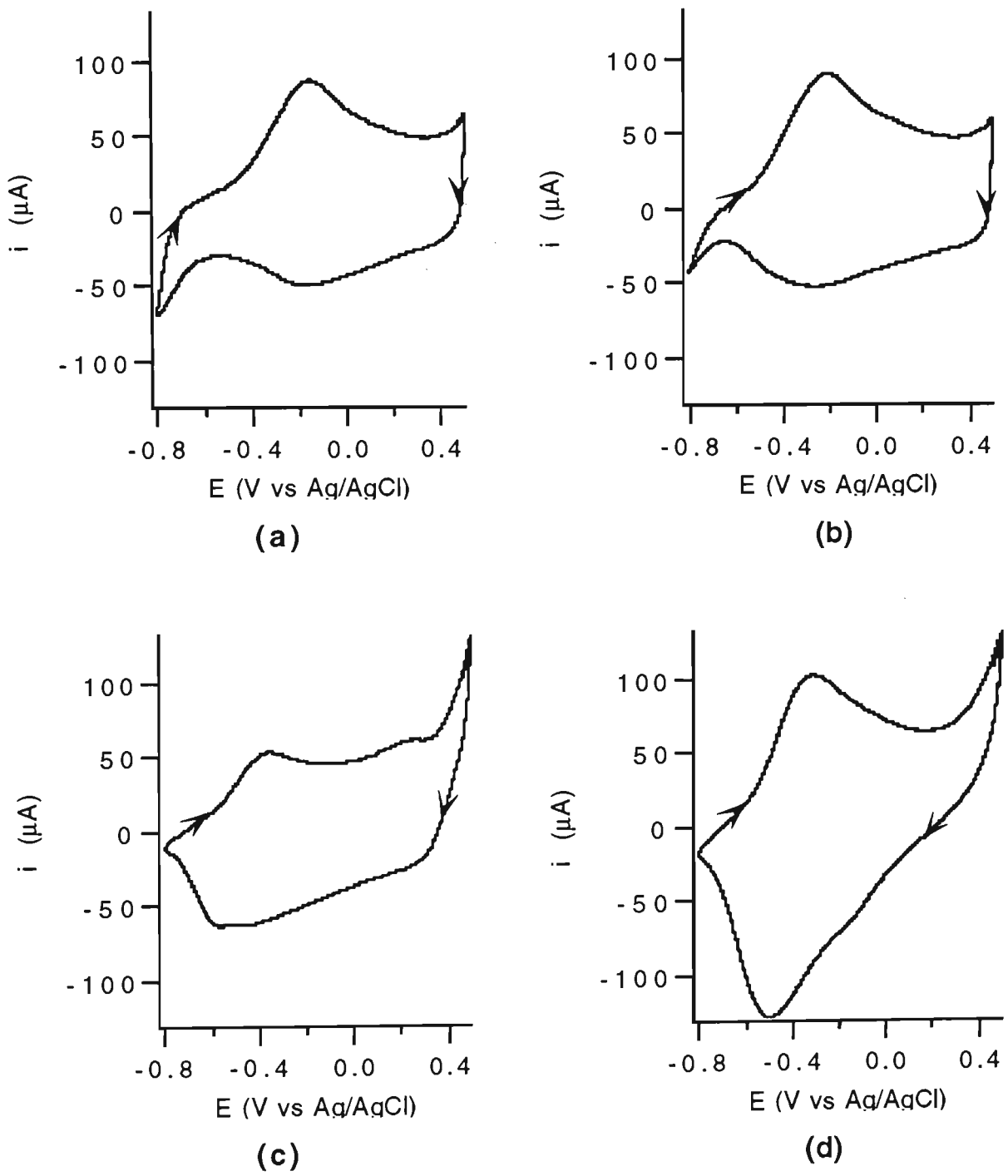

***Figure 2.4**: Cyclic voltammograms of PPy/(+)CSA in 0.1M (a) NaCl, (b) $NaNO_3$, (c) Na_2SO_4, and (d) Na_2CO_3. Scan rate=50mV/s. Polymer was grown from 0.2M Py/0.1M CSA at 1mA/cm^2 for 2min.*

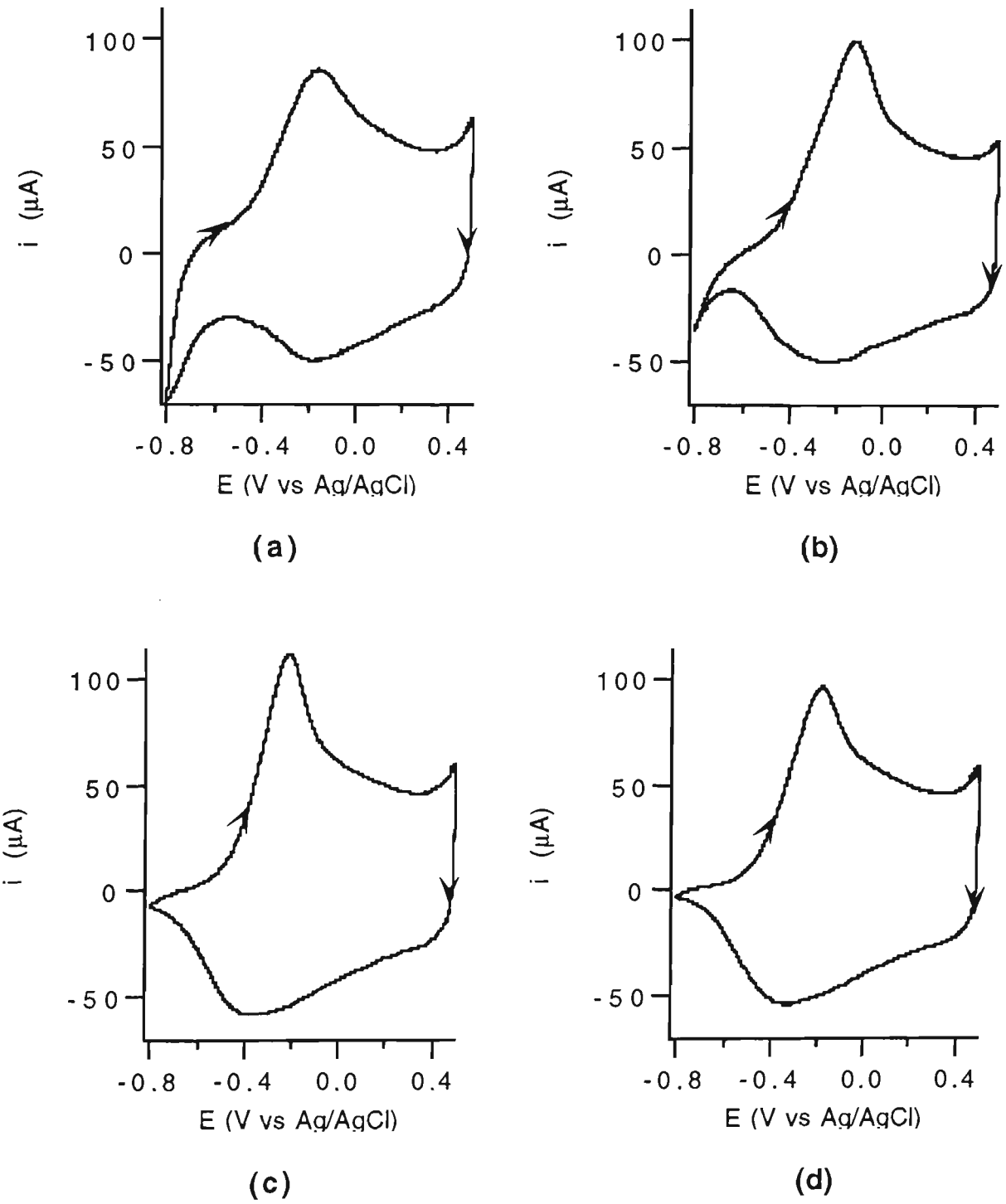

***Figure 2.5**: Cyclic voltammograms of PPy/(+)CSA in 0.1 M (a) NaCl, (b) LiCl, (c) $BaCl_2$, and (d) $MgCl_2$. Scan rate=50 mV/s. Polymer was grown from 0.2 M Py/0.1 M CSA, at 1 mA/cm^2 for 2 min.*

2.3.1.2 Influence of Dopant on Electroactivity of Polypyrrole

The effect of dopant anions incorporated during electrosynthesis has also been investigated. The PPy/Cl, PPy/DS, PPy/PTS, PPy/SBA, PPy/HBSA and PPy/PVS were synthesised as described in Section 2.3.1. Under consistent experimental conditions the electrochemistry was investigated in 0.1 M $NaNO_3$. The CV's for the above mentioned polymers are shown in Figure 2.6(a-f). Polypyrrole doped with small mobile anions (Cl^-) gives a broad reduction wave (-0.3 V peak potential) and a sharp oxidation peak (-0.25 V peak potential) typical for polypyrrole (Figure 2.6-a) [231].

For PPy/DS the CV (Figure 2.6-b) is drastically different with anion expulsion peak (A') at -0.5 V indicating that the expulsion of bulky DS^- was difficult to attain. A cation incorporation peak (B') at -0.7 V was also obtained [69]. On the reverse scan a cation expulsion peak (B) was observed at -0.5 V. A rather small peak at 0.1 V is probably due to some NO_3^- incorporation. The well defined cation redox peaks (B/B') indicate that the DS^- was immobilised during the polymerisation and charge was neutralised by cation movement during the redox process.

Polypyrrole doped with PTS^-, SBA^- and $HBSA^-$ (Figure 2.6 (c-e)) shows somewhat similar electrochemistry, with two couples of peaks associated with anion and cation movements. The reduction peaks (A') are broad (-0.2 V peak potential) and are associated with anion expulsion. During the reduction scan to more negative potentials, well defined cation incorporation peaks (B') were obtained at -0.7 V.

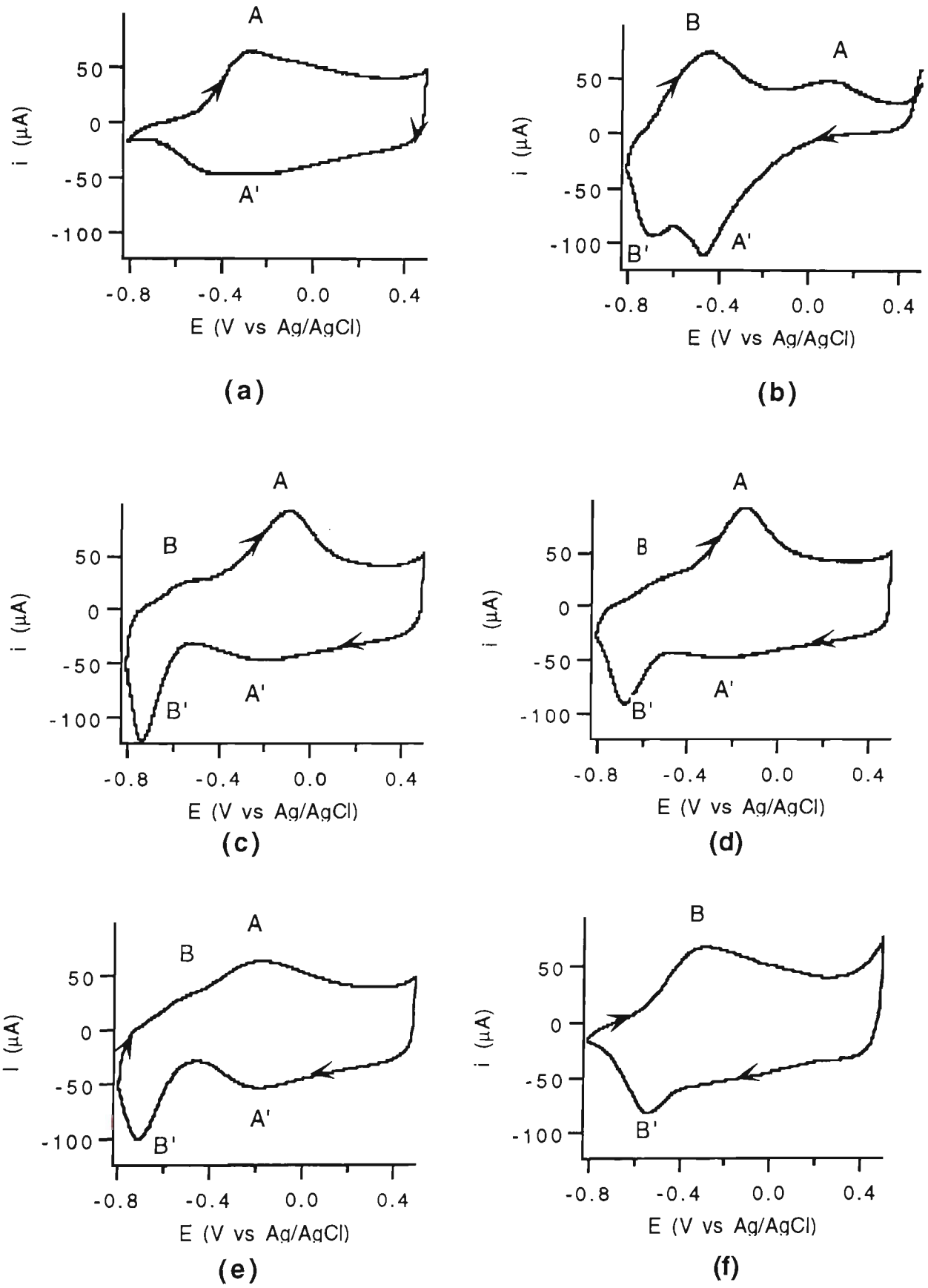

Figure 2.6: *Cyclic voltammograms of (a) PPy/Cl, (b) PPy/DS, (c) PPy/PTS, (d) PPy/SBA, (e) PPy/HBSA, and (f) PPy/PVS in 0.1M $NaNO_3$. Polymer prepared as in Figure 2.3. Scan rate=50 mV/s.*

Upon the reversal of the scan direction, the cation expulsion peak was not prominent (B), while sharper oxidation peaks (A) (compared with PPy/Cl) associated with anion incorporation were obtained at around -0.1 V. The polymers exhibit high electrochemical stability under redox cycling where several tens of voltammetric cycles have been performed without any apparent loss of electroactivity.

The results observed above (Figure 2.6 (b-e)) are in agreement with Zong and Doblhofer's findings [121]. It was described that the incorporation of the fixed negative charge into the polymer film can produce any one of the following situations:

(i) the number of fixed negative sites are larger than the PPy^+ sites. In this situation polymer would act as a cation-exchanger for charge neutrality;

(ii) the concentration of negative fixed groups is equal to PPy^+ sites;

(iii) the concentration of negative fixed groups is lower than PPy^+ sites. In this situation the polymer film acts as anion-exchanger.

The situations (i) to (iii) are shown in Figure 2.7.

In the case of a polyelectrolyte (PVS^-) the only species which was acting as charge carrier was Na^+ [237] which clearly indicates that negative fixed charges were introduced by the incorporation of polyelectrolytes as shown in Figure 2.8. The 'pseudo-cathodic doping' [115] becomes significant as the dopant size increases or the dopant ion mobility decreases. For completely immobile dopant such as a polyelectrolyte (PVS), the 'pseudo-cathodic doping' covers the whole redox range.

These observations suggest that the behaviour of an incorporated anion in the polymer matrix during polymerisation plays a significant role in the electrochemical properties of the polypyrrole. Therefore, electrochemical

polymerisation allows us to vary the nature of the polymer simply by changing the electrolyte used in polymerisation. The selection of the anion could be a useful means in producing a polymer with desired properties.

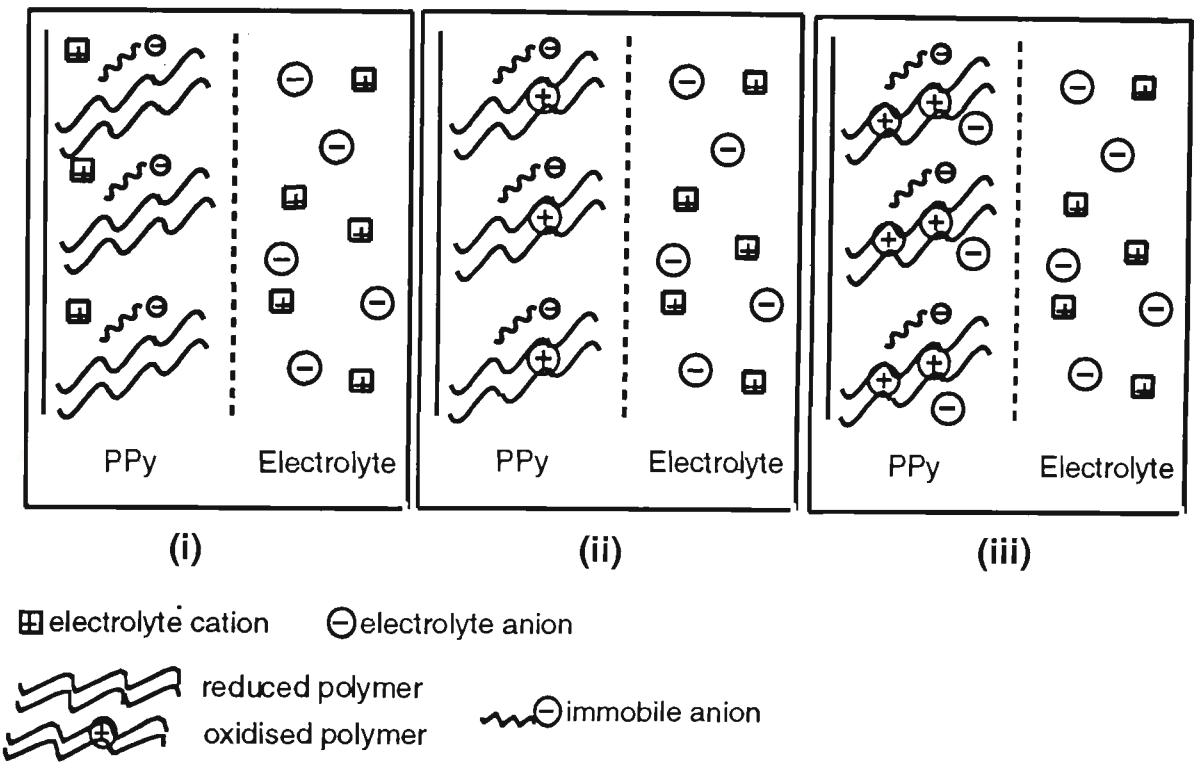

Figure 2.7: *An illustration of the polymer 'switching between cation- and anion-exchanger' in electrolyte such as NaCl, at three characteristic potentials. (i) reduced, (ii) neutral, (iii) oxidised.*

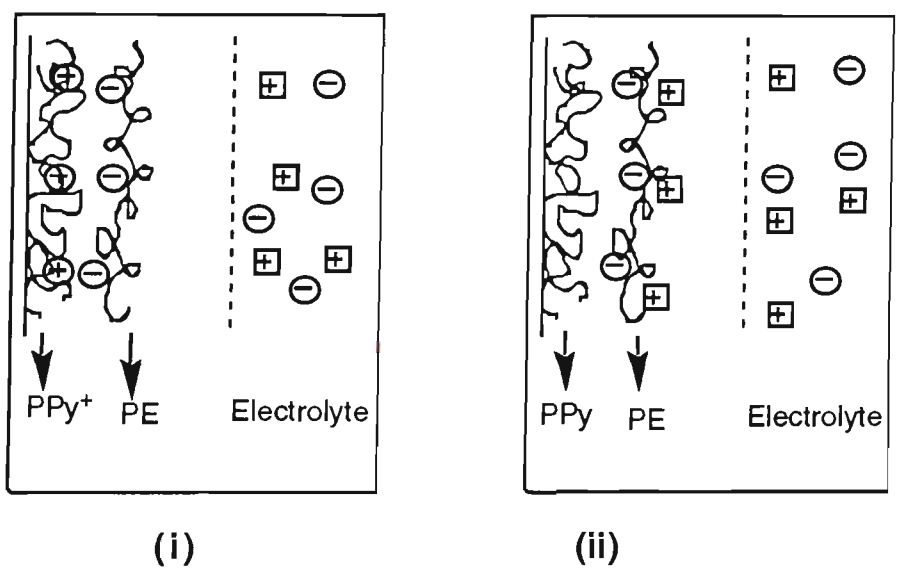

Figure 2.8*: An illustration of the redox process in polyelectrolyte incorporated polypyrrole. (i) Oxidised, (ii) Reduced.*
PPy⁺=oxidised polypyrrole, PPy=reduced polypyrrole, PE= polyelectrolyte.

2.3.1.3 Preparation and Characterisation of Poly (3-methyl pyrrole-4-carboxylic acid)

PMPC was also deposited by applying a constant current of 1 mA/cm^2 for 2 minutes from solutions containing 0.1 M monomer and 0.1 M electrolyte in acetonitrile. In all cases the polymerisation potential was 1 V or above (Table 2.2) and remained constant during the course of the polymerisation, indicating the deposition of a conductive polymer. Irrespective of the nature of the counterion, a red shiny polymer was deposited and was adherent to the electrode surface.

Table 2.2 *Polymerisation potentials attained during galvanostatic growth of PMPC with different counterions*

Polymer	Ep(V)	Observations
PMPC/(+)CSA	1.6	red polymer deposited
PMPC/PF_6	1.0	red polymer deposited
PMPC/ClO_4	1.0	red polymer deposited
PMPC/PTS	1.1	red polymer deposited

Conditions: MPC=0.1 M, electrolyte=0.1 M, electrode=3 mm diameter Pt, current density=1 mA/cm^2, time=2 min. Ep=Polymerisation potential after 1minute of polymerisation.

After polymerisation the electrodes were washed with acetonitrile, allowed to dry, and then cycled in 0.1 M $NaNO_3$. The cyclic voltammogram of PMPC/CSA is shown in Figure 2.9. The first cycle shows a broad reduction peak, over the range of -0.3 to +0.4 V, for expulsion of anions and, at -0.75 V a cation incorporation peak. On the reverse scan a cation expulsion peak (-0.55 V) and a less prominent anion incorporation wave between 0.0 and 0.4V are obtained. The two polymer redox couples of peaks, for both anion and cation exchange, have clearly been demonstrated for PMPC. Similarly,

polymer electrodes with other counterions given in Table 2.2 also did show anion and cation exchange behaviour.

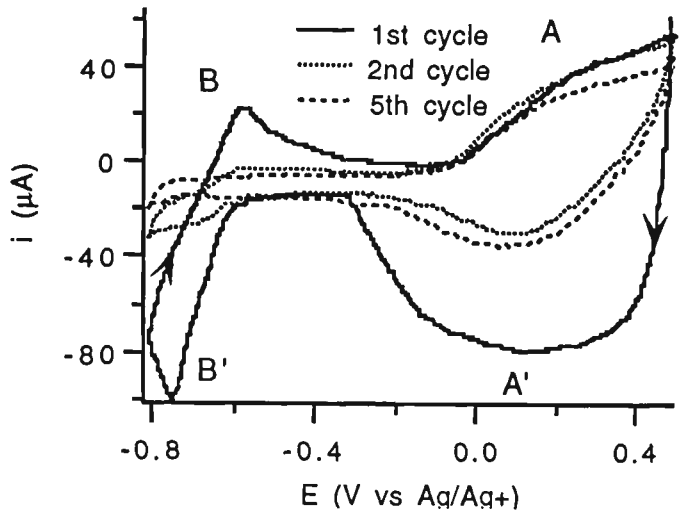

Figure 2.9: *Cyclic voltammograms of PMPC/(+)CSA in 0.1 M $NaNO_3$. Scan rate=50 mV/s. Polymer deposited from Py (0.1M)/(+)CSA (0.1 M) at Pt electrode using current density of 1 mA /cm^2 for 2 min.*

For all polymers, the cyclic voltammograms changed during successive scans as shown for 1,3,5 scans in Figure 2.9 for PMPC/CSA. This is probably because the polymer electrode lost adherence to the substrate as detected by visual observation. The electroactivity was completely lost after 10 cycles. A polymer electrode without drying was cycled in $NaNO_3$ solution but no improvement of the adhesion of the polymer to the platinum substrate was observed. A Nafion precoated electrode was used to deposit the polymer as described previously [238] but the adhesion of the polymer did not improve. It is possible that the hydrophilic nature of the polymer, because of the -COOH substituted pyrrole molecule, causes the polymer to be hydrated in aqueous media and peel off. So these polymer electrodes were not considered for any further work.

2.3.2 Electrochemical Quartz Crystal Microbalance Analysis of Chiral Polymers

2.3.2.1 Electrochemical Polymerisation to give PPy/(+)CSA and PPy/(-)CSA

The polymerisation was carried out using the constant current method with 2 mA/cm^2 current density for 2 minutes. The process was monitored by chronopotentiograms. The polymerisation potential was less than +0.8 V and remained constant throughout the polymerisation. The mass deposition as a function of time was recorded for PPy/(+)CSA and PPy/(-) CSA and is illustrated in Figure 2.10. It was observed that equivalent amounts (34 μg) of polymer were deposited irrespective of which hand of CSA^- was employed. In all cases black, shiny adherent polymer was deposited on the electrode. The polymerisation was linear with time and the slope was constant throughout the polymerisation. This linear growth fulfils the requirement of a rigid film for EQCM [157].

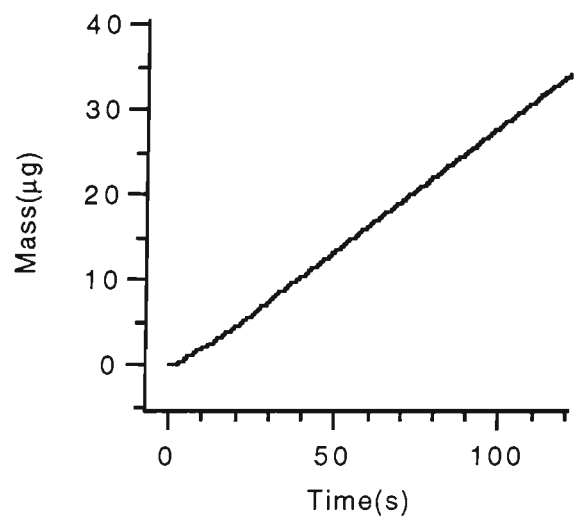

(a)

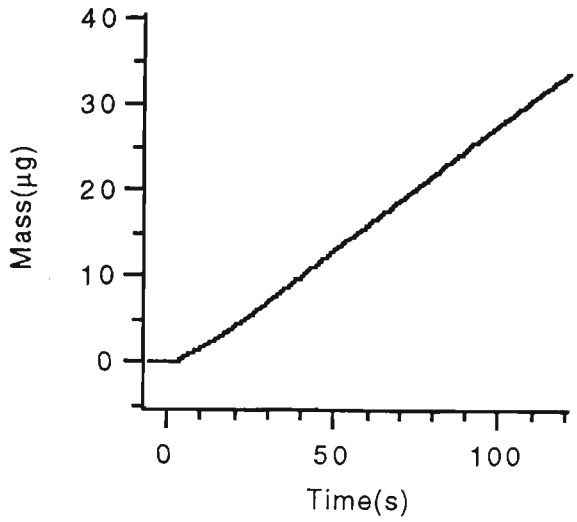

(b)

Figure 2.10: *Gain of mass as a function of time recorded during polymerisation of (a) PPy/(+)CSA and (b) PPy/(-)CSA.*
Current density=2mA/cm^2, time=2min. Monomer solution composed of 0.2 M pyrrole and 0.05M of corresponding hand of CSA.

Elemental analysis of PPy/(+)CSA and PPy/(-)CSA shows that the polymers had identical composition. The N/S ratio is 3.3 (n=ca 3) as given in Table 2.3.

Table 2.3 *Elemental analysis of PPy/(+)CSA and PPy/(-)CSA*

Polymer	C%	H%	N%	S%	N/S
PPy/(+)CSA	56.5	5.4	9.3	6.4	3.3
PPy/(-)CSA	56.7	5.3	9.4	6.5	3.3

Conditions: Polypyrrole was prepared on Pt plates (2.5 cm x1.3 cm) by current density of 2mA/cm^2 , time=30 min, Py(0.2 M)/(+) or (-)CSA (0.05 M).

The CD spectra of the polymer films grown on ITO-glass were recorded to investigate the optical activity of the polymer backbone. The CD spectra of the films between 800 and 350 nm were too noisy, due to high absorption. However, the long wavelength edge of the CD band associated with the

incorporated (+) CSA^- or (-) CSA^- ion was observed in each case near 300 nm where the absorption is less intense.

2.3.2.2 Electrochemical Characterisation of PPy/(+)CSA and PPy/(-)CSA

The electroactivity of the polymer films grown on quartz crystal was checked in 0.1 M $NaNO_3$ between -0.4 to 0.6 V. The cyclic voltammetry and mass changes on PPy/(+) CSA in $NaNO_3$ are shown in Figure 2.11. The polymer was electroactive with a reduction peak around 0.0 V and an oxidation peak around 0.1 V. Both redox peaks were broad over the range of -0.2 V to 0.2 V. The i vs E and Δm vs E responses become quantitatively reproducible from the fourth scan onwards. Presumably at this stage NO_3^- is the only species compensating the charge neutrality (see Equations 2.3 and 2.4 previously for analogy).

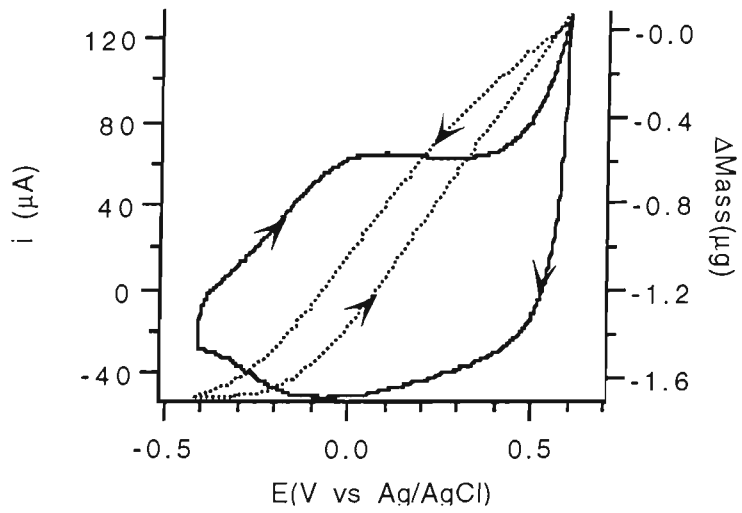

***Figure 2.11**: PPy/(-)CSA in 0.1 M $NaNO_3$. i/E(—), and Δ m/E(----). Scan rate=10 mV/s. Polymerisation conditions as given in Figure 2.10.*

The mass decrease started immediately after the imposition of the reduction potential and continued throughout the reduction scan. This additional

information about the kinetics of the redox process could only be obtained by EQCM. On reversal of the scan direction, mass uptake starts from -0.3 V and continues until the scan is completed. The Δm in NO_3^- is 1.7 μg (Figure 2.11). However, in the first cycle, mass loss was larger than the gain because of loss of heavy CSA^- and incorporation of lighter NO_3^- ions. Quantitatively identical behaviour was obtained on PPy/(+) CSA and PPy/(-) CSA.

The polymer films were also characterised in the electrolyte solutions used as dopant (i.e. in the corresponding hands of CSA^-) in order to observe the redox behaviour which is characteristic of the dopant ion itself. The current and mass response during potential cycling are shown in Figure 2.12. During the reduction scan, the polymer reduction peak appeared at 0.1 V (anion expulsion), and was sharp as compared with the nitrate peak. On continuation of the cathodic scan, a second reduction peak was observed at -0.25 V. The presence of this redox peak is ambiguous, this peak could be due to expulsion of deeply trapped anions.

As far as the mass changes are concerned during redox cycling, initially there was a mass increase over the potential range of +0.6 to +0.4 V. This increase in mass could be due to some solvent incorporation [160] because solvent molecule and neutral electrolyte salt can diffuse into the film until equilibrium is obtained. As the potential scan continued to negative potentials, the mass decreased rapidly, which is consistent with the expulsion of CSA^- anions. The fact that the second reduction peak was due to expulsion of deeply trapped anions can be confirmed from the mass flux in this region (-0.1 V to -0.4 V) where the polymer mass continued to decrease. Overall, a substantial mass loss occurred during the full cathodic scan from +0.6V to -0.4 V. The overall mass loss during reduction of the

polymer is 0.27 μg in CSA^-. This behaviour was reversed upon re-oxidation when there was an initial decrease in the mass flux between -0.4 V to 0.0 V, which could be due to slow anion expulsion continuing in this region, or possibly that some solvent was flowing out of the polymer film. Subsequently mass increase was observed from 0.1 V to 0.6 V, due to anion incorporation. Reproducible responses were obtained with the repeated cycles. Analogous cyclic voltammetric and EQCM experiments with PPy/(+)CSA showed, as expected, quantitatively similar responses in (+) CSA^- during redox cycling .

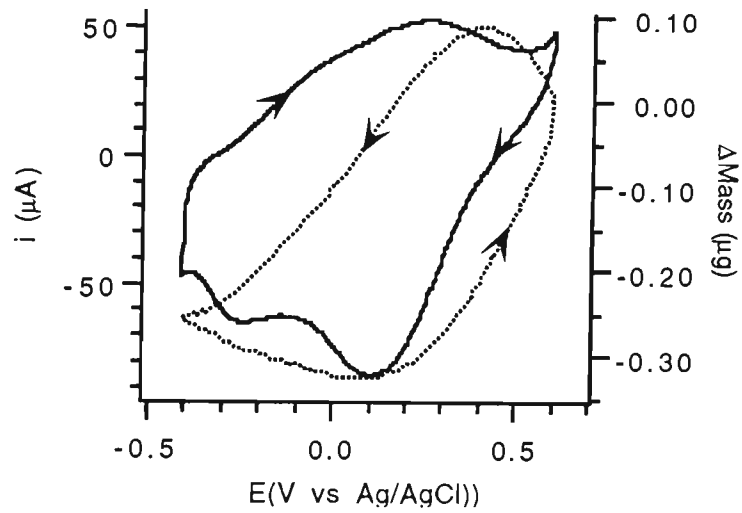

***Figure 2.12**: PPy/(-)CSA in 0.1 M (-)CSA. i/E(—), and Δ m/E(----). Scan rate=10 mV/s. Polymerisation conditions as in Figure 2.10.*

The influence of applied potential pulses on mass changes was then investigated. In potential pulse experiments the polymer was pulsed between 0.6V to -0.4V. Potentials were applied for 15 seconds each. Figure 2.13 shows the mass changes and chronoamperogram for the PPy/(-)CSA polymer. As can be predicted from the CV response, the mass of the polymer decreased during the reduction pulse and increased during the oxidation pulse (Figure 2.13-a). This loss and increase in mass is associated with the expulsion and incorporation of the counterions. The

corresponding chronoamperogram also reveals similar electrode behaviour (Figure 2.13-b). These results are consistent with cyclic voltammetric responses where similar behaviour was observed in this electrolyte. Quantitatively similar responses were obtained with PPy/(+)CSA. The reproducibility of the system was monitored for 300 sec when reproducible responses were obtained.

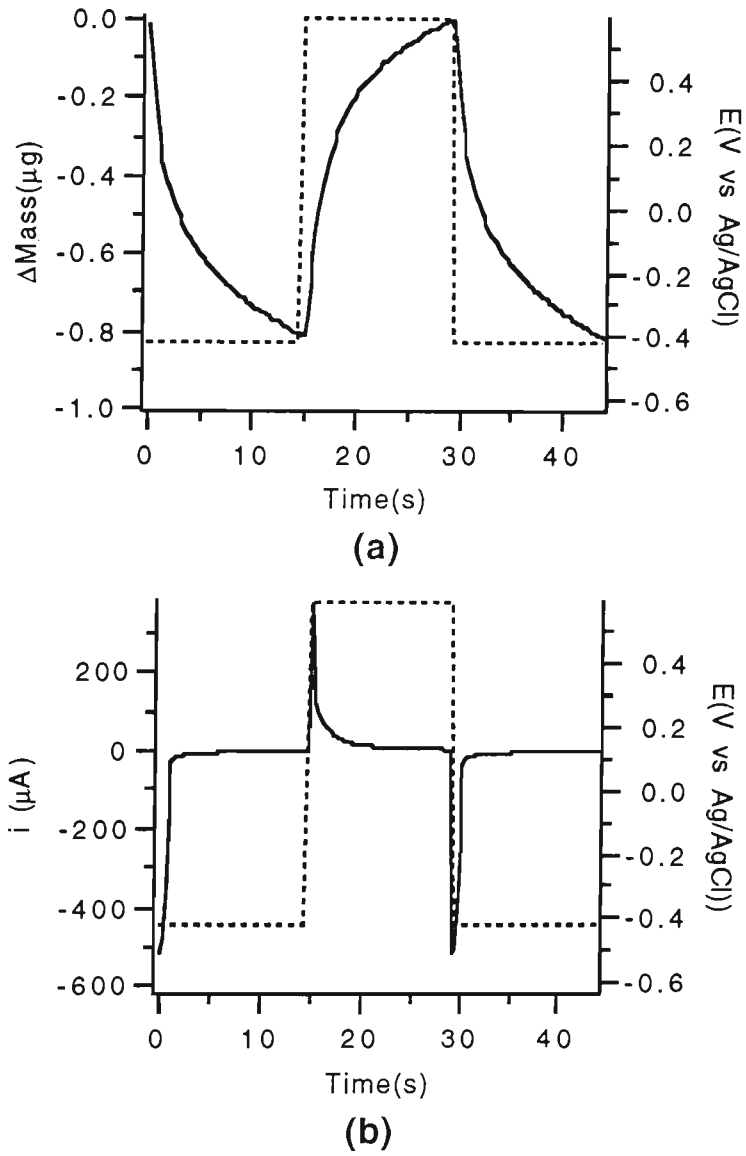

***Figure 2.13**: EQCM of PPy/(-)CSA under potential pulse conditions in 0.1M (-)CSA. (a) Mass change(—), and potential applied(----). (b) Current response (—), and potential applied (----). Potential pulse applied: E_1=-0.4V, E_2=0.6V, t_1=t_2=15 sec.*

The EQCM results obtained at PPy/CSA electrodes indicate that the polymer predominantly behaves as an anion exchanger. The dopant ions exist in

shallowly trapped and deeply trapped states. This was confirmed by the mass exchanges during redox cycling.

2.3.3 Synthesis and Characterisation of Poly{N-[(1S)-(+)-1-phenylethyl]pyrrole} and Poly{N-[(1R)-(-)-1-phenylethyl]pyrrole}

The electrochemical polymerisation was carried out using the constant current method from monomer solution of 0.1M N-[(1S)-(+)-1-phenylethyl]pyrrol (+PEP) or N-[(1R)-(-)-1-phenylethyl]pyrrole (-PEP) and 0.1M TBAP prepared in acetonitrile. A constant current density of $2mA/cm^2$ over periods of 90 seconds and 2 min. was applied to deposit the polymer. The polymerisation potential (Ep) continued to increase slightly, showing deposition of resistive polymer. The chronopotentiograms are shown in Figure 2.14. The Ep was 1.10 V, taken from the potential/time curve, after 1min. An anodic shift in the polymerisation potential for N-substituted pyrrole as compared with those of pyrrole have been shown before. The extent of this shift depends on the size of the substituents [126]. The electropolymerisation could be represented by the following equation.

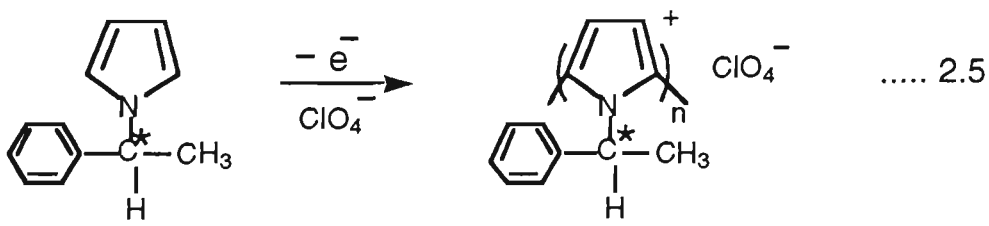

..... 2.5

Mass deposition with time during polymerisation is shown in Figure 2.15 for (+)PPEP/ClO_4 and (-)PPEP/ClO_4. The mass deposition was slow initially, probably due to the formation of some oligomers which did not deposit on to the crystal, but soon after 20 seconds mass increased linearly with time. The polymer mass deposited was 26 μg and 27 μg for (+)PPEP/ClO_4 and

(-)PPEP/ClO_4, respectively.

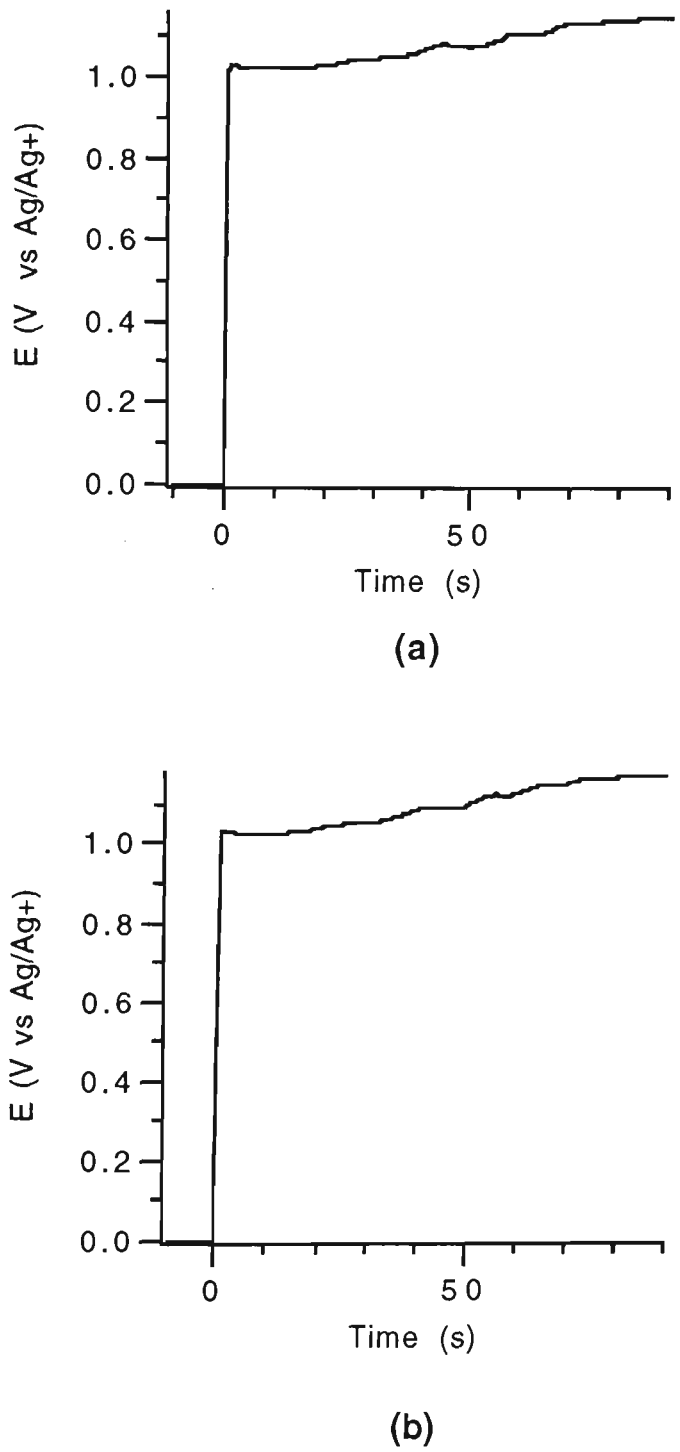

***Figure 2.14**: Chronopotentiograms for deposition of (a) (+)PPEP/ClO_4, (b)(-)PPEP/ClO_4.. Monomer solution contained 0.1 M (+) or (-) PEP and 0.1M TBAP. Current density=2mA.cm^{-2}, time=90 seconds, solvent=CH_3CN.*

It was observed that when polymerisation continued for 2 minutes the polymer mass was 40μg. This value is close to the critical value for this

EQCM apparatus. So the polymerisation duration was kept to 90 seconds. The black-brown polymer was not a continuous film but was powdery in nature. This is characteristic of N-substituted pyrrole, where the mechanical properties become worse on increase in the size of the side chain [123].

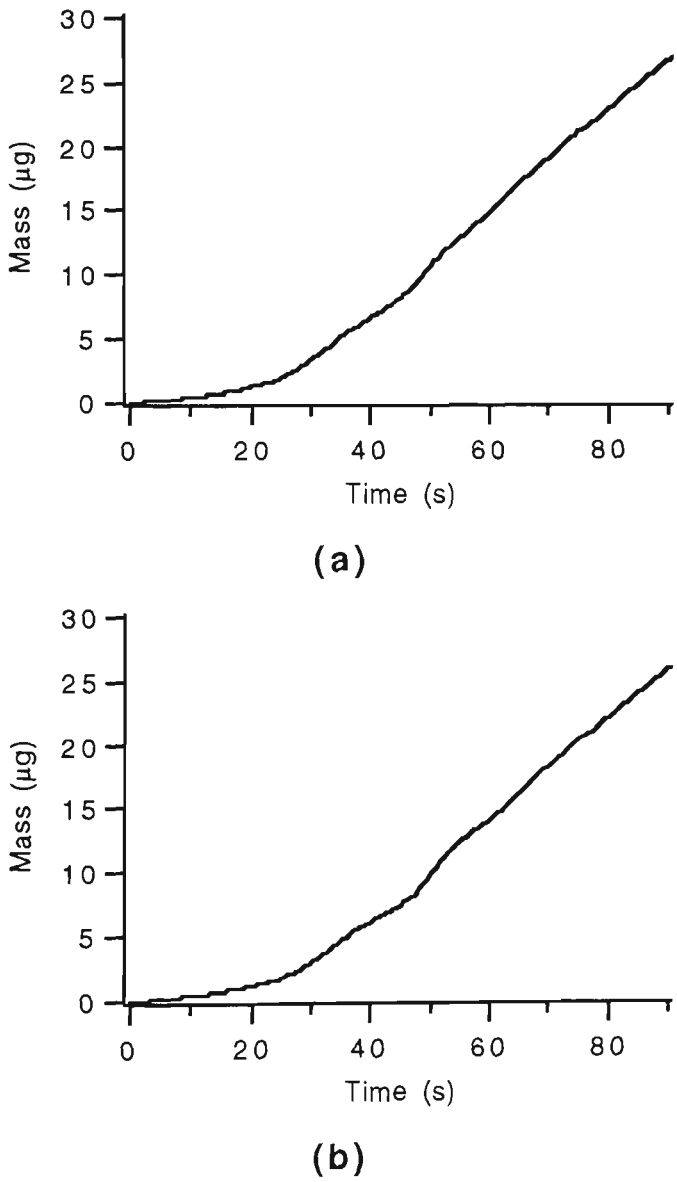

***Figure 2.15**: Mass deposited vs time during galvanostatic polymerisation. (a) (+)PPEP/ClO_4, (b)(-)PPEP/ClO_4. Monomer solution contained 0.1 M (+) or (-) PEP and 0.1 M TBAP. Current density=2 mA.cm^{-2}, time=90 seconds, solvent=CH_3CN.*

Elemental analysis results, given in Table 2.4, show that the materials deposited are identical irrespective of the handedness of the monomer. The

ratio N/ClO_4 is 5 to 4.5 (n=ca 5) indicating that the polymer was less heavily doped than polypyrrole (n=2-4).

Table 2.4 *Elemental analysis of (+) PPEP/ClO_4 and (-)PPEP/ClO_4.*

Polymer	C%	H%	N%	ClO_4%	N/ClO_4
(+)PPEP/ClO_4	74.36	6.24	7.73	3.80	5.0
(-)PPEP/ClO_4	69.69	7.12	6.88	3.89	4.5

Conditions: Polymer was deposited on Pt plate (2.5 cm x1.3 cm). Polymerisation solution contained 0.1 M (+) or (-) PEP and 0.1 M TBAP. Current density=2 mA.cm^{-2}, time=30 min, solvent=CH_3CN.

The degree of oxidation of the polymer chain is 0.20. In under-doped or less doped polymer the polarons and bipolarons are not fully supported and stabilised, which leads to low conductivity of the polymer. The decrease in the electrical conductivity for N- and 3-alkylpyrrole with increasing substituent size has been reported before [123,239-241]. The lower conductivities of substituted pyrrole as compare to unsubstituted ones could be due to electronic and steric effects of the substituents on the structural arrangement of monomeric units.

The CD spectra of the polymers deposited on ITO-glass were recorded between 300 and 800 nm. No chiroptical properties were obtained in this region. The polymer backbone there did not possess macroasymmery.

2.3.3.1 Electrochemical Characterisation of Poly{N-[(1S)-(+)-1-phenylethyl]pyrrole} and Poly{N-[(1R)-(-)-1-phenylethyl]pyrrole}

Under consistent experimental conditions the cyclic voltammetry was carried out on these films. The CV of the polymers were recorded in 0.1 M

sodium nitrate solutions. The electroinactivity and loss of mechanical stability of PPEP/ClO_4 in $NaNO_3$ hampered any further analysis in aqueous solutions. These experiments were then performed with solutions containing ClO_4^- anion prepared in acetonitrile to observe polymer electroactivity in solutions containing its dopant ion.

The polymer film was cycled between 0.0 and +0.8 V. Figure 2.16 shows the effect of cyclic potential scans on i/E and Δmass/E for (+)PPEP. The polymer is electroactive in TBAP with broad oxidation and reduction peaks at around 0.4 V. The redox potential has shifted anodically compared with polypyrrole. Such potential shifts were observed before [74,242,243]. However, more cathodic and anodic potentials were also tried, but no additional oxidation/reduction responses were obtained. The redox process could be presented as follows:

$$PPEP^{+}/ClO_4^{-} \underset{ClO_4^{-}}{\overset{+e^{-}}{\rightleftharpoons}} PPEP^{0} + ClO_4^{-} \qquad \text{..... 2.6}$$

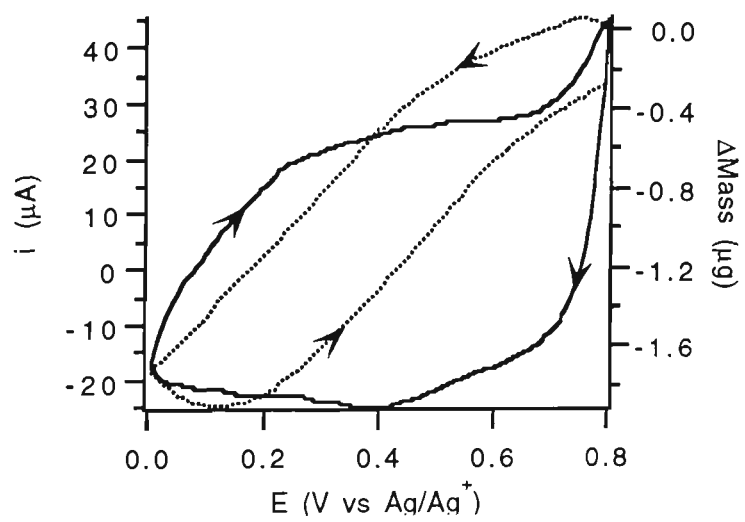

Figure 2.16: *Mass and current changes during cyclic voltammetric studies of (+)PPEP/ClO_4 in 0.1 M TBAP. i/E(—), and Δm/E(----). Scan rate = 10 mV/s. Polymer electropolymerised using 2 mA/cm^2 for 2 min.*

As far as mass changes are concerned the polymer mass decreased on reduction throughout the scan. On the reversal of the scan (oxidation), the mass continued to decrease until the potential scan reached 0.1 V, but the decrease was slow. This mass decrease could probably be due to slow anion expulsion that continued at this potential. Then an increase in the polymer mass was obtained as the potential scan was continued anodically. The polymer mass, however, did not recover to its initial value, and during each scan there was a net decrease of 0.3 μg in polymer mass. The mass decrease on reduction and increase on re-oxidation must be due to the expulsion and incorporation of counterion (ClO_4^-) from the polymer film. The decrease in the mass exchange capacity indicates that the polymer lost its stability with time. Analogous responses were manifested by (-)PPEP in TBAP solution during cyclic voltammetry under similar experimental conditions.

Potential step experiments were also carried out to investigate the doping/dedoping process in ClO_4^- solution. The responses are shown in Figure 2.17. Similarly to CV, upon reduction the polymer mass decreased by 0.7 μg. On oxidation, an increase in mass was observed. These changes in mass are associated with the ClO_4^- ion expulsion and incorporation, respectively. The current response (Figure 2.17-b) is similar to the responses observed in the mass change. The rate of mass change was potential dependent. During the reduction pulse potential, the mass loss continued throughout the pulse, whereas mass uptake (on oxidation) was faster; the increase in mass was completed in 3 seconds.

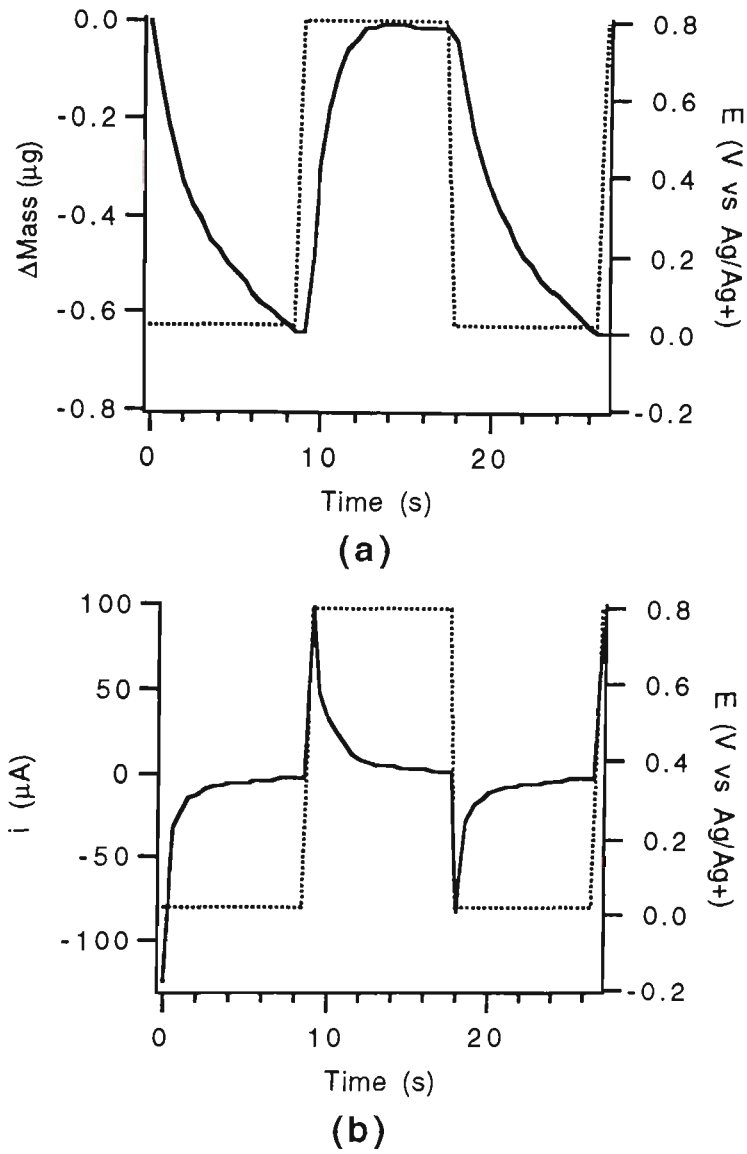

Figure 2.17: *Potential step responses at (+)PPEP/ClO_4 in 0.1 M TBAP. (a) Mass change (—), potential applied (----), (b) current response (—), potential applied (---). Pulses applied: E_1=0.0 V, E_2=0.8 V; pulse width, t_1=8 sec, t_2=10 sec.*

The reproducibility of the system was investigated for 10 repetitive pulses. The anion exchange capacity of the polymer decreased with repetitive pulses as shown in Figure 2.18. The mass uptake decreased linearly with each successive cycle and, over 10 cycles, 0.35 μg of mass loss was observed.

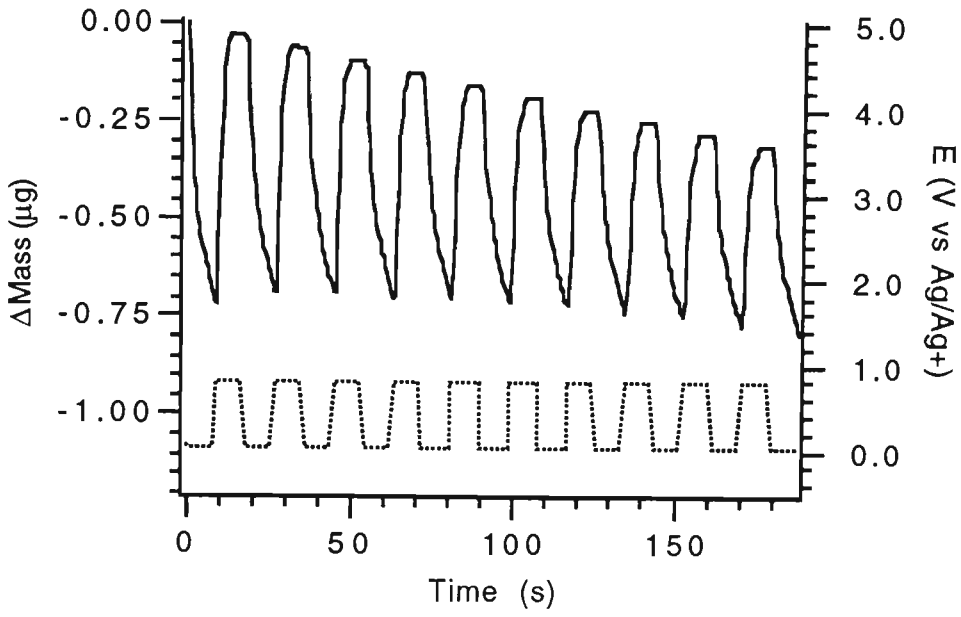

Figure 2.18: *Mass changes during 10 repetitive pulses at (+)PPEP/ClO_4 in 0.1 M TBAP. Mass change (—), potential applied (----). Conditions as in Figure 2.17.*

The EQCM analysis of the polymer reveals that the redox process is accompanied by anion movement in and out of the polymer. The responses during CV and pulse potential analysis complement each other. The polymer films showed some instability during the electrochemical analysis.

2.4 CONCLUSIONS

Conductive electroactive polymers can be easily prepared by single step electrochemical polymerisation of monomers. The electrochemical polymerisation technique has the advantage over chemical polymerisation in that it facilitates the incorporation of a range of counterions. The anodic doping process in the electrochemical polymerisation, which was applied to deposit the polymer, was not much affected by the size of the electrolyte anion (Ep ranges from 0.55-0.65 V). On the contrary, the redox process of the resulting film was influenced considerably by the size of the anion

incorporated. The ion-exchange behaviour can be categorised into three different types:

(i) the polymers that showed predominantly anion exchange behaviour (PPy/Cl) due to the mobile small counterion;

(ii) the polymers with less mobile counterions showed both anion and cation exchange processes (PPy/DS, PPy/PTS, PPy/SBA and PPy/HBSA);

(iii) the polymers with completely immobile counterions (PPy/PVS), where the polymer acts as a cation exchanger.

The 'pseudo-cathodic doping' of the polymer films increases with the decrease in the counterion mobility and the effect is maximised in polyelectrolyte incorporated polymers.

The electrolyte solutions employed during cyclic voltammetry also play an important role in determining the properties of the polymer films. Monovalent anions are incorporated and expelled easily during the redox process at PPy/CSA electrodes. The incorporation of di-anions was not easily achieved, resulting instead in monovalent cations being incorporated as charge compensating species. Similarly, the di-cation incorporation was not obtained at the polymer electrodes in redox processes.

PMPC, which has anionic substituents, shows cation exchange properties as expected but mechanical instability of these polymers in aqueous solutions hinders their application.

The identification of the species undergoing transport during switching reactions is of considerable importance to the ultimate goal of manipulating the properties of conducting polymers for their applications. The EQCM is an excellent tool for such analysis. The mass deposition recorded for both

PPy/(+)CSA and (-)CSA showed that an equal polymer mass (34 μg) was deposited. The EQCM analysis of the PPy/CSA confirmed its anion exchange property, both in NO_3^- and in CSA^- solutions. The potential step experiment also showed mass decrease and mass increase with reduction and oxidation potentials, respectively. The presence of deeply trapped anions in the polymer; as indicated by mass decrease at more cathodic potentials corresponding to a second peak in the CV of this region. The polymerisation process of PPEP studied by EQCM showed that the polymerisation efficiency was lower at the beginning of the polymerisation, probably due to formation of some oligomers. The anion exchange properties of the polymer with ClO_4^- in cyclic voltammetry and potential step experiments was corroborated by the mass decrease and increase during reduction and oxidation, respectively. The polymer was powdery in nature and lost its stability with time.

The general conclusion is that the electropolymerisation of pyrrole and substituted pyrrole is a versatile way of manipulating the characteristics of modified electrodes in order to tailor them for specific applications.

CHAPTER 3

DETECTION OF AMINO ACIDS AT CONDUCTING POLYMER MODIFIED MACROELECTRODES USING FLOW INJECTION ANALYSIS

3.1 INTRODUCTION

Amino acid analysis is of great importance in biological materials [244], sea water [244,245] and food samples [246,247]. Due to the complex nature of the samples encountered and the similar properties of a number of amino acids, chromatography with UV or fluorescence detection has emerged as a most useful method in their determination [248,249]. However amino acids do not fluoresce, and only phenylalanine, tryptophan and tyrosine have sufficient UV-vis absorbance. Consequently, such methodologies often require pre or post-column derivatisation to improve the UV or fluorescence activity of the amino acids [245,250,251]. There are several drawbacks to this approach. For example, in some cases [252,253] the reagents themselves and reaction by-products are fluorescent and so they can become serious interferents in the analysis. Also, some reagents such as o-phthaladehyde (OPA) (a fluorescent derivatising agent) and the amino acid derivatives of OPA, are not stable [254,255]. A detection methodology that does not require pre- or post-column derivatisation is preferable due to the greater simplicity and convenience such a technique would offer.

Electrochemical (EC) detection of amino acids in FIA, and subsequent to HPLC separation, is preferred compared with photometric detection because the EC method is simple, selective and low cost [256-260]. A review of EC detection of electroinactive amino acids is given as the present work addresses the detection of electroinactive amino acids.

Potentiometric detection on a copper tubular electrode subsequent to reverse phase high performance liquid chromatography (RPHPLC) has been investigated with the detection limits for glycine, valine, and isoleucine of 75, 200 and 300ng/μl respectively [261-264].

In 1972 Fleishmann et al. reported that amines and alcohols can be oxidised on a nickel electrode in alkaline solution [265]. This lead to the amperometric detection of amino acids on nickel electrodes in FIA and HPLC. The mechanism involved the catalytic oxidation of amino acids by higher oxidation state species of nickel (NiOOH) formed anodically on the surface of the electrode. The stated advantages included ease of detector maintenance, low cost of components, direct detection and sensitivity comparable to UV-vis methods [258,266]. Wang and Lu [260] have investigated the use of Eastman-AQ/Ni^{II} (poly(ester sulphonic acid)polymer from Eastman Kodak) chemically modified glassy carbon electrodes. The detection limits are better than those reported using bare nickel electrodes. For glycine the detection limit is 1.0×10^{-6} mol/l (0.075ppm) compared with 0.30µg/25µl (12ppm) on the nickel electrode [258]. Glassy carbon electrodes at 0.9V [267] and ruthenium oxide modified glassy carbon electrodes [268] have also been used for amino acid detection. The catalytic DC detection on metal electrodes is accompanied by a loss of electrode activity with subsequent rapid decay of the analytical signal.

Polta and Johnson reported the use of triple step potential waveforms in the amperometric detection of amino acids in alkaline solution on platinum [259] and gold [269,270] electrodes in FIA and post-chromatographic analysis. The amino acid was detected by anodic oxidation and the multi-step waveform was applied in order to clean the electrode surface via anodic polarisation and reactivation by reductive polarisation after the detection step. The detection limit with this method is 13ng/50µl (0.26ppm) for glycine and the optimum sensitivity was obtained using solutions of pH > 11 [259]. Therefore post-column addition of base is often required [269], which makes the system more complicated. A comparison of various EC detection methods is given in Table 3.1.

Table 3.1 *A comparison of EC detection of amino acids*

Electrode	Amino Acids	Analysis Method	Limit of Detection	Notes	Ref.
Cu	Gly	RPHPLC-EC	75ppm (75ng/μl)	Potentiometric detection	263
Ni^{II}	Gly	FIA-EC	12ppm (0.30μg/ 25μl)	Anodic oxidation with NiOOH formation	258
Eastman AQ/Ni^{II}	Gly	FIA-EC	0.075ppm ($1x10^{-6}$ mol l^{-1})	Oxidation of amino acid with surface catalysed NiOOH formation	260
Pt	Gly	FIA-EC	0.26ppm (13ng/50μl)	Use of triple step waveform for oxidation of adsorbed amino acid	259
Au	Lys	HPLC-PCD	0.22ppm (11ng/50μl)	Surface catalysed oxidation of amine functionalities of amino acids	269
		HPLC-PS-PCD	0.06ppm (3ng/50μl))		
Au	Cys	LC-PED	$0.109x\ 10^{-3}$ppm (0.9 pmol)	Use of fast cyclic potential sweep with electronic integration of electrode current	270
	Met		$0.463x\ 10^{-3}$ppm (3.1pmol)		

The literature on the separation and detection of amino acids is vast, and only some key findings that involve EC-detection in flowing solutions are included here.
Values and units in brackets (as stated in the literature) are converted to the same units for comparison purposes and are given outside the brackets.

Conducting polymers such as polypyrrole, polythiophene and polyaniline have been employed as electrochemical sensors. Selectivities towards electroinactive anions may be obtained by changing the nature of the polymer or the counterions (Section 1.5) [190,102,271-278]. Therefore, conducting polymers could be useful for the detection of amino acids with

appreciable selectivities in FIA. Previous work indicated that amino acids showed predominantly anionic interactions with polypyrrole and polyaniline when the amino acids were employed as molecular probes with an inverse TLC technique [279,280].

Chromatographic columns packed with polypyrrole/tosylate (PPy/OTs) coated glassy carbon spheres have been used for the separation of dansylamino acids in electrochemically modulated liquid chromatography (EMLC). With electrochemically modulated liquid chromatography, capacity factors and hence the separations of dansyl amino acids, were affected by application of voltages prior and during elution [281].

Thus the unique ability of conducting polymers to interact selectively with particular amino acids and the ability to influence such interactions through electrochemical control should then form the basis of an unique analytical system for the determination of amino acids.

3.1.1 Amino Acids

Amino acids have a distinctive side chain that gives these molecules chemical individuality. All 20 amino acids naturally found in proteins have two functional groups in common, a carbonyl group and an amino group which are bonded to the same carbon atom. The side chain, or R groups, are different in each amino acid. These R groups vary in structure, size, electrical charge and solubility in water. The general structure of amino acids found in proteins is shown below (I) in the non-ionic form.

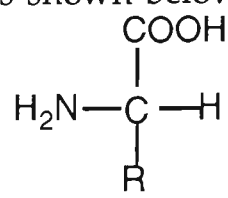

(I)

The amino acids can be grouped on the basis of the properties of their R groups:

-Non polar R-groups

-Polar but uncharged R-groups

-Acidic R-groups

-Basic R-groups

Within each group, R groups vary in polarity, size and shape. The type of chemical interactions predicted are neutral (non-polar, polar), anion exchange (acidic), and cation exchange (basic) interactions. The four amino acids selected from each group are shown in Table 3.2 along with the structure of their side chains and their chemical nature.

Amino acids in aqueous solution are ionised and can act as acids and bases. At the isoelectric point (pI, the arithmetic mean of the two pK' values) all amino acids are in the dipolar or zwitterion form, which is fully ionised but has no net electric charge. At any pH above the isoelectric point, the amino acid has a net negative charge and at any point below its isoelectric pH, it has a net positive charge as shown below (II).

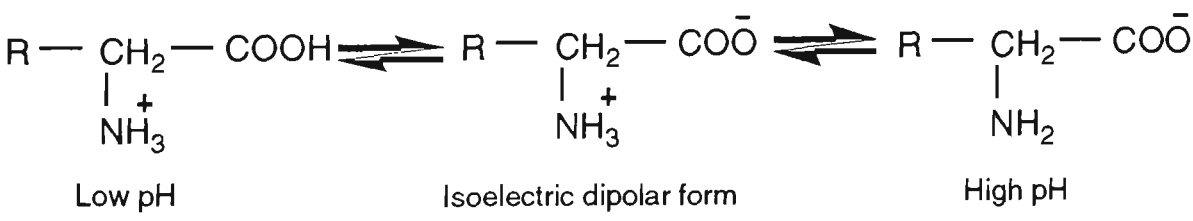

(II)

The further the pH of the solution is from the isoelectric point, the greater the net electric charge of the population of amino acid molecules.

Table 3.2 *List of amino acids selected for detection on polymer electrodes*

Amino acid	Symbol	Structure	Mol.Wt	pI	R-group
L-Alanine	Ala	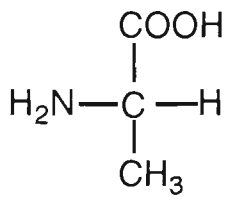	89.09	6.00	non-polar
L-Serine	Ser	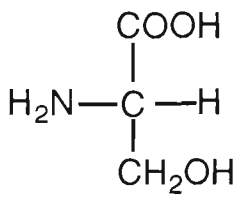	105.09	5.68	polar but uncharged
L-Aspartic acid	Asp	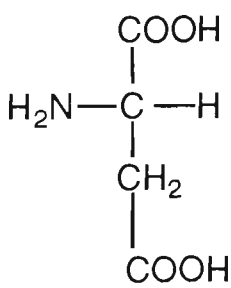	132.10	2.77	acidic
L-Arginine	Arg	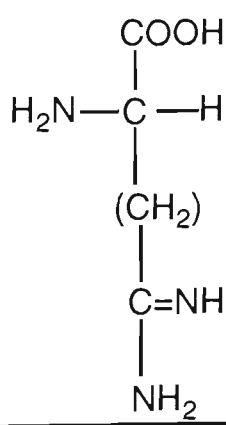	174.02	10.76	basic

3.1.2 Aims and Approach of this Chapter

The objective of this section of research work is to achieve the detection of amino acids on conducting polymer electrodes without the prior derivatisation of amino acids which is required for more conventional analysis techniques. The amino acids selected for this work were L-alanine, L-serine, L-aspartic acid, and L-arginine (one from each of the four main groups) listed previously (Section 3.1.1), and for chiral selectivity, D-phenylalanine, L-phenylalanine and D-tryptophan, L-tryptophan. The polymer electrodes chosen include PPy/CSA, PPy/Cl, PPy/DS, PPy/SBA, PPy/PTS, PPy/HBSA, and PPy/PVS.

The conventional electrochemical experiments used were cyclic voltammetry (CV), normal pulse voltammetry (NPV) and chronoamperometry (CA). Optimisation of the electrochemical detection system was carried out using the PPy/(+)CSA electrode as a test case. The technique employed for this was electrochemical detection using flow injection analysis (FIA). The effect of the electrochemical parameters employed in DC amperometry, pulsed potential analysis (varying pulse width, magnitude and current sample point) have been investigated. Once this was completed with the PPy/(+)CSA electrode, the analysis was extended to other polymer coated electrodes and the selectivity for particular amino acids was in this way evaluated for the range of polymers listed above.

Sodium nitrate (0.1M, pH=5.7) was used as an eluent. Due to the complex chemical nature of amino acids it is important first to analyse the amino acid/polymer interactions without the presence of buffer salts. Thus a comparison of the interactions between each of the amino acids and

polymers can be made. Also, a system which eliminates the use of buffer will be of advantageous because of its simplicity. FIA was also carried out in phosphate buffer (pH 7) where the eluent and amino acid solutions were of uniform pH .

3.2 EXPERIMENTAL

3.2.1 Reagents and Standard Solutions

All reagents used were of analytical reagent (AR) grade. Pyrrole was obtained from Sigma, distilled and kept in a cool dry place. L-alanine, L-serine, L-aspartic acid, L-arginine, L-glutamic acid, D-phenylalanine, L-phenylalanine, D-tryptophan and L-tryptophan were obtained from Sigma. Standard stock solutions (0.02M) of these amino acids were prepared in deionised Milli-Q water and further diluted in the appropriate eluents, as required. $NaNO_3$ (BDH), Na_2HPO_4 (BDH) and NaH_2PO_4 (BDH) were all used as received. Eluents were filtered using a 0.45μm filter (nylon from ACTIVON) and deoxygenated with nitrogen. A blanket of nitrogen was maintained over the eluent during analysis.

3.2.2 Instrumentation

An in-house built galvanostat was used for constant current polymerisation. Cyclic voltammograms were obtained using a BAS model CV-27, normal pulse voltammetry with an ElectroLab Workstation (ADI) and chronoamperometry was carried out with a BAS 100 Electrochemical Analyser. The recording system was comprised of a computerised Macintosh/MacLab system with Chart v3.2.8 software (ADI). Data

manipulation was also performed out using an Igor software package (Wavemetrics).

For stationary cell work, a platinum disc (3 mm diameter) served as the working electrode. The electrode was polished on 0.3μm followed by 0.05μm alumina (Leco) and ultrasonicated for approximately 1 minute in Milli-Q water. A platinum mesh was used as the auxiliary electrode and the reference electrode was a BAS Ag/AgCl (3M NaCl) with a in-house built salt bridge.

Flow injection analysis was performed using a Dionex chromatography module (CHB-2) with a 50μl sample injection loop. A Dionex thin layer flow cell, with 3mm diameter platinum working electrode, Dionex reference electrode (Ag/AgCl-pH) and a stainless steel cell body as the auxiliary electrode, was employed as the electrochemical cell. The electrochemical cell was controlled with a Dionex Pulsed Electrochemical Detector (PED-II) and the recorder was an ICI Instruments DP 600 chart recorder. The schematic of the system is shown in Figure 3.1 with the exploded view of the Dionex thin layer cell.

Conductivity measurements were made with a Phillips PW9501 conductivity meter. Solution pH was measured with a digital pH/mV meter (model SA520) (Orion).

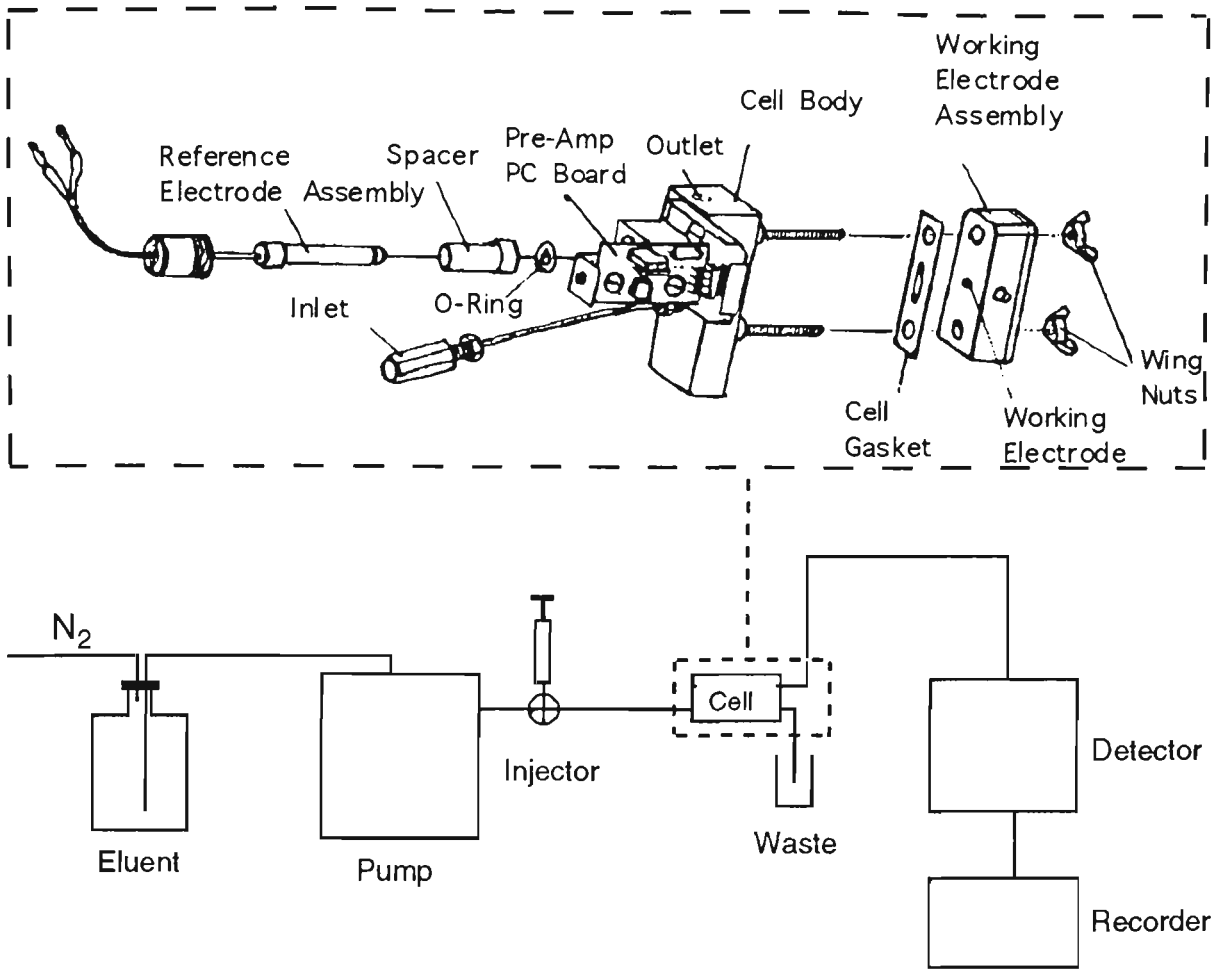

***Figure 3.1**: Schematic of Flow Injection Analysis System with the exploded view (in dotted lines) of the Dionex thin layer cell.*

3.2.3 Electrode Preparation

The polymer electrodes PPy/CSA, PPy/Cl, PPy/DS, PPy/SBA, PPy/PTS, PPy/HBSA and PPy/PVS were deposited on working electrodes by the method described in Chapter 2 and Section 2.3.1.

3.2.4 Electrochemical Characterisation

All polymer electrodes were characterised in 1 mM amino acid solutions by cyclic voltammetry. A scan rate of 50 mV/s was applied between potential values of 0.5V and -0.8V (where 0.5V was also the initial potential). Normal

pulse voltammetry and chronoamperometry were also performed in 1mM amino acid solutions.

3.3 RESULTS AND DISCUSSION

3.3.1 Electrode Preparation

All polymer electrodes were prepared galvanostatically from monomer solutions containing pyrrole and an appropriate electrolyte as described in Chapter 2, Section 2.3.1. The polymer electrodes were subjected to cyclic voltammetry in 0.1M $NaNO_3$ supporting electrolyte before flow injection analysis in order to check the electroactivity of the polymers. Only polymers having cyclic voltammetric responses similar to those obtained in Section 2.3.1.1 and 2.3.1.2, i.e. good electroactivity, were employed in FIA.

3.3.2 Electrochemistry in Amino Acid Solutions

The electrochemistry of the PPy/CSA electrodes was investigated in 1 mM amino acid solutions. The cyclic voltammograms are shown in Figure 3.2. The polymer did not show electroactivity in alanine, serine and arginine. That is, electrochemically controlled ion-exchange processes (described previously, Section 2.3.1.1) were not observed in these amino acids, but the upper and lower limits of current is variable depending on the amino acid employed. Such behaviour is typical of a system with high solution resistance due to lack of ions in the solutions and/or because it is difficult to incorporate larger ions into conducting polymers during the oxidation/reduction process. It has also been shown by Heineman et al. [8] that polypyrroles do not respond to zwitterions such as neutral amino acids. The conductance of the 1mM amino acid solutions is given in Table 3.3.

The low conductance of these amino acid solutions prevent their electrochemical analysis in conventional electrochemical experiments because the high solution resistance causes iR drop problems. Straight line cyclic voltammograms were obtained with the PPy/TBAP electrode in distilled water, glycine (1M) and non-zwitterionic electrolytes (such as 10^{-4}M KCl) of similar conductance [278].

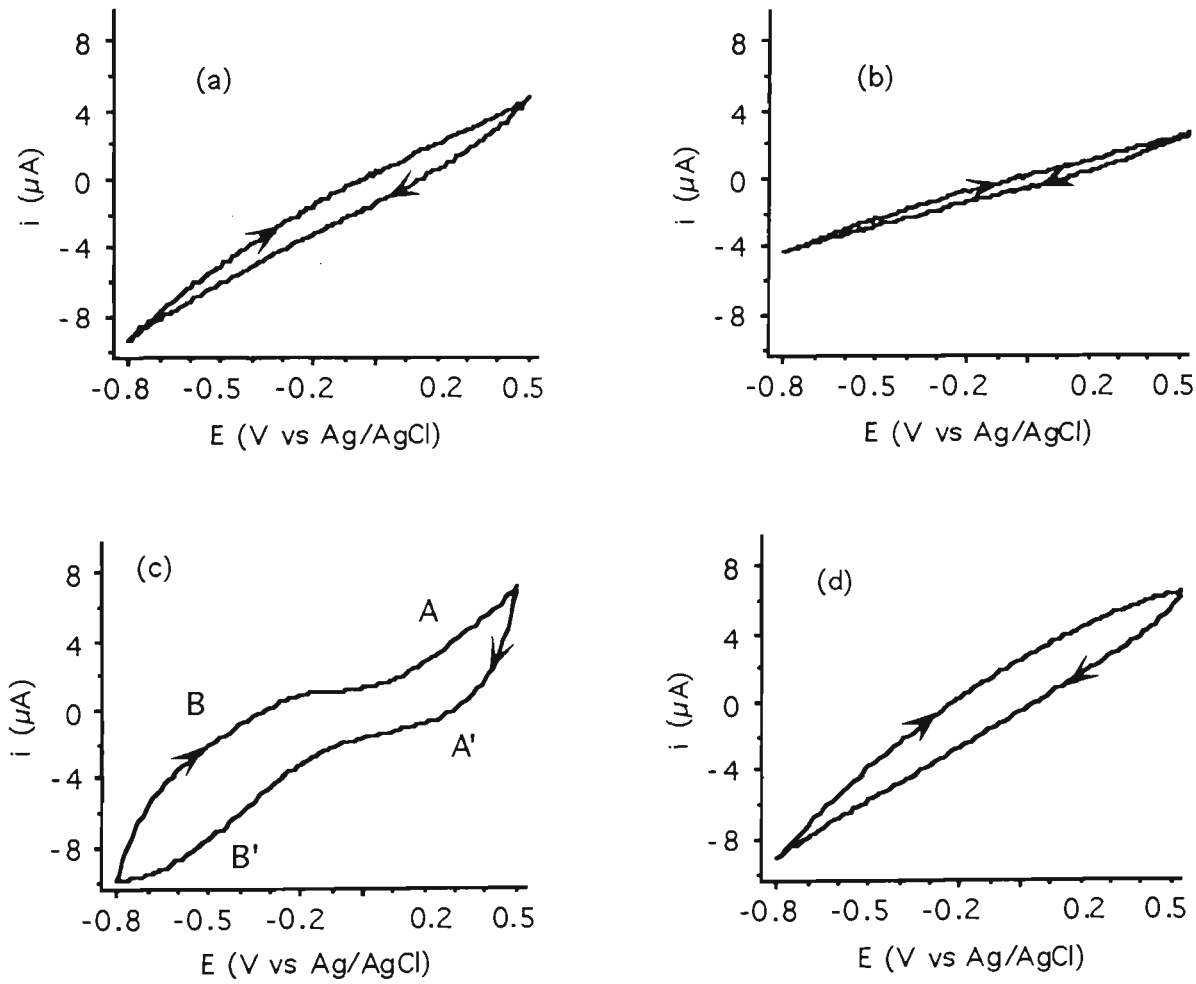

Figure 3.2: *Cyclic voltammetry of PPy/CSA in 1mM (a) alanine (b) serine (c) aspartic acid and (d) arginine solutions. Scan rate=50mV/s. Polymer electro-polymerised from Py (0.2M)/CSA (0.05M), current density=1mA/cm^2, and deposition time of 2min.*

In the case of aspartic acid, two oxidation/reduction peak couples were observed (A/A' and B/B', corresponding to the anion and cation movement in the redox process of the polymer (Section 1.3)). The current observed

with cyclic voltammetry is low compared to those recorded in the electrolytes tested in Chapter 2, which is perhaps due to the lower aspartic acid solution (1mM) conductivity (115.4μS). These observations suggest that the responses are highly effected by the resistive nature of the solutions which overrides any effects due to the interaction of the amino acid with the polymer.

However, it is important to note that the amino acid solutions have different pH values. Alanine and serine are of approximately pH 6, aspartic acid acid pH 3.5, and arginine pH 9.2. Presumably however, the cyclic voltammetric responses are unaffected by the amino acid solution pH, as conductivities of polypyrrole were shown to be less affected between pH 1-10 [282-284].

Table 3.3: *Conductance and pH of 1mM amino acid solutions*

Solutions	Conductance (μS)	pH
Water	1.4±0.2	5.7
Alanine	2.1±0.1	5.8
Serine	2.4±0.1	6.1
Aspartic Acid	115.4±0.2	3.5
Arginine	29.5±0.1	9.2

Condition; Amino acid solutions prepared in Milli-Q water. Conductance and pH of solutions were measured as described in Section 3.2.2.

The electrochemistry of the PPy/CSA electrode in amino acid solutions containing additional supporting electrolyte (0.1M $NaNO_3$) was also investigated (Figure 3.3). In solutions containing both alanine and $NaNO_3$, the voltammetric responses are equal to those recorded for $NaNO_3$ only (Section 2.3.1.1). Similar voltammetric behaviour was observed in serine

and arginine prepared in nitrate solutions. These results indicate that the presence of alanine, serine and arginine has no effect on the cyclic voltammetric responses for the polymer in 0.1M $NaNO_3$.

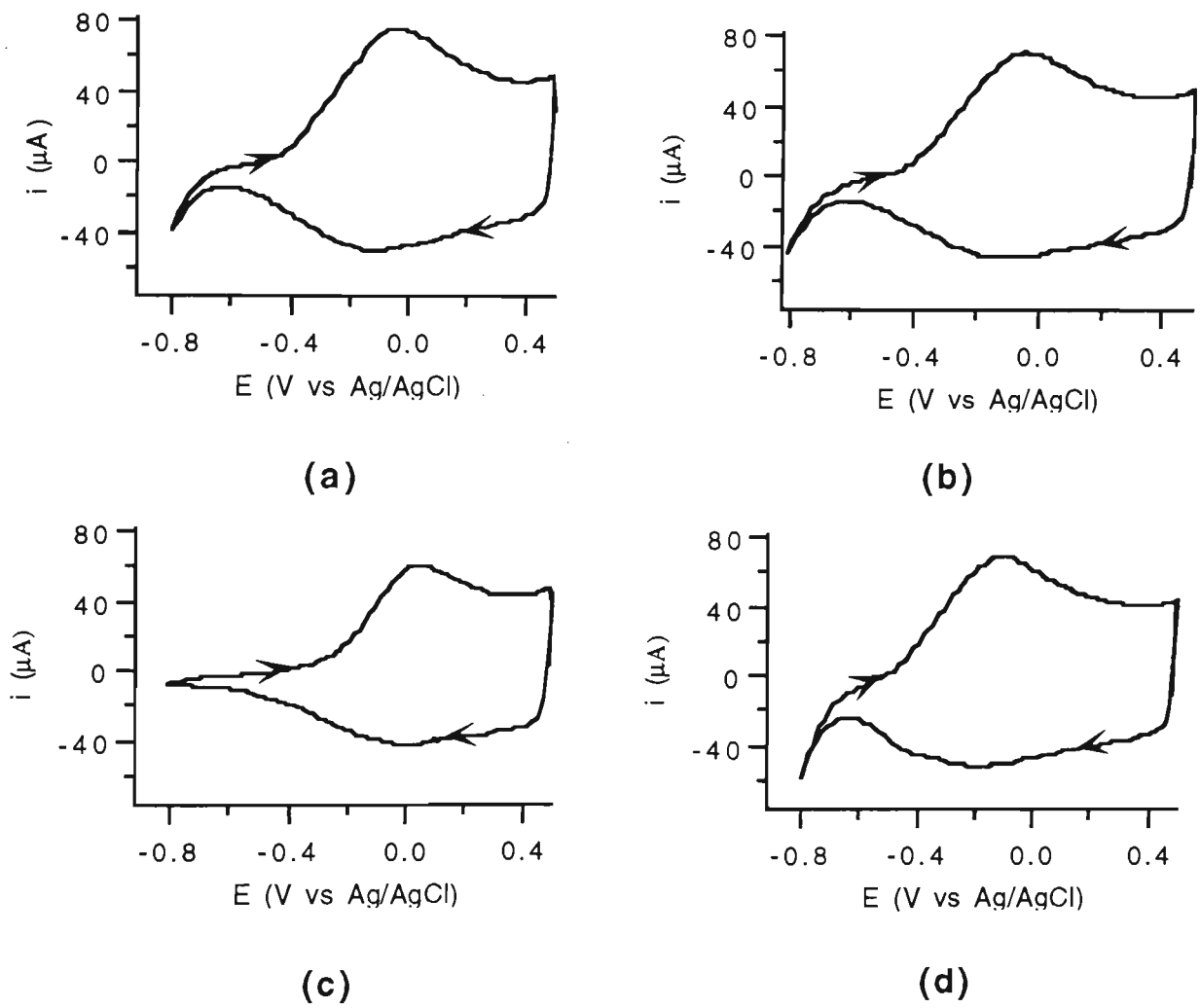

***Figure 3.3**: Cyclic voltammograms of PPy/CSA in 1mM amino acid prepared in 0.1M $NaNO_3$. (a) alanine, (b) serine, (c) aspartic acid and (d) arginine. Scan rate=50mV/s.*

In the presence of aspartic acid, the current decreased at more negative potentials, and the oxidation/reduction peaks were shifted positively by 100mV. However, no additional voltammetric responses due to aspartic acid were observed. The highly conductive $NaNO_3$ electrolyte masks any relatively low current due to the amino acid, where the conductance of 0.1M sodium nitrate and 1mM amino acid solutions is approximately 10mS. It is also possible that the presence of aspartic acid in sodium nitrate complicates

the ion-exchange process at the polymer electrodes by competing in the ion-exchange process. Reproducible cyclic voltammograms (up to 10 cycles) can be obtained without the loss of electroactivity of the polymer.

3.3.3 Normal Pulse Voltammetry

The use of normal pulse voltammetry (NPV) was also investigated using a PPy/CSA electrode. Normal pulse voltammetry is an important technique used to study the kinetics of anion doping at the polymer electrodes. Potential pulses of increasing pulse heights are applied and the sampled current output is plotted against the applied potential.

The NPV behaviour in sodium nitrate solution is shown in Figure 3.4. At lower concentrations of supporting electrolyte, no oxidation/reduction responses were observed. The increase in the nitrate concentration to 0.5M gave an asymmetric response due to anion doping at around 0.1V. Increasing the nitrate concentration to 1M produced a well defined a symmetric peak for anion doping at around 0.0V.

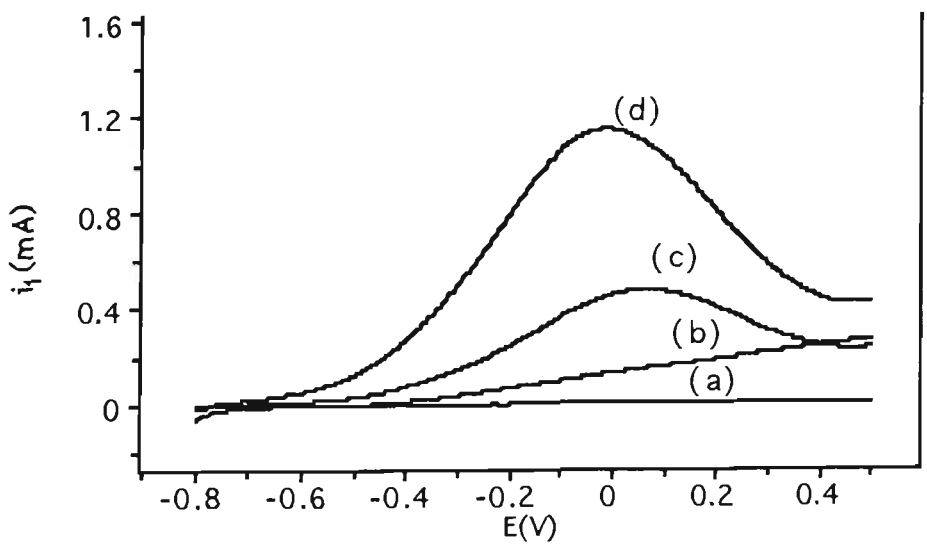

***Figure 3.4**: Normal pulse voltammograms obtained with a PPy/CSA electrode in $NaNO_3$ concentrations of (a) 0.0 M, (b) 0.1M, (c) 0.5 M and (d) 1M. E_i=-0.8V, E_f=0.5V, scan rate=20mV/s, step width=200ms, step height=4mV, pulse width=120ms, current sampled for 5ms at 115 ms.*

The anodic current was also recorded in alanine solutions of different concentration (Figure 3.5-i). No peak current potential was obtained in alanine solutions because of poor solution conductivity and/or limited polymer doping. Similar behaviour was observed in serine and arginine solutions.

In aspartic acid solutions the curves obtained (Figure 3.5-ii) show some response at anodic potentials, probably due to anion doping/dedoping. The curve is not very well defined and again this may be attributed to the low solution conductivity and/or the bulky nature of the anion [285]. The limited solubility of the amino acid in water prevents the increase of the acid concentration. The current obtained is dependent on the concentration, showing a drop with decrease in amino acid concentration culminating in a straight line in 1mM solutions. The ascending order of current magnitudes obtained was alanine ~ serine< arginine <aspartic acid.

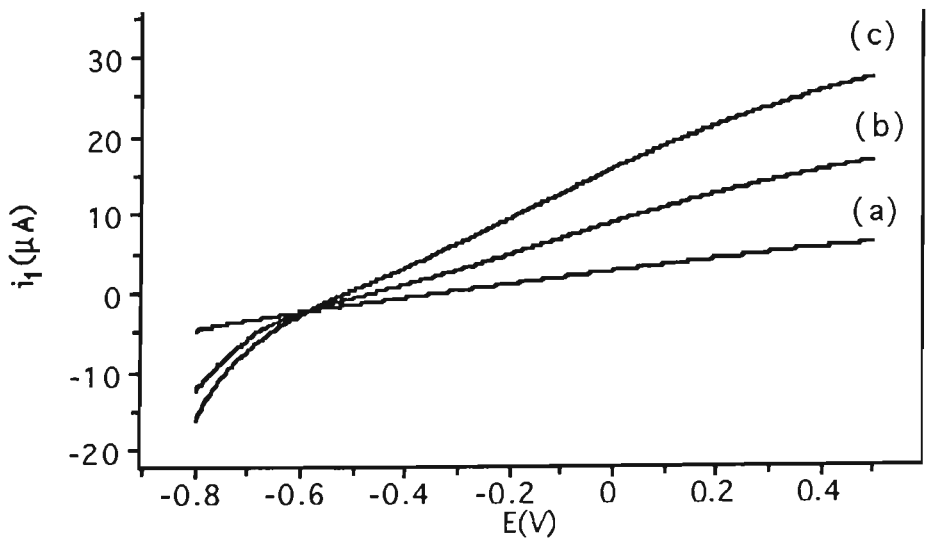

(i)

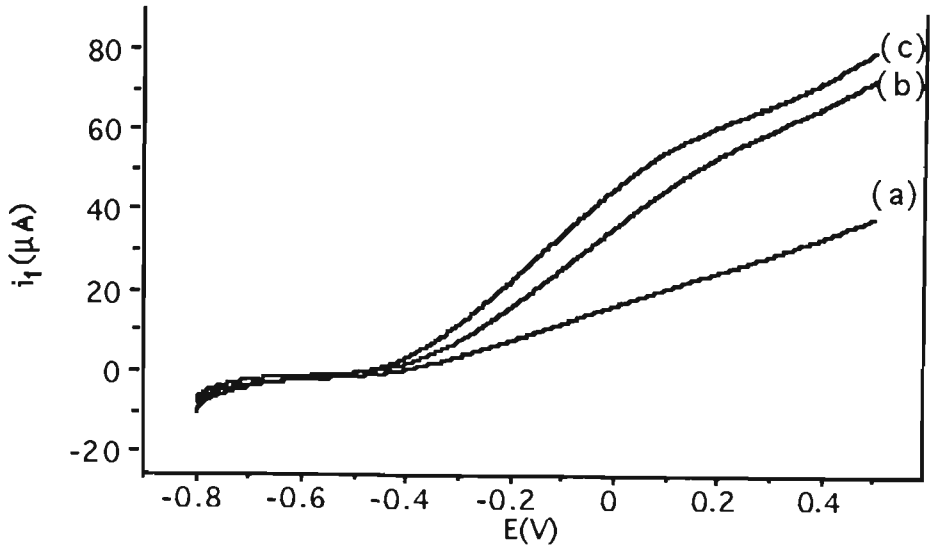

(ii)

***Figure 3.5**: Normal pulse voltammograms obtained at PPy/CSA in (i) alanine and (ii) aspartic acid. (a) 0.001 M (b) 0.01M (c) 0.02 M, E_i=-0.8V, E_f=0.5V, scan rate=20mV/s, step width=200ms, step height=4mV, pulse width=120ms, current sampled for 5ms at 115 ms.*

Since no significant NPV responses were obtained in alanine, serine and arginine, the NPV was not considered in 0.1M $NaNO_3$ in the presence of these amino acids. However, the NPV was performed in aspartic acid solutions prepared in sodium nitrate (Figure 3.6). The peak current and peak potential due to nitrate were affected by the presence of aspartic acid in the nitrate solutions. The peak potential was shifted by 200mV positively and a decrease was observed in the current. This suggests that the presence of aspartic acid affects the ion-exchange process of the nitrate in and out of the polymer by affecting the polymer properties.

The analysis can be carried out repeatedly without any loss in response, so it is not likely that the lower current and shift in peak potential indicate some deterioration in the electrochemical properties of the polymer in the presence of aspartic acid in the nitrate solution. This was confirmed by re-analysing the polymer electrode in nitrate solution alone after the above experiment in the presence of aspartic acid.

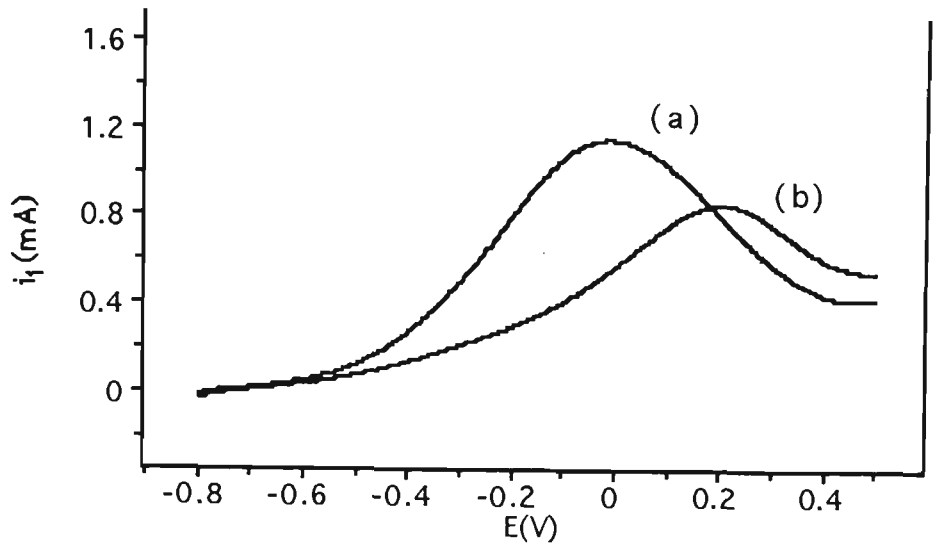

Figure 3.6: *Normal pulse voltammograms obtained at PPy/CSA in (a) 1M $NaNO_3$, (b) 0.02M aspartic acid in 1M $NaNO_3$. E_i=-0.8V, E_f=0.5V, scan rate=20mV/s, step width=200ms, step height=4mV, pulse width=120ms, current sampled for 5ms at 115 ms.*

3.3.4 Chronoamperometry

Chronoamperometry was performed in flowing solutions using the polymer coated (PPy/CSA) electrodes so as to more fully understand the time dependence of electrochemical ion-exchange processes. The responses of the system in these experiments provides information on polymer/amino acid interactions with applied pulse potential and flowing solutions.

The potential was first held at -0.8V and was stepped to 0.5V for 10ms. The potentials were selected to ensure that the polymer was reduced and oxidised. The current transients recorded in amino acid solutions are shown Figure 3.7. The i/t profile recorded varied accordingly with different amino acids. In alanine and serine, low currents were recorded, typical of i/t profiles observed with more resistive solutions. A well defined response

was observed in aspartic acid solution with greater current flowing compared to the other amino acids investigated. The current decay continued throughout the potential scan, but did not reach zero within this time frame (10ms). This indicates strong interaction between polymer and aspartic acid. In the case of arginine the current flow was less than that recorded in aspartic acid, probably due to the low conductivity of the arginine solution. However, the effect of the nature of the analytes on the rate of current decay was also evident. The anodic current flow follows the ascending order of alanine ~ serine< arginine< aspartic acid.

Chronoamperometry (CA) was also carried out in amino acid solutions prepared in $NaNO_3$ eluent (Figure 3.8). It was observed that the currents were lower at the polymer electrodes in the presence of amino acids. Also, the current decay was faster in the amino acids solutions compared with the nitrate solution. However, no distinction could be made between the individual amino acids. The high conductivity of the nitrate solution (~10mS) probably masks the effect of the amino acids. Also, the competition from NO_3^- for the doping sites is high.

Chronoamperograms obtained in amino acid solutions with no added $NaNO_3$ electrolyte showed that currents decayed at varying rates depending on solution composition. These differences demonstrate the importance of the solution ions on the electrochemical behaviour of the polymer.

However, it could be misleading to select the detection conditions from the observed chronoamperograms. This is because in CA the current has been measured throughout the scan and background current has not been eliminated.

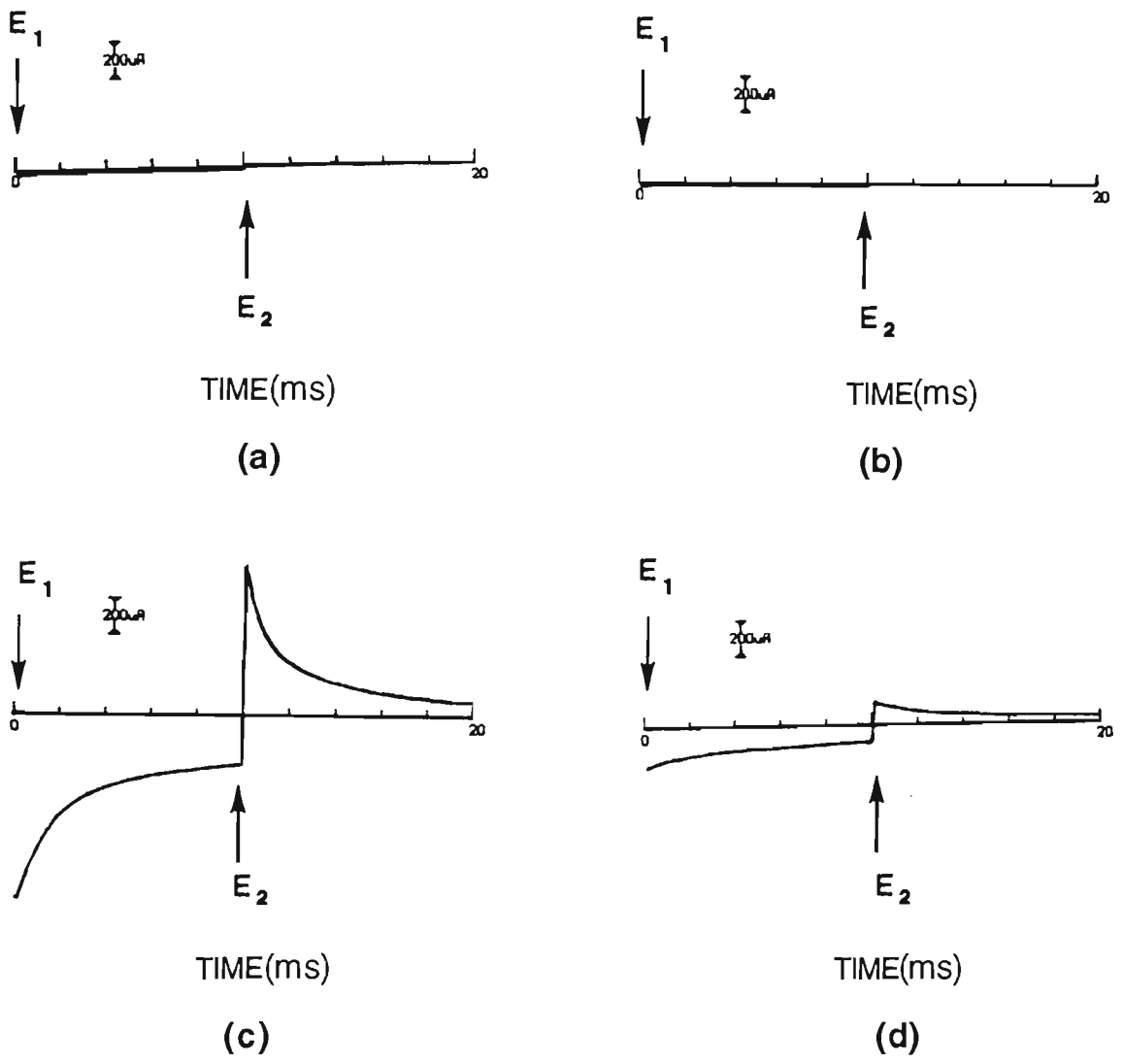

***Figure 3.7**: Chronoamperograms obtained using PPy/CSA in 1mM (a) alanine, (b) serine, (c) aspartic acid and (d) arginine. E_1=-0.8V, E_2=0.5V, pulse width=10ms. Flow rate = 1ml/min.*

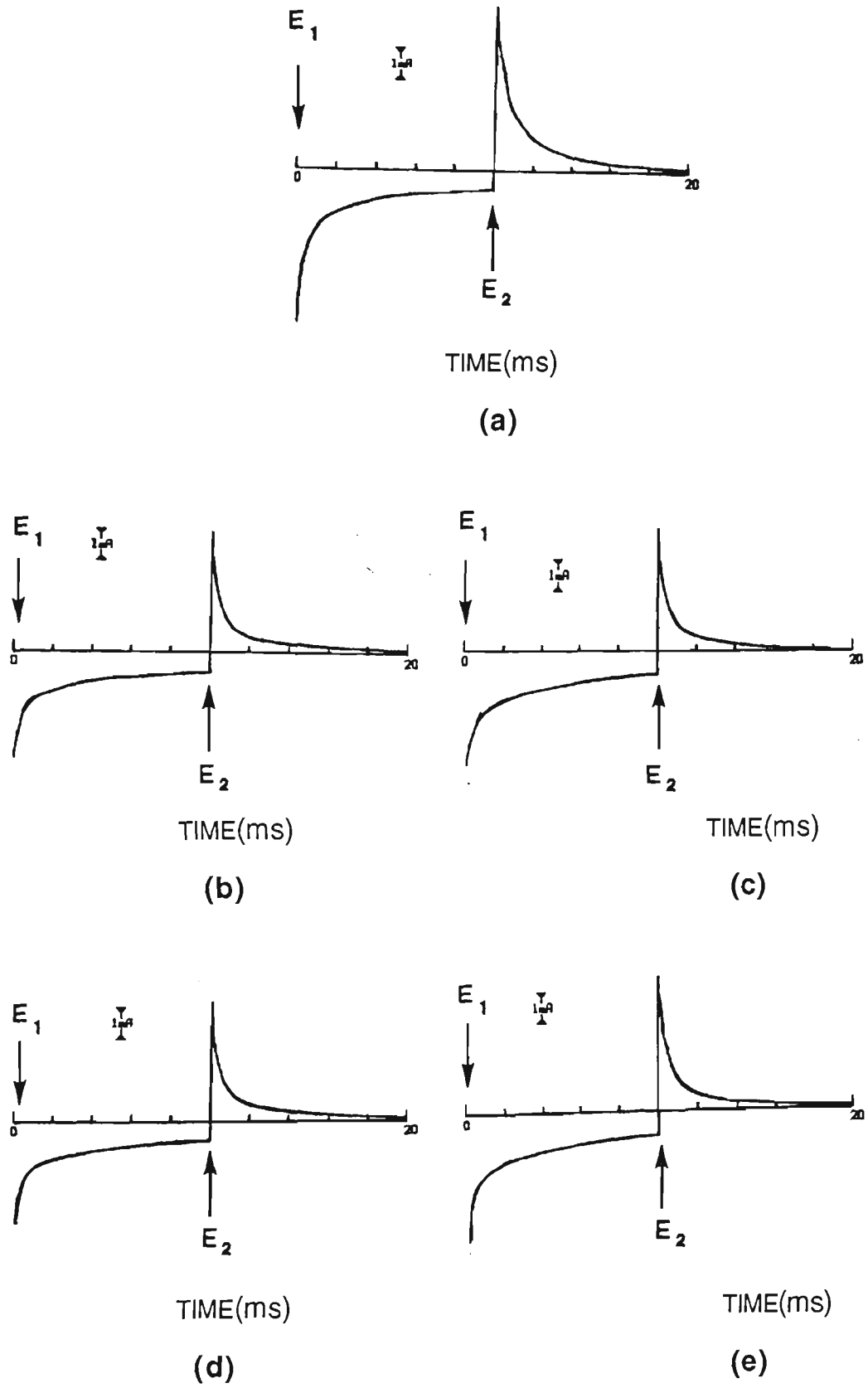

Figure 3.8: *Chronoamperograms at PPy/CSA in (a) 0.1M $NaNO_3$ and 1mM amino acids prepared in 0.1M $NaNO_3$, (b) alanine, (c) serine, (d) aspartic acid and (e) arginine. E_1=-0.8V, E_2=0.5V, pulse width=10ms. Flow rate = 1ml/min.*

3.3.5 Flow Injection Analysis

The electrochemical conditions that influence the detection of amino acids were optimised at PPy/(+)CSA. The following analyses were carried out.

1) Constant potential analysis.

2) Pulsed potential analysis; including the investigation of:

- effect of E_1 and E_2,
- effect of pulse width,
- effect of current sample point.

3.3.5.1 Constant Potential Amperometric Detection

A series of anodic and cathodic potentials between -0.4V to +0.5V were applied to the polymer electrode such that the electrode exists in either the conductive or resistive state. The current responses were measured and peak height (μA) was used as the analytical signal.

The peak height (amperometric responses) as a function of applied potential are shown in Figure 3.9. The signal generated on polymer electrodes for particular amino acids was found to be potential dependent. For alanine and serine the FIA responses were not very large. The peak magnitude was the same for both acids and increased with increasing applied potential value. No response was observed with an applied potential of below 0.2V. The small responses observed may be due to the fact that hydrophobic interactions and hydrogen bonding (with alanine and serine because of non-polar and polar R-groups respectively) are not strong enough to produce strong signals. The responses observed could be due to some disruption of the polymer electrode/eluent equilibrium as the analyte plug passes over the electrode surface.

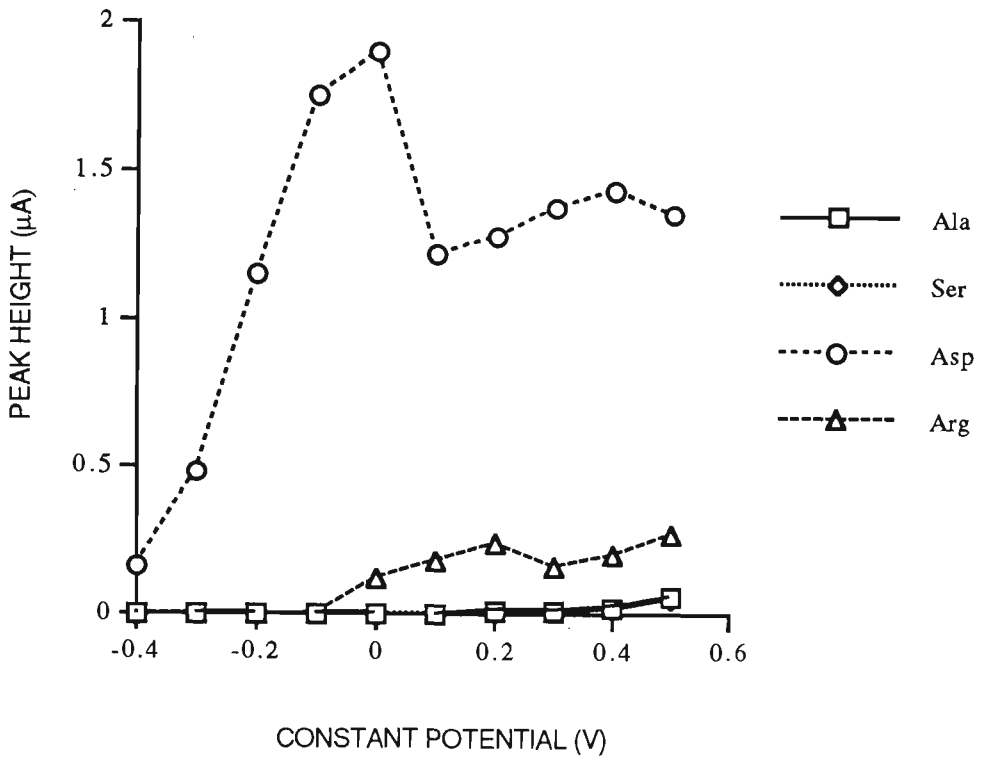

***Figure 3.9**: Amperometric responses at PPy/(+)CSA during FIA of 0.2mM alanine, serine, aspartic acid and arginine. Eluent: 0.1M $NaNO_3$. Flow rate=1ml/min. Injection volume=50μl. Values plotted represent the average of 3 measurements. (alanine and serine have the same response values, therefore serine is not visible in the plot).*

Well defined FIA responses were obtained for aspartic acid tat each applied potential. However, noise and baseline drift at extreme potentials (0.5V and -0.4V) were observed. The peak height increased with increasing potential, a maximum response obtained at 0.0V. Between 0.0V to 0.1V a decrease in peak magnitude was observed and responses were little affected by further potential increases. The peak widths did not change with applied potential. The FIA peaks for aspartic acid at 0.0V are shown in Figure 3.10-a. The peak broadness indicates strong interaction between the aspartic acid and polymer film. The relatively large current and the presence of maxima in the hydrodynamic voltammogram (HDV) reflect the polymer switch from non-conducting to conducting state as the potential was shifted positively. This

also indicates that the doping/dedoping of the polymer was occurring in the acidic amino acids and the current obtained was faradaic in nature.

Compared with aspartic acid, the signal for arginine was smaller and the polymer was not responsive below 0.0V. The broader, tailing peaks obtained for that amino acid are indicative of stronger interactions between arginine and polymer (or of interactions of a different nature). The signal obtained is shown in Figure 3.10-b.

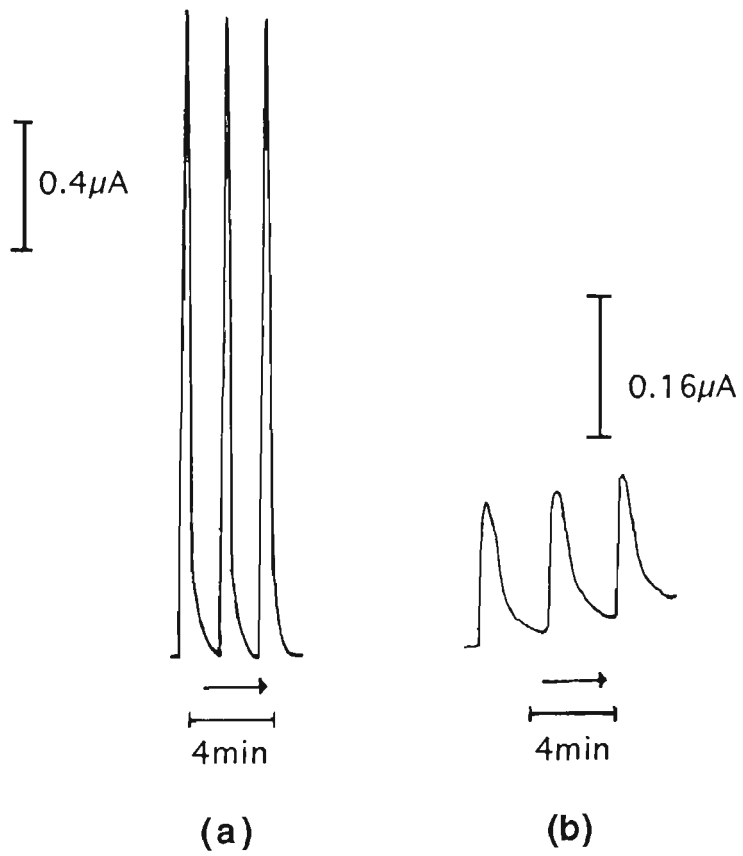

***Figure 3.10**: FIA peak for (a) aspartic acid (0.2mM) and (b) arginine (0.2mM) at PPy/(+)CSA at 0.0V. Eluent=0.1M $NaNO_3$. Flow rate=1ml/min. Sample loop=50μl.*

The conductance and pH of amino acids in the eluent is given in Table 3.4. Since the eluent and amino acid solutions injected have the same solution conductance, the current responses are mainly faradaic in nature. The other factor that may contribute to the signal might be the difference in pH of the

analyte and eluent. Although the conductivity of the PPy is less affected in the pH range 1-10 [282-284], it is possible that part of the responses for arginine and aspartic acid solutions is due to the pH differences of the analytes and eluent. Some rearrangement of the polymer chain [204] or the electrostatic interactions between the polymer chain and the dopant can also be important factors in the pH dependence of polymer conductivity [286].

Table 3.4 *Conductance and pH of 0.2mM amino acids in 0.1 M $NaNO_3$**

Solutions	Conductance (mS)	pH
Sodium nitrate	~10	5.7
Alanine	~10	5.7
Serine	~10	5.8
Aspartic acid	~10	4.2
Arginine	~10	8.0

* *Concentration of sodium nitrate solution=0.1M. Conductance and pH of the solutions were measured as described in Section 3.2.2.*

The same response magnitude could not be obtained when the DC amperometric detection experiment of aspartic acid was repeated on the same electrode. The response magnitude suffered a 50% decreased at 0.0V, the potential of maximum aspartic acid response. This may have been due to polymer electrode fouling, since the polymer was not regularly oxidised and reduced.

3.3.5.2 Pulsed Integrated Amperometry

Pulsed electrochemical detection was also employed to eliminate the limitations associated with constant potential amperometric detection, such as low sensitivity for alanine, serine, and arginine and to avoid electrode fouling. A sequence of repetitive symmetric pulses were applied to the polymer. E_1 was fixed at 0.0 V where the signal was maximum for aspartic acid (with DC) and the current was sampled at this potential. E_2 was varied from -0.2V to +0.5V. The current sampling point was chosen at the end of the pulse to avoid the charging current and thereby maximise the S/N ratio. Sampling point duration was 30 ms and kept constant throughout the experiment. The analytical signal is expressed in coulombs, as the detector (PED-II) integrates the current over the sampling period. The applied potential waveform is shown in Figure 3.11.

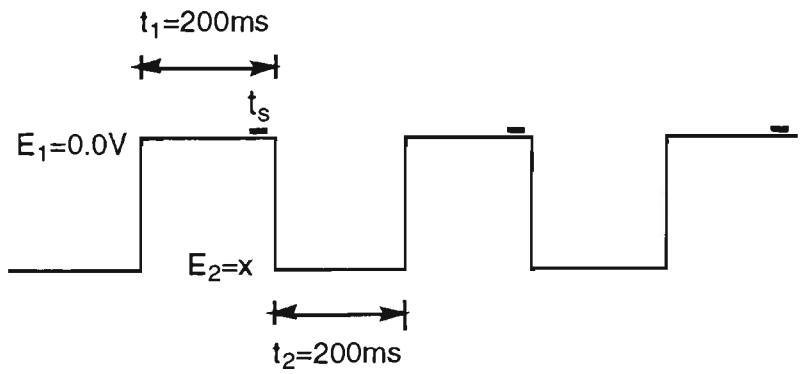

Figure 3.11: *Pulsed potential waveform for integrated amperometry. E_1=electrode potential fixed at 0.0V, E_2=electrode potential varied between -0.2V and 0.5V, t_1=time period for E_1, t_2=time period for E_2, t_s= current sampling point.*

It took almost 2 hours for the base line to stabilise where E_2=-0.2V. The base line drift was 20μC/min in the first hour, and only gradually decreased and then stabilised. The FIA responses in the form of histograms are shown in Figure 3.12.

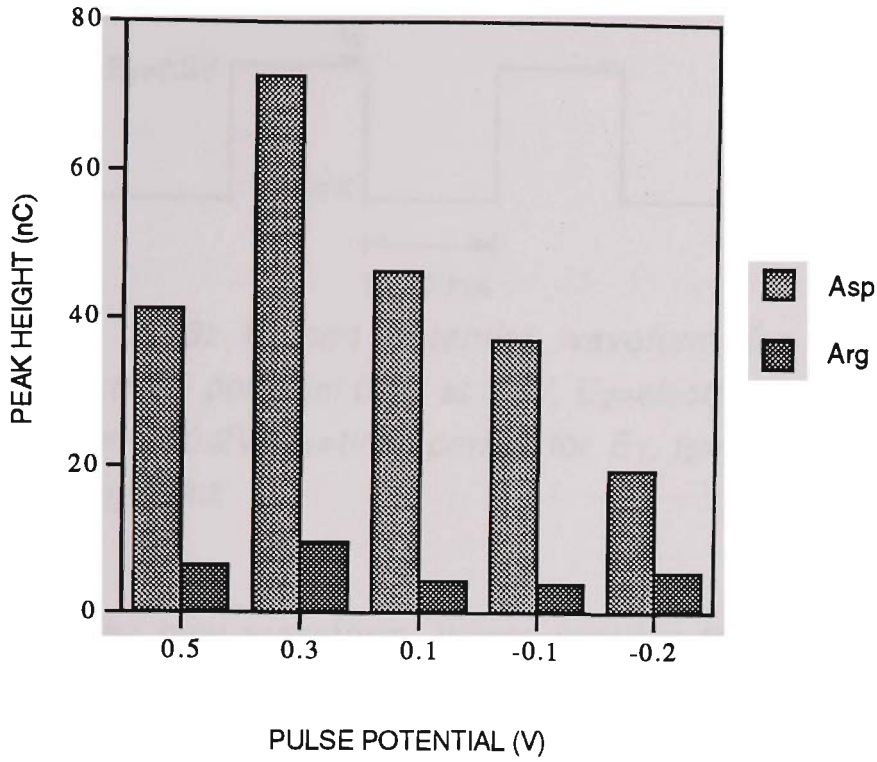

***Figure 3.12**: Responses for amino acids at PPy/(+)CSA with pulsed integrated amperometry. E_1=0.0V, E_2 varied as in x-axis. t_1=t_2=200ms, t_s=160-190ms and sampled at E_1. Amino acid concentration=0.2mM. Eluent =0.1M $NaNO_3$. Flow rate=1ml/min. Injection volume=50µl.*

No responses were obtained for either alanine or serine for E_2 between -0.2V and 0.5V. These two amino acids are not in an ionic state and any disruption in the ion-exchange process due to eluent ions is unmeasurable under these electrochemical conditions. As E_2 was varied from -0.2V to 0.5V, the signal for aspartic acid increased with a response maximum obtained at E_2=0.3V. For arginine, the magnitude of the response was lower than that obtained for aspartic acid at all E_2 potentials applied but as for aspartic acid, the maximum was obtained at E_2=0.3V.

Consequently, E_1 was fixed at +0.3V and the current was sampled at this potential over 30ms at the end of the pulse. E_2 was varied from -0.6V to -0.2V. The waveform is shown in Figure 3.13.

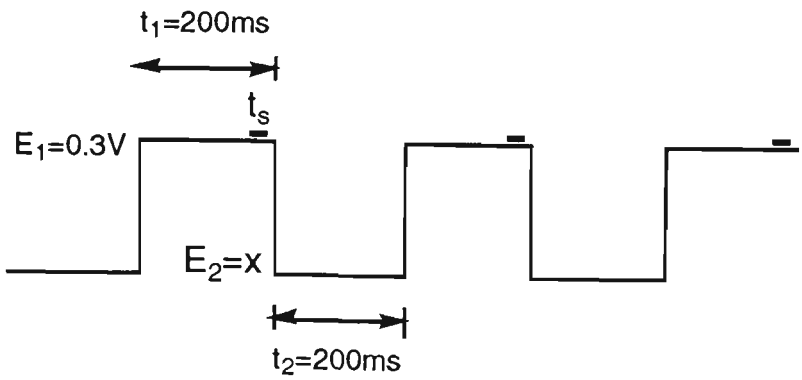

Figure 3.13: *Pulsed potential waveform for integrated amperometry. E_1=electrode potential fixed at 0.3V, E_2=electrode potential varied between -0.6V and -0.2V, t_1=time period for E_1, t_2=time period for E_2, t_s=current sampling point.*

Using the new waveform, it was possible to obtain responses for all four amino acids (Figure 3.14). The responses were dependent on the E_2 potential applied. Between the reduction potentials -0.6V and -0.4V, the aspartic acid response was little affected, perhaps because the polymer reduction states does not change between these potentials as also indicated in the CV (Figure 3.3-c). Consequently, the component of the signal arising from the anion exchange was not affected. This may suggest that anion exchange is the dominant factor contributing to the signal for aspartic acid. The FIA peaks for aspartic acid are shown in Figure 3.15.

The electronic conductivity of the polymer at a particular potential is also important. A further shift in the applied reduction potential to -0.2V had a marked effect on the responses observed. Aspartic acid gave smaller responses and a post-peak dip was observed, indicating that if the polymer is not fully oxidised and reduced, the analyte/polymer interactions are not completed.

The signals for alanine and serine could be due to some disruption to the eluent anion and cation accessibility to the polymer electrode which occurs

as the analyte plug passes over the polymer electrode (also suggested by the peak direction, which was negative). This effect was influenced by the shift in E_2 potential. For alanine and serine the response decreased with decreasing potential.

For arginine, the response may be due to cation movement therefore a more negative potential is favourable for such interactions.

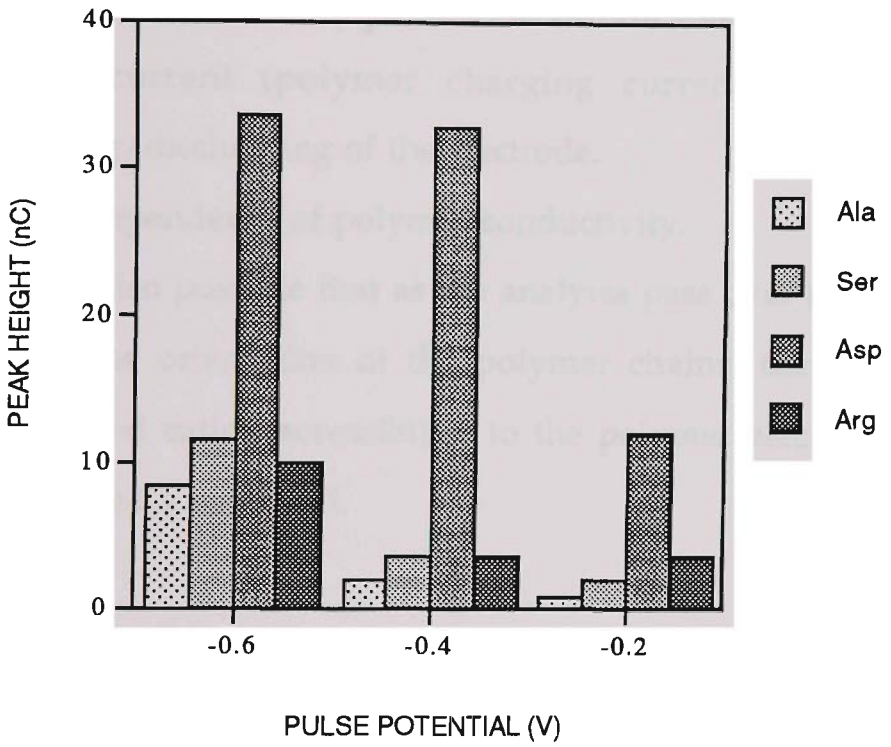

***Figure 3.14**: FIA responses for the four amino acids at PPy/(+)CSA electrode. E_1=0.3V; E_2=-0.6V, -0.4V and -0.2V; t_1=t_2=200ms, t_s=160-190ms and current sampled at E_1. Eluent=0.1M $NaNO_3$. Flow rate=1ml/min. Analytes were 0.2mM amino acids in 0.1M $NaNO_3$. Injection volume=50µl.*

These observations suggest that the signals generated at the polymer electrodes are complex, as the responses differ so drastically between the amino acid species. Each signal may be the result of the combined effects of several factors [29]. That is, the signal is not just due to simple doping/dedoping of the polymer electrodes. It has been observed that the potential applied (DC or pulsed) affects the signal magnitude, direction and

shape. The factors which may contribute to the signal as a function of applied potential are as follows:-

1) The electronic conductivity of the polymer electrode [185] is a function of potential applied. The i_{pd} current (current due to polymer doping/dedoping) is produced as the doping/dedoping of the eluent ions occur.

2) The ion-exchange process due to analyte incorporation/expulsion contributes current as i_{pa} (anodic current due to analyte ion movement).

3) i_{pc} current (polymer charging current) is produced due to the charging/discharging of the electrode.

4) pH dependence of polymer conductivity.

5) It is also possible that as the analytes pass over the electrode surface, they affect the orientation of the polymer chains, thereby affecting the eluent anion and cation accessibility to the polymer electrode. This factor would affect the i_{pc} produced.

From the observation that the responses differ so drastically between the amino acid analytes it can be concluded that the nature of the analyte plays the predominant role.

The experimental conditions with E_1=0.3V and E_2=-0.6V were selected for further analysis because responses for all four analytes were obtained under these conditions.

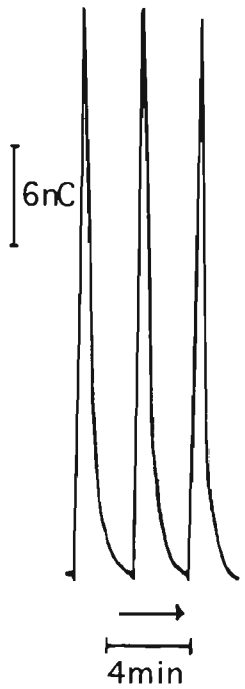

***Figure 3.15**: FIA peaks for aspartic acid (o.2mM) at PPy/(+)CSA pulsed integrated amperometry. E_1=0.3V, E_2=-0.6V, t_1=t_2=200ms, t_S=160-190ms. Eluent=0.1M $NaNO_3$. Flow rate=1ml/min. Injection volume=50µl.*

The effect of the current sampling point on the FIA response was investigated for aspartic acid as it gave the most sensitive FIA peaks. The current was sampled at three different points for a period of 10ms along E_1 (0.3V). Two pulse widths were considered; pulse waveform 1 and pulse waveform 2 shown in Figure 3.16 and Figure 3.17 respectively.

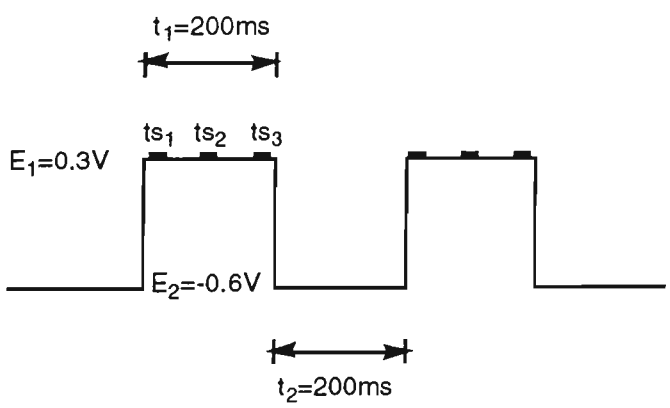

***Figure 3.16:** Potential pulse waveform 1 with current sampling point positions. E_1=0.3V, E_2=-0.6V, ts_1=10-20ms, ts_2=100-110ms, ts_3=180-190ms, t_1=t_2=200ms.*

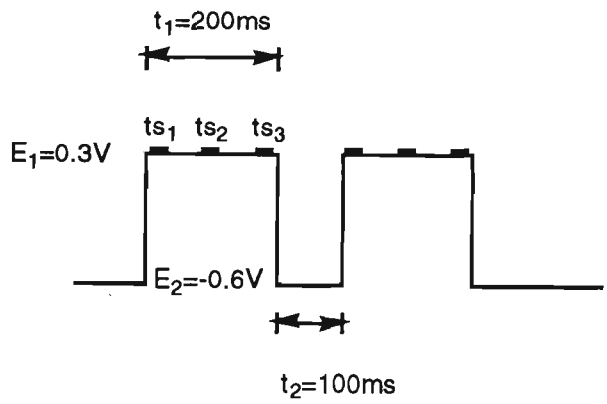

Figure 3.17: *Potential pulse waveform 2 with current sampling point positions. E_1=0.3V, E_2=-0.6V, ts_1=10-20ms, ts_2=100-110ms, ts_3=180-190ms, t_1=200ms, t_2=100ms.*

Sampling the current at the beginning of the pulse produces a bigger response. This could be due to electrode charging effects. There was no significant difference in aspartic acid sensitivity (Figure 3.18) between sampling in the middle or at the end of the pulse.

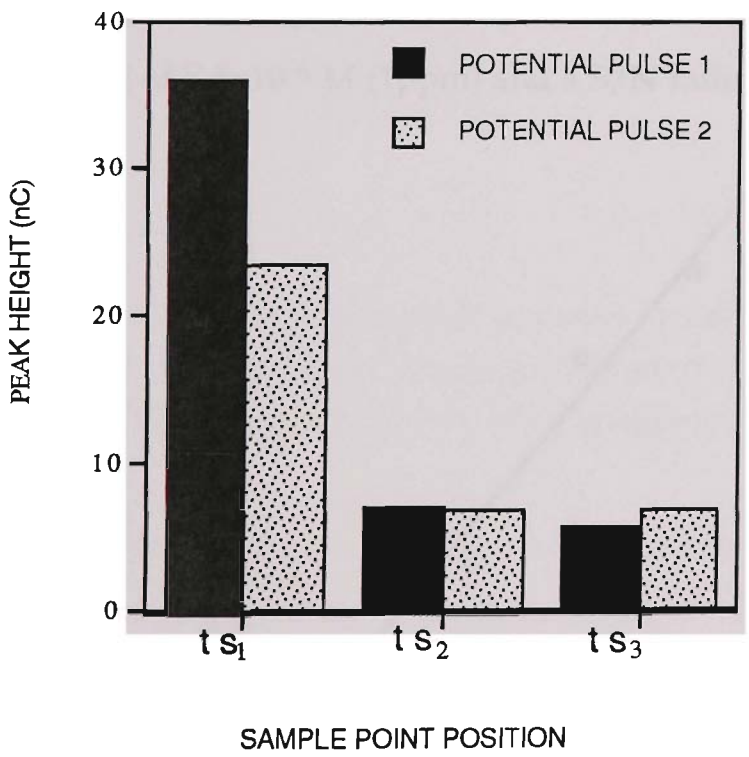

Figure 3.18: *Effect of current sampling point position on the responses of 0.1mM aspartic acid. E_1=0.3V, E_2=-0.6V, ts_1=10-20ms, ts_2=100-110ms, ts_3=180-190ms, t_1=t_2=200ms for pulse 1, t_1=200ms, t_2=100ms for pulse 2. Eluent=0.1M $NaNO_3$. Flow rate=1ml/min. Injection volume=50µl.*

When the width of the negative pulse was decreased to 100ms, the response at the beginning of the pulse decreased, which once again might reflect the charging of the electrode. However, the responses at the ts_2 and ts_3 positions were similar in magnitude for both pulses. This indicates that the magnitude of the responses was unaffected by the width of the negative pulse when sampled later in the pulse (at ts_2 and ts_3). The S/N ratio was 1 at ts_1 whereas S/N was 3 at ts_3. For this reason current sampling at ts_3 is preferable.

3.3.5.3 Sensitivity, Stability and Reproducibility

Using the optimised conditions, a calibration curve was obtained for a series of aspartic acid concentrations (Figure 3.19). The linear response concentration range was between $7.5x10^{-6}$ M and $6x10^{-5}$M with a limit of detection of $7.5x10^{-6}$ M (1ppm) and a S/N ratio of 3.

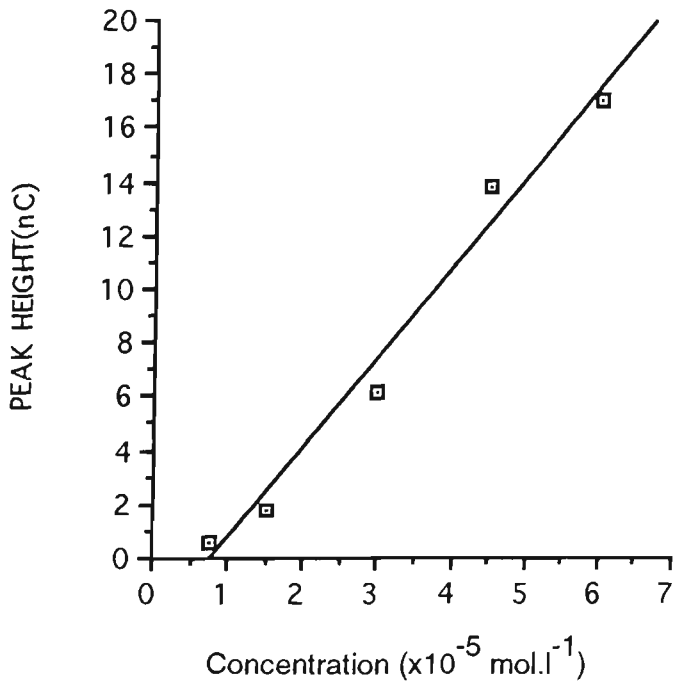

***Figure 3.19**: Calibration curve for aspartic acid at PPy/CSA. E_1= 0.3V, E_2=-0.6V, t_1=t_2=200ms, t_S=160-190ms. Flow rate=1ml/min. Eluent=0.1M $NaNO_3$. Injection volume=50µl.*

The sensitivity calculated from this calibration curve for aspartic acid is 334μC/mol.l^{-1}, with intercept -2.66 nC and correlation coefficient of 0.979 (99% confidence level, 3 degrees of freedom). Responses are given in Figure 3.20. It can be seen that the responses are well defined even at low analyte concentrations.

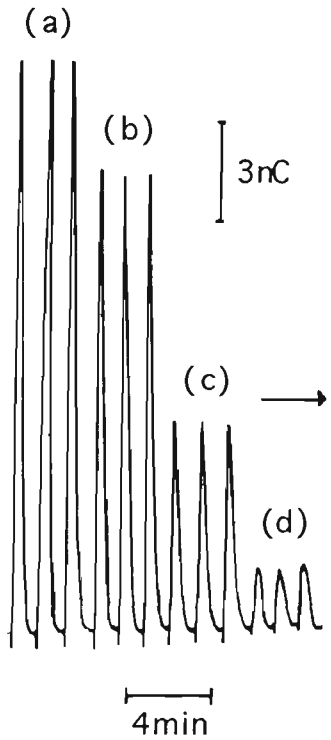

***Figure 3.20**: Typical responses obtained for aspartic acid using a PPy/CSA electrode. Concentrations of aspartic acid were (a)6x10^{-5}M, (b) 4.5x10^{-5}M, (c) 3x10^{-5}M and (d) 1.5x10^{-5}M. FIA Conditions same as in Figure 3.19.*

The reproducibility of the method was estimated by making eight repetitive injections of 4.5x10^{-5}M aspartic acid (Figure 3.21). The responses obtained were reproducible (13.88±0.21nC) with no sign of response deterioration over a period of approximately 20 minutes.

During pulsed integrated amperometry, the long term stability of the polymer response was monitored over 12 hours. In general, the electrode showed a gradual decrease in response during continuous use over this

extended period of time. The response decreased 25% after 12 hours of analysis (Figure 3.22). However, responses vary for every fresh electrode prepared.

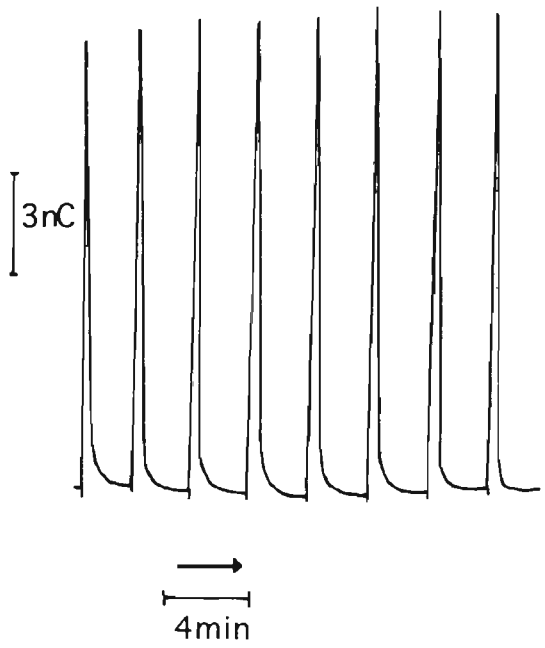

Figure 3.21 *Reproducibility of the polymer response for eight injections at PPy/(+)CSA electrode. E_1=0.3V, E_2=-0.6V, t_1=t_2=200ms, t_s=160-190ms. Aspartic acid concentration=4.5x10^{-5}M. Flow rate=1ml/min. Eluent=0.1M $NaNO_3$. Injection volume=50µl.*

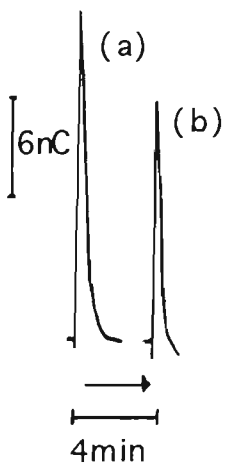

Figure 3.22: *Stability of the 0.1mM aspartic acid FIA response at PPy/(+)CSA electrode (a) At the beginning of the analysis and (b) After 12 hrs. FIA conditions as in Figure 3.21.*

Cyclic voltammetry of the polymer after use in FIA (12 hr) indicated no apparent electrode fouling. The polymer was still electroactive with well defined oxidation/reduction peaks (Figure 3.23). However, the electroactivity of the polymer electrode deteriorated upon storage in 0.1M $NaNO_3$ for 24 hours. Therefore, long term stability from day to day was not investigated.

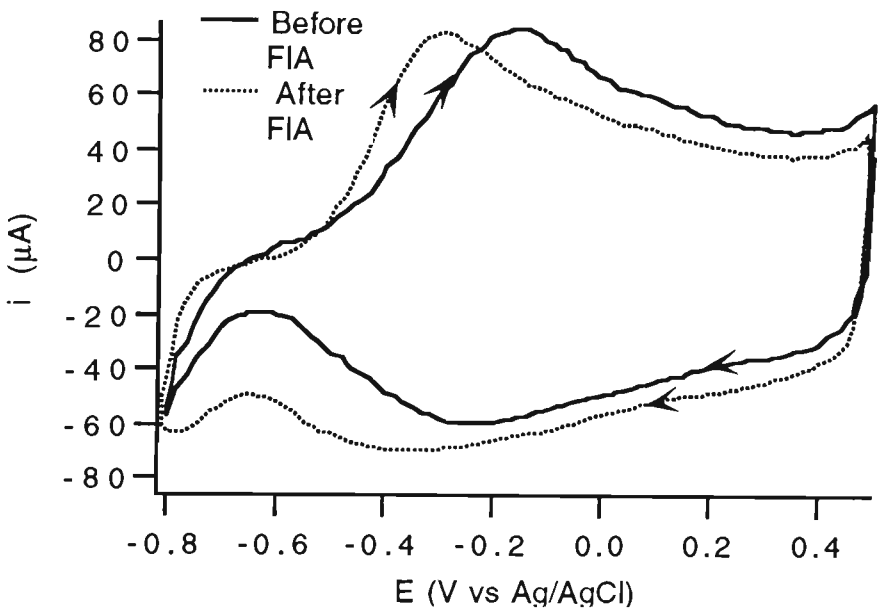

Figure 3.23 *Cyclic voltammograms of PPy/(+)CSA in 0.1M $NaNO_3$ before and after 12 hours of aspartic acid FIA. Scan rate=50mV/s.*

3.3.5.4 Effect of Polymer Composition on Sensitivity and Selectivity towards Amino Acids

The selectivity for anions of potentiometric polypyrrole sensors were reported to be influenced by the anion incorporated during polymer synthesis. The sensor electrodes were found to be most selective for the parent dopant [184]. This concept is important for improving the selectivity of a chemical sensor, as it suggests that selectivity can be improved by changing the doping ion and the polymerisation conditions used [285]. The

effect of the counterions incorporated during polymerisation, on the selectivity of the electrode for the amino acids was investigated. The polymer electrodes were prepared by incorporating a range of counterions, Cl^-, DS^-, SBA^-, PTS^-, $HBSA^-$, and PVS^- as described in Section 2.3.1. The optimal conditions found for PPy/(+)CSA in Section 3.3.5.2 were also applied here to detect amino acids on these polymer electrodes. The magnitude of responses on these electrodes are shown in Figure 3.24.

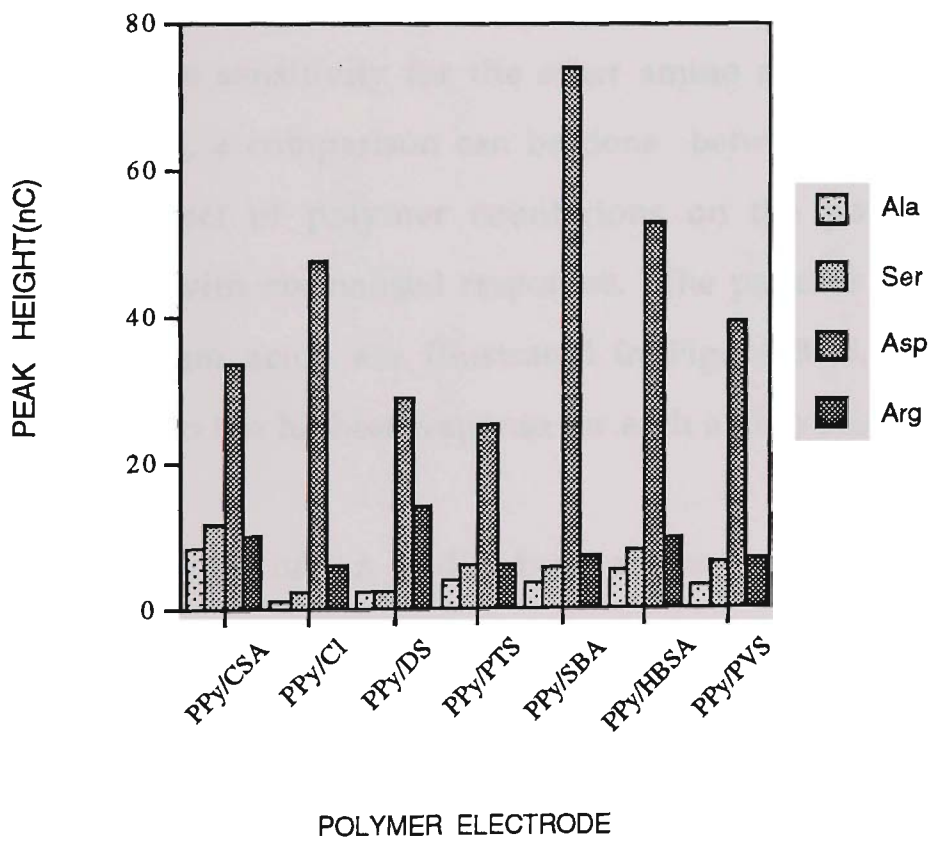

***Figure 3.24**: Magnitude of FIA responses for four amino acids on seven different polymer electrodes. E_1= 0.3V, E_2=-0.6V, t_1=t_2=200ms, t_S=160-190ms. Flow rate=1ml/min. Eluent=0.1M $NaNO_3$. Analytes injected =0.2mM amino acids. Injection volume=50µl.*

The sensitivity of each amino acid varies with the counterions incorporated in the polymer. This suggests that each particular polymer electrode has a different affinity for the four amino acids. This also indicates that all those

factors previously described (Section 3.3.5.2) which contribute to the signal currents, such as doping/dedoping of the polymer by eluent ions, analyte ion doping/dedoping, charging current, effect of pH on polymer conductivity and polymer chain movement are also dependent upon the polymer composition. However, aspartic acid produced the maximum response on each electrode considered and sensitivity was maximum at PPy/SBA. This could be due to the intrinsic anion exchange ability of the polymer film which suggests that the major component of the signal produced arises from anion exchange processes.

Although the sensitivity for the other amino acids is lower than that for aspartic acid, a comparison can be done between individual amino acids and the effect of polymer counterions on the polymer selectivity, by histograms with normalised responses. The patterns observed in response to four amino acids are illustrated in Figure 3.25, where the graph is normalised to the highest response for each amino acid.

The selectivity of an individual amino acid is dependent on the composition of the polymer. As patterns given in Figure 3.25 show, the neutral amino acids (alanine and serine), acidic and basic amino acids, have different affinity for the polymer electrodes. The patterns for alanine and serine correlate closely, with maximum sensitivity obtained at PPy/CSA. For aspartic acid, maximum signal was produced at PPy/SBA, and arginine shows most affinity for the PPy/DS, where cation incorporation at negative potentials is expected [69,189,287].

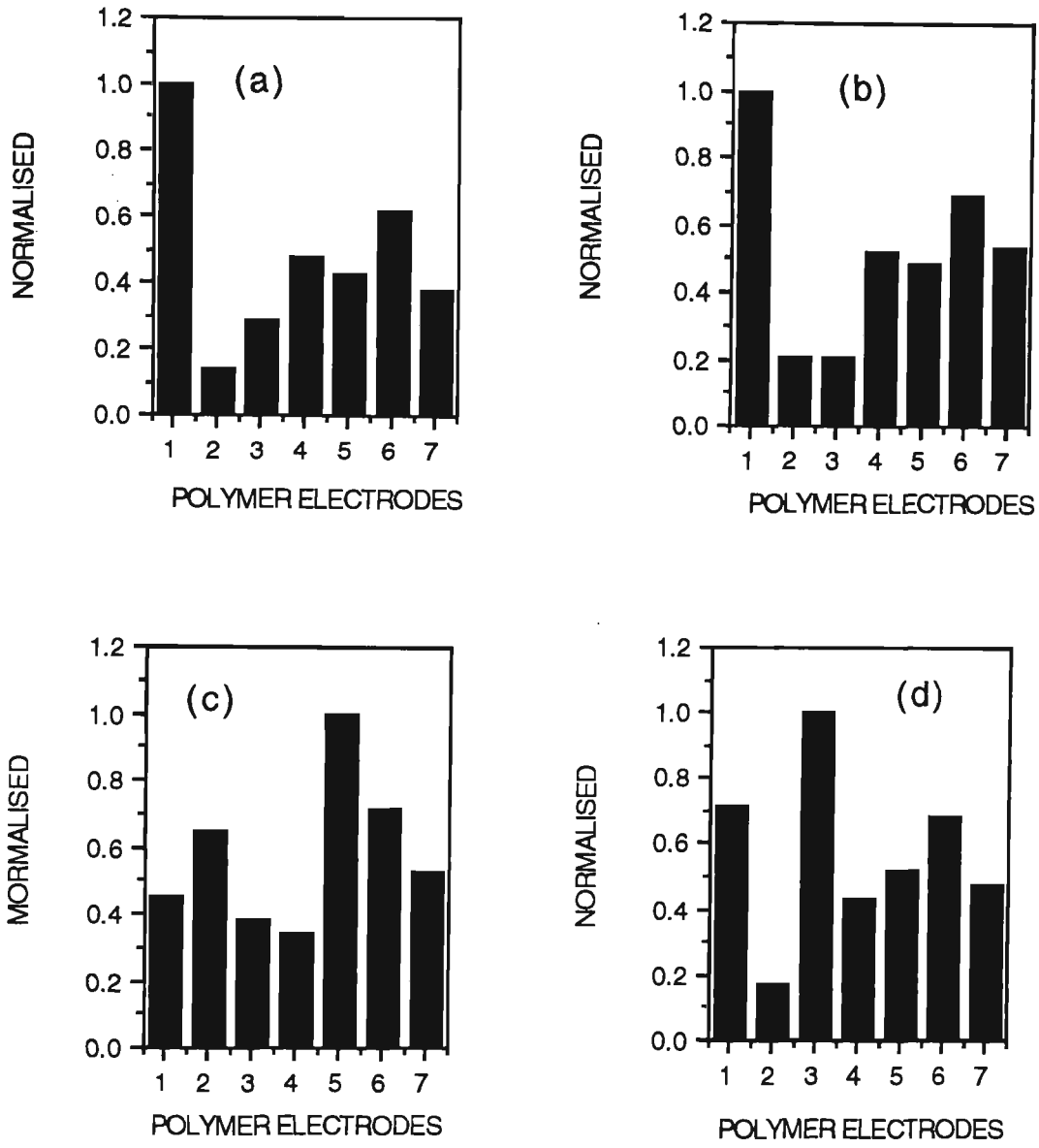

Figure 3.25: *Normalised patterns obtained from multiple sensors. (a) alanine (b) serine, (c) aspartic acid and (d) arginine. Sensors are:- 1=PPy/CSA, 2=PPy/Cl, 3=PPy/DS, 4=PPy/PTS, 5=PPy/SBA, 6=PPy/HBSA and 7=PPy/PVS. Data taken from Figure 3.24.*

These patterns obtained on multi-electrode systems show that conducting polymer electrodes may be used to distinguish between neutral, acidic and basic amino acids. The ability to obtain finger-prints for different amino acids is an important breakthrough in their analysis because this may potentially lead to the identification of amino acids in mixtures, eliminating the need for (eg. HPLC) separation. Absolute sensor selectivity

is a noble concept but in reality it is often difficult to achieve. Therefore the use of a multiple electrode system, with each electrode possessing only partial selectivity for an analyte producing a finger-print, would be required to improve the selectivity of the analysis.

The selectivity for alanine over serine, and aspartic acid over arginine at each individual polymer electrode may be expressed as the ratio of their response magnitudes, defined as a selectivity factor. The selectivity factor of Ala/Ser peaks and Asp/Arg peaks (as α_1 and as α_2 respectively) are given in Table 3.5.

Table 3.5 *Selectivity factor of amino acids at polymer electrodes*

Polymer Electrode	α_1 (Ala/Ser)	α_2 (Asp/Arg)
PPy/CSA	0.7	3.6
PPy/Cl	0.5	7.9
PPy/DS	1.0	2.0
PPy/PTS	0.7	4.1
PPy/SBA	0.6	10.2
PPy/HBSA	0.6	5.5
PPy/PVS	0.5	5.9

Data obtained from Figure 3.24

The order of selectivity of alanine/serine (α_1) is:

PPy/DS > PPy/PTS = PPy/CSA > PPy/HBSA = PPy/SBA > PPy/PVS= PPy/Cl

The selectivity series for aspartic acid/arginine (α_2):

PPy/SBA > PPy/Cl > PPy/PVS > PPy/HBSA > PPy/PTS > PPy/CSA > PPy/DS.

These results indicate that the selectivity at conducting polymer electrodes can be manipulated by changing the counterion incorporated into the polymer at the time of synthesis.

3.3.5.5 Intra Group Selectivity towards Acidic Amino Acids

It has been shown that the conducting polymers are responsive to all four amino acids analysed, with maximum responses obtained for the acidic amino acids. Consequently a systematic study to consider the responses for aspartic acid and glutamic acid on the polymer systems was performed. The responses of the study are given in Figure 3.26.

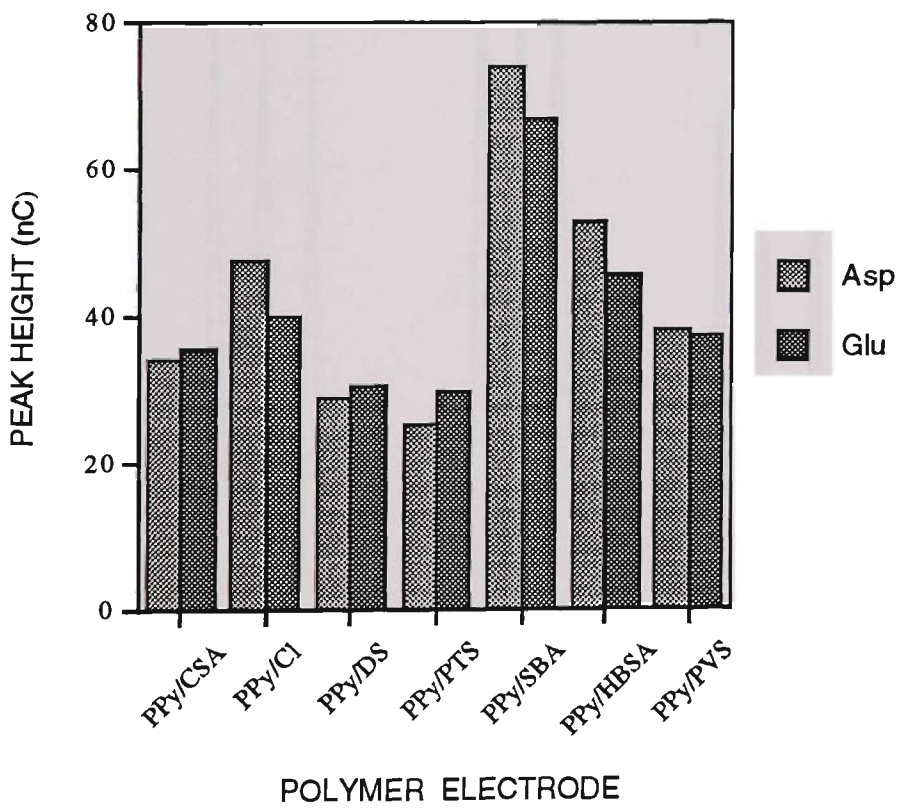

***Figure 3.26**: A graph showing the similar selectivities of polymer electrodes for aspartic acid and glutamic acid. Amino acid concentration=0.2mM. E_1=+0.3V, E_2=-0.6V, t_1=t_2=200ms, t_S=160-190ms. Eluent=0.1M $NaNO_3$. Flow rate=1ml/min. Injection volume=50µl.*

The magnitude of responses are almost equal for both amino acids on each particular polymer electrode, except for PPy/Cl, PPy/SBA and PPy/HBSA. The selectivity factors for Asp/Glu peaks are 1.19 for PPy/Cl, 1.11 for PPy/SBA and 1.16 for PPy/HBSA. The presence of an extra -CH_2- group on the R-group of glutamic acid does not seem to influence the selectivity drastically even though glutamic acid is slightly larger than aspartic acid.

The well defined responses on PPy/CSA, PPy/Cl and PPy/PTS are shown in Figure 3.27. Similar FIA peaks were obtained on other polymer systems investigated.

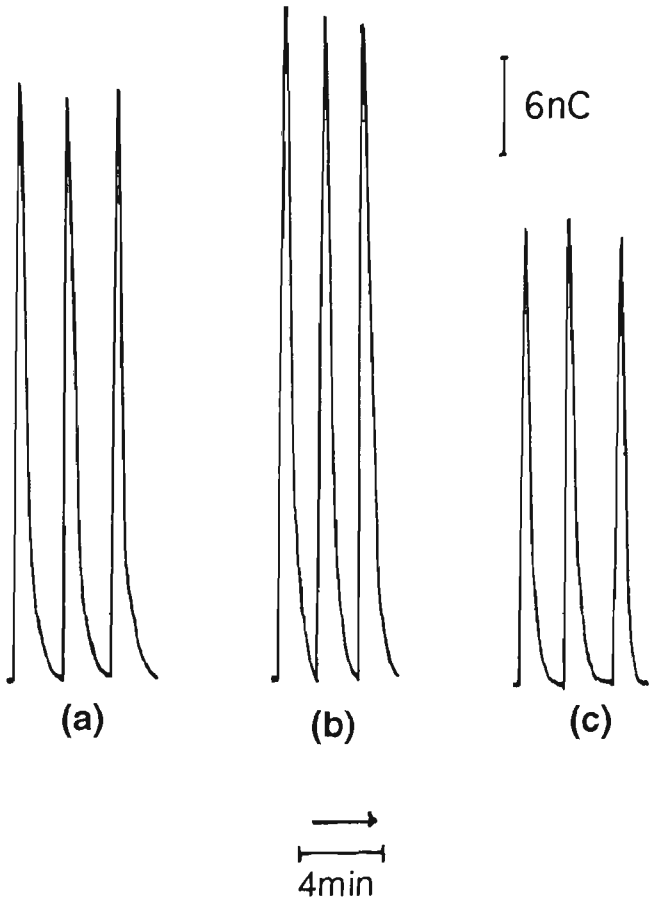

***Figure 3.27**: FIA peaks for 0.2mM glutamic acid at (a)PPy/CSA, (b)PPy/Cl and (c) PPy/PTS electrodes. E_1=+0.3V, E_2=-0.6V, t_1=t_2=200ms, t_S=160-190ms. Eluent=0.1M $NaNO_3$. Flow rate=1ml/min. Injection volume=50µl.*

3.3.5.6 Flow Injection Analysis Using a Phosphate Buffer Eluent

FIA was carried out using phosphate buffer (0.05M, pH 7) as eluent. At pH 7 alanine and serine are neutral, aspartic acid is negatively charged and arginine is positively charged. The cyclic voltammetric analysis in solutions containing amino acids and buffer showed that the voltammetric responses were equal to those recorded for buffer only.

In FIA, the background current was in the range of 200nC on PPy/CSA and the base line did not stabilise even after four hours. Rather, a constant baseline drift of 2.7nC/min was observed. The base line drift and noise are shown in Figure 3.28.

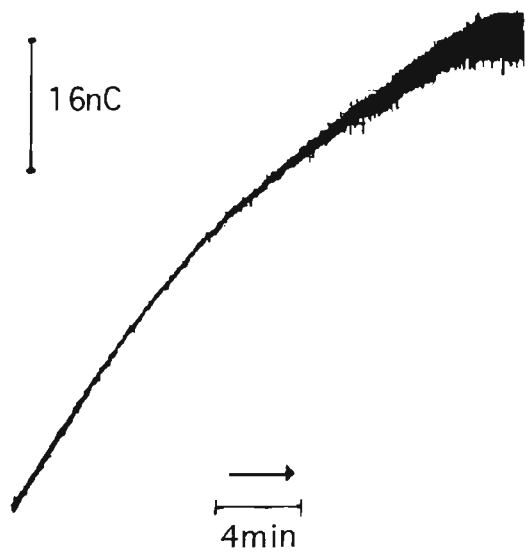

Figure 3.28: *Baseline drift and noise recorded with PPy/(+)CSA in 0.05M phosphate buffer (pH=7). E_1=+0.3V, E_2=-0.6V, t_1=t_2=200ms, t_S=160-190ms. Flow rate=1ml/min.*

The visual inspection of the electrode showed mechanical deterioration of the polymer which was observed even after as little as 15 minutes. Subsequently, the eluent concentration was decreased to 0.01M, producing a background current in the range of 200nC and a base line drift of

0.96nC/min. No responses were obtained for any analytes injected. It is possible that there is some interaction between polymer and amino acids but, due to the high background noise and drift in base line, these responses cannot be detected. The CVs in 0.05 and 0.01M buffer solutions are shown in Figure 3.29.

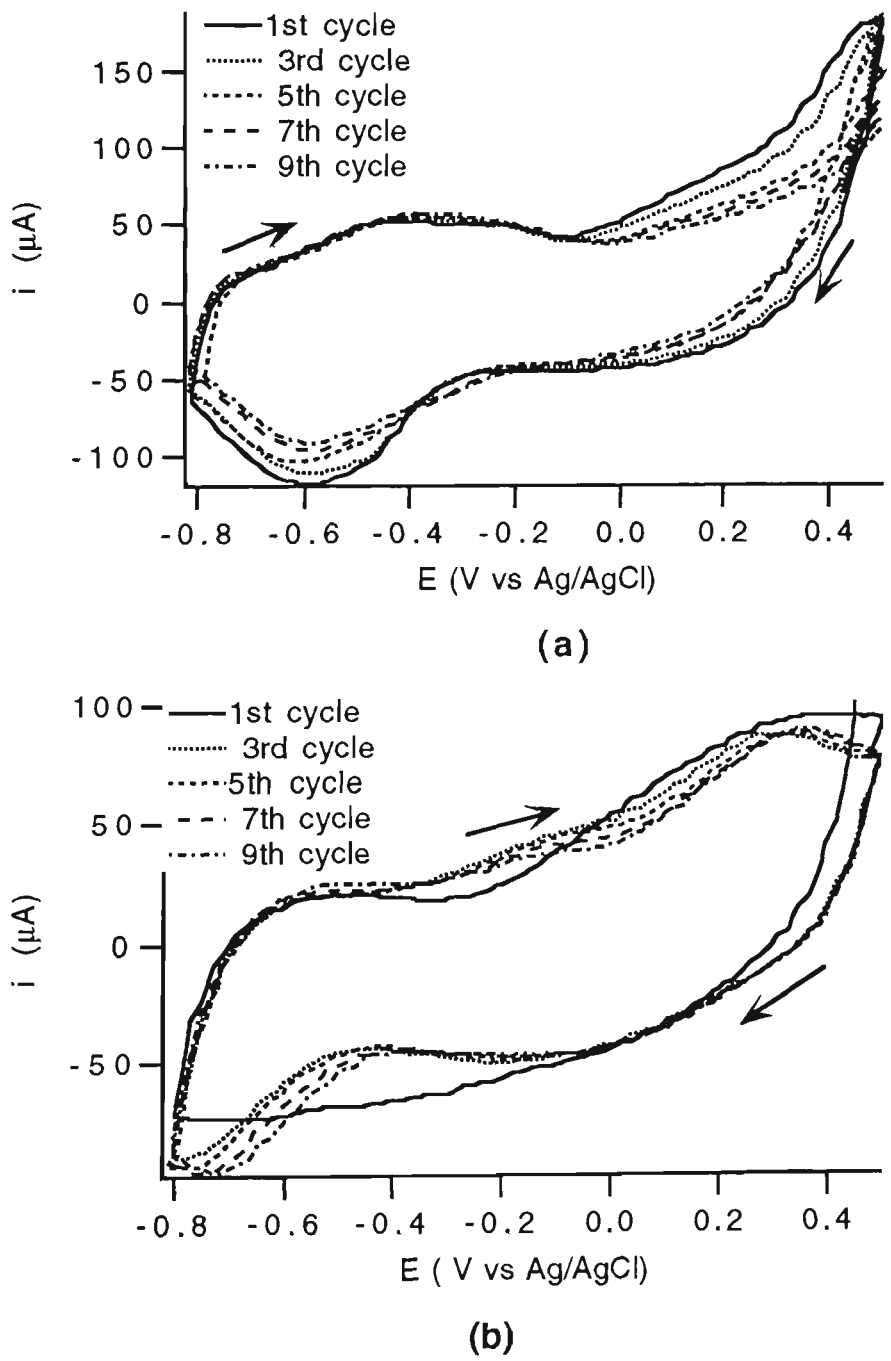

Figure 3.29: *Cyclic voltammograms of PPy/CSA in phosphate buffer pH=7 (a) 0.05M, (b) 0.01M. Scan rate=50mV/s.*

These CVs show that the polymer does not stabilise in buffer solutions until at least the 9th cycle. Along with the cation (Na^+), the charge neutralising species (the phosphate ion) is also incorporated. It might be that to incorporate the double negative charge into the polymer, the polymer chains get distorted which adversely affects the mechanical stability. It is also important to note that the extent of damage to the polymer (visually) appeared greater in 0.05M buffer compared to 0.01M buffer.

Other polymer systems were also considered using phosphate buffer at pH 7 (0.05M) as eluent. The PPy/Cl electrode was allowed to equilibrate for more than two hours. The base line drifted constantly and only broad drawn out responses were obtained; even when $3x10^{-4}M$ amino acids was injected (Figure 3.30).

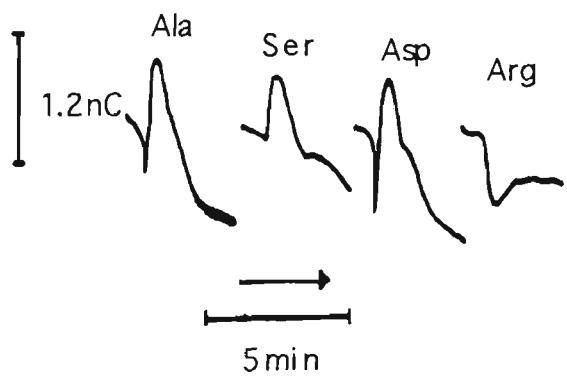

***Figure 3.30**: FIA responses at PPy/Cl. E_1=+0.3V, E_2=-0.6V, t_1=t_2=200ms, t_s=160-190ms. Eluent=0.05M phosphate buffer, pH=7. Amino acid concentration=$3x10^{-4}$M. Flow rate=1ml/min. Injection volume=50µl.*

Following these observations, the ionic strength of the phosphate buffer was decreased to 0.01M in an attempt to minimise the effects of the phosphate ions. However, the decrease in concentration did not produce any significant improvement in responses. Injections of aspartic acid did give rise to a signal but with low sensitivity (Figure 3.31-a). With PPy/PTS electrodes, responses were similar to those observed with other polymer

systems (Figure 3.31-b). The base line drifts observed with all electrodes investigated are given in Table 3.6.

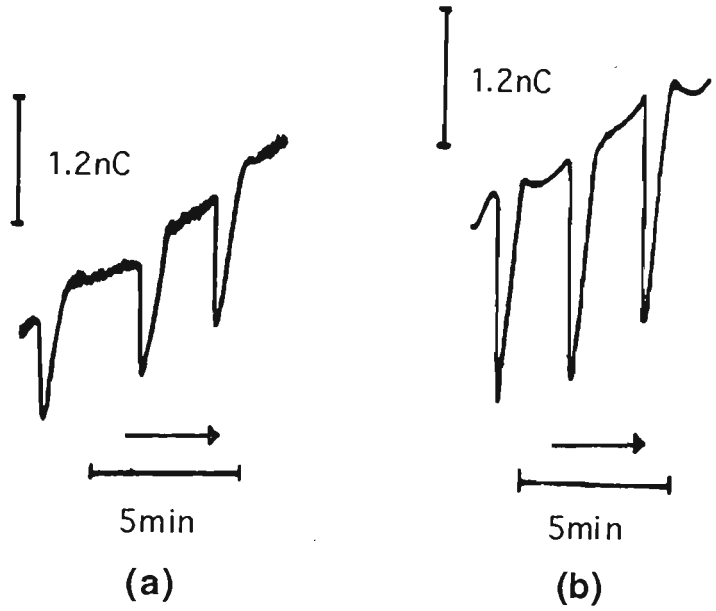

***Figure 3.31**: FIA responses for amino acids at (a)PPy/Cl and (b) PPy/PTS electrode. Eluent=0.01M phosphate buffer (pH=7). Aspartic acid concentration=0.3mM. Flow rate=1ml/min. Injection volume=50µl.*

Table 3.6 *Base line drift in phosphate buffer (pH 7)*

Electrode	Concentration of buffer eluent (M)	Base line drift (nC/min)
PPy/CSA	0.05	2.70
PPy/CSA	0.01	0.90
PPy/Cl	0.05	0.21
PPy/Cl	0.01	0.20
PPy/HBSA	0.01	0.06
PPy/PTS	0.01	0.04

Detection Conditions; E_1=0.3V, E_2=-0.6V, t_1=t_2=200ms, t_d=160-190ms. Flow rate=1ml/min. Average of three measurements.

The base line drift was lower with a decrease in the buffer ionic strength. It also decreased when the polymer counterion was changed from Cl^- to

$HBSA^-$ and to PTS^-, where the incorporation of phosphate ions are difficult. The stability of the polymers was further investigated by cyclic voltammetry in the phosphate buffer (Figure 3.32).

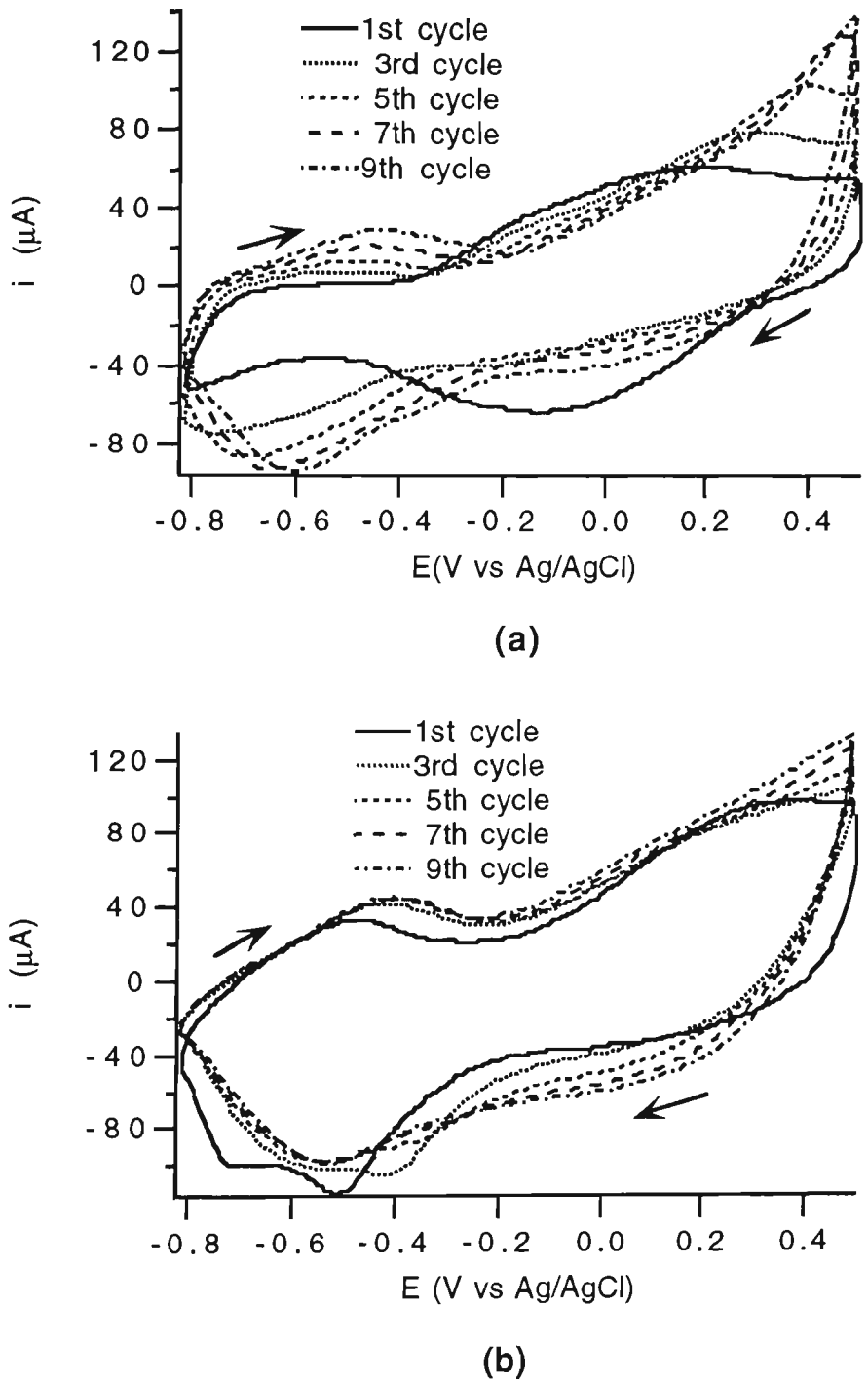

***Figure 3.32**: Cyclic voltammograms of (a)PPy/Cl and (b) PPy/HBSA in phosphate buffer (0.05M, pH=7.0,). Scan rate=50mV/s. Polymerisation by applying 1mA/cm^2 for 2min, Py=0.2M, counterion=0.05M.*

The current responses changed with each cycle but the change was more marked for PPy/Cl, compared to PPy/HBSA. After cyclic voltammetry a visual inspection of the electrode surface also showed some mechanical deterioration of both electrode surfaces.

3.3.5.7 Chiral Selectivity of PPy/(+)CSA for D/L-phenylalanine and D/L-tryptophan

The use of PPy/(+)CSA electrodes to achieve chiral selectivity in for D- and L-phenylalanine and D- and L-tryptophan detection was investigated. Limitations from the use of phosphate buffer meant that the option to employ 0.1M $NaNO_3$ as an eluent was preferred. Initially, the conditions optimised previously (Sections 3.3.5.2) were employed for the analysis but later the reduction potential was also changed to alter the selectivity. The responses for D-phenylalanine, L-phenylalanine and D-tryptophan, L-tryptophan are shown in Figure 3.33 and Figure 3.34. The results indicate poor selectivity towards the different hands of amino acids, but that the response was dependent on the potential applied.

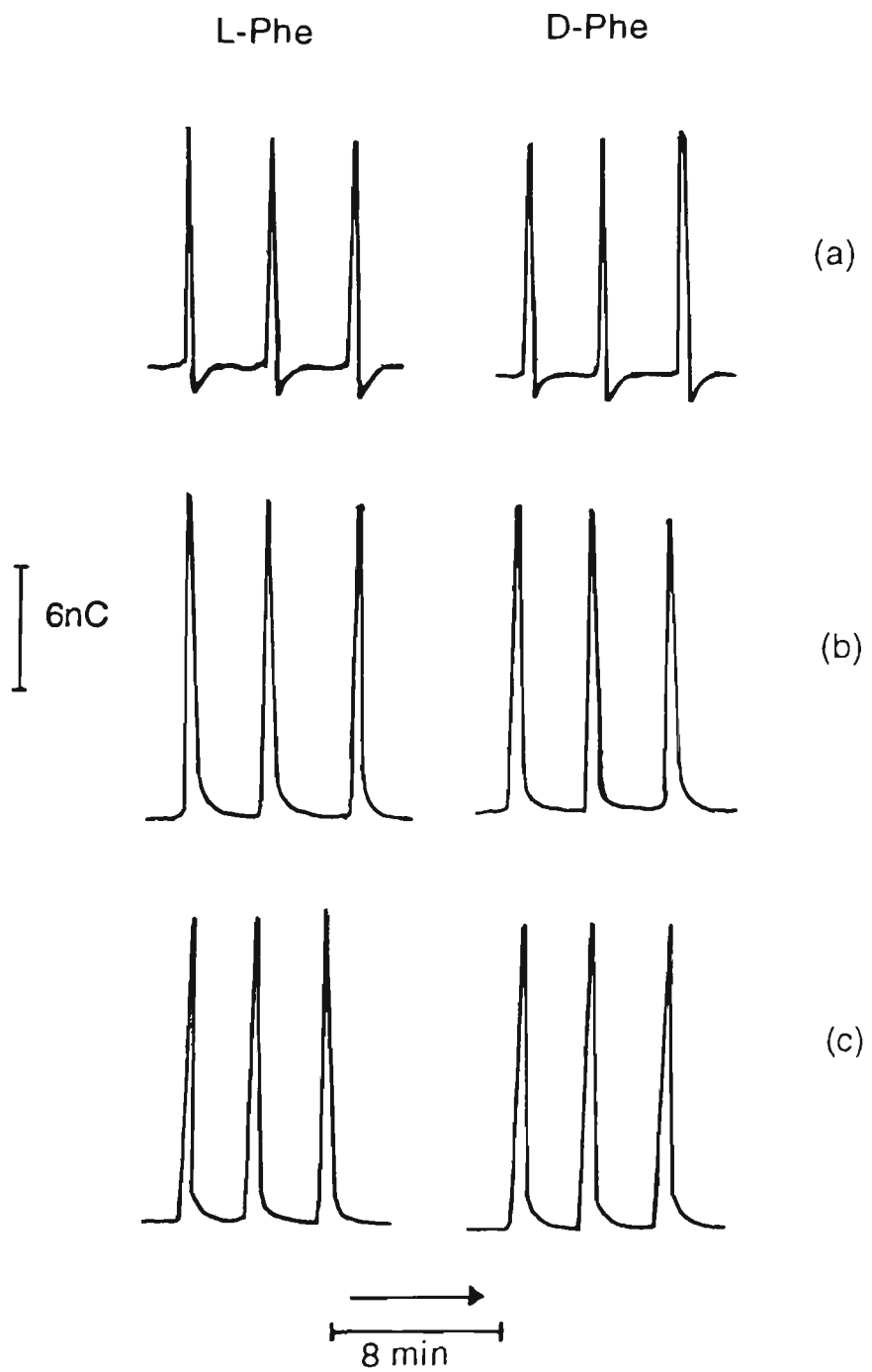

***Figure 3.33**: FIA responses for L-phenylalanine and D-phenylalanine with PPy/(+)CSA. E_1=0.3V, t_1=t_2=200ms, t_S=160-190ms, (a) E_2=-0.6V (b) E_2=-0.7V (c) E_2=-0.8V. Eluent=0.1M $NaNO_3$. Flow rate=1ml/min. Amino acid concentration=0.1mM. Injection volume=50µl.*

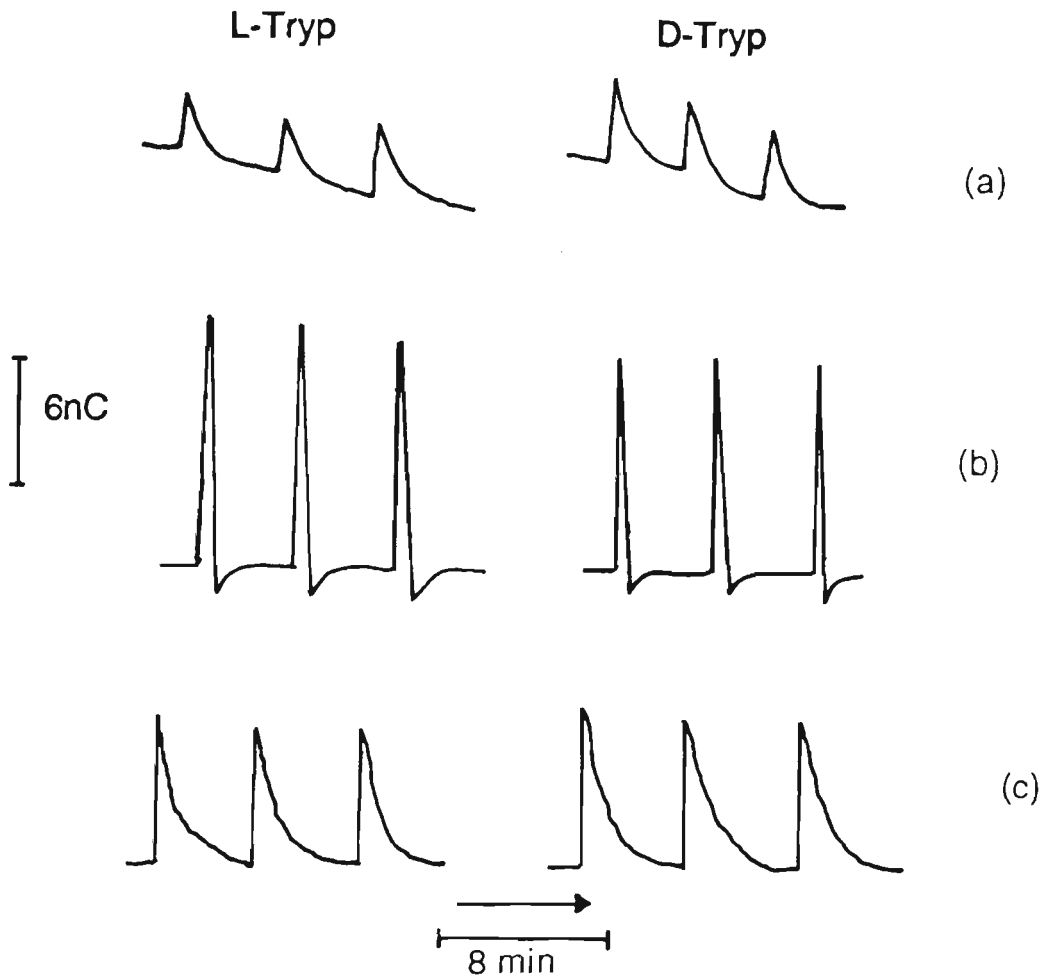

***Figure 3.34**: FIA responses for L-tryptophan and D-tryptophan with PPy/(+)CSA. E_1=0.3V, t_1=t_2=200ms, t_S=160-190ms, (a) E_2=-0.6V (b) E_2=-0.7V (c) E_2=-0.8V. Eluent=0.1M $NaNO_3$. Flow rate=1ml/min. Amino acid concentration=0.1mM. Injection volume=50µl.*

3.4 CONCLUSIONS

It has been shown in this chapter, that conducting electroactive polymers can be used for the detection of amino acids. Amino acid/polymer interactions can be characterised as either neutral, anionic or cationic. The selectivity of polymers for amino acids can be manipulated by changing the counterion incorporated into the polymer upon its synthesis.

The mechanism of signal generation is complex, and is probably a multi-component process [29]. The factors which contribute to the signal as a function of applied potential included:

1) Polymer conductivity [185], which is dependent on the potential applied, and gives rise to i_{pd} (current due to doping/dedoping of the eluent ions).

2) Current due to doping/dedoping of analyte, i_{pa} (the anodic current).

3) Current due to charging/discharging of the electrode, i_{pc}.

4) The pH dependence of the polymer conductivity.

It is important to note that the analyte responses differ markedly, suggesting that it is the nature of the analyte which plays the most important role in signal generation. The dominant factor is proposed to be the anion exchange properties of the polymers. The limitations encountered with the use of phosphate buffer, hinders a complete understanding of the mechanism of amino acid/polymer interactions.

These observations are consistent with literature which report that the R_f values on polypyrrole and polyaniline conducting polymer TLC plates were lowest for acidic amino acids. Non-polar, polar and cationic amino acids show high R_f values and so the polymers were found to behave as anion exchangers [279,280].

The limit of detection (1ppm) for aspartic acid is relatively high, compared with other EC-detection methods (Table3.1). Further work will concentrate on improving the limit of detection and the selectivity of conducting polymers for amino acids.

CHAPTER 4

DETECTION OF AMINO ACIDS AT CONDUCTING POLYMER MODIFIED MICROELECTRODES USING FLOW INJECTION ANALYSIS

4.1 INTRODUCTION

In Chapter 3, the detection of amino acids at polymer modified macroelectrodes was discussed. It was shown that selectivity can be varied with the counterion incorporated. The influence of electrochemical parameters on the responses obtained was also demonstrated. The detection suffered from high limit of detection. This could be due to low signal-to-noise ratio or due to strong competition between analyte and eluent ions during redox processes.

With microelectrodes many limitations associated with macroelectrodes have been minimised or greatly reduced; for example the minimisation of electrode diameter results in spherical diffusion leading to enhanced mass transport. In voltammetric studies this gives rise to steady state currents. An ohmic potential drop (iR) causes significant errors to the actual potential applied to the electrode with respect to the value set at the potentiostat. The decreased ohmic (iR) and capacitance effects under steady state conditions, allows analysis in media with low electrolyte concentrations or no added electrolyte [288-292]. Voltammetry at microelectrodes with very dilute electrolyte or without any added electrolyte is now a routine form of measurement [289,293-301]. In pure water self dissociation occurs according to:

$$H_2O = H^+ + OH^- \qquad .....4.1$$

which provides enough conductivity to enable voltammetry to be achieved without any added electrolyte [302-310].

Microelectrodes have also been modified by polypyrrole, polythiophene and polyaniline [311,312]. Conducting polymer coated microelectrodes are capable of fast switching as compared to macroelectrodes during redox process [311,313,314]. A scan rate as large as 300,000 V/s [311] can be applied without deteriorating the cyclic voltammetric response and well defined oxidation reduction peaks were obtained for polyaniline, poly(3-methyl-thiophene) and poly(3,4-dimethylpyrrole). Conducting polymer coated chemical [315] and biosensors [198] have also been reported. PPy/Cl modified electrode applied for silver detection showed 20-50 times greater sensitivity than macroelectrodes [316]. The limit of detection for electroinactive ions were reported to improve 10-40 fold at PPy/Cl modified electrodes in FIA by overcoming the limitation associated with low conductivity solution (glycine) [315]. Microelectrodes are advantageous since an increase in the faradaic-to-charging current ratio [292,317] and reduced competition between analyte and supporting electrolyte species for the detector in low supporting electrolyte concentration [318-320] offers improvement in the limit of detection [292,317]. These features of microelectrodes should enhance the limit of detection and selectivity for the amino acids.

4.1.2 Aims and Approach of this Chapter

The aim of this study is to use conducting polymer coated microelectrodes for the detection of amino acids in FIA. In Chapter 3 it was observed that maximum selectivity was obtained on PPy/SBA for aspartic acid. Here we focus on further improving the selectivity and LOD for amino acids using this polymer.

4.2 EXPERIMENTAL

4.2.1 Reagents and Standard Solutions

All reagents and chemicals were the same as in Chapters 2 and 3.

4.2.2 Instrumentation

An in-house nanogalvanostat was used to deposit the polymer on the microelectrodes. Cyclic voltammetric experiments were carried out with ElectroLab Work Station(ADI). The data was recorded with ElectroLab software on Macintosh Computer. The data manipulation was carried out using Igor software package (Wavemetrics). 10μm disc microelectrodes were prepared by sealing the 10μm platinum wire (Goodfellow) in a glass tube. The electrodes were polished using 0.30μm and 0.05μm alumina (Leco) respectively, and ultrasonicated for 1 minute in Milli-Q water. The auxiliary electrode was a platinum mesh and the reference electrode was a BAS Ag/AgCl (3M NaCl) with a salt bridge.

Flow injection analysis was performed using a Dionex chromatography module (CHB-2) with a 50μl injector loop. A Dionex flow cell, with a Dionex Ag/AgCl-pH reference electrode and a stainless steel cell body as auxiliary electrode, was employed as an electrochemical cell. The working electrode cell block was modified by drilling a hole to screw in the working electrode. The working electrode assembly was housed in a Faraday cage to insulate against interference from electrical noise. The Faraday cage had a built in amplifier to record the low level currents to be monitored. The electrochemical cell was controlled with a Dionex Pulsed Electrochemical

Detector (PED-II) and the recorder was an ICI Instruments DP 600 chart recorder. The schematic of the system is shown in Figure 4.1.

Conductivity measurements were made with a Phillips PW9501 conductivity meter. Solution pH was measured with a digital pH/mV meter (model SA520) (Orion).

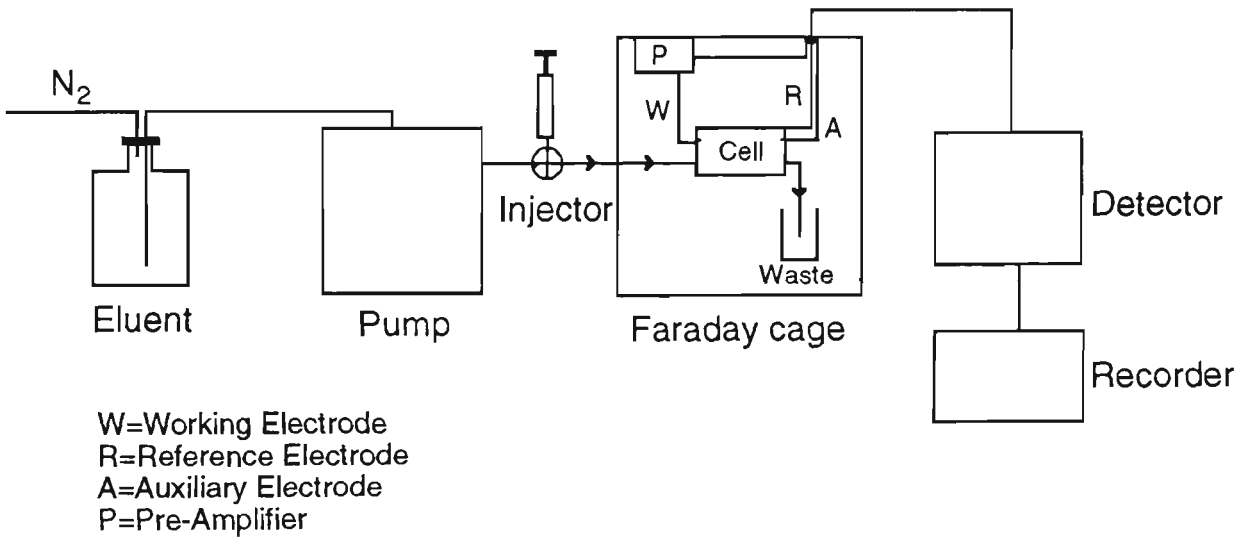

Figure 4.1: *Schematic of flow system with Faraday cage.*

4.2.3 Polymerisation Procedure

The polymerisation solution consisted of 0.2-0.5M pyrrole. The concentration of counterions was 0.05M except for chloride where the concentration was 1M. The monomer solutions were purged with nitrogen for five minutes before polymerisation and a constant current method was used to deposit the polymer.

4.2.4 Electrochemical Characterisation

The polymer electrodes were characterised by cyclic voltammetry in 0.1M $NaNO_3$ as well as in the 0.001M $NaNO_3$ to be used as eluent in FIA. Cyclic voltammetry and chronoamperometry were also performed in amino acid solutions.

4.3 RESULTS AND DISCUSSION

4.3.1 Preparation of Polymer Electrodes

Attempts to polymerise PPy on microelectrodes using the conditions used for macroelectrodes were unsuccessful for all polymers considered. For example in the case of PPy/SBA the potential increased to more than 2.0 V when the polymerisation was carried out from 0.2M pyrrole and using 0.05M counterion with $1mA/cm^2$ current density for 2 minutes. No (electroactive) polymer was deposited on the electrode (as confirmed by CV). Subsequently the current density was increased to $2mA/cm^2$, but still there was no polymer on the electrode and the potential obtained was now 2.0 V. The reason for this is that at microelectrodes, due to spherical diffusion, high mass transport **to** and **from** the electrode occurs. Thus the radical cation formed during monomer oxidation does not have enough time to combine with other oligomeric cation radicals and deposit on the electrode surface [312]. To overcome this, the monomer concentration was increased from 0.2 to 0.5M. A conducting polymer was obtained from this solution using $2mA/cm^2$ current density during galvanostatic polymerisation. The chronopotentiogram recorded during polymerisation showed an initial increase in potential which is associated with the nucleation of the polymer

growth [316]. The potential decreased during polymerisation indicating that the polymer formed was conductive. The growth potential levelled out at 0.6V (Figure 4.2).

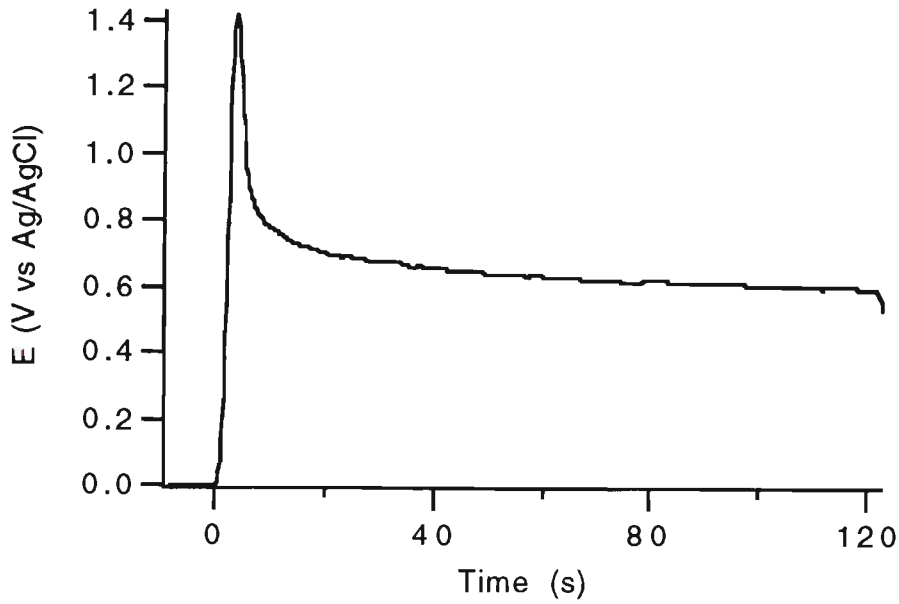

***Figure 4.2**: Chronopotentiogram during polymerisation of PPy/SBA on a 10µm Pt disc electrode. Py=0.5M, SBA=0.05M, current density=2mA/cm^2, time=2min.*

Three different thicknesses of polymer film were deposited on the electrode by varying the deposition time. These polymer electrodes were characterised by cyclic voltammetry. The polymer doping current during oxidation in the CV increased linearly with the polymer thickness. A plot of polymer film doping current at -0.1V vs deposition time is shown in Figure 4.3. Well defined oxidation/reduction responses were obtained for polymer deposited for 6 minutes. The polymerisation time of 6 minutes was selected for preparation of the electrodes.

Using chloride as the counterion (0.5M) during growth the potential observed was 2.0V and no polymer was deposited on the electrode surface.

When the chloride concentration was increased to 1M a polymer was obtained (confirmed by CV) with the polymerisation potential at 0.5V.

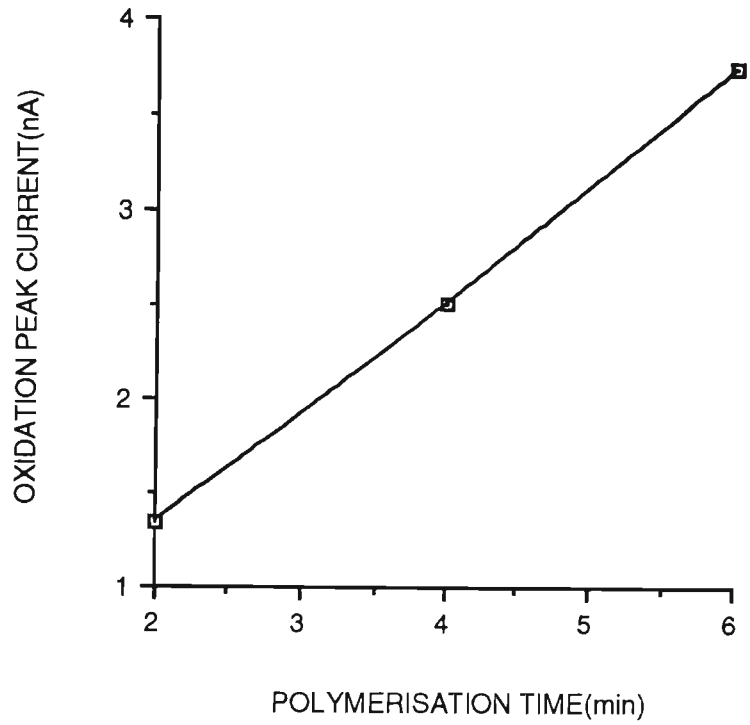

***Figure 4.3**: Polymer doping current at PPy/SBA during cyclic voltammetry in 0.1M $NaNO_3$ at -0.1V for three different polymer thicknesses. Scan rate=50mV/s.*

PPy/CSA, PPy/HBSA, PPy/DS and PPy/PTS were grown successfully (as confirmed by CV) from 0.5M pyrrole and 0.05M counterions using $2mA/cm^2$ current density. No polymer deposit was obtained with PVS on microelectrodes.

The polymerisation potentials, measured after 3 minutes of polymerisation, are given in Table 4.1. The polymerisation potential decreased during the course of polymerisation indicating the deposition of conducting polymer. In all cases, potentials were lower than that on macroelectrodes which indicate the easy oxidation of the monomers on microelectrodes under ideal situation.

Table 4.1 *Polymerisation potential during the growth of PPy with different counterions.*

Electrode	Ep(V)
PPy/SBA	0.60
PPy/CSA	0.60
PPy/DS	0.45
PPy/HBSA	0.60
PPy/Cl	0.50
PPy/PTS	0.60

Conditions: Py=0.5M, counterion=0.05 M (CSA, DS, PTS, HBSA or SBA) and 1.0 M Cl, Current density=2mA/cm^2, time=6min. Ep=Polymerisation potential after 3 minutes of polymerisation.

4.3.2 Electrochemistry at Microelectrodes

Using selected consistent experimental conditions the polymer coated microelectrodes were characterised in 0.1M $NaNO_3$. The cyclic voltammograms are shown in Figure (4.4, a-f). Each of the voltammograms in Figure 4.4 showed reasonably well defined electrochemistry associated with elecrochemically controlled ion-exchange process. The resultant currents were lower compared to macroelectrodes for each corresponding polymer due to the smaller electrode size.

For PPy/SBA (Figure 4.4-a), there were two sets of redox peaks (A/A' and B/B') corresponding to anion and cation exchange respectively. The anion expulsion/incorporation peaks were broad at around -0.1V. The cation

incorporation peak at around -0.7V and a broad cation expulsion peak at -0.6V were observed.

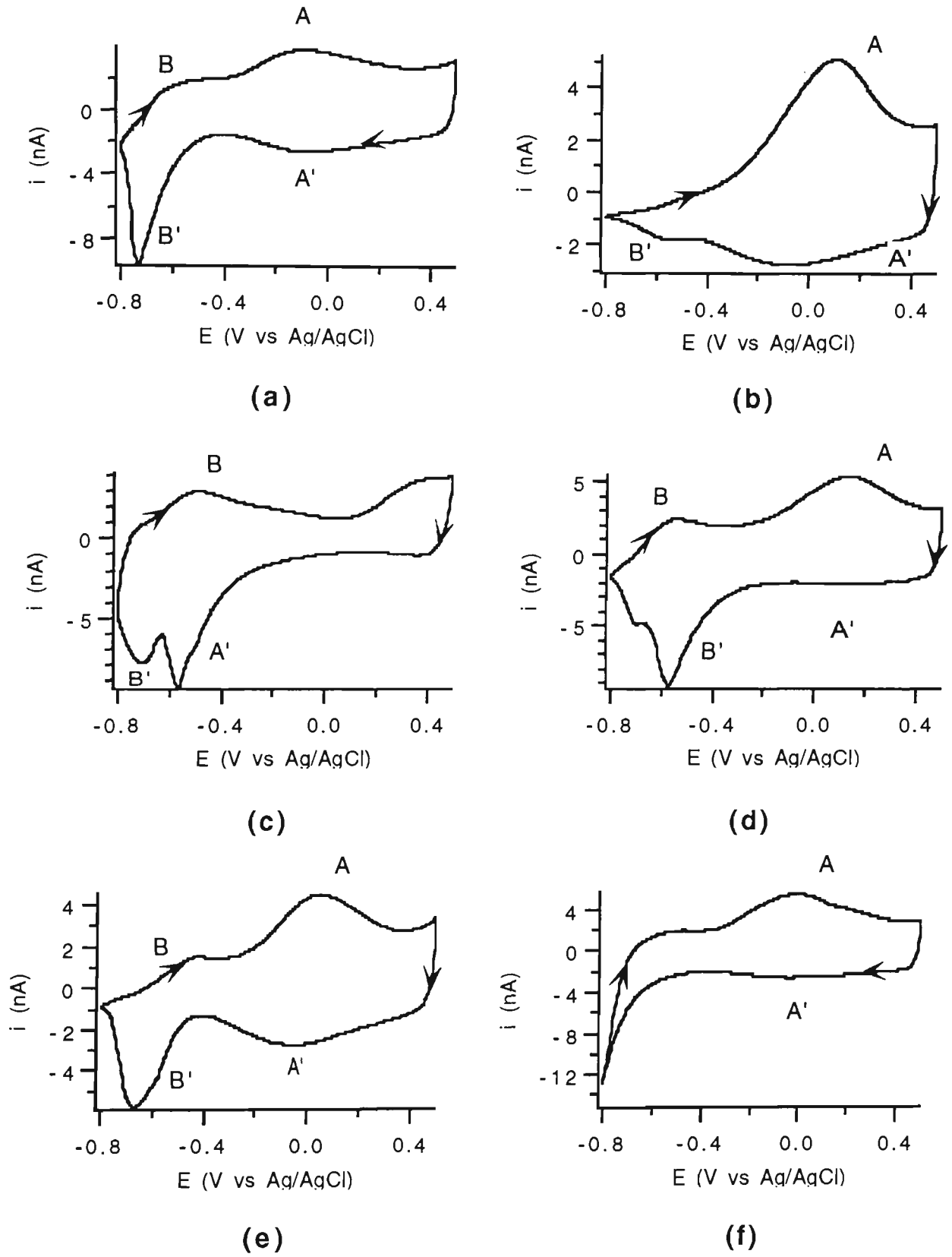

Figure 4.4: *Cyclic voltammograms of (a) PPy/SBA, (b) PPy/Cl, (c) PPy/DS, (d) PPy/PTS, (e) PPy/HBSA and (f) PPy/CSA in 0.1M $NaNO_3$. Scan rate=50mV/s. Polymerisation condition as in Table 4.1.*

At PPy/Cl (Figure 4.4-b) a broad reduction peak appeared at around -0.1V when the polymer switched from the conducting to neutral state. The polymer oxidation occurred at 0.1V producing a well defined anion incorporation peak. The cation incorporation peak was also clearly present at -0.6V, whereas no similar peak was obtained at the macroelectrode (Section 2.3.1.2).

For PPy/DS (Figure 4.4-c) during cyclic voltammetry the main charge compensating species were cations (B/B'), along with some anion expulsion. This anion expulsion peak was located at -0.6V indicating that the expulsion of incorporated anion, due to its bulky nature, required extreme reduction potentials.

For PPy/PTS (Figure 4.4-d) there were anion oxidation/reduction peaks (A/A') around 0.1V, while cation incorporation / expulsion peaks were present at -0.6V.

For PPy/HBSA (Figure 4.4-e) a reduction peak was obtained at -0.1V and a better defined oxidation peak was obtained at around 0.1V. The well defined cation insertion peak was obtained at -0.7V and, upon reversal of scan, the cation expulsion peak was present at -0.45V.

In the case of PPy/CSA (Figure 4.4-f) the electrochemistry was not well defined compared to above polymers. Only anion redox peaks were obtained during polymer switching from conductive to nonconductive states. The polymer reduction peak was broad at 0.0V while oxidation was also broad at 0.0V.

These CVs were stable for repetitive cycles without loss of electroactivity. These observations showed that conducting polymers could be successfully grown using a range of counterions with well defined electrochemically controlled ion-exchange behaviour. The current magnitude was dependent on the counterion incorporated. The excellent electrochemistry could be due to fast mass transfer [311] and lower iR drop in microelectrodes.

In 0.001M $NaNO_3$ the polymer electroactivity was less prominent for all polymer electrodes. The low electroactivity could be due to the low ion concentration of the electrolyte. The cyclic voltammograms are shown in Figure 4.5 (a-f).

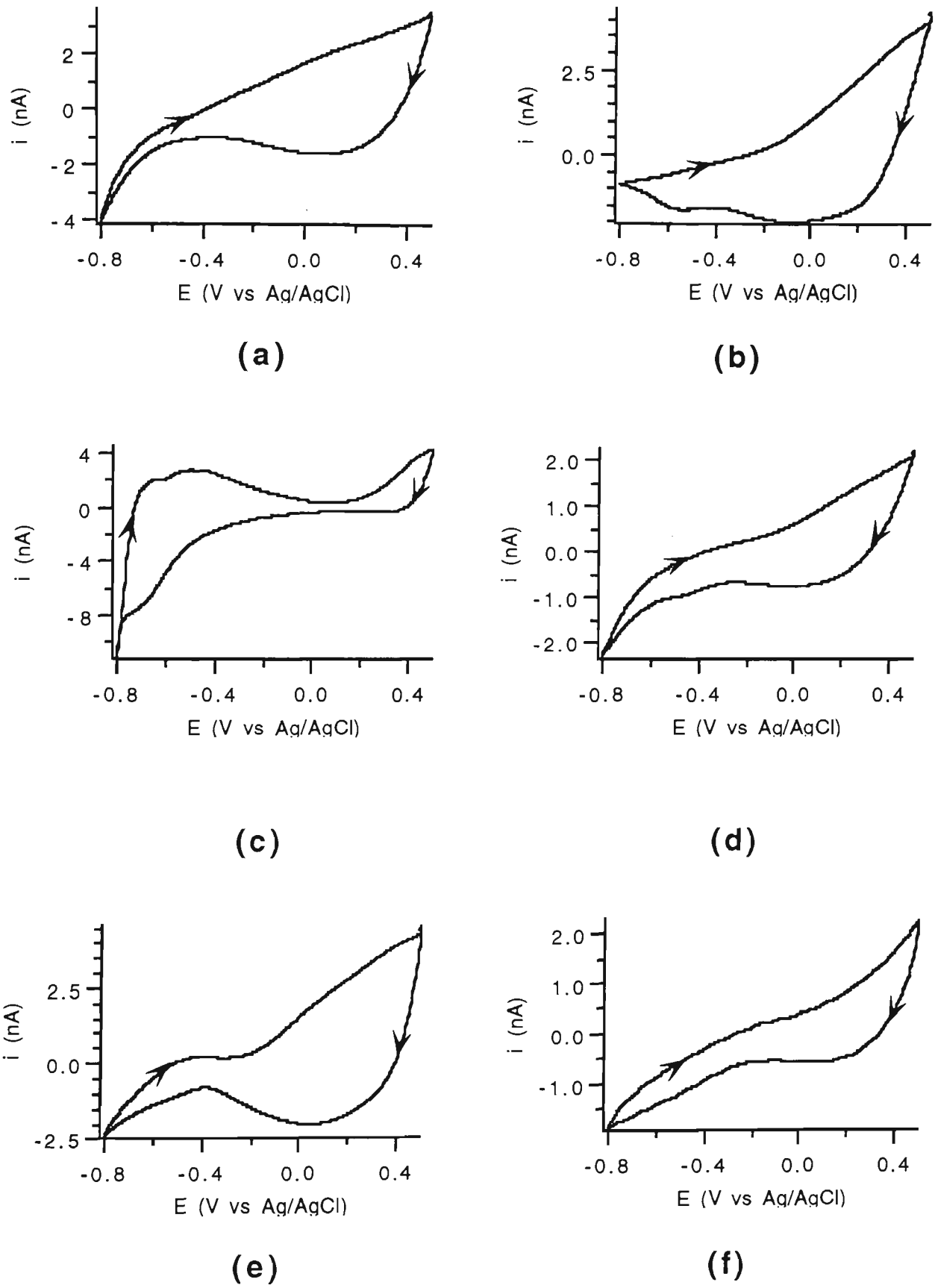

***Figure 4.5**: Cyclic voltammograms of (a) PPy/SBA, (b) PPy/Cl, (c) PPy/DS, (d) PPy/PTS, (e) PPy/HBSA and (f) PPy/CSA in 0.001M $NaNO_3$. Scan rate=50mV/s. Polymerisation conditions as in Table 4.1.*

4.3.3 Comparison of the Electrochemistry of PPy/SBA coated Microelectrode and Macroelectrode

The cyclic voltammograms of PPy/SBA films grown under identical conditions at both micro and macroelectrodes were compared. The polymerisation solution contained 0.5M pyrrole and 0.05M SBA as counter ion. The polymer electrodes were deposited using a current density of $2 mA/cm^2$ for 6 min. The polymerisation potential attained at the macroelectrode was 0.7V, which is higher than that observed on the microelectrode (0.6V).

The electrochemistry of both micro and macroelectrodes was studied in 0.1M $NaNO_3$. As discussed in Section 4.3.2 microelectrodes showed well defined electrochemistry during redox cycling. At macroelectrodes the electrochemistry was slow (Figure 4.6), the oxidation/reduction peaks were not well defined. The anion incorporation peak was located at more positive potentials. The cation insertion and expulsion peaks were not observed. This could probably be due to the difference in the mass transfer, which is faster at microelectrodes.

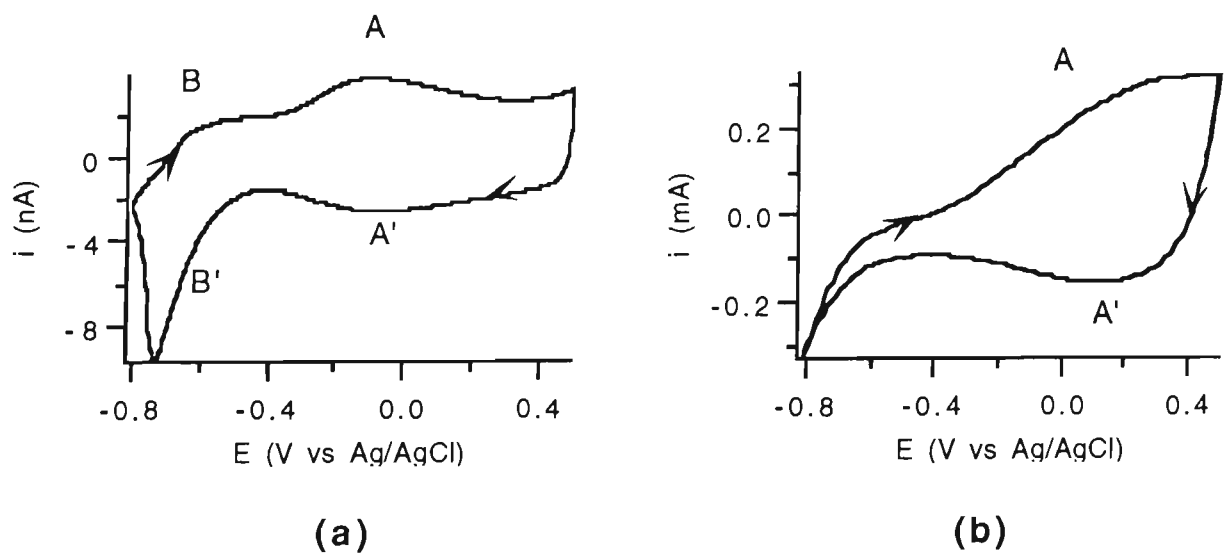

***Figure 4.6** : Cyclic voltammograms recorded at PPy/SBA. (a) microelectrode (10μm), (b) macroelectrode (3mm) in 0.1M $NaNO_3$. Scan rate= 50mV/s.*

The polymers deposited on micro and macroelectrodes were cycled in ferricyanide media to gain information on electron transfer across the polymers. The solution contained 10mM $K_3Fe(CN)_6$ in 0.1M $NaNO_3$ supporting electrolyte. The peaks, labelled as C/C', associated with $Fe(CN)_6^{3/4-}$ are present at both micro and macroelectrodes (Figure 4.7). The redox pair is better defined at the microelectrode probably because the mass transport of electroactive ferricyanide/ferrocyanide anion is faster at the microelectrode than at the macroelectrode and with microelectrodes iR drop problems are also minimised.

Both anion doping/dedoping (A/A') and cation doping/dedoping (B/B') were present at the microelectrode and anion doping/dedoping (A/A') peaks were present at the macroelectrode, while a reduction peak at -0.8V could be due to solvent reduction.

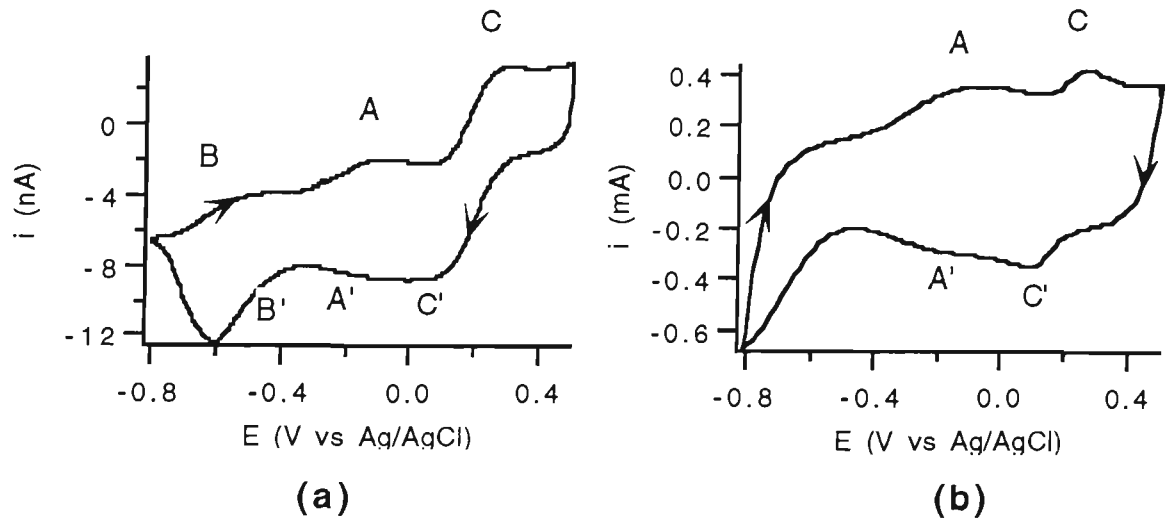

***Figure 4.7**: Cyclic voltammograms of PPy/SBA. (a) microelectrode (10μm) (b) macroelectrode (3mm) using 1mM $K_3Fe(CN)_6$ in 0.1M $NaNO_3$. Scan rate=50mV/s.*

4.3.4 Cyclic Voltammetry in Amino Acid Solutions

The electroactivity of the PPy/SBA (microelectrode) in amino acid solutions was investigated under constant experimental conditions. Cyclic voltammetry was performed in 1mM amino acid solutions without the addition of any external electrolyte. The CVs are shown in Figure 4.8.

The polymer was not electroactive in alanine and serine solutions. This type of behaviour indicates that alanine and serine did not incorporate during redox cycle. The conductance and pH of the 1mM amino acid solutions are given in Table 3.3 (Chapter 3) and the effect of solution conductance was discussed. In the case of aspartic acid the anion expulsion and cation incorporation was prominent during reduction which was followed by the less distinct cation expulsion and anion incorporation during oxidation of polymer film. For arginine the cation incorporation and expulsion peaks were present at -0.4V and at -0.2V respectively.

Cyclic voltammetry was also carried out on macroelectrodes, grown under the same experimental conditions, (Figure 4.9) to compare the electrochemistry of the polymer in amino acid solutions.

In alanine and serine, CVs were straight lines due to solution resistance which becomes more prominent in macroelectrodes. In the case of aspartic acid the anion and cation peaks were not prominent compared to results obtained at microelectrodes. Furthermore no peaks were obtained in arginine solutions. These observations indicate that the responses on microelectrodes were more favourable than macroelectrodes.

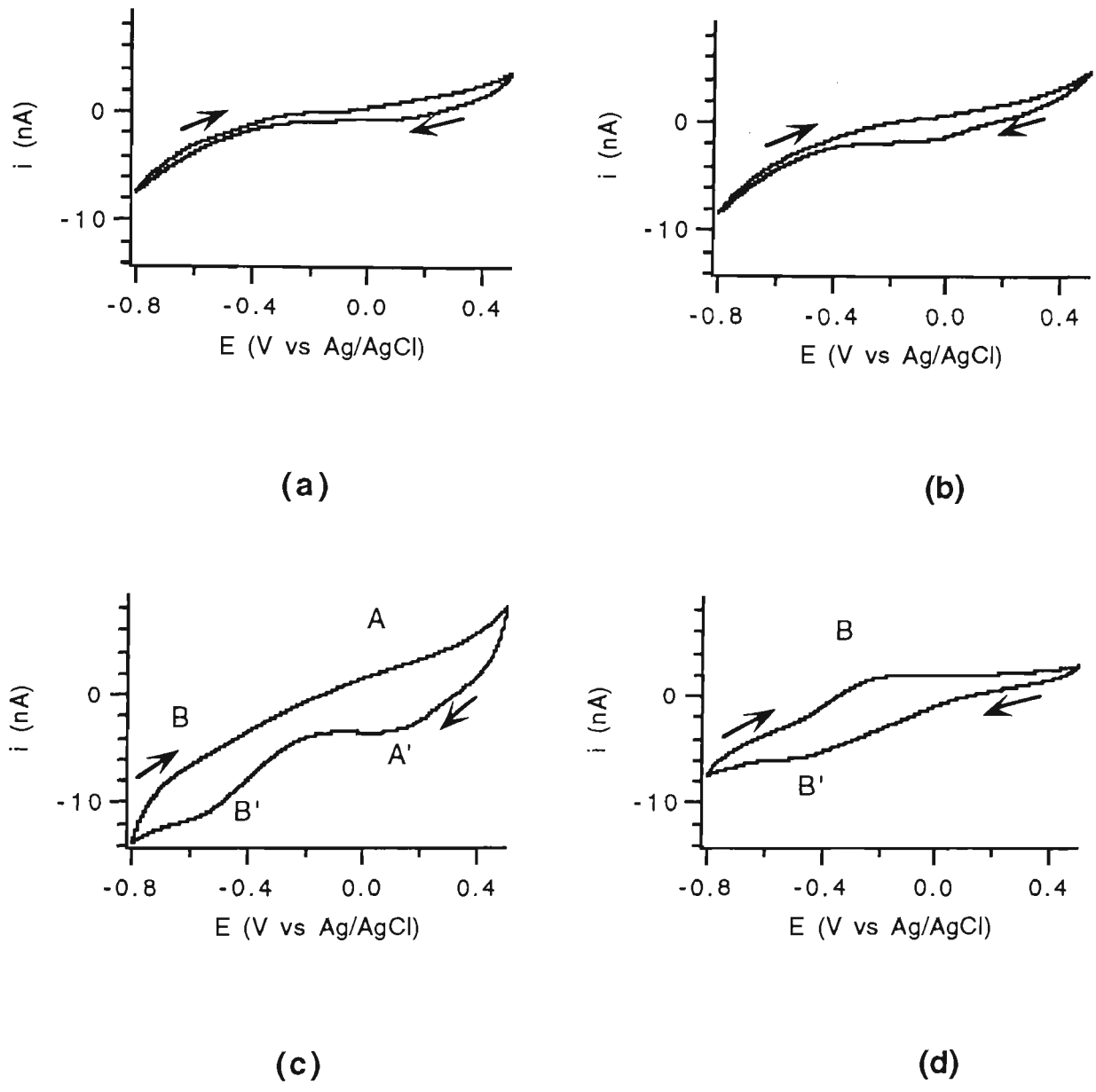

***Figure 4.8**: Cyclic voltammetry of PPy/SBA in 1mM amino acid solutions. (a) alanine, (b) serine, (c) aspartic acid and (e) arginine. Scan rate=50mV/s.*

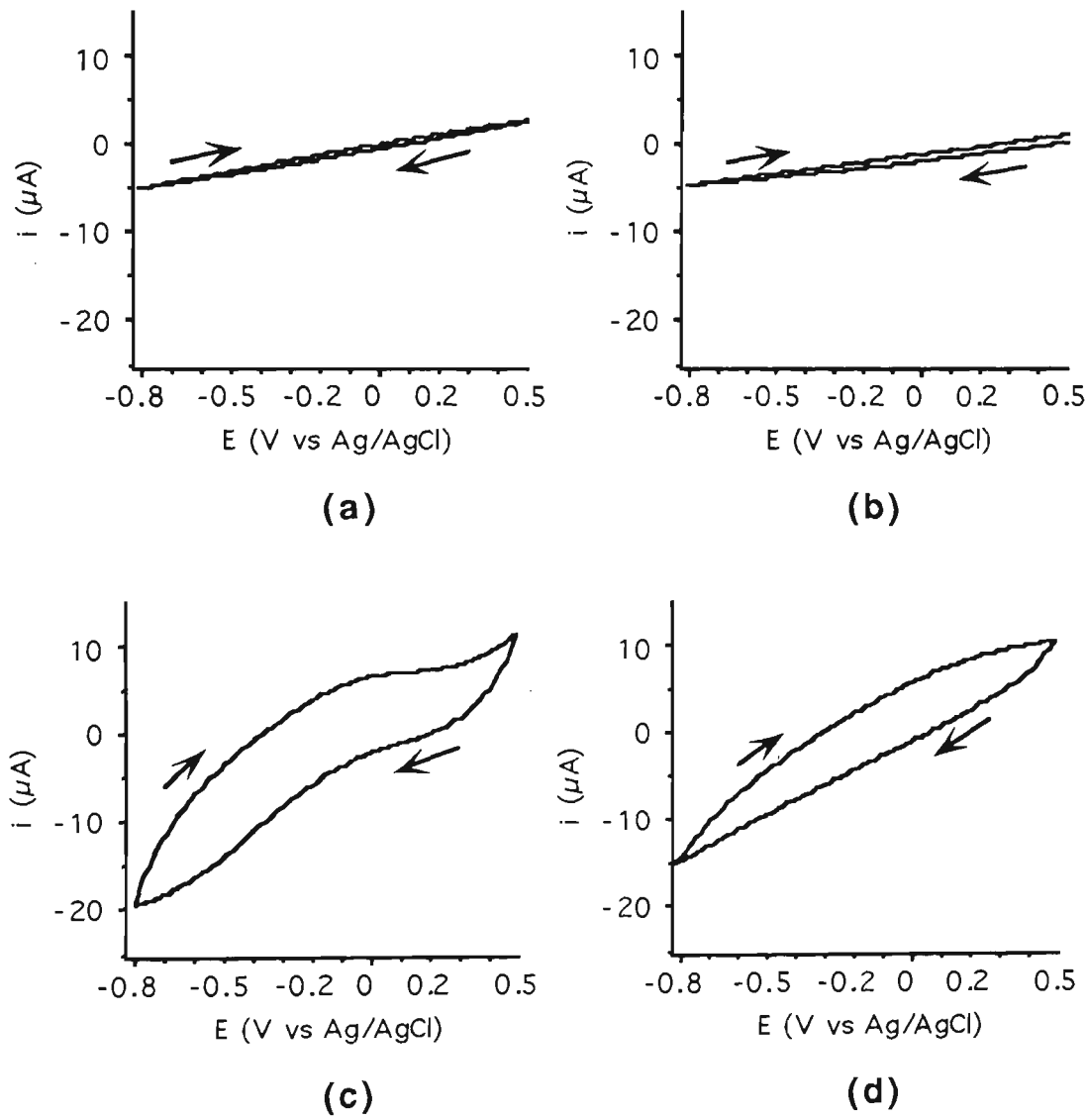

Figure 4.9: *Cyclic voltammograms recorded on PPy/SBA (macroelectrode) in 1mM amino acid solutions. (a) alanine, (b) serine, (c) aspartic acid and (d) arginine. Scan rate=50mV/s.*

Cyclic voltammetric experiments at microelectrodes in the presence of added electrolyte in the amino acid solution were also performed. The cyclic voltammograms are shown in Figure 4.10 and compared with Figure 4.5-a (in electrolyte alone). The addition of 1mM alanine or serine to 0.001M $NaNO_3$ did not have any effect on the cyclic voltammetry. The conductance and pH of the solutions are given in Table 4.2. For alanine and serine the conductance and pH are similar to that of nitrate solution alone.

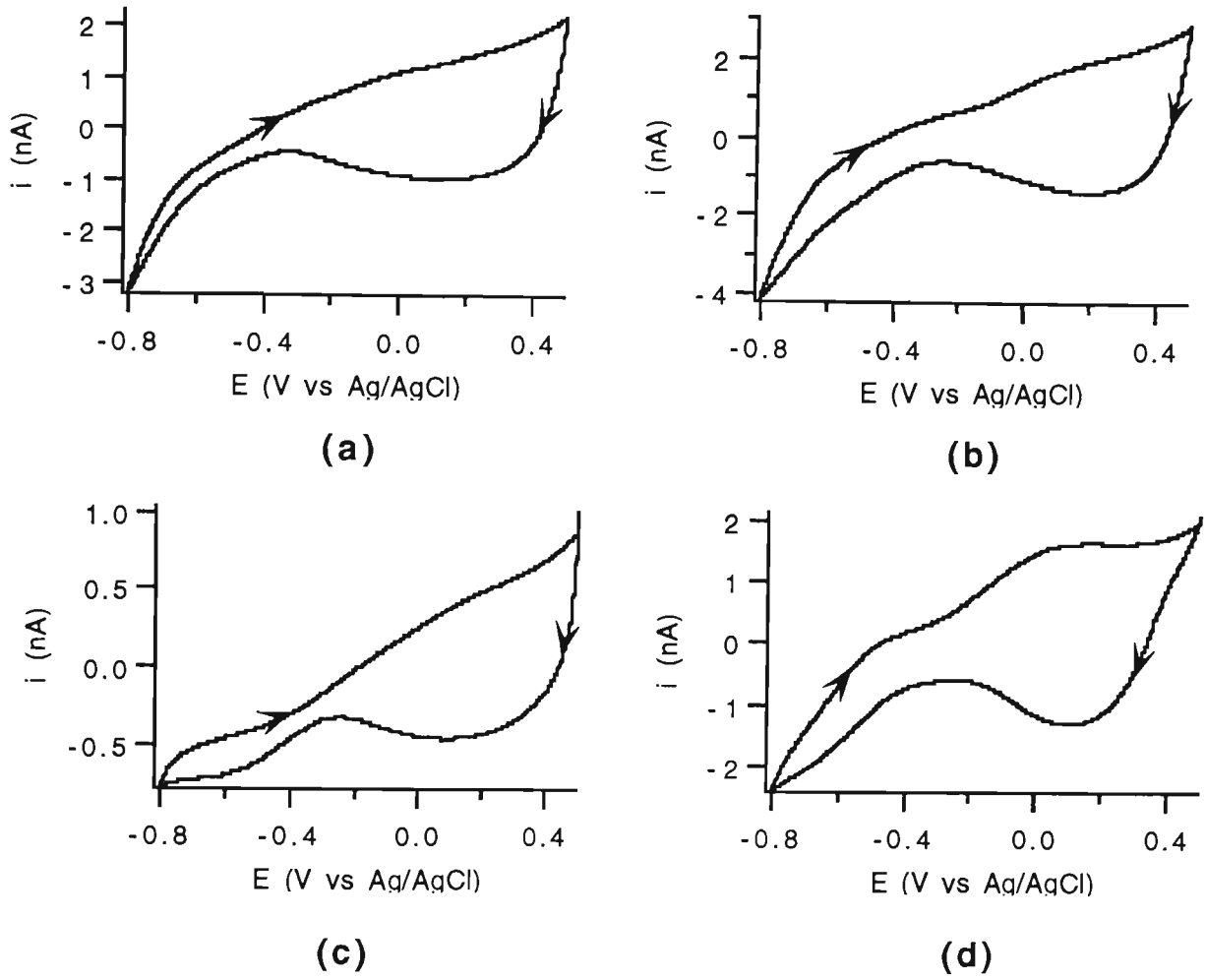

***Figure 4.10**: Cyclic voltammograms of PPy/SBA in 1mM amino acid solutions prepared in 0.001M $NaNO_3$. (a) alanine , (b) serine, (c) aspartic acid and (d) arginine. Scan rate=50mV/s.*

***Table 4.2** Conductance and pH of 1mM amino acid solutions in 0.001M $NaNO_3$**

Solutions	Conductance (μS)	pH
Sodium Nitrate	123.5± 0.2	5.5
Alanine	124.3± 0.1	5.8
Serine	124.5± 0.2	6.1
Aspartic Acid	241.3± 0.3	3.5
Arginine	145.5± 0.1	9.2

**Amino acid solutions prepared in Milli-Q water. Conductance and pH of solutions were measured as described in Section 4.2.2.*

In the case of aspartic acid the cation peak was present at extreme reduction potentials. But unexpectedly the current had decreased in the cyclic voltammogram. Although the solution conductivity was higher than the nitrate solution, the presence of the amino acid in the solution affects polymer redox behaviour. In arginine the oxidation and reduction has become prominent but the exact role of amino acids is unclear. It is concluded that under the applied experimental conditions the redox behaviour is affected more for microelectrodes as compared with macroelectrdes.

4.3.5 Chronoamperometry

Oxidation and reduction of PPy/SBA (in flowing solution) was also investigated using potential step experiments. Useful information regarding the affinity of the polymer for the amino acids had already been obtained using chronoamperometry at macroelectrodes. This technique, therefore, was also applied to microelectrodes to obtain information about the rate of current decay and affinity of amino acids at polymer modified microelectrodes.

The PPy/SBA was first reduced at -0.8V for 10ms and then the potential was stepped to 0.5V for 10ms. The current transients recorded in 0.1M $NaNO_3$ at both microelectrode and macroelectrode are shown Figure 4.11. Well developed maxima were obtained on both micro- and macroelectrodes. The current discharge was 85% in 2ms at the microelectrode, whereas at the macroelectrode the current discharge was 75% in 2ms. The observations are consistent with the literature [311,314].

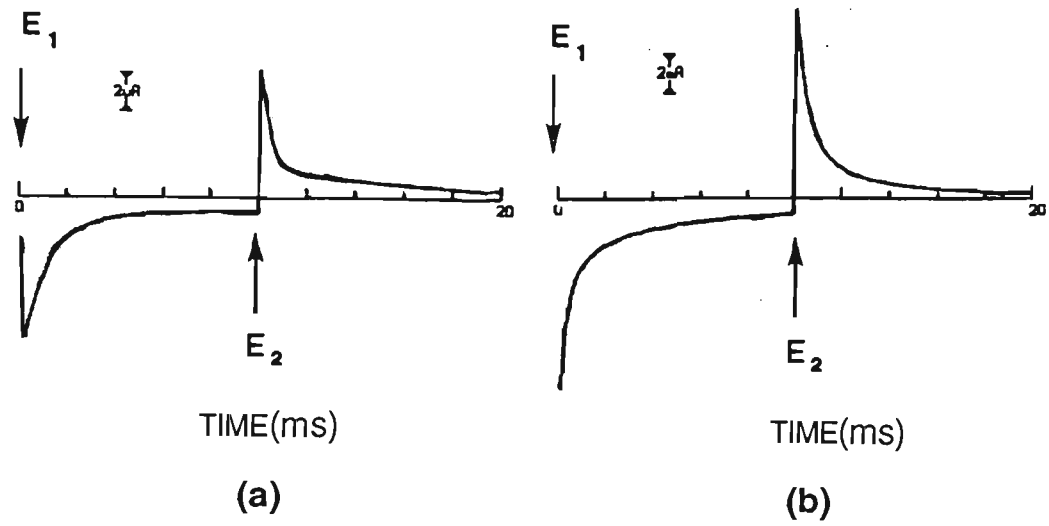

Figure 4.11: *Chronoamperograms recorded at PPy/SBA in 0.1M $NaNO_3$. (a) microelectrode (b) macroelectrode. E_1=-0.8V, E_2=0.5V, pulse width=10ms. Flow rate=1ml/min.*

The i/t profile was also recorded in amino acid solutions at PPy/SBA microelectrodes (Figure 4.12). In alanine and serine the responses were similar. Only the oxidation current decayed in less than 1ms. Maximum current was obtained in aspartic acid solutions. The current discharge was completed in 4ms. In the case of arginine the current decay was slow and continued throughout the pulse period. This indicates some strong interaction between the polymer and amino acid.

Chronoamperometry was also carried out in amino acid solutions prepared in 0.001M $NaNO_3$ (Figure 4.13). No distinction could be made between the alanine or serine from that of sodium nitrate solution. The polymer electrode showed a very slow decaying current in the presence of aspartic acid and the current decay continued throughout the potential pulse. The polymer showed strong affinity for the acid. In the case of arginine the current decay was slower than that in the nitrate solution indicating some affinity between polymer/amino acid.

These observations indicate that the response on the polymer electrode is dependent on the nature of amino acid. The polymer/amino acid interaction differs in zwittrions (alanine and serine), anionic and cationic amino acids.

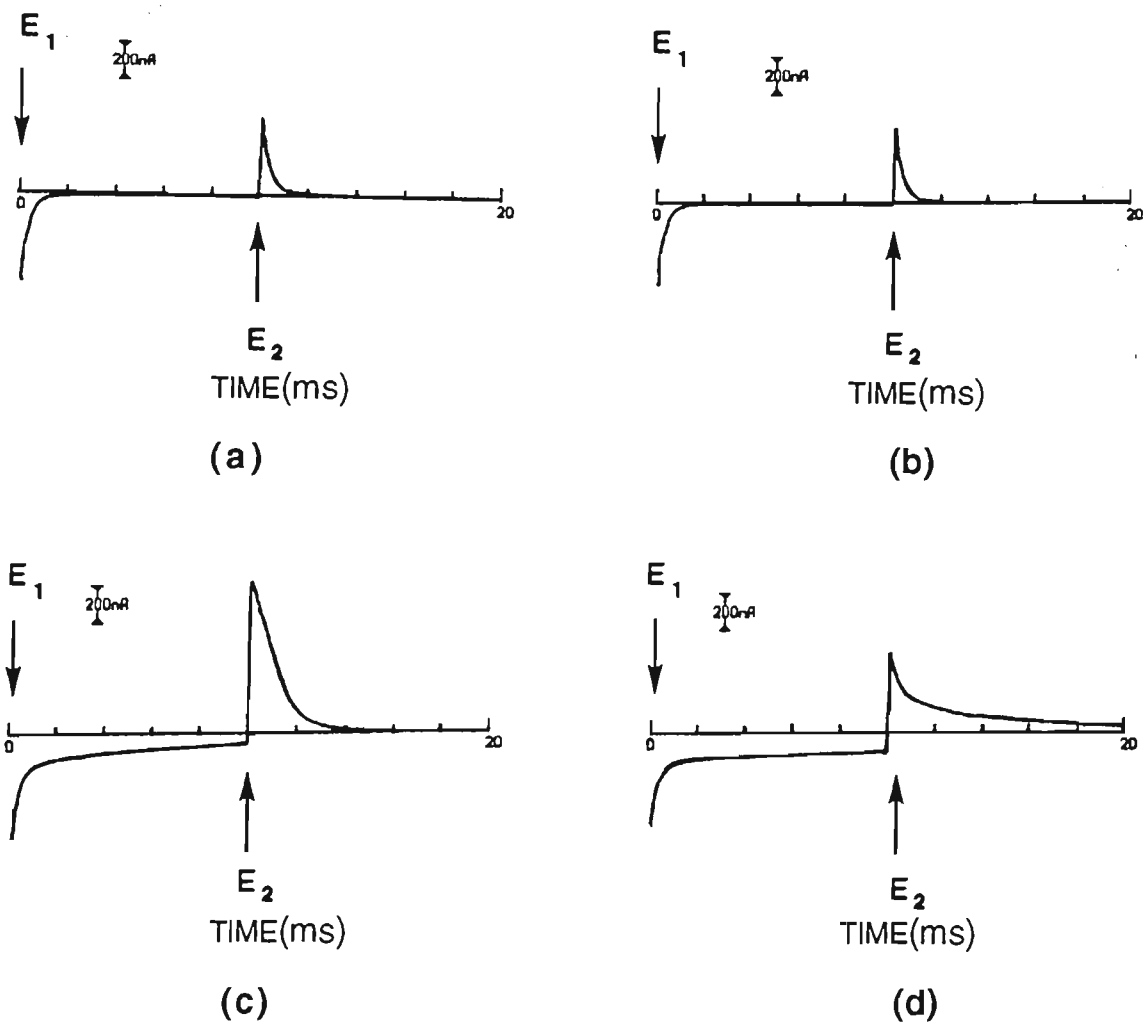

***Figure 4.12**: Chronoamperograms recorded at PPy/SBA (microelectrode) in 1mM amino acid solutions. (a) alanine ,(b) serine,(c) aspartic acid and (d) arginine. E_1=-0.8V, E_2=0.5V, pulse width=10ms. Flow rate=1ml/min*

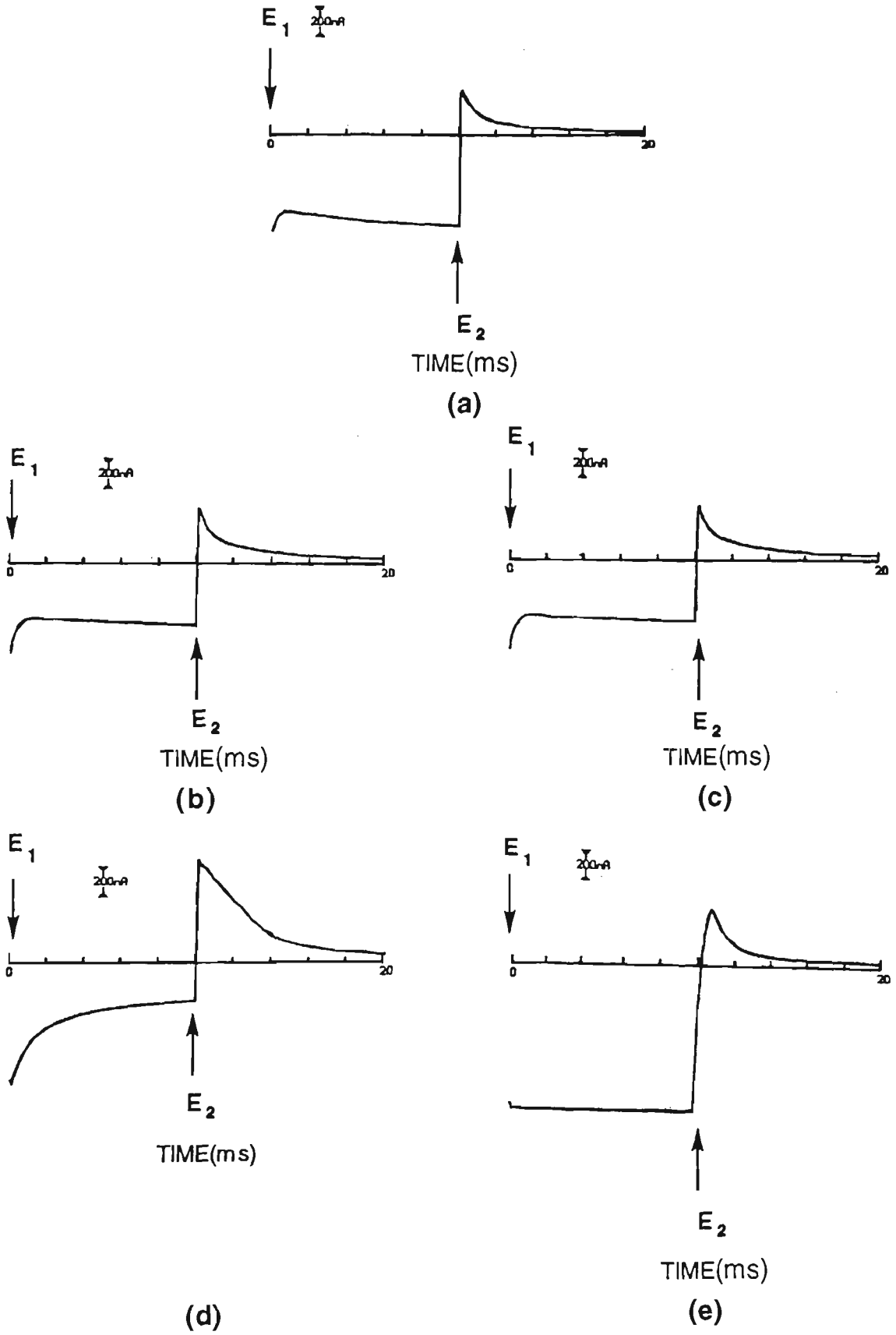

***Figure 4.13**: Chronoamperograms recorded at PPy/SBA (microelectrode). In $NaNO_3$ (a) 0.001M, and 1mM amino acid solutions prepared in 0.001M $NaNO_3$: (b) alanine, (c) serine, (d) aspartic acid and (e) arginine. E_1=-0.8V, E_2=0.5V, pulse width=10ms. Flow rate=1ml/min.*

4.3.6 Flow Injection Analysis

FIA experiments were carried out to determine the optimum detection conditions for of amino acids. Constant potential analysis, and pulse potential analysis with current sampled at different points, were considered.

4.3.6.1 Constant Potential Amperometric Detection

A constant potential hydrodynamic voltammogram (HDV) was obtained on PPy/SBA for aspartic acid. The potential applied was varied from -0.8V to 0.5V with 100 mV intervals. The responses obtained are shown in Figure 4.14. From -0.8V to -0.3V there was an increase in the polymer response. The maximum response was obtained at -0.3 V. Subsequently, there was a decrease in the response magnitude.

The presence of maxima in the current responses with respect to the applied potential indicates that the polymer switched from the non-conductive to the conductive state as the potential was scanned from -0.8 to 0.5V. These observations also suggest that the ion exchange processes were occurring and that responses were not ohmic in nature.

The conductance and pH of the analyte solutions are given in Table 4.3. The aspartic acid analyte conductance is higher than the eluent. The change in conductance of the flowing solution as the analyte plug passes over the electrode also contributed to the signal produced. It is possible that, like macroelectrodes, the change in the solution pH might also have affected the polymer conductivity by affecting the access of the analyte or eluent ions to the polymer chains, or by affecting the polymer chain orientation.

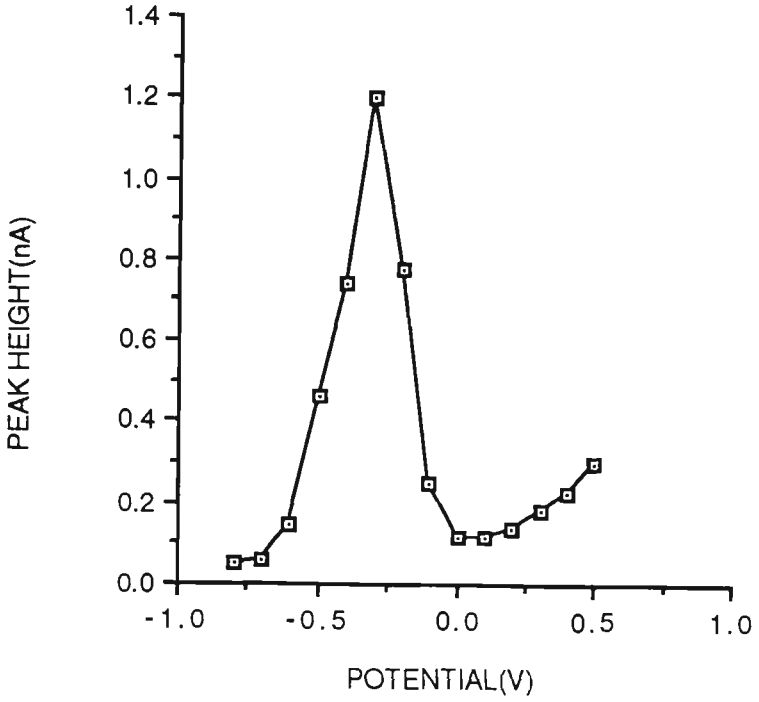

***Figure 4.14**: Constant potential HDV obtained using PPy/SBA for 0.1mM aspartic acid. Potential varied from -0.8 V to 0.5V with 100mV steps. Eluent=1x10^{-3}M $NaNO_3$. Flow rate =1ml/min. Injection volume=50µl.*

***Table 4.3** Conductance and pH of 0.1mM amino acid in 0.001 M $NaNO_3$*

Solutions	Conductance (µS)	pH
Sodium nitrate	123.5± 0.2	5.5
Alanine	124.3± 0.1	5.2
Serine	124.5± 0.2	5.3
Aspartic acid	156.1± 0.2	4.1
Arginine	130.8± 0.1	8.0

Concentration of sodium nitrate solution=0.001M. Conductance and pH of the solutions were measured as described in Section 4.2.2.

The FIA peaks were well defined between 0.5V and -0.4V (Figure 4.15). A base line drift was observed between -0.8V and -0.5V which was severe at more negative potentials. Reproducible responses were not obtained when the analysis was repeated at the same electrode, a 40% decrease in the

response magnitude was observed. The drift in the base line and the lack of reproducibility of the system suggest fouling of the electrode surface.

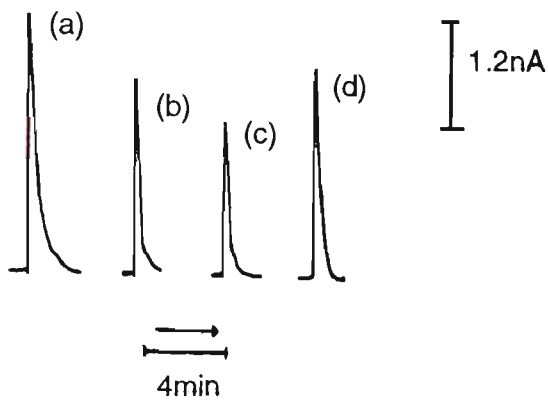

***Figure 4.15**: FIA responses at PPy/SBA during amperometric detection of 0.1mM aspartic acid. (a)=0.5V, (b)=0.4V, (c)=0.3V, (d)-0.1V and (e)-0.2V, Eluent=1x10^{-3} M $NaNO_3$. Flow rate =1ml/min. Injection volume=50µl.*

4.3.6.2 Pulsed Integrated Amperometry

Pulsed integrated amperometry was also used to investigate the detection of aspartic acid on PPy/SBA coated microelecrodes. A series of repetitive pulses were applied to the electrode. During this analysis E_1 was kept constant at +0.5V and E_2 varied from -0.8V to 0.3V. The current was sampled at the end of the E_1 pulse (at exactly the same position as for macroelectrode experiments) and at the end of the E_2 pulse, which includes the potential where the maximum response for the aspartic acid was obtained during amperometric detection. The waveform with the current sample points is shown in Figure 4.16.

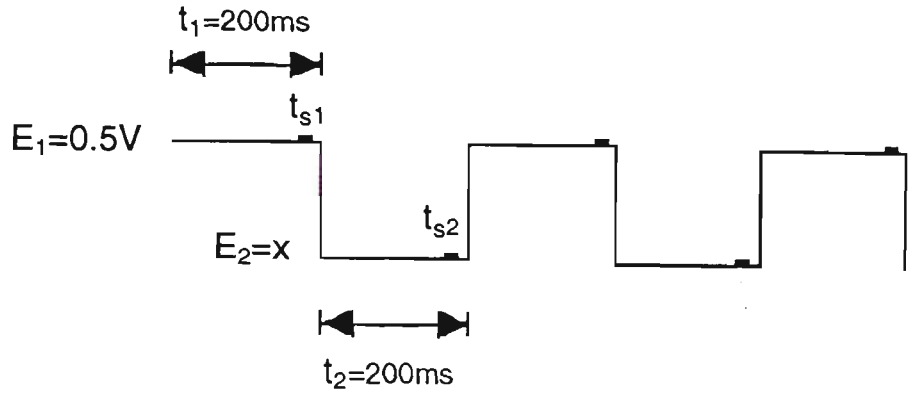

Figure 4.16: *Pulsed potential waveform with current sampling point positions. E_1= electrode potential fixed at 0.5V, E_2=electrode potential varied between -0.8V and 0.3V. t_1=time period for E_1, t_2=time period for E_2, t_{s1}=current sampling point at E_1, t_{s2}=current sampling point at E_2.*

It was observed with microelectrodes in 0.001M $NaNO_3$ eluent that the background current was low (charge monitored in pC range) compared to macroelectrodes and fast to stabilise, about 15 minutes. Figure 4.17 shows the pulsed potential hydrodynamic voltammogram on PPy/SBA. Peak current magnitude (monitored as charge) did not change between 0.3V and -0.1V, with low current response for both E_1 and E_2. This was probably due to the lower reduction potential (E_2) and so the polymer was not fully reduced. As discussed for the case of macroelectrodes, the signal might also consist of multicomponents. The ion-exchange process was not efficient because the polymer was not fully reduced. The signal obtained also consisted of the electrode charging current as well as the current arising from the change in the solution conductivity as the analyte passed over the electrode.

The magnitude of the response, however, started to increase with the application of more cathodic potentials and the maximum was obtained at E_2=-0.8V with current sampled at E_1. This was probably because the ion-exchange process was more efficient with the application of more cathodic potentials. Other factors contributing to the current signal were: polymer

conductivity and the charging of the electrode which was also influenced by the applied potential.

The responses at E_2 were lower than E_1 between -0.3 and -0.8V. It was observed that the response was not a maximum when the current was sampled at -0.3V, which was the potential which produced maximum response in constant potential analysis. The condition E_1=0.5V and E_2 =-0.8V with current sampled at E_1 was selected for all further analyses.

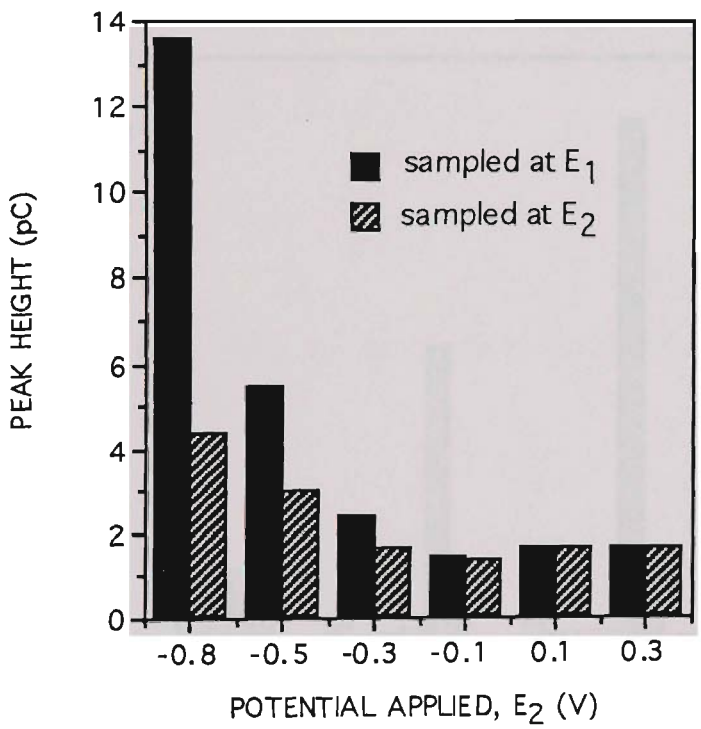

Figure 4.17: *Pulsed potential HDV at PPy/SBA for 0.1mM aspartic acid. E_1=+0.5V, E_2 varied as give in x-axis, t_1=t_2=200ms, t_{s1}=160-190 ms, t_{s2}=360-390 ms. Eluent=1x10^{-3}M $NaNO_3$. Flow rate=1ml/min. Injection volume=50µl.*

4.3.6.3 Effect of Polymer Composition on the Selectivity towards Amino Acids

The optimised experimental conditions were applied to detect other selected amino acids (alanine, serine and arginine) as well as to investigate the effect of polymer composition on selectivity of amino acids. Figure 4.18 shows the

comparison of responses obtained for four amino acids on different electrodes. The polymers investigated were responsive to all four amino acids to varying degrees but the heighest response was for aspartic acid. The maximum aspartic acid response was obtained at PPy/SBA followed by the PPy/DS electrode. The sensitivity for alanine and serine was very low irrespective of the nature of the electrode. Similar to macroelecrodes, PPy/DS showed the highest response for arginine due to cation exchange properties [69,189,287].

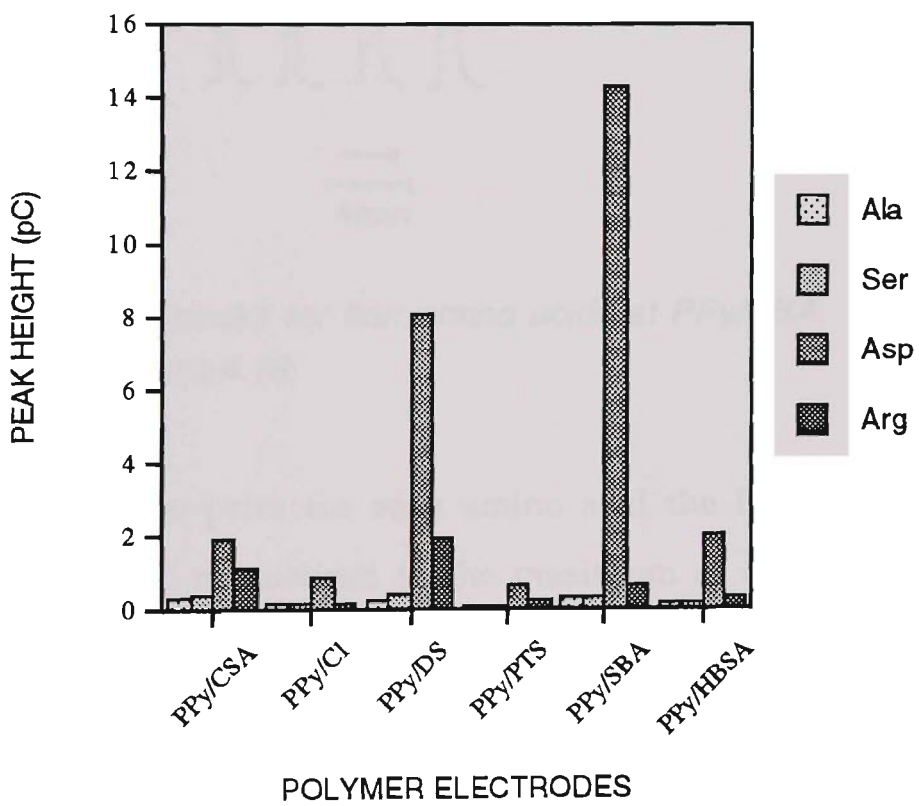

***Figure 4.18**: A comparison of FIA responses at polymer electrodes for alanine, serine aspartic acid and arginine solutions. E_1=+0.5V, E_2=-0.8V, t_1=t_2=200ms, t_s=160-190ms. Eluent=1x10^{-3}M $NaNO_3$. Flow rate=1ml/min. Concentration of amino acid=0.1mM. Injection volume=50µl.*

These results indicate that the selectivity for aspartic acid among the electrodes has been improved on microelectrodes compared to macroelectrodes (Section 3.3.5.4). Figure 4.19 shows the FIA peaks for four amino acids at PPy/SBA. FIA peaks were well defined with no peak tailing.

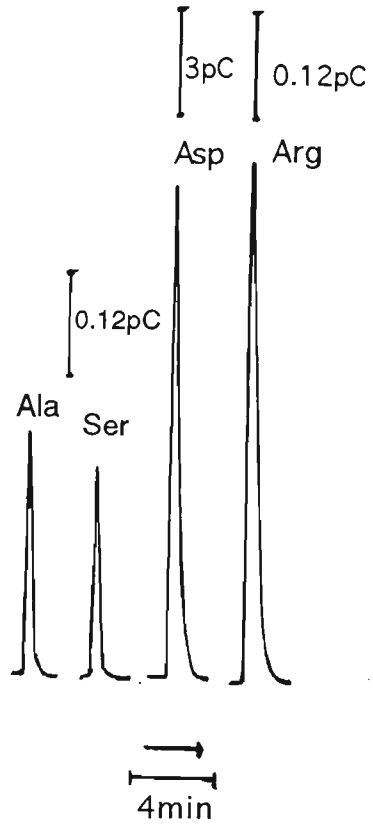

Figure 4.19: *FIA peaks for four amino acids at PPy/SBA. Experimental conditions as in Figure 4.18.*

To obtain a finger-print for each amino acid the FIA responses for four amino acids were normalised to the maximum of each amino acid. The pattern obtained is shown in Figure 4.20. It is observed that a specific pattern was obtained for each amino acid. The differences in the histograms for alanine, serine, aspartic acid and arginine are sufficient to permit identification of each compound. A distinction can be made between alanine and serine based on the responses of electrode 3 (PPy/DS) and 5 (PPy/SBA). On the other hand the pattern obtained at microelectrodes (Figure 4.20) for aspartic acid and arginine could easily be distinguished from alanine and serine as compared with the patterns obtained at macroelectrodes (Figure 3.25).

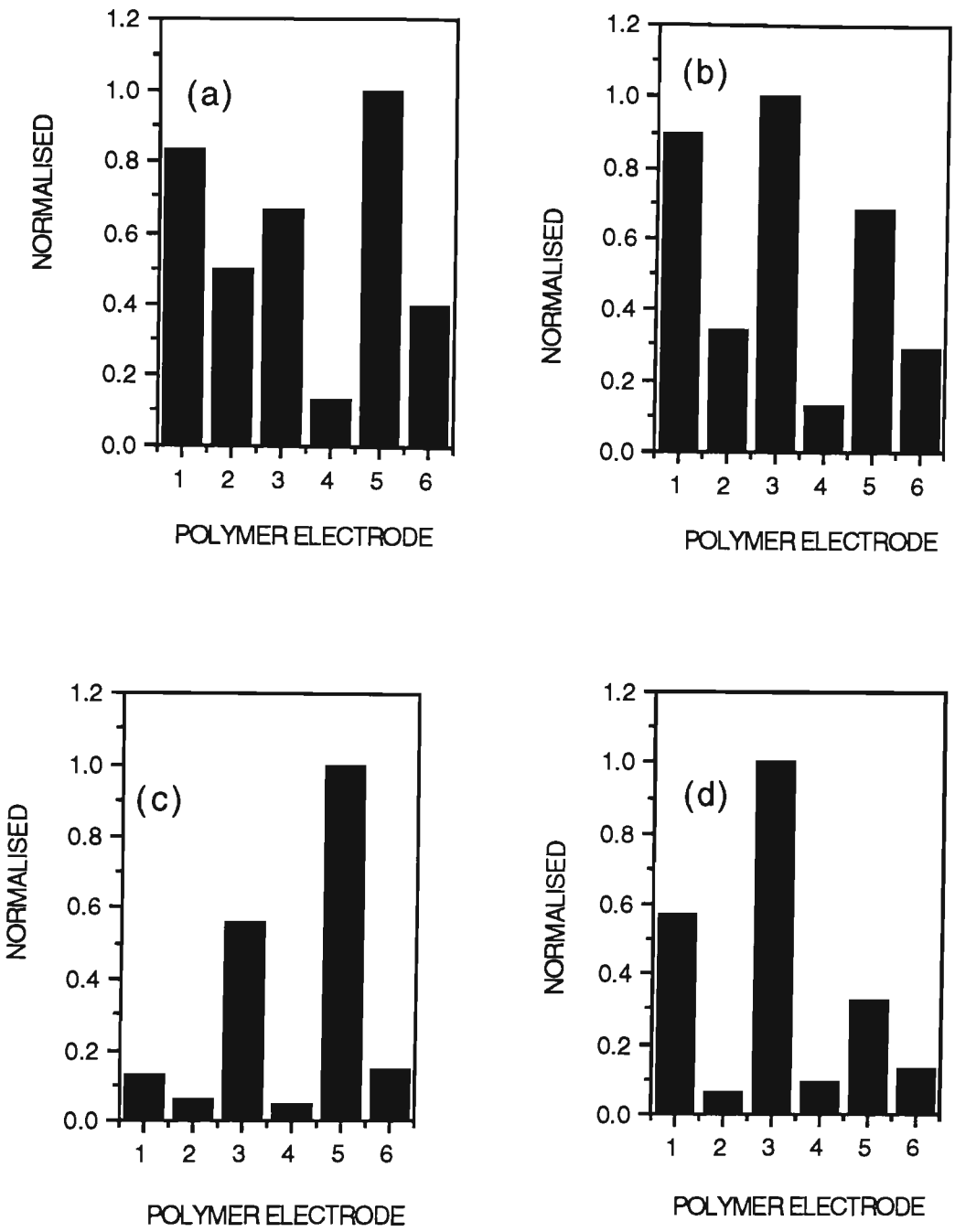

Figure 4.20 *Normalised patterns obtained at multielectrode sensors. Data taken from Figure 4.18. (a) alanine, (b) serine, (c) aspartic acid, and (d) arginine. 1=PPy/CSA, 2=PPy/Cl, 3=PPy/DS, 4=PPy/PTS, 5=PPy/SBA, and 6=PPy/HBSA*

The selectivity factor for alanine to serine is given as the ratio of peak heights (Ala-to-Ser) denoted as α_1 and aspartic acid to arginine as the ratio of peaks (Asp-to-Arg) is given as α_2 respectively in Table 4.4. The selectivity, like that obtained with macroelectrodes, is maximum at PPy/SBA and has

increased by more than 100% at the microelectrode. These observations show that it is possible to improve the selectivity of amino acid analysis with appropriate polymer systems and electrochemical conditions.

Table 4.4 *Selectivity factors of amino acids at polymer electrodes*

Polymer Electrode	α_1 Ala/Ser	α_2 Asp/Arg
PPy/Cl	1.1	7.25
PPy/DS	0.5	4.23
PPy/PTS	0.8	3.44
PPy/SBA	1.1	23.06
PPy/HBSA	1.0	8.00
PPy/CSA	0.7	1.72

Data obtained from Figure 4.18

4.3.6.4 Intra-Group Selectivity towards Amino Acids

The intra-group selectivity (for aspartic acid and glutamic acid) was also considered on polymer coated microelectrodes. The response magnitude for both acids were of the same order at each particular electrode. The selectivity between these two acids could not be improved at any of the microelectrodes considered. The FIA responses obtained for these polymer systems are shown in Figure 4.21 and the FIA peaks for PPy/Cl, PPy/PTS and PPy/HBSA are given in Figure 4.22 (a-c). The FIA peaks are sharp and suffer from very little tailing.

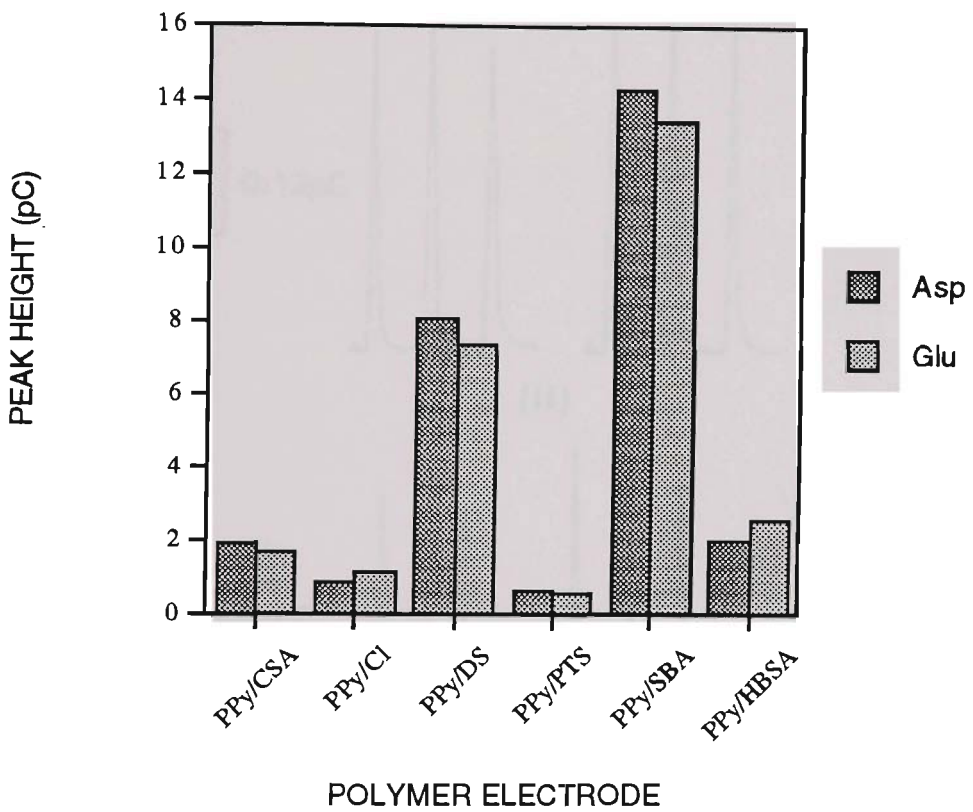

***Figure 4.21**: Intra-group selectivity at polymer electrodes for 0.1mM aspartic acid and 0.1mM glutamic acid. Conditions same as in Figure 4.18.*

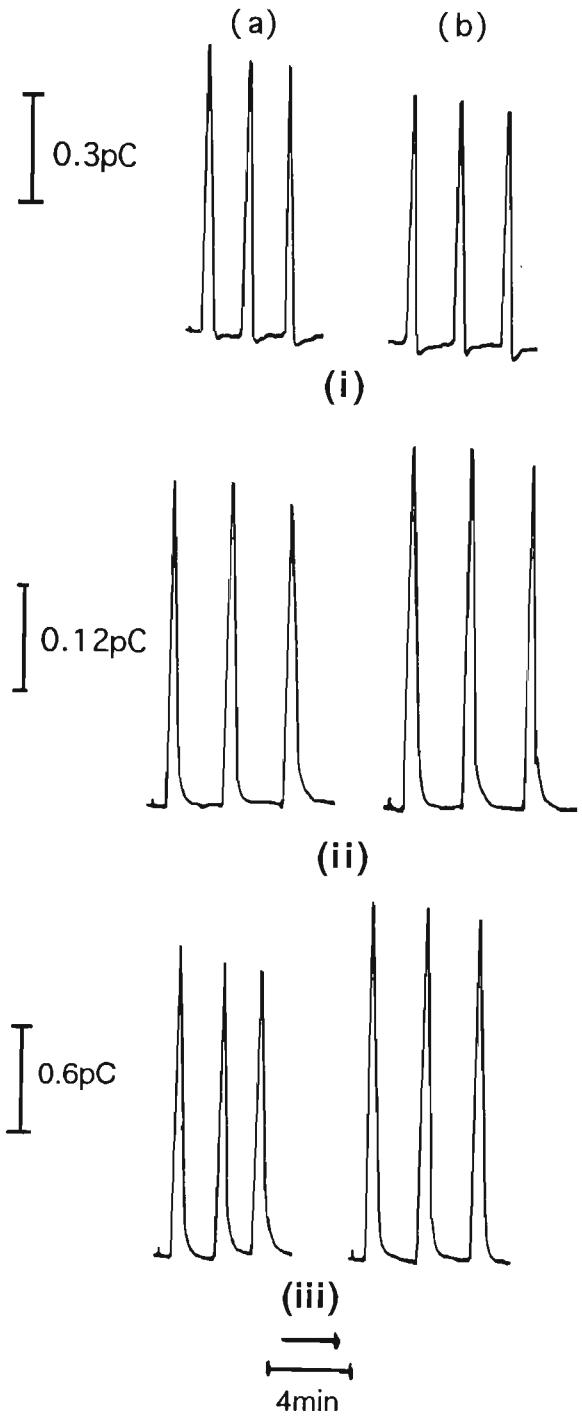

***Figure 4.22**: FIA peaks obtained for (a) aspartic acid and (b) glutamic acid at (i) PPy/Cl, (ii) PPy/PTS and (iii) PPy/HBSA. Conditions same as in Figure 4.21.*

4.3.6.5 Calibration for Aspartic acid and Glutamic acid

Calibration curves were obtained for aspartic acid and glutamic acid using optimised conditions (Figure 4.23). The linearity of response was obtained over the concentration range $7.5x10^{-6}$M to $1x10^{-4}$M. The data analysis is given in Table 4.5. The limit of detection (LOD) is $3x10^{-6}$M (0.4ppm) for both aspartic and glutamic acid with correlation coefficients for the calibration of 0.992 and 0.982 for aspartic and glutamic acid respectively. This corresponds to confidence levels of 99.9% for both aspartic and glutamic acid (for 4 degrees of freedom). The LOD has improved, as compared to that obtained with the PPy/CSA macroelectrode (1ppm), due to the higher faradaic-to-charging current ratio. Some FIA responses are shown in Figure 4.24.

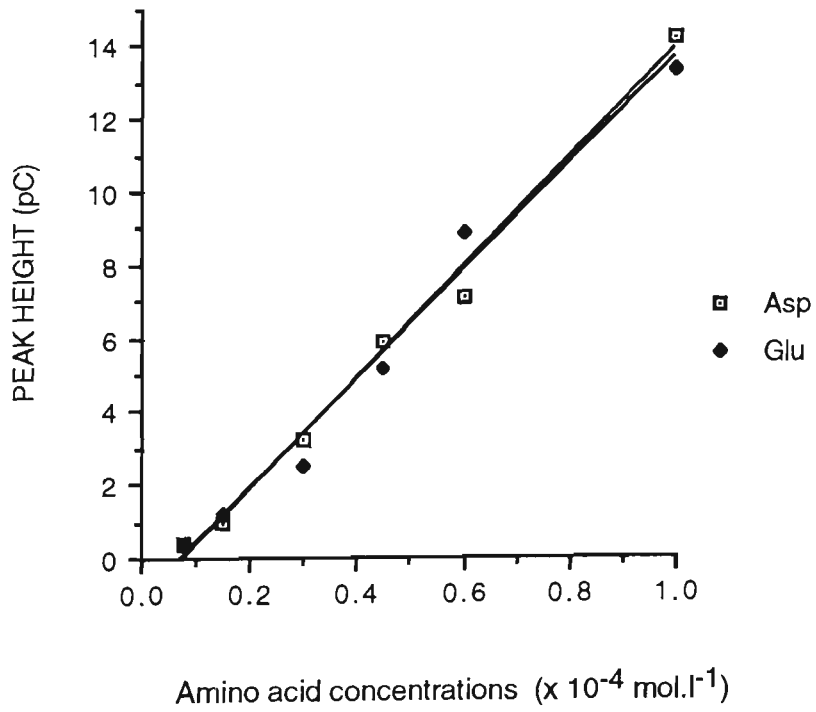

Figure 4.23: *Calibration graph for aspartic acid and glutamic acid at PPy/SBA. E_1=+0.5V, E_2=-0.8V, t_1=t_2=200 ms, t_S=160-190ms. Eluent $1x10^{-3}$M $NaNO_3$. Flow rate=1ml/min. Injection volume=50µl.*

Table 4.5 *Calibration data obtained for aspartic acid and glutamic acid at PPy/SBA for concentration range 7.5x10^{-6} M to 1x10^{-4} M*

Amino acid	Intercept	Slope pC/10^{-4} mol.l^{-1}	Correlation Coefficient	Limit of Detection
Aspartic acid	-1.18	15.10	0.992	3x10^{-6} M
Glutamic acid	-1.07	14.75	0.982	3x10^{-6} M

Calibration data obtained from Figure 4.23

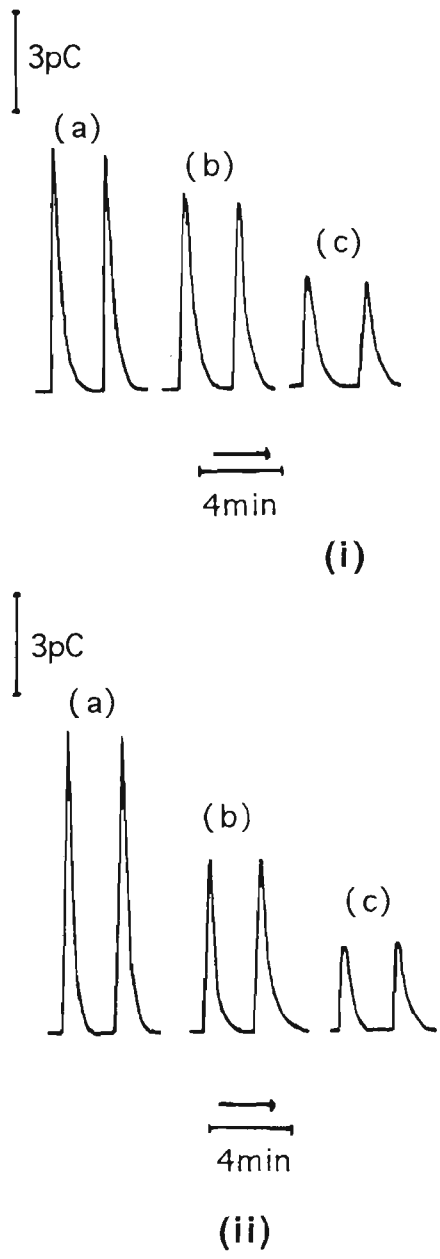

Figure 4.24: *FIA responses for (i) Aspartic acid and (ii) Glutamic acid at PPy/SBA microelectrode (10μm). (a) 6x10^{-5}M, (b) 4.5x10^{-5}M, and (c) 3x10^{-5}M. E_1=+0.5V, E_2=-0.8V, t_1=t_2=200 ms, t_S=160-190ms. Eluent =1x10^{-3}M $NaNO_3$. Flow rate=1ml/min. Injection volume=50μl.*

4.3.6.6 Reproducibility and Stability of the Polymer Based Detection System

The reproducibility of the response on PPy/SBA was investigated by making six consecutive injections. Reproducible responses, 13.6±0.15pC, were obtained without loss in the response signal (Figure 4.25). The long term stability of the microelectrode during use was less than that of the macroelectrode. Often a sudden loss in polymer response without any prior indication of polymer deterioration occurred. There was an initial rapid deterioration of the response which subsequently stabilised. The polymer lasted for a maximum of 3 hours and, over this time reproducibility was satisfactory. The response, showing little loss of sensitivity after 3 hours of FIA analysis, is shown in Figure 4.26. The cyclic voltammograms of the polymer in $NaNO_3$ (0.1M and 0.001M) after the stability test are also given (Figure 4.27) and they indicate that the polymer was still electroactive.

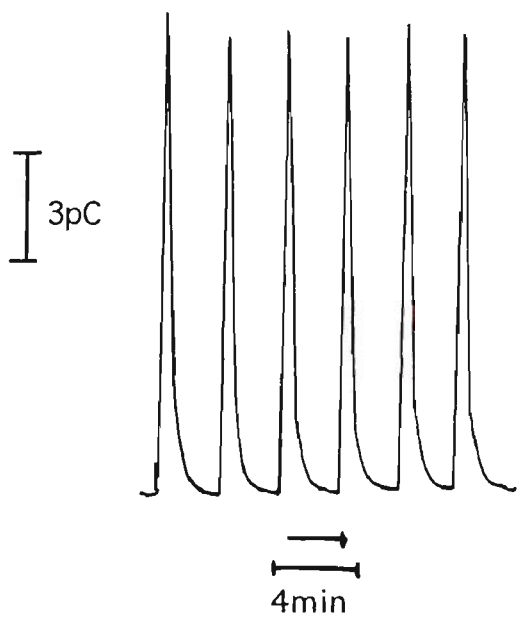

***Figure 4.25**: FIA response reproducibility at PPy/SBA for 0.1mM aspartic acid. FIA conditions as in Figure 4.18.*

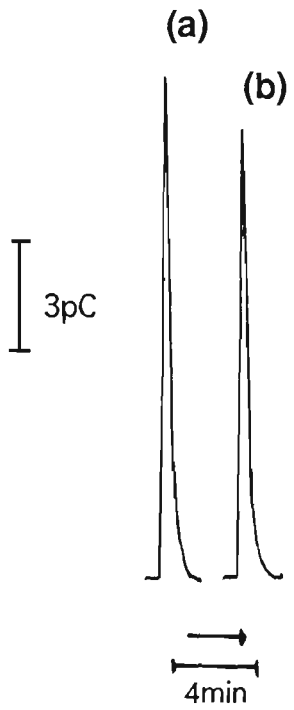

***Figure 4.26**: Stability of the PPy/SBA microelectrode for detection of aspartic acid (0.1mM). (a) Response at the beginning of analysis, (b) After 3hrs. FIA conditions as in Figure 4.18.*

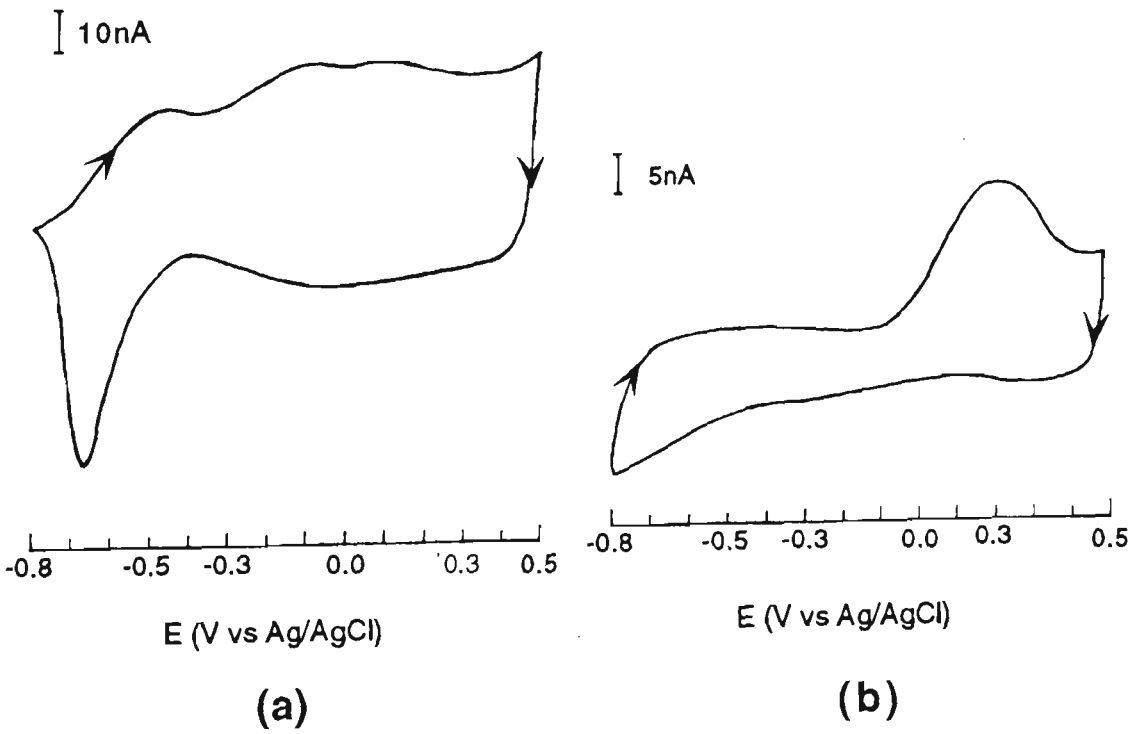

***Figure 4.27**: Cyclic voltammograms of PPy/SBA in (a) 0.1M $NaNO_3$ and (b) 0.001M $NaNO_3$ after 3 hours of FIA. Scan rate = 50mV/s.*

4.4 CONCLUSIONS

In this chapter it has been shown that conducting polymers can be deposited successfully on microelectrodes and that a range of counterions can be incorporated. The conditions required for polymerisation were harsher, requiring higher current density and monomer concentrations. The polymer showed adequate redox characteristics and satisfactory stability.

FIA demonstrated that the microelectrodes were also responsive to the amino acids, but the magnitude of response remained higher for aspartic acid and the selectivity had increased by more than 100%. A pattern of response could be obtained for each amino acid at different polymers. The patterns for aspartic acid and arginine, however, have become more selective. It is also possible to distinguish between alanine and serine.

The LOD of aspartic acid has also improved as compared with that obtained with macroelectrodes. Although the stability of the microelectrodes was not as good as that of the macroelectrodes, it has been demonstrated that they are stable for up to 3 hours in FIA mode. Nevertheless, a limitation of the microelectrodes could be that, for some electrodes, a sudden loss of polymer response can occur without prior indication or warning.

In general, amino acid responses and sensitivities at these microelectrodes are superior to those obtained at macroelectrodes.

CHAPTER 5

DETECTION OF HALOACETIC ACIDS AT CONDUCTING POLYMER MODIFIED MICROELECTRODES

5.1 INTRODUCTION

Chlorination of drinking water has been shown to result in the production of chlorinated and fluorinated organic acids [321-323]. Haloacetic acids are carcinogenic even at low concentrations [324-328], therefore a reliable detection method is necessary at low ppb levels.

Disinfecting of drinking water with chlorine results in halogenated by-products due to the reaction of chlorine (as hypochlorous acid and hypochlorate anion) with natural 'humic and fulvic' matter present in the source water. Christman and others [329-332] have shown that chloroform and chlorinated aliphatic acids, especially dichloro- and trichloroacetic acids, are major by-products of chlorination of humic and fulvic acid. In the presence of bromide, chlorination of humic acid results in production of all nine possible chloro/bromoacetic acids [333].

The standard method for determination of haloacetic acids is by liquid-liquid extraction followed by derivatization with diazomethane and then gas chromatography (GC) with electron capture detection. This is applicable to drinking water and ground water for the detection of six halogenated acetic acid (monochloroacetic acid, dichloroacetic acid, trichloroacetic acid, monobromoacetic acid and dibromoacetic acid). This method is the US EPA method 552 (United States Environmental Protection Agency) [334]. The detection limits are in the 0.05 to 0.1 μg/l range (for MCAA, DCAA, TCAA, DBAA) but this method is complicated as it require diazomethane derivatization.

High performance liquid chromatography with UV detection at 210 nm has been applied to detect di- and trichloroacetic acid [335]. Mono-, di-, and

trichloroacetic acids were also detected with refractive index detection while separation was carried out by ion-exchange chromatography on silica based anion-exchanger [336].

Recently two chromatographic methods have been described. The first employs anion exchange separation with suppressed conductivity detection, and the second method is anion exclusion chromatographic separation with UV detection. The detection limits are in the 5 to 90 μg/l range, which is higher than those observed by GC detection [337] and so cannot be used for real applications. But this method is simple, inexpensive and includes simultaneous separation and detection of inorganic and organic acids.

The detection of partially ionised inorganic and organic acids, however, has always presented a challenge for conductivity detection. In the suppressed mode, the reduction of the background conductance leads simultaneously to the suppression of ionisation of analyte weak acids. This renders their detection by conductivity very difficult. A method is required that will simultaneously detect the organic acids subsequent to ion chromatography.

5.1.1 Aim and Approach of this Chapter

The work in this chapter focuses on the development of conducting polymer sensors for detection of halogenated organic acids. The electrochemical behaviour of these acids at conducting polymers was considered. The electrochemical detection was carried out in the suppressed mode subsequent to anion exchange separation of organic acids. Electrochemical detection was optimised by considering the influence of the potential and current sampling point. The performance of these detectors was compared with results obtained from conductimetric detection.

Polymer electrodes selected for this work were PPy/Cl, PPy/DS, PPy/SBA and PPy/PTS. Both 10μm and 50μm platinum electrodes were considered in order to gain the benefits from using microelectrodes and to improve the stability of the electrodes. The haloacetic acids include monochloroacetic acid (MCAA), dichloroacetic acid (DCAA), trichloroacetic acid (TCAA), monobromoacetic acid (MBAA), dibromoacetic acid (DBAA) and tribromoacetic acid (TBAA).

5.2 EXPERIMENTAL

5.2.1 Reagents and Standard Solutions

All reagents used were analytical reagent (AR) grade. Pyrrole was obtained from Merck, distilled and kept in a cool place protected from light. Monochloroacetic acid (MCAA), Monobromoacetic acid (MBAA), Dibromoacetic acid (DBAA) and Tribromoacetic acid (TBAA) were obtained from Fluka. Dichloroacetic acid (DCAA) and Trichloroacetic acid(TCAA) were obtained from Sigma. NaOH (BDH), sulfuric acid (Ajax), NaCl (BDH), NaDS (Sigma), SBANa (Aldrich) and PTSNa (Merck) were used as received. 5000ppm of stock solutions of haloacetic acids from Dionex were used for chromatography. Eluent was prepared from 50% w/w solution of NaOH. All eluents were filtered through a 0.45μm filter (Nylon from ACTIVON) and degassed with nitrogen before and during use.

5.2.2 Instrumentation

An in-house built nanogalvanostat was used for constant current polymerisation. Cyclic voltammograms were obtained with a CV-27 voltammograph (BAS) and ElectroLab workstation. Data were acquired via

a Macintosh/MacLab set-up with Chart v3.2.8 or ElectroLab software. Data manipulation was also carried out using the Igor software package (Wavemetrics).

For stationary cell work, the working electrode was a platinum disc, either 10 µm or 50 µm electrodes (the preparation method is described in Chapter 4). The working electrode was polished on 0.3µm and 0.05µm alumina (Leco) respectively, and ultrasonicated for 1 minute in Milli-Q water before polymerisation experiments. A platinum mesh was used as the auxiliary electrode. The reference electrode was a BAS Ag/AgCl (3MNaCl) with a in-house built salt bridge.

Chromatography was performed with a Dionex Basic Chromatography Module (CHB-2). The injector loop was 50µl. A Dionex anion separation column Ion Pac AS11 Analytical Column (4mm x 250mm, P/N 044076) was used for anion exchange separation of haloacetic acids. The column is composed of 13µm size highly cross-linked polyethylvinylbenzene/divinylbenzene particles agglomerated with anion exchange latex. The Anion Micromembrane Suppressor (AMMS 11) was used for eluent suppression. The Dionex flow cell was modified in that the working electrode was replaced with a teflon block and a hole was drilled through the block to screw in the microelectrode. The reference electrode was a Dionex Ag/AgCl-pH, and the stainless steel body was the auxiliary electrode. The Dionex conductivity cell was used for conductivity detection. The conductivity cell and electrochemical cell were controlled with Dionex Pulsed Electrochemical Detector (PED-II). The recorder was an ICI Instrument DP 600 chart recorder. The microelectrode set up was kept in a Faraday cage to avoid electrical interferences. A preamplifier fitted in the

Faraday cage was used whenever necessary. The schematic of the flow system is shown in Figure 5.1.

The EQCM apparatus described in Chapter 2.

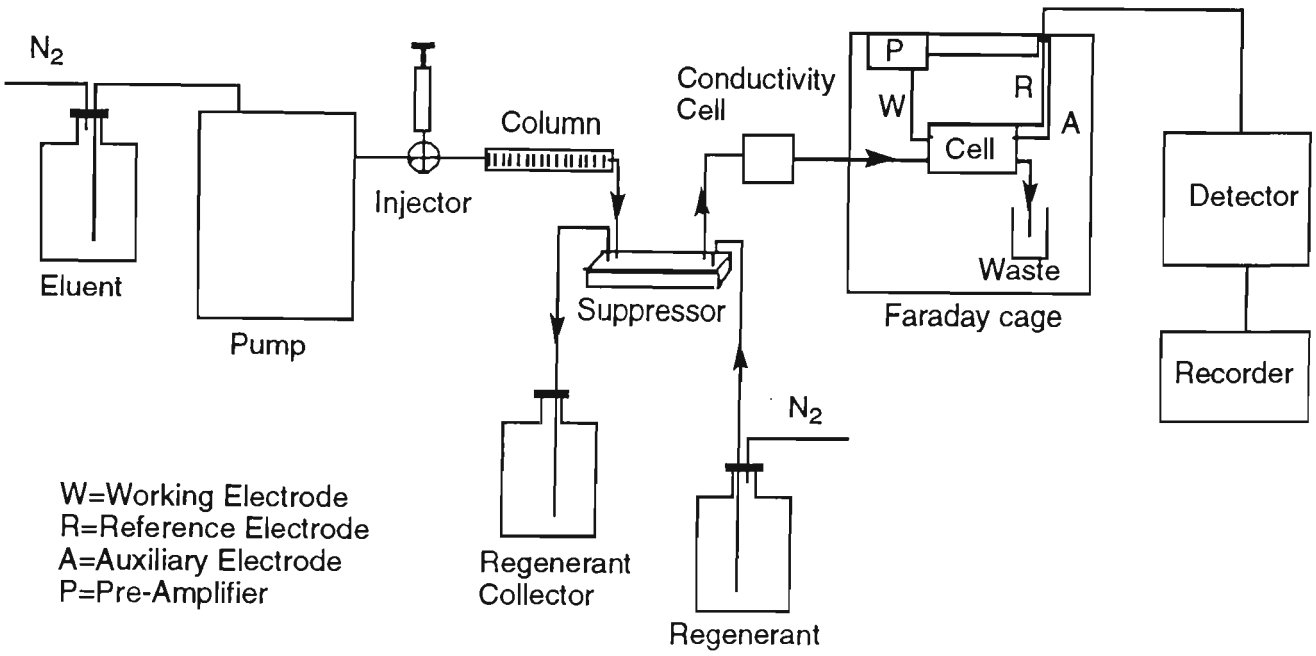

Figure 5.1: *Schematic of the flow system with suppressor.*

5.2.3 Polymerisation Procedure

The monomer solution consisted of 0.5M pyrrole and 0.05M DS, PTS or SBA, but in the case of chloride 1M supporting electrolyte was used. The monomer solution was purged with nitrogen for 5 minutes to remove dissolved oxygen. The constant current mode was employed to deposit the polymer and the polymerisation process was monitored by recording the chronopotentiogram.

5.2.4 Electrochemical Characterisation

The polymer electrodes were characterised in 21mM NaOH, suppressed NaOH and 0.1M haloacetic acid solutions. The polymers were cycled between -0.8V and 0.5V with a scan rate of 50mV/s starting from positive potentials. EQCM was performed in 0.1M $NaNO_3$ and 0.1M MCAA at PPy/SBA.

5.2.5 Chromatographic Method

The standard conditions for the Dionex AS11 column for anion separation were used without any modification. The chromatographic conditions are given below.

Column	Ion Pac AS11
Suppressor	AMMS11
Eluent	21.0mM NaOH
Regenerant	12.5mM H_2SO_4
Regenerant flow rate	2.5-3.0 (ml/min)
Sample loop	50 µl

5.2.6 Suppressor Function

The membrane suppressor is placed between the separator column and the detector. The column eluent enters the membrane suppressor between two membranes made of a cation exchange polymer. A dilute solution of sulfuric acid (the regenerant) flows in the opposite direction, as shown in Figure 5.2. The membranes have fixed sulfonic acid groups and therefore exclude anions. Positive ions can pass through the membrane freely.

Sodium ions leave the eluent and pass through the membrane and enter the regenerant side. An equal number of hydrogen ions from the regenerant flow exchange through the membrane and enter the eluent. The neutralisation of eluent (NaOH) proceeds to form H_2O thus lowering the eluent conductivity. The efficiency of the membrane suppressor is dependent upon the flow rate as well as the regenerant concentration.

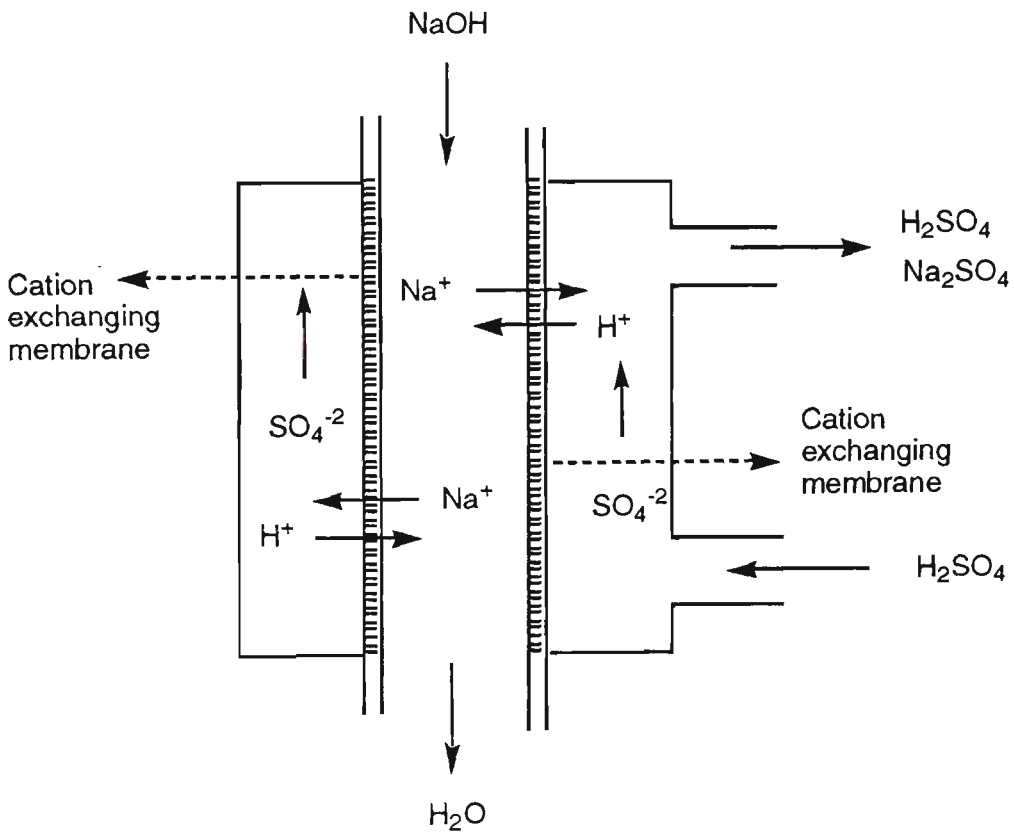

***Figure 5.2**: Operation of membrane suppressor for anion-exchange chromatography.*

5.3 RESULTS AND DISCUSSION

5.3.1 Preparation of Polymer Film

The procedure developed for polymerisation on 10μm microelectrodes (Chapter 4, Section 4.3.1) was applied to 10μm and 50μm electrodes to deposit the polymer. It was found that polymers deposited readily on a

50μm diameter microelectrode. The polymerisation process was monitored by recording the chronopotentiogram. After an initial rise associated with the nucleation process, the potential levelled off to a constant value indicating that no extra resistance was added to the system, that is, a conducting polymer was deposited. Polymerisation was initiated at lower potentials and settled at lower potentials compared to macroelectrodes. Compared with 10μm electrodes the potentials obtained during electropolymerisation were similar for all the polymers, except for PPy/Cl where the potential was 0.55V which is 0.05V higher at the 50μm electrode.

5.3.2 Electrochemistry in Chromatographic Eluent

The electrochemistry at the polymer electrodes was investigated in both suppressed and unsuppressed eluent. The cyclic voltammograms for 10μm are shown in Figure 5.3. The polymers were electroactive in unsuppressed eluent (21.0mM NaOH, pH=12) where the peaks appearing in the reductive region could be related to the high solution resistance, as the electrolyte concentration was low.

At PPy/Cl the reduction peak appeared at -0.6V, while the oxidation peak potential was not defined. For PPy/DS the polymer reduction peak potential was -0.5V. The polymer oxidation peak was broad at around -0.4V. Well defined electrochemistry was observed for PPy/SBA with the reduction peak at -0.45 V and the corresponding rather broad oxidation peak around -0.2V. At PPy/PTS the reduction peak was at -0.6V, whereas the oxidation peak was broad at -0.25V. The current magnitude on these polymer electrodes vary depending on the counterion incorporated into the polymer during polymerisation; as all polymers were prepared under similar experimental

conditions. The current response (electroactivity) of the polymer decreased with successive cycles.

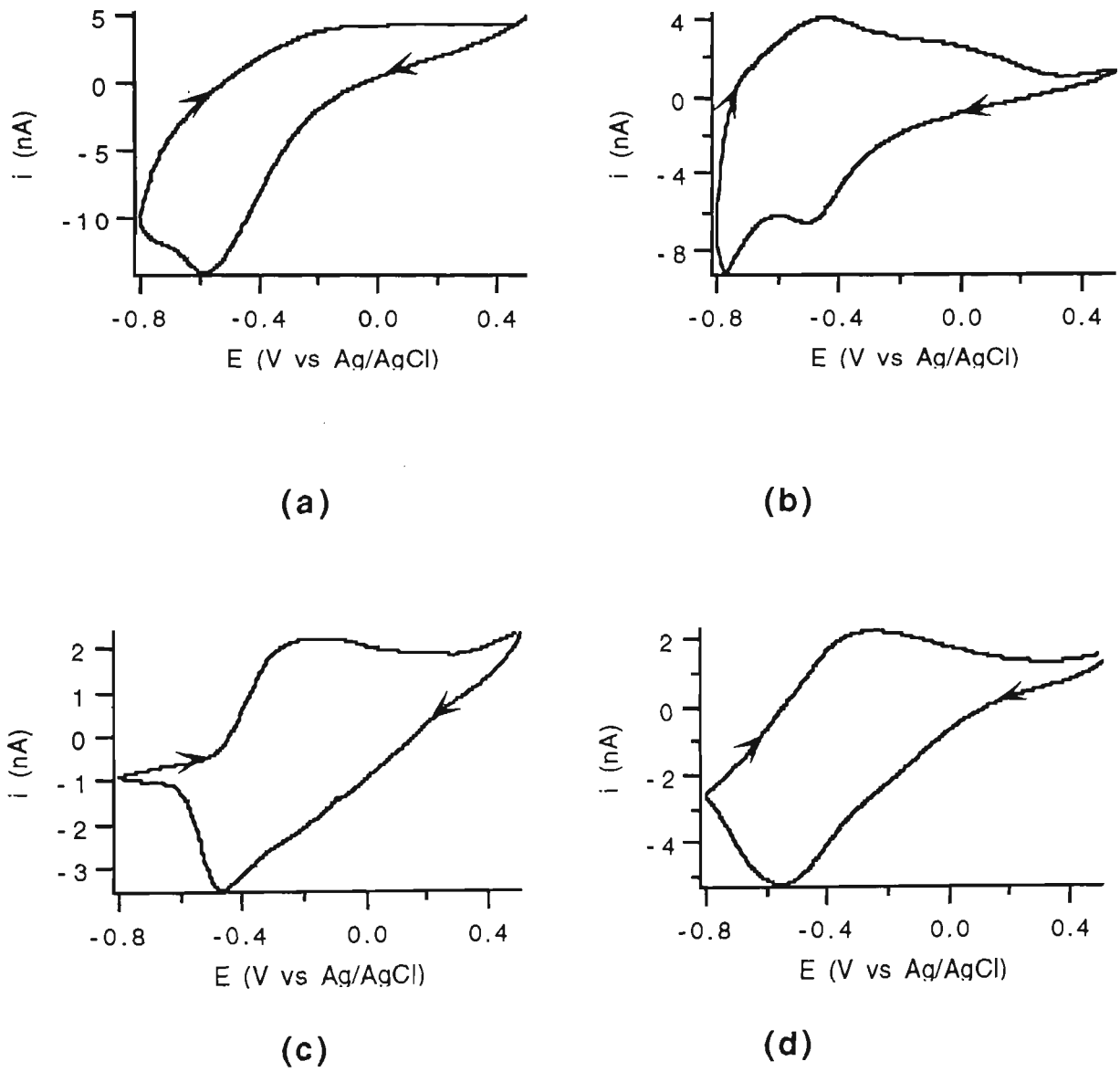

***Figure 5.3**: Cyclic voltammogram at 10μm (a) PPy/Cl, (b) PPy/DS, (c) PPy/SBA, and (d) PPy/PTS electrodes in unsuppressed eluent (21.0mM NaOH, pH=12). Scan rate= 50mV/s.*

Similarly the polymers grown on 50μm electrodes were also characterised in unsuppressed eluent. The cyclic voltammograms obtained at polymer coated 50μm electrodes are depicted in Figure 5.4. These voltammograms have qualitative similarities with those obtained at 10μm electrodes, but quantitative characteristics (e.g. peak position and current magnitude) of the

electrodes were quite sensitive to the size of the electrodes. The current magnitude on 50μm electrodes was higher due to the larger size of the electrodes and shifts in the peak potentials were also observed. The cyclic voltammetric responses are better defined at 50μm electrodes compared with 10μm electrodes. A comparison of electrochemical data is given in Table 5.1. This could be related to the nature of the polymer deposited on two different size electrodes. The effect of fast mass transport is probably more severe at 10μm electrodes. This results in thinner and less stable polymers at 10μm electrodes.

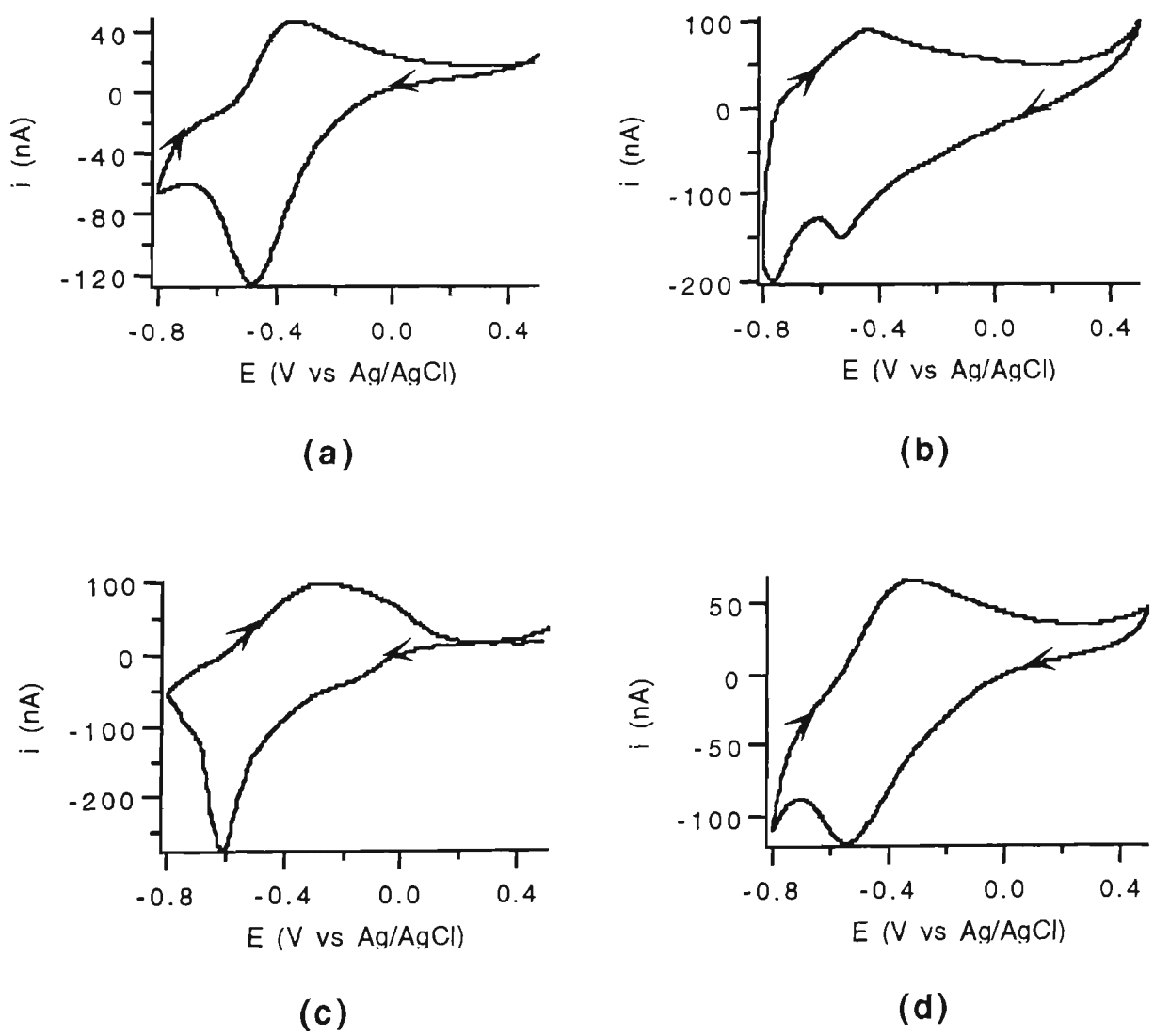

***Figure 5.4**: Cyclic voltammograms at 50μm (a) PPy/Cl, (b) PPy/DS, (c) PPy/SBA and (d) PPy/PTS electrodes in unsuppressed eluent (21.0mM NaOH, pH=12). Scan rate= 50mV/s.*

Table 5.1 *Comparison of electrochemical data obtained at 10μm and 50μm polymer modified microelectrodes, in unsuppressed eluent (21mM NaOH, pH=12)*

Polymer	E_{pa} (V)	E_{pc} (V)	i_{pa} (nA)	i_{pc} (nA)
PPy/Cl	N.D	-0.6	N.D	15
	(-0.4)	(-0.5)	(45)	(120)
PPy/DS	-0.4	-0.5	4	10
	(-0.4)	(-0.5)	(90)	(50)
PPy/SBA	-0.2	-0.45	2	3.5
	(-0.25)	(-0.6)	(90)	(270)
PPy/PTS	-0.25	-0.6	2.2	6.2
	(-0.3)	(-0.55)	(70)	(120)

Values given in brackets obtained at 50μm microelectrodes
N.D= not defined
E_{pa}=anodic peak potential
E_{pc}=cathodic peak potential
i_{pa}=anodic peak current
i_{pc}=cathodic peak current

The polymer electroactivity decreased with increasing number of cycles. This is due to high pH of the solution [338]. It has been reported before that the decrease in the conductivity and mechanical properties of polypyrrole films occurred when the films were treated with aqueous solutions of NaOH [339,340]. The OH^- ions bind covalently with polypyrrole [166] as shown below (Equation 5.1).

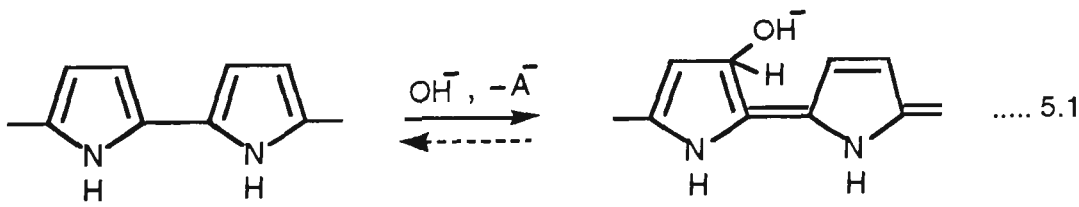

..... 5.1

This results in the discharge of the ionic structure and decreased conjugation length, and lower electronic conductivity. As a consequence of this the conducting polymer becomes an insulator.

To determine the long term stability of the polymers in eluent (NaOH), CVs were recorded over an extended period of time (100cycles). The cyclic voltammograms shown in Figure 5.5 illustrate the electrochemical behaviour of a PPy/Cl microelectrode immersed in NaOH during 100 cycles. The electroactivity of the polymer film deteriorated after the first cycle and continued to decrease with each successive cycle.

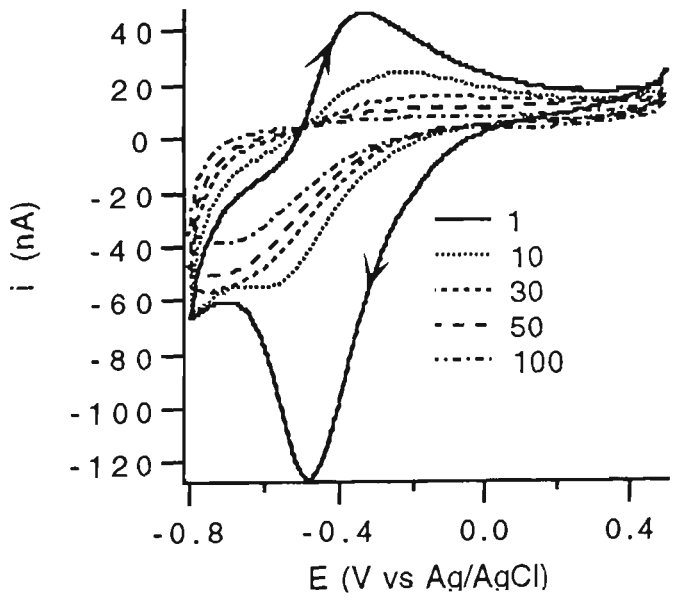

Figure 5.5: *Cyclic voltammograms obtained at (50μm) PPy/Cl microelectrode in 21mM NaOH with multiple cycles (100 cycles). Scan rate=50mV/s.*

Similar behaviour was observed for other polymer systems investigated. The decrease in the i_{pa} and i_{pc} with increasing number of cycles for PPy/Cl, PPy/DS, PPy/SBA and PPy/PTS are given in Figure 5.6. The most pronounced effect observed upon prolonged cycling in NaOH was a general

decrease in the current magnitude over the entire potential range. For all polymer electrodes the oxidation and reduction peak currents decreased with increasing number of cycles. The other general feature was the increase in separation between anodic and cathodic peak potentials due to increased resistivity of the polymer. The slow degradation could be due to low concentration of sodium hydroxide [340]. The instability of the polymer films in NaOH hinders the electrochemical detection on polymer films.

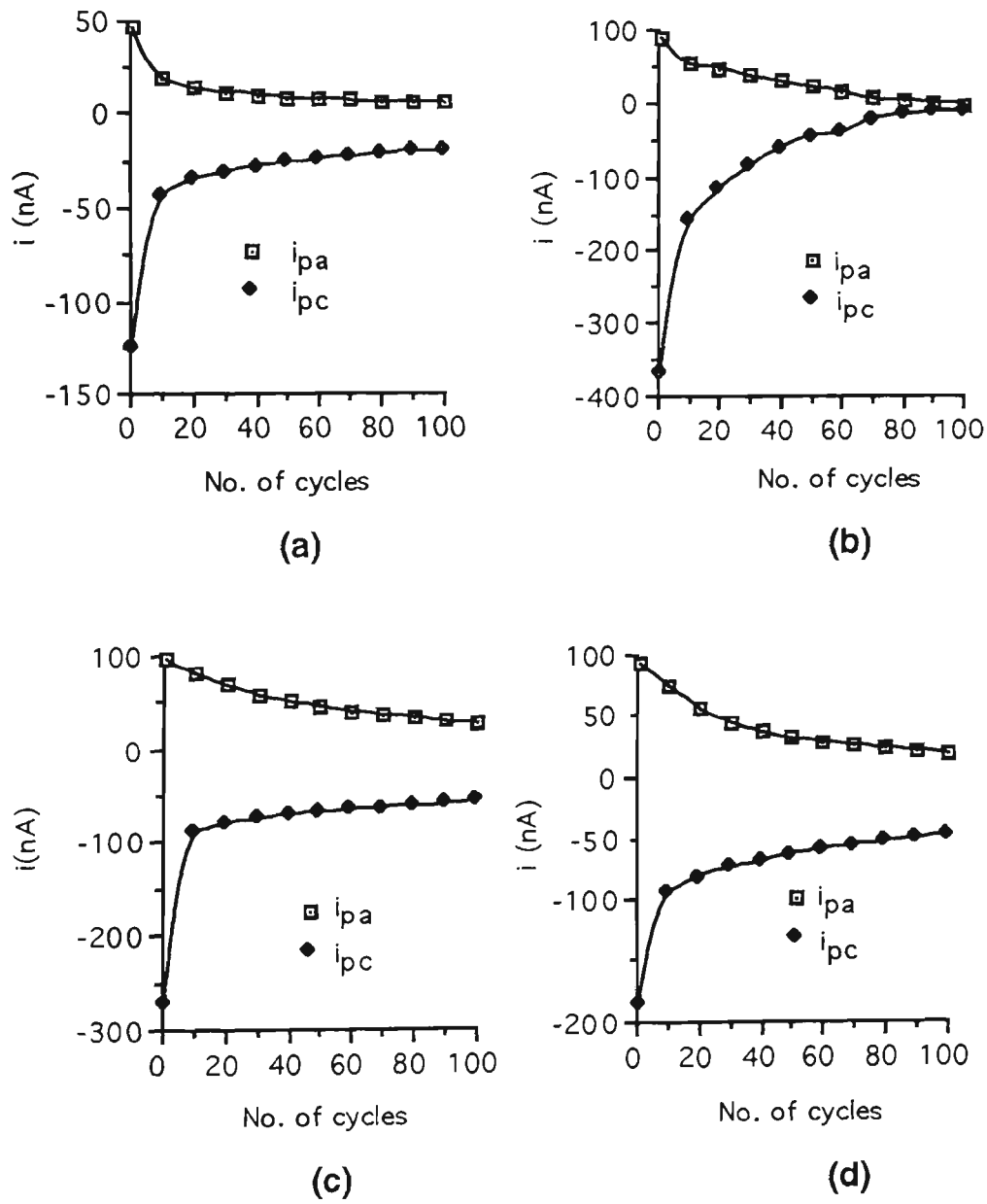

Figure 5.6: *The effect of multiple cycling on the i_{pa} and i_{pc} of 50 µm (a) PPyCl, (b) PPy/DS, (c) PPy/SBA and (d) PPy/PTS. Scan rate=50mV/s.*

The CVs in suppressed eluent show lower level of currents due to lack of ions to facilitate the oxidation /reduction process. The CVs for 10μm and 50μm microelectrodes are given in Figure 5.7 and Figure 5.8 respectively. The current magnitude at both 10μm and 50 μm electrodes were dependent upon the counterion incorporated into the polymer during polymerisation. The effect of the size of the electrode was also manifested in the current obtained in CVs; with larger currents at 50 μm compared to 10 μm electrodes. The current was maximum at PPy/SBA. In general, the shape of the CVs were different for different polymers but were quite independent of the two microelectrode sizes.

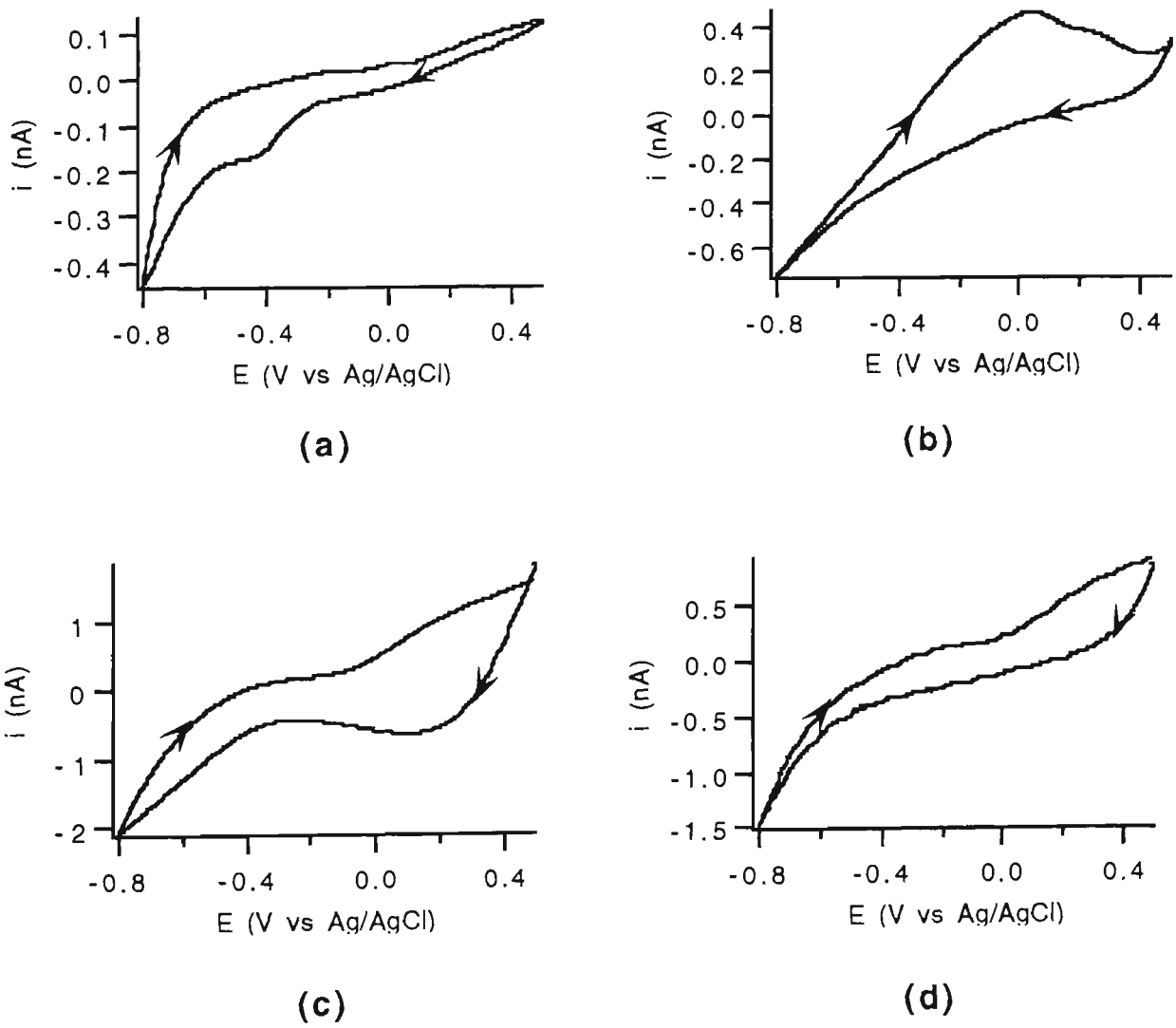

Figure 5.7: *Cyclic voltammograms obtained at 10μm (a) PPy/Cl, (b) PPy/DS, (c) PPy/SBA and (c) PPy/PTS microelectrodes in suppressed eluent. Scan rate= 50mV/s.*

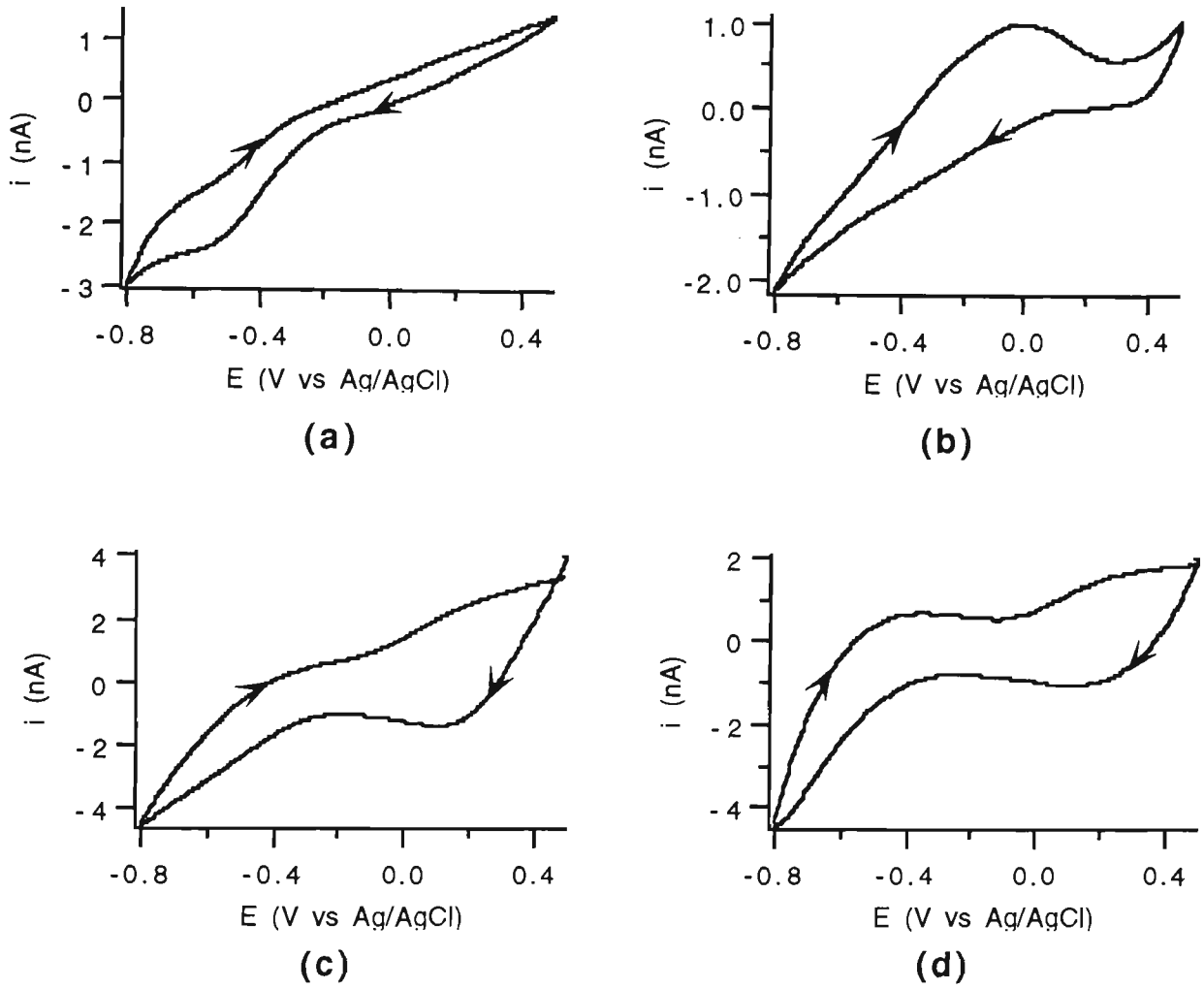

Figure 5.8: *Cyclic voltammograms obtained at 50μm (a) PPy/Cl, (b) PPy/DS, (c) PPy/SBA and (c) PPy/PTS microelectrodes in suppressed eluent. Scan rate= 50mV/s.*

Even though the electrochemistry of the polymers were not well defined, the polymers did switch from the non-conductive to the conducting state and vice versa during cyclic voltammetry. The voltammograms in suppressed eluent were stable for the repetitive number of cycles (100 cycles) as investigated for unsuppressed eluent.

5.3.3 Electrochemistry in Haloacetic Acid Solutions

Using a stationary cell, the cyclic voltammetric responses for haloacetic acids (0.1M) on polymer electrodes were recorded. Solutions were prepared in suppressed eluent in order to understand the polymer/haloacetic acid interactions.

PPy/Cl (10μm) electrodes indicated some incorporation and expulsion of ions ($ClCH_2COO^-$, $BrCH_2COO^-$) during oxidation and reduction in MCAA and MBAA (Figure 5.9). The polymer reduction potential for both analytes were at -0.55V and -0.50V for MCAA and MBAA respectively. The oxidation potential was less distinct and broad over the potentials 0.0V and 0.3V. No such responses were observed for DCAA, TCAA, DBAA and TBAA. The dissociation constant for the haloacetic acids are given in Table 5.2. The acid dissociation becomes more favourable with increasing number of halide-substituents. Therefore the acid activity increases from mono- to trichloro acetic acid. So it could be the size of the anions which makes them difficult to incorporate into the polymer during oxidation.

The cyclic voltammetric responses on PPy/SBA (10μm) are shown in Figure 5.10. Responses were obtained in all six acids. For the chloroacetic acid series (Figure 5.10 a-c) the reduction potential was around -0.4V to -0.3V. But the oxidation peaks were shifted for trichloroacetic acid by 0.1V to more positive potentials. This shift in the potential indicated that the larger size analyte ions were difficult to incorporate into the polymer.

For the bromoacetic acid series (Figure 5.10 d-f) the reduction potential lies between -0.4V to -0.3V for mono- and dibromoacetic acid. The responses in

tribromoacetic acid was not well defined which is also related to the size of the analyte. The CVs became less defined from MBAA to TBAA.

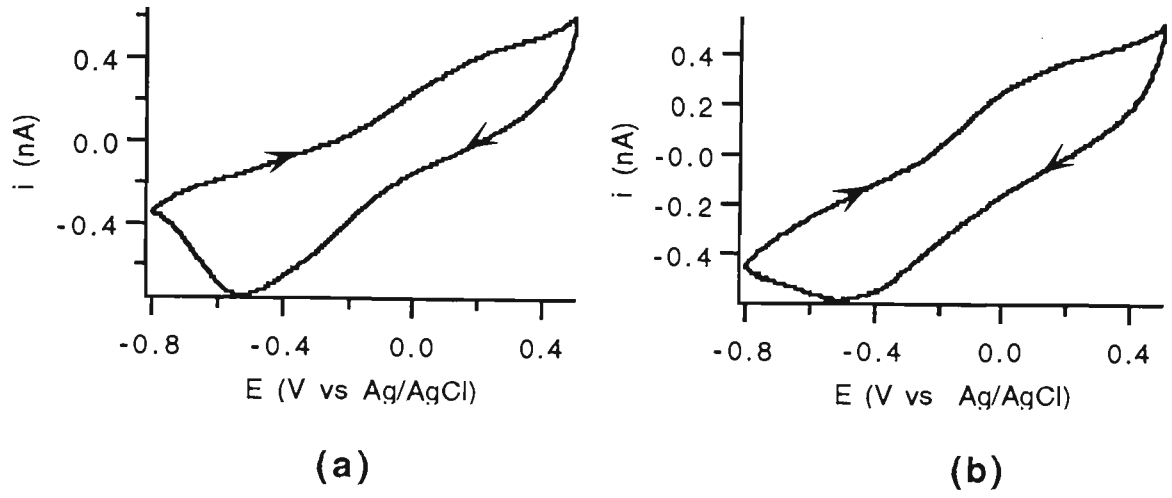

***Figure 5.9**: Cyclic voltammetric responses at PPy/Cl (10μm) in 0.1M (a) MCAA and (b) MBAA. Scan rate=50mV/s.*

***Table 5.2** Dissociation constants of haloacetic acids*

Acid	Dissociation constant $pK_a=(-\log K_a)$	Ionisation constant K_a	Formula
MCAA	2.867	1.36×10^{-3}	$CH_2ClCOOH$
DCAA	1.26	5.50×10^{-2}	$CHCl_2COOH$
TCAA	0.52	3.02×10^{-1}	Cl_3COOH
MBAA	2.902	1.25×10^{-3}	$CH_2BrCOOH$
DBAA	1.39	$4.10 \times^{-2}$	$CHBr_2COOH$
TBAA	-0.147	1.40	Br_3COOH

Data taken from reference 341

The current level was also dependent on the nature of the analyte which decreased from monochloro- to trichloroacetic acid and also from monobromoacetic acid to tribromoacetic acid with the tribromoacetic acid having the least defined responses in the series. The CVs were reproducible

over a number of cycles (10 cycles). However, the other polymer systems investigated (PPy/DS and PPy/PTS) were not electroactive in any of the haloacetic acid solutions.

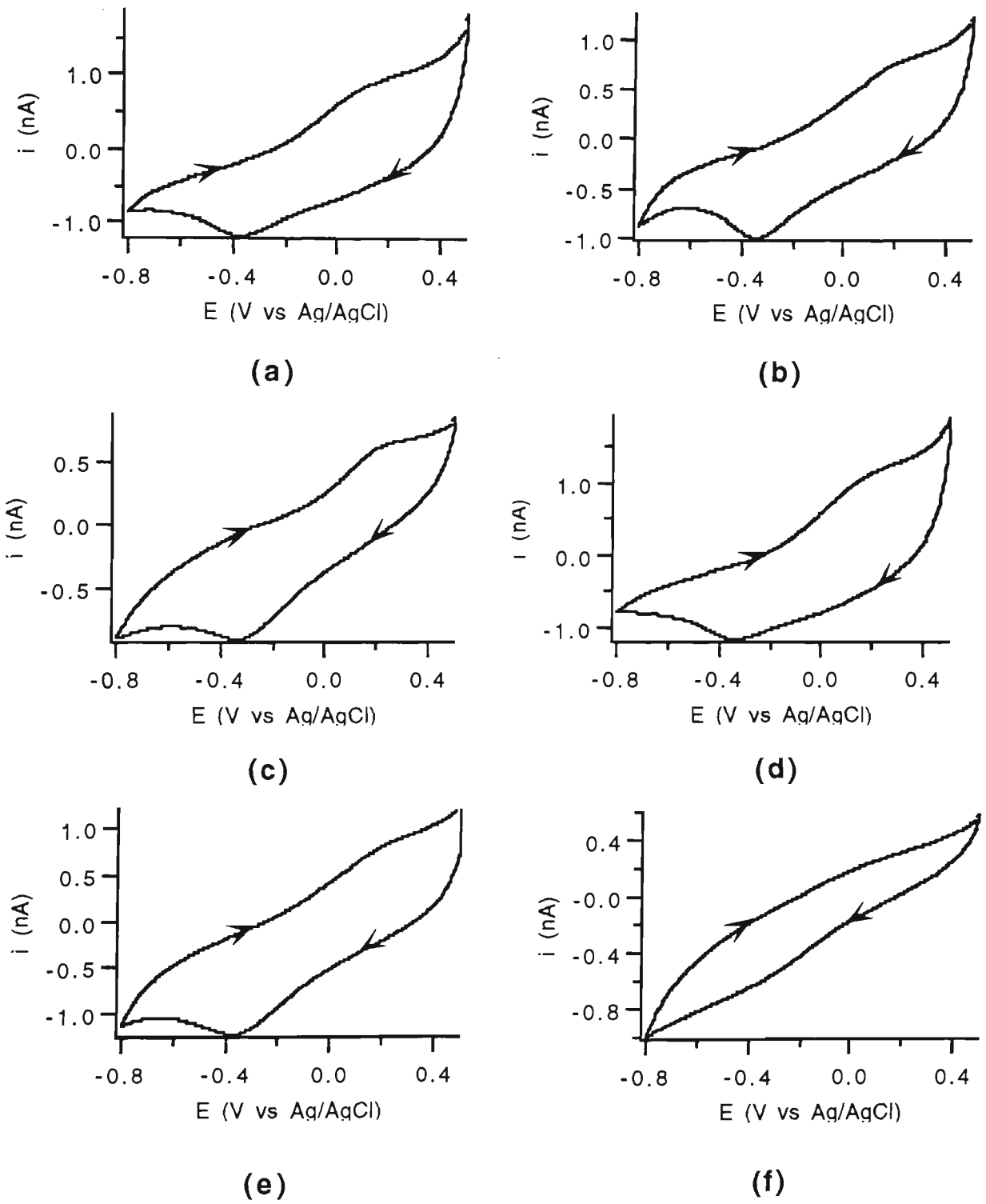

***Figure 5.10**: Cyclic voltammetric responses at PPy/SBA (10μm) in 0.1M (a) MCAA, (b) DCAA, (c) TCAA, (d) MBAA, (e) DBAA and (f) TBAA. Scan rate=50mV/s.*

The electroactivity of the polymer films coated on 50μm electrodes were also investigated. The cyclic voltammograms at PPy/Cl (50μm) electrodes are shown in Figure 5.11. The CV response was prominent in MCAA compared to DCAA and TCAA, with the reduction peak at -0.4V and oxidation occurring around -0.1V to 0.1V. The current magnitude decreased from MCAA> DCAA > TCAA.

At PPy/SBA (50μm) the voltammograms (Figure 5.12) were well defined compared to PPy/Cl (10μm, 50μm) and PPy/SBA (10μm). The current magnitude decreased in the order MBAA > DBAA > TBAA. Such responses were not obtained on other systems investigated: PPy/DS and PPy/PTS electrodes. The most obvious explanation for the effects reported here (Figure 5.11 and Figure 5.12) for different anions is that the presence of anions capable of diffusing into the polymer was required to offset the buildup of the positive charge generated by oxidation of the film.

The current magnitude was higher on both 50 μm microelectrodes of PPy/Cl and PPy/SBA compared to corresponding 10μm polymer coated electrodes because of the electrode area.

In general, therefore, somewhat less ideal CVs were obtained with haloacetic acids where the currents were smaller (compared to NaOH) and the anodic peak was broader and shifted to higher potentials. The large separation between anodic and cathodic peaks is the common feature for all the electrodes investigated and is due to the slow diffusion of the ions. The difference in the shape of the CV for PPy/Cl and PPy/SBA also suggests that the counterions play a role in the polymer/analyte interaction. It might be the case that the incorporation of ions is easier in PPy/SBA as compared to

PPy/Cl and this was displayed by the peaks being more prominent for the former polymer together with higher current levels.

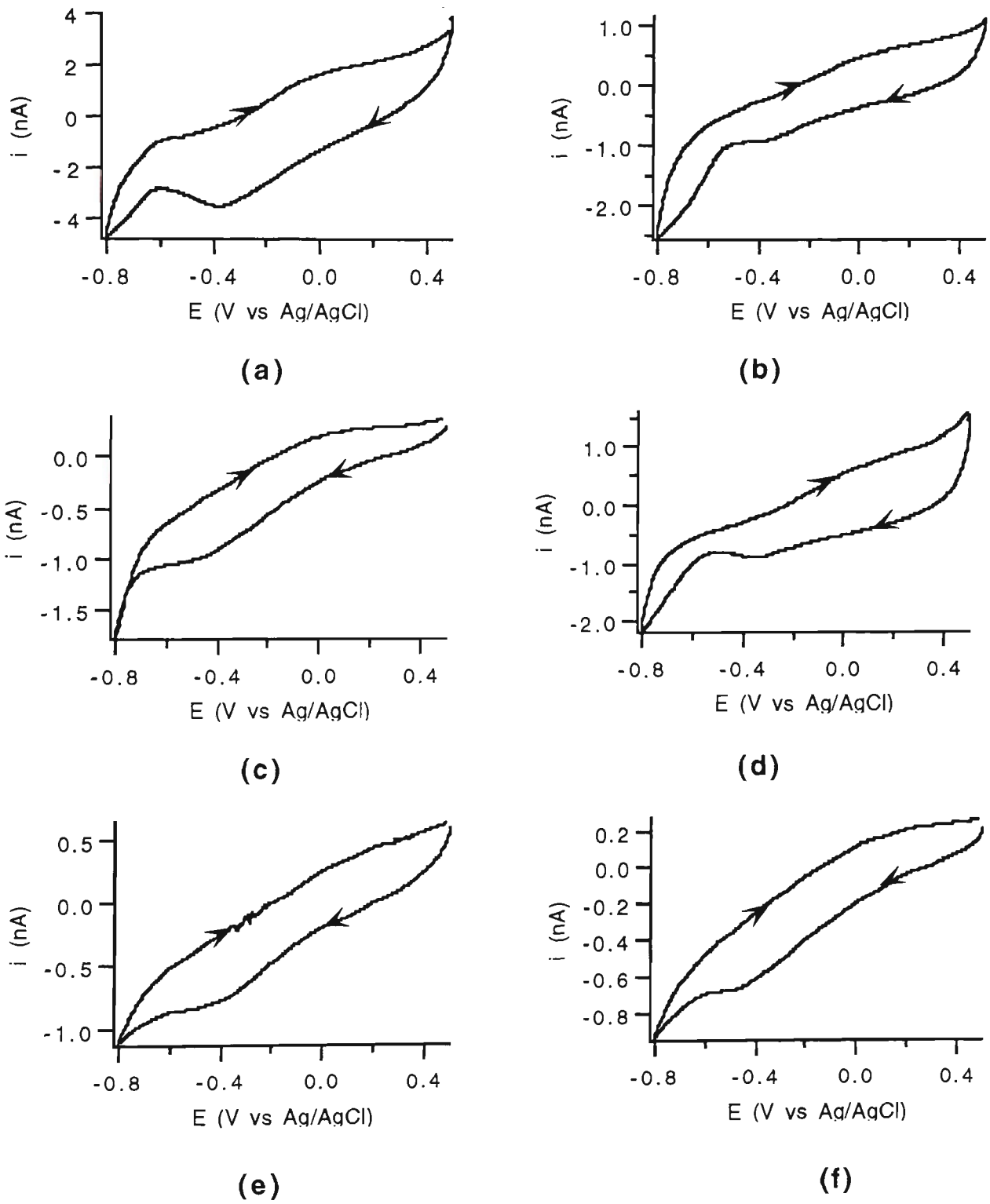

***Figure 5.11**: Cyclic voltammetric responses at PPy/Cl (50μm) in 0.1M (a) MCAA, (b) DCAA, (c)TCAA , (d) MBAA, (e) DBAA and (f) TBAA. Scan rate=50mV/s.*

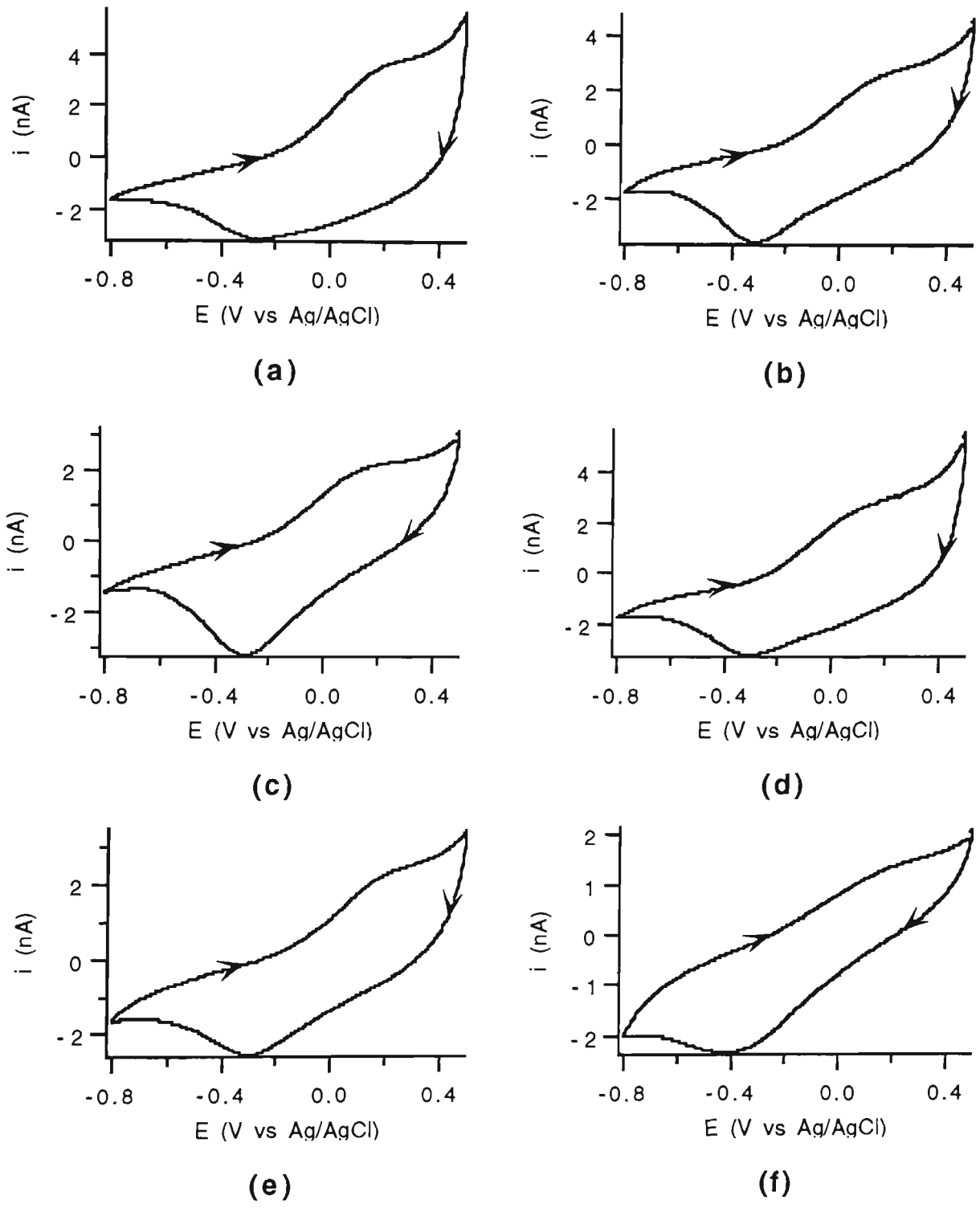

***Figure 5.12**: Cyclic voltammetric responses at PPy/SBA (50μm) in 0.1M (a) MCAA , (b) DCAA, (c) TCAA, (d) MBAA, (e) DBAA and (f) TBAA. Scan rate=50mV/s.*

5.3.4 Mass Changes During Redox Cycling of PPy/SBA

In order to investigate the nature of the ions involved in ion-exchange processes during redox cycling, the mass changes associated with incorporation/expulsion of MCAA at the PPy/SBA electrode during cyclic voltammetry were considered. The mass and current changes are shown in Figure 5.13. The mass change obtained in MCAA is compared with that obtained in sodium nitrate.

In nitrate solution the two distinct regions are evident. Firstly the polymer mass decreased during reduction between 0.5V to -0.4V (Figure 5.13-i(a)). This decrease is associated with anion expulsion, as evident from the corresponding reduction peak in this potential region of the CV (Figure 5.13-i(b)). This is followed by a mass increase at more cathodic potentials (-0.4V to -0.8V) which is associated with cation incorporation [118,162] (corresponding reduction peak also appeared in Figure 5.13-i(b). The reverse was observed during oxidation of the polymer film. On oxidation of the polymer the mass initially decreased because of expulsion of cations and this was followed by a mass increase related to anion incorporation.

By contrast, in MCAA there was only one region in the mass response (Figure 5.13-ii (a)). The EQCM of polymer showed a decrease in mass during reduction and an increase upon oxidation. This process, as can be seen from the CV (Figure 5.13-ii(b)), was associated with the movement of anions of MCAA during redox cycling of the polymer.

This observation indicates that during redox cycling of the PPy/SBA in monochloroacetic acid, the charge compensating species was the anion

($ClCH_2COO^-$) of the acid. From these observations the mechanism of signal generation could be predicted. It can be presumed that the major signal component would be due to the anion exchange of the analyte with the polymer film but not the cation of the analyte.

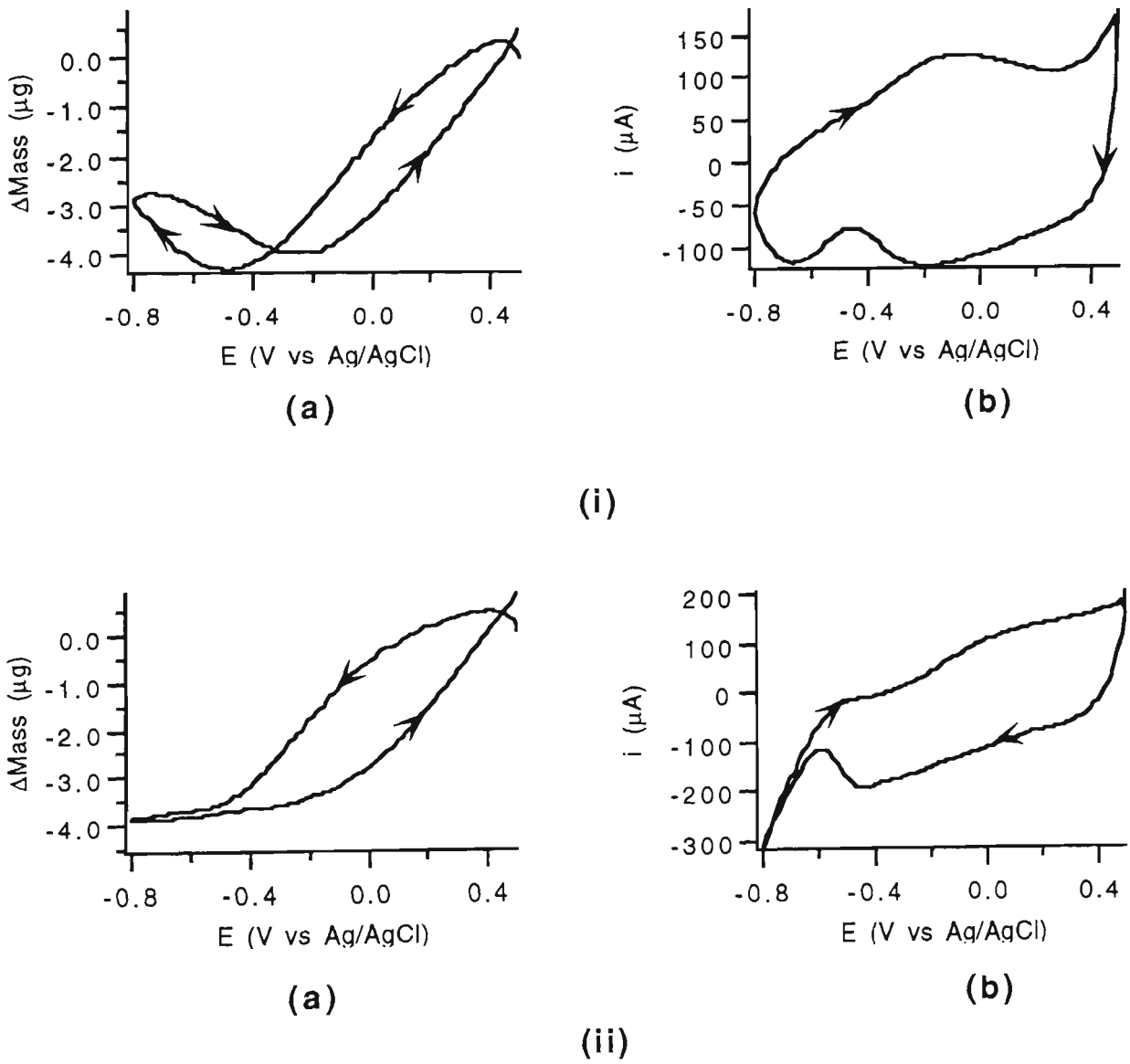

***Figure 5.13**: EQCM of PPy/SBA . (a)Mass change, (b) cyclic voltammograms in (i) 0.1M $NaNO_3$ and (ii) 0.1M MCAA. Scan rate=50mV/s. Polymer electropolymerised from Py (0.2M)/SBA (0.5M). A current density of 2mA/cm^2 was applied for 2min.*

5.3.5 Conductivity Detection of Haloacetic Acids

A suppressor based anion-exchange chromatography method with conductivity detection was used for the separation of haloacetic acids (conditions given in Section 5.2.4). A standard mixture of six haloacetic acids was injected and were separated on an anion-exchange column with 21mM sodium hydroxide. The column effluent flowed through a suppressor device before entering the conductivity detector. The eluent suppression takes place as described in Section 5.2.5. This results in a decrease in conductivity for the eluent and an increase in conductivity for the sample. The chromatogram obtained is shown in Figure 5.14. It was found that MCAA and MBAA co-eluted and TBAA did not elute at all because it had high affinity towards the stationary phase while all other acids were well resolved from each other. The retention data is given in Table 5.3. The order of elution was MCAA > DCAA > DBAA > TCAA with the maximum sensitivity for MCAA.

Table 5.3 *Retention data obtained by conductivity detection*

Haloacetic acids	Retention time (minutes)	Peak Height (μS)
MCAA	1.31	17.4
DCAA	2.10	15.0
DBAA	2.52	7.6
TCAA	6.10	1.8

The peaks were identified by injecting the individual haloacetic acids.

In our case the separation of four acids were completed within 8 minutes with excellent resolution and sensitivity, where Nair et al. [337] separated MCAA, DCAA and TCAA in 18 minutes. Nair at al. [337] have also

discussed the co-elution of MCAA and MBAA on Alltech Universal Anion 300 column with carbonate/sodium hydrogen carbonate eluent. So the analysis for chloroacetic acids and bromoacetic acids were performed separately while separation of TBAA was not discussed [337]. The elution of TBAA on AS 11 was obtained by methanol gradient according to the Dionex method [342]. In our case, further work was concentrated on the detection of MCAA, DCAA, TCAA and DBAA.

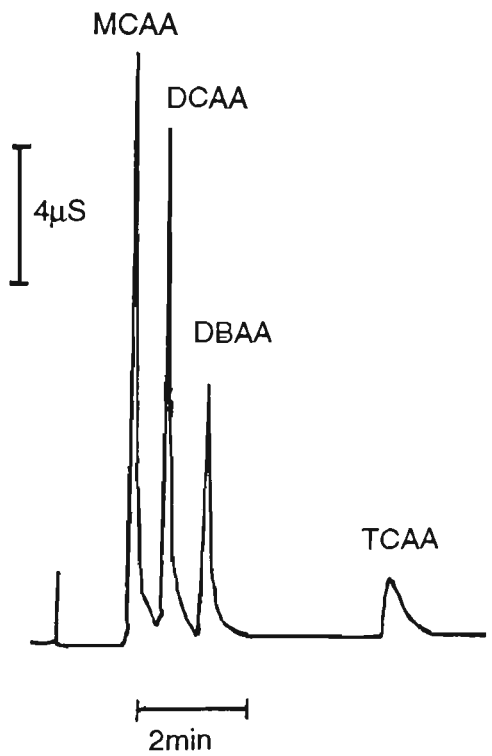

***Figure 5.14**: Chromatogram obtained by conductivity detection. Column : AS11, eluent: 21.0 mM NaOH, suppressor: AMMS11. Flow rate=1ml/min. Background conductivity: 3.5μS. Analyte concentration=10μg/l. Injection volume=50μl.*

5.3.6 Detection of Haloacetic Acid at Polymer Electrodes

Once the chromatogram was established the analysis was carried out on polymer electrodes by pulsed integrated amperometry. It was established in Chapter 3 and Chapter 4 that pulsed potential is required to prevent the polymer electrode fouling.

To optimise the electrochemical detection, the electronic state of the polymers was varied systematically by applying positive and negative potentials. Two pulsed waveform schemes were applied. In waveform 1 (Figure 5.15), E_1=0.5V (kept constant) and E_2 varied from -0.6V to 0.0V with 200mV steps and the current was sampled at the beginning of E_1.

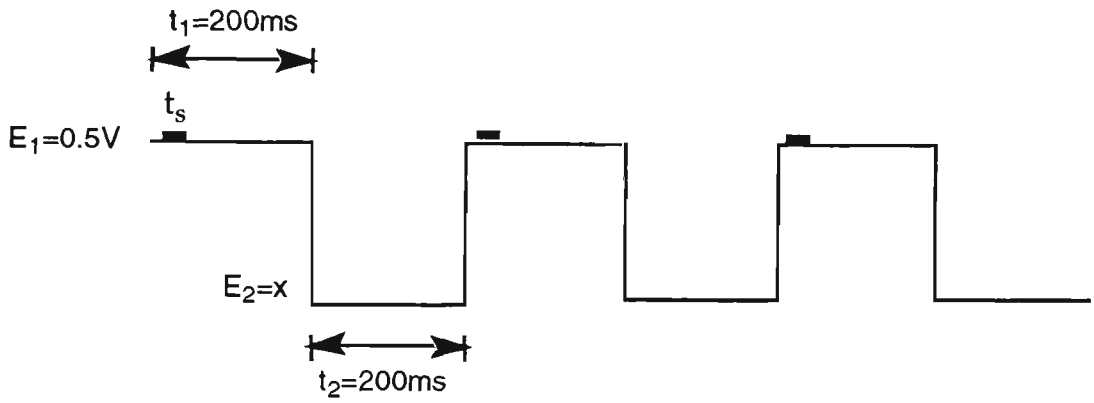

Figure 5.15: *Pulsed potential waveform 1 with current sampling point position. E_1= electrode potential fixed at 0.5V, E_2=electrode potential varied between -0.6V and 0.0V. t_1=time period for E_1, t_2=time period for E_2, t_{s1}=current sampling point.*

Waveform 2 (Figure 5.16) consists of E_2=-0.8V (kept constant) and E_1 varied from 0.3 V to 0.6V with 100mV steps while current was sampled at the beginning of E_1.

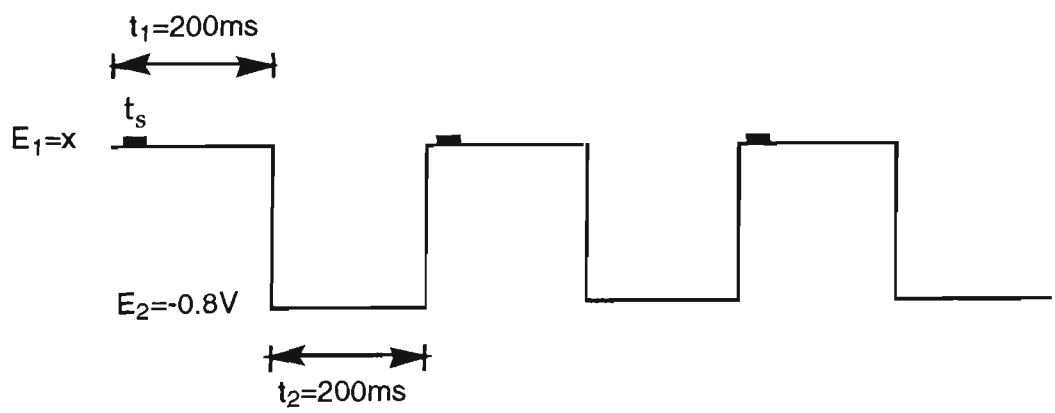

Figure 5.16: *Pulsed potential waveform 2 with current sampling point position. E_1= electrode potential varied between 0.3V and 0.6V, E_2=electrode potential fixed at -0.8V. t_1=time period for E_1, t_2=time period for E_2, t_{s1}=current sampling point .*

Current responses were obtained for all four analytes. Of particular interest are the changes in relative sensitivities and hence selectivity factors obtainable with different electrode compositions. The electrode sensitivity varied with the change in the potential applied. For 10μm polymer coated electrodes, when the current was sampled at the end of E_1 (160-190ms) the responses were unmeasurable, and so the sampling was carried out at the beginning of the pulse. Among the large number of chromatograms, the one with prominent differences in acid selectivity are discussed to highlight the effect of potentials applied and the polymer composition.

The effect on selectivity by deliberate changes in the potential applied at the working electrode was demonstrated with the use of PPy/Cl (10μm) and PPy/SBA (10μm). The ability to tune the selectivity at PPy/Cl are shown in Figure 5.17. With E_1=0.5V and E_2=-0.6V and -0.2V. Figure 5.17 shows that the selectivities obtained for MCAA, DCAA, TCAA and DBAA differ as the potential becomes more negative. The selectivity factors (the peak ratios) obtained for MCAA/DCAA peaks were 1.30 and 1.06 at potentials E_2=-0.6V and -0.2V respectively. Changes in selectivities were also recorded for DCAA/DBAA peaks. The selectivity factors obtained for these acids were markedly different, 2.7 and 1.4 in Figure 5.17-a and Figure 5.17-b respectively. This indicates that DCAA is more selective over DBAA at E_2=-0.6V. The selectivity factors for MCAA/TCAA peaks were 12.5 and 3.5 for conditions (a) and (b) in Figure 5.17.

The influence of the reduction potential on selectivity factors at PPy/DS electrodes are shown in Figure 5.18. The most noticeable difference between the two chromatograms is that the TCAA has a dip rather than a peak at E_2= -0.6V. The selectivity factors for DCAA/DBAA peaks were 2.5 and 1.6 for E_2=-0.6V and E_2=-0.2V respectively.

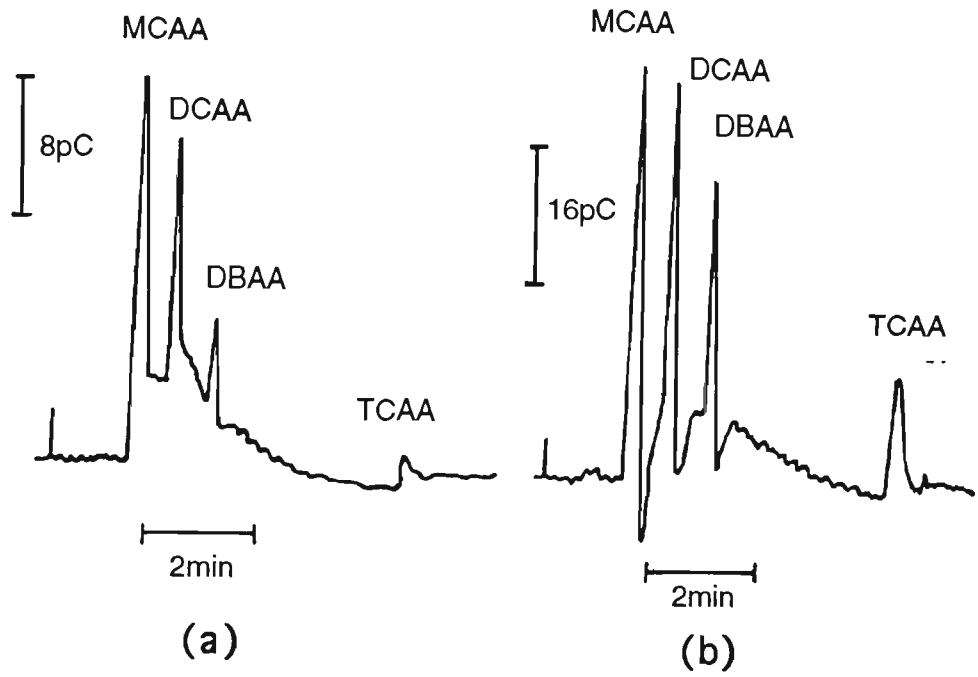

***Figure 5.17**: Chromatograms obtained at PPy/Cl (10μm).*
E_1= +0.5V, (a) E_2=-0.6V, (b) E_2=-0.2V and t_1=t_2=200ms, t_S=10-60ms.
Chromatographic conditions as in Figure 5.14.

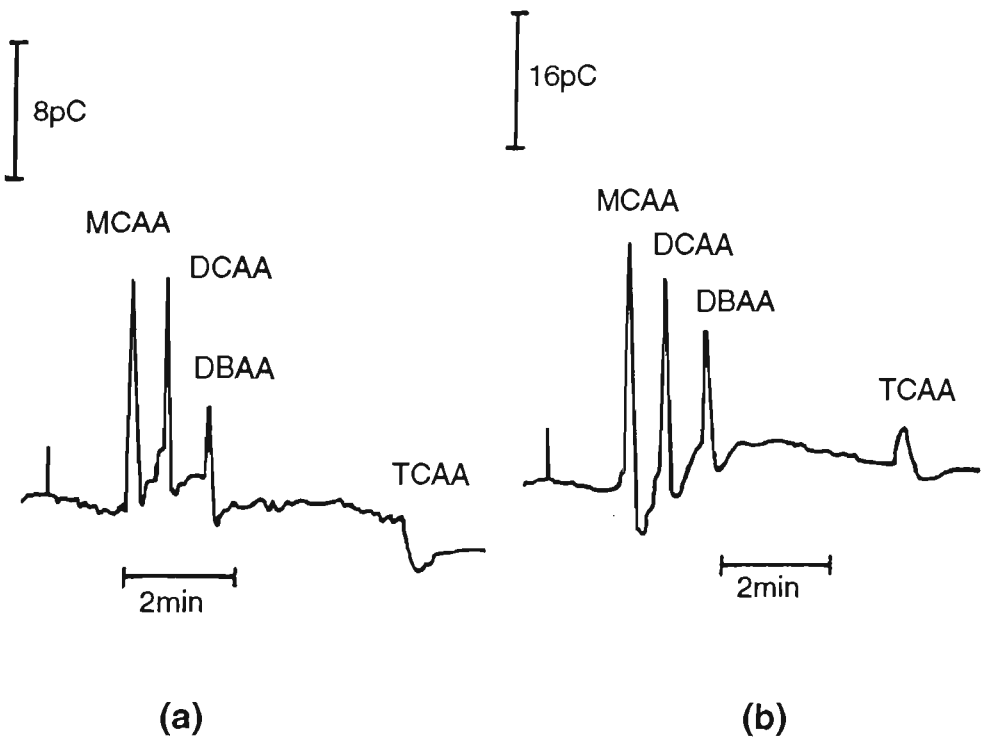

***Figure 5.18**: Chromatograms obtained at PPy/DS (10μm).*
E_1=+0.5V, (a) E_2=-0.6V, (b) E_2=-0.2V, t_1=t_2=200ms, t_S=10-60ms.
Chromatographic conditions as in Figure 5.14.

It was observed that at 10μm polymer coated electrodes, that the current level was very low (charge in pC range) and often chromatograms were unreadable due to mixed base line and noise. A sudden loss in the electrode response was also common at 10μm electrodes.

The pulsed integrated amperometric detection was also carried out at 50μm polymer coated electrodes. The histograms shown in Figure 5.19 demonstrate the versatility of the polymer electrodes for haloacetic acid detection.

In general, the sensitivities for the analytes changed when the reduction potential changed from -0.6V to 0.0V. Unlike CV, drastically different results were obtained, depending on the potential applied, with the maximum responses either at the E_2=-0.2 V or E_2=-0.4V.

This dependence of selectivity upon the potential applied indicates that electrochemically controlled ion-exchange processes were occurring on the electrodes. These ion-exchange processes were favourable at a particular potential for each polymer electrode. This is important because it clearly indicates that sample-related changes in solution-phase properties were not (entirely) responsible for the signals seen at the polymer electrodes.

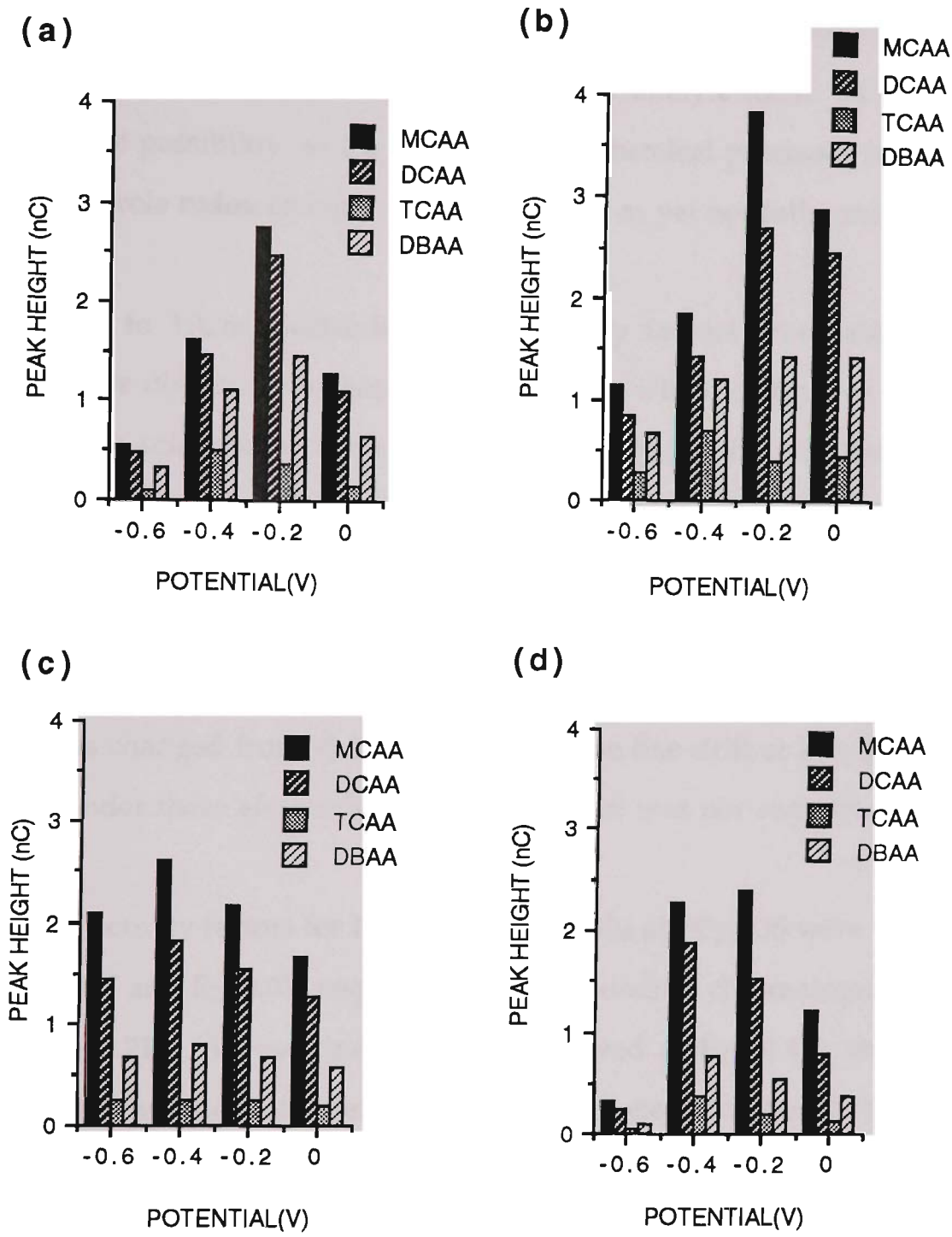

***Figure 5.19**: Effect of reduction potential in pulsed integrated amperometric detection for haloacetic acids at (a) PPy/Cl, (b) PPy/DS, (c) PPy/SBA and (d) PPy/PTS. E_1=0.5V, E_2 varied as in x-axis. t_1=t_2=200ms, t_s=10-60ms. Chromatographic conditions as in Figure 5.14.*

The fact, that different sensitivities were obtained for the polymer electrodes when different counterions were employed in the polymer synthesis, suggests that the polymer electrodes may be detecting the haloacetic acids by oxidation/reduction when pulsing the potential of the electrode; thus facilitating the ion-exchange process of the analyte ions. Of course, this is only one possibility, as the electronic and chemical processes occurring upon polypyrrole redox changes are complex and as yet not fully understood.

Similar to 10μm electrodes the selectivity factors were also influenced. Here, we discuss only those chromatograms where distinctive differences in the peak selectivities were obtained. For PPy/Cl the selectivity factors for DCAA/DBAA peaks were 1.3 and 1.7 as E_2 was changed from -0.4V to E_2=-0.2V (the corresponding chromatograms are shown in Figure 5.20). It is worth noting that the sensitivities for MCAA, DCAA and DBAA increased but the sensitivity for TCAA decreased (Figure 5.20-a to Figure 5.20-b) when E_2 was changed from -0.4V to -0.2V. A base line drift at E_2=-0.4V, indicates that under these electrochemical the polymer was not completely dedoped.

The selectivity factors for DCAA/DBAA peaks at PPy/DS were 1.2 and 1.7 for E_2=-0.4V and E_2=0.0V respectively (corresponding chromatograms shown in Figure 5.21). A base line drift was observed at E_2=-0.4V, this shows the electrode was not fully dedoped under these electrochemical conditions.

At PPy/SBA when reduction potential was changed from E_2=-0.6V to E_2=-0.4V, the sensitivity for MCAA, DCAA and DBAA increased while response for TCAA remained unchanged (Figure 5.22-a and Figure 5.22-b). The selectivity factors for MCAA/TCAA were 8 and 10, for DCAA/TCAA were 5.5 and 7, and for DBAA/TCAA were 2.6 and 3.1 (Figure 5.22-a and Figure 5.22-b).

At PPy/PTS with the change in the reduction potential from E_2=-0.4V to E_2=-0.2V, the sensitivity for MCAA was increased while the sensitivity for DCAA, TCAA and DBAA decreased (Figure 5.23-a and Figure 5.23-b). The selectivity factors for MCAA/DCAA were 1.2 and 1.6 fo r E_2=-0.4V and E_2=-0.2V respectively. The selectivity factors for DCAA/DBAA were 2.5 and 2.8 (Figure 5.23-a and Figure 5.23-b)).

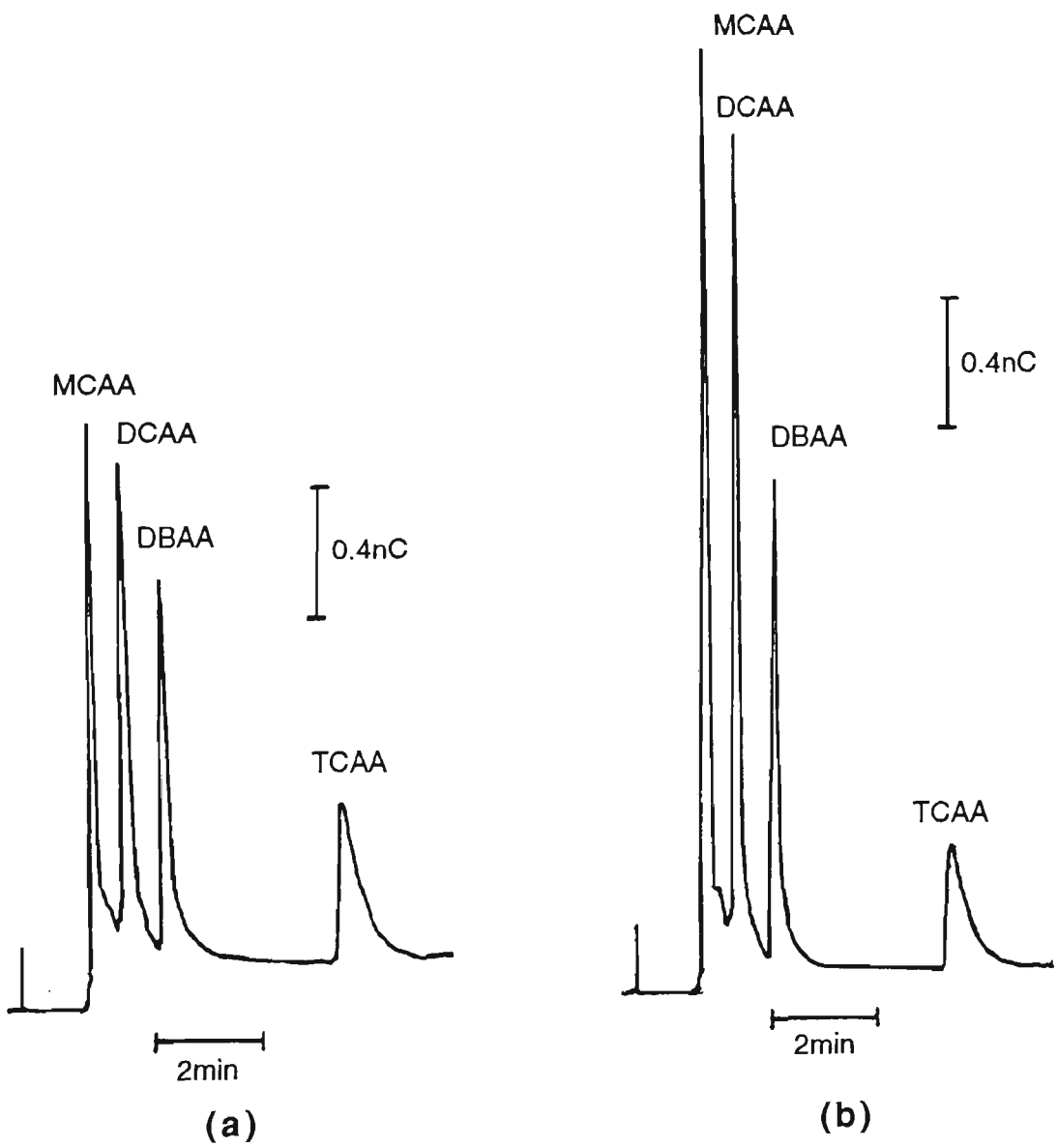

***Figure 5.20**: Chromatograms obtained at PPy/Cl (50μm). E_1=+0.5V, (a) E_2=-0.4V and (b) E_2=-0.2V, t_1=t_2=200ms, t_S=10-60ms. Chromatographic conditions as in Figure 5.14.*

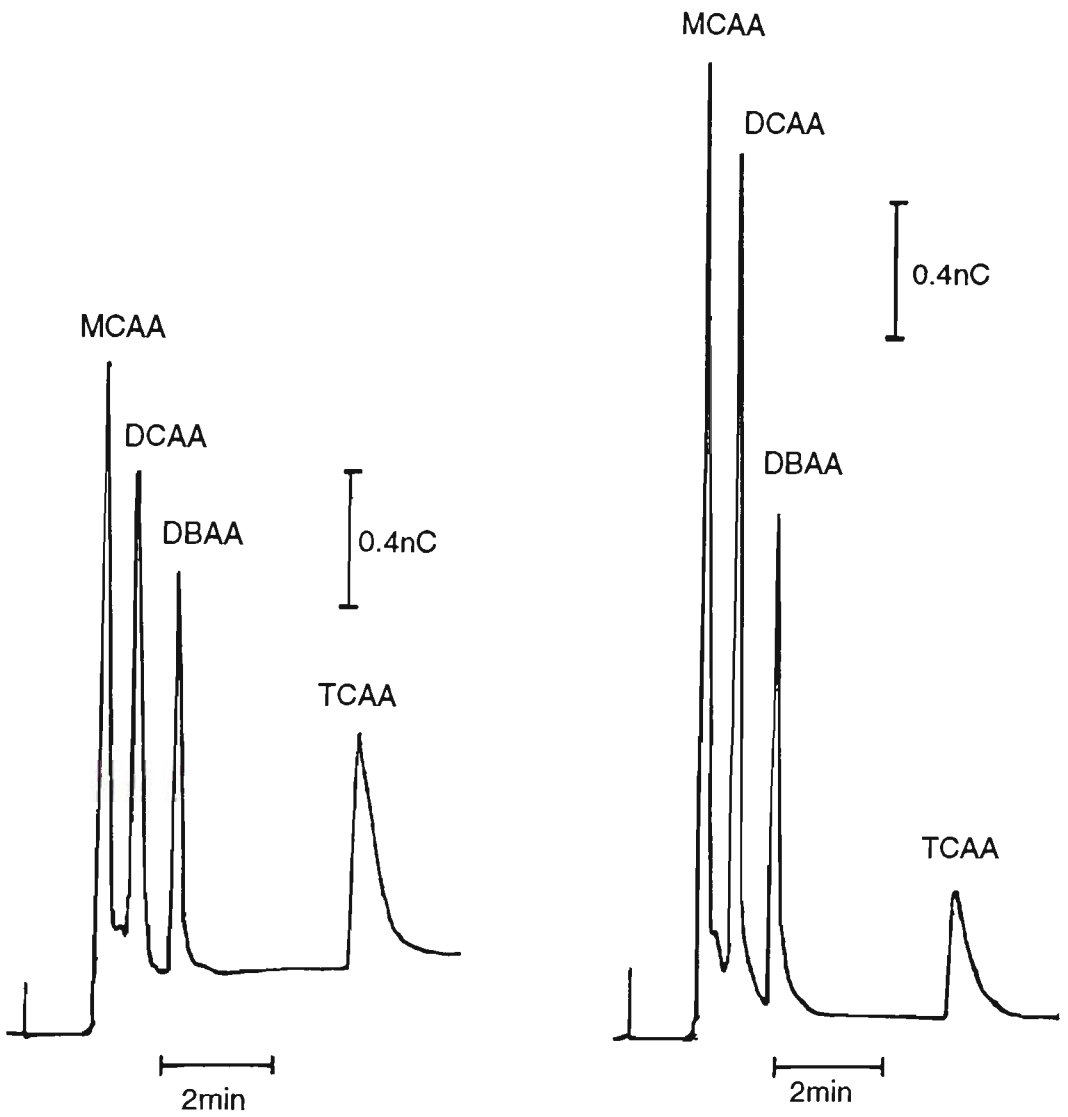

***Figure 5.21**: Chromatograms obtained at PPy/DS (50μm). E_1=+0.5V, (a) E_2=-0.4V, (b) E_2=0.0V, $t_1=t_2$=200ms, t_S=10-60ms. Chromatographic conditions as in Figure 5.14.*

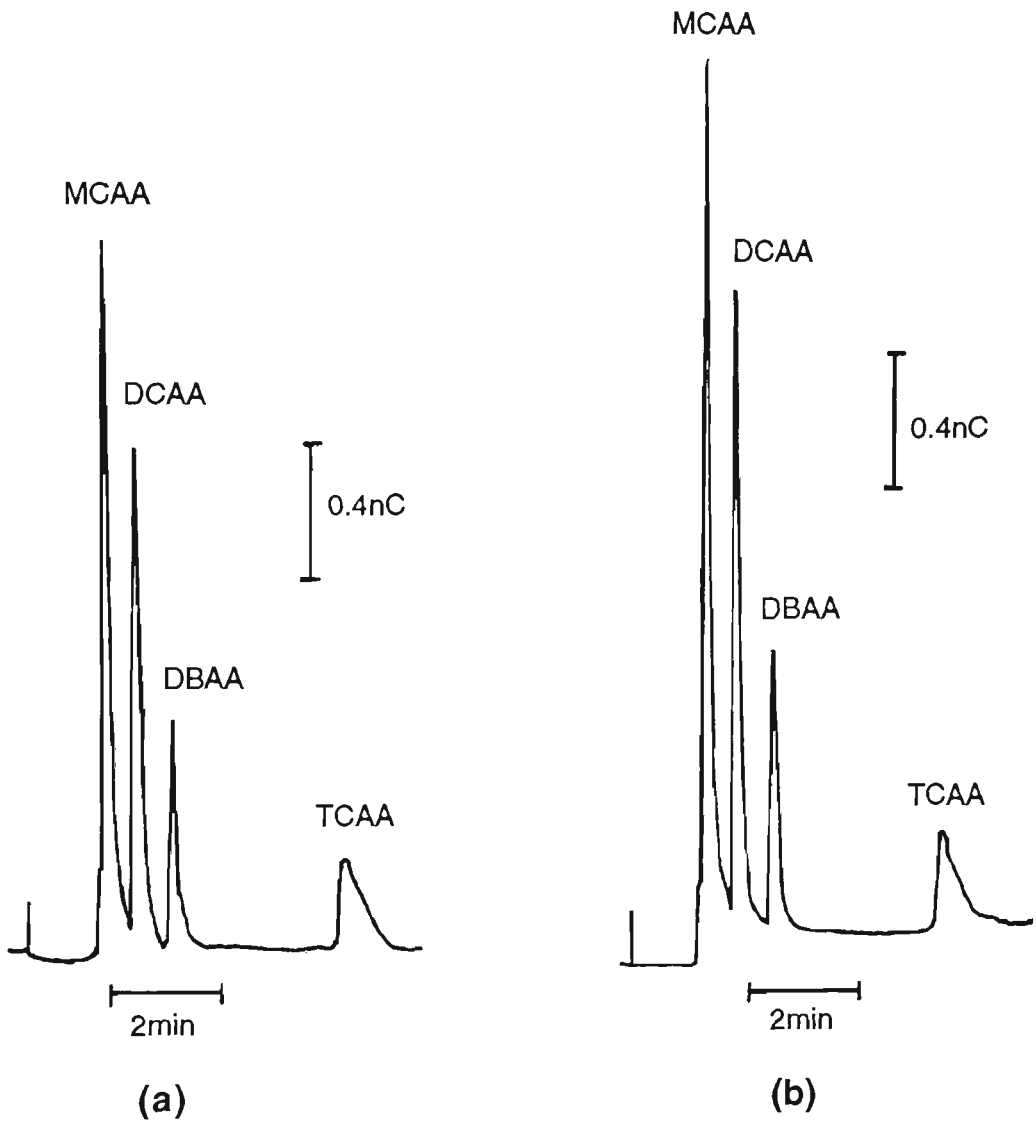

***Figure 5.22**: Chromatograms obtained at PPy/SBA (50μm). E_1=+0.5V, t_1=t_2=200ms, t_S=10-60ms. (a) E_2=-0.6V, (b) E_2=-0.4V. Chromatographic conditions as in Figure 5.14.*

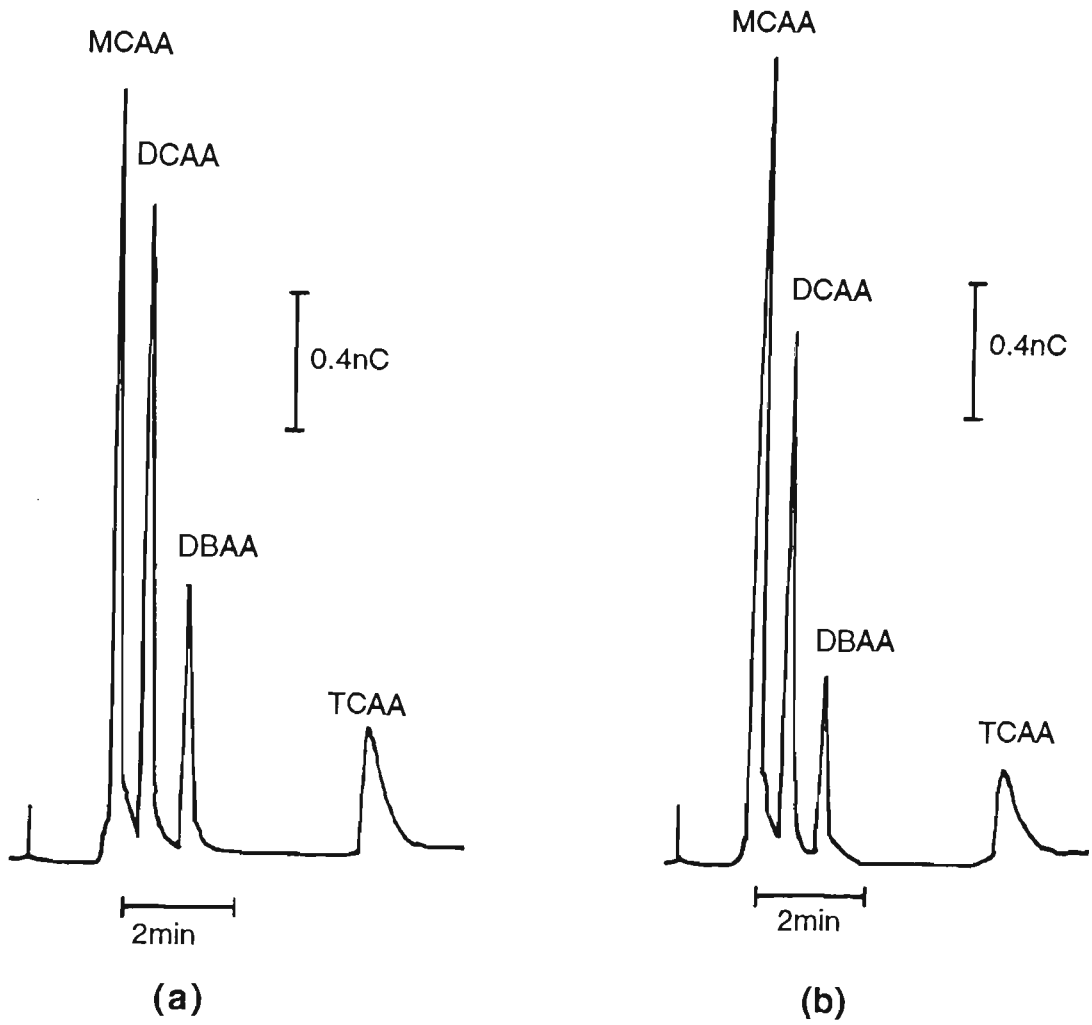

***Figure 5.23**: Chromatograms obtained at PPy/PTS (50μm). E_1=+0.5V, $t_1=t_2$=200ms, t_S=10-60ms. (a) E_2=-0.4V, (b) E_2=-0.2V. Chromatographic conditions as in Figure 5.14.*

The effect of counterions on the selectivity factor has also been studied. For DCAA/DBAA peaks the selectivity factor were 1.7 and 2.8 for PPy/Cl and PPy/PTS respectively at E_2=-0.2V.

These observations indicate that the selectivity could be manipulated simply by changing the electrochemical conditions at the polymer electrodes as well as polymer composition. This flexibility is not offered by the conductivity method.

The effect of changing the positive potentials in pulsed integrated amperometric analysis was also considered where E_2=-0.8V and E_1 was varied from +0.6 to +0.3V (Waveform 2).

The responses obtained at the four polymer electrodes (PPy/Cl/, PPy/DS, PPy/SBA and PPy/PTS) are shown as histograms in Figure 5.24. It can be seen that the sensitivity for all haloacetic acids increased as the positive potentials were increased. In addition, the effect of counterions incorporated into the polymer have also been manifested in the trend of increase of the responses. For PPy/Cl the signal magnitude increased significantly from E_1=0.5V to E_1=0.6V probably because high oxidation potentials were favourable for signal generation. On the other hand the responses increased gradually with increases in potential values at PPy/DS electrodes. The responses, however, were large for all potentials at PPy/SBA compared to other electrodes investigated. At PPy/PTS the responses also increased gradually with increasing potentials but the sensitivity was higher than at PPy/Cl and PPy/DS.

It has also been found that the selectivity factors did not change dramatically when these pulses were applied. The only significant changes in the selectivity factors were observed at PPy/DS electrodes. The selectivity factor for MCAA/DCAA peaks were 1.4 when E_1=0.5V, and 1.2 when E_1=0.6V (Figure 5.25-a and Figure 5.25-b). For DCAA/DBAA peaks the selectivity factors were 1.9 and 1.7 respectively (Figure 5.25-a and Figure 5.25-b). The greatest effect was seen for selectivity factors for MCAA/TCAA peaks which changed from 7.2 to 5.3 (Figure 5.25-a and 5.25-b respectively).

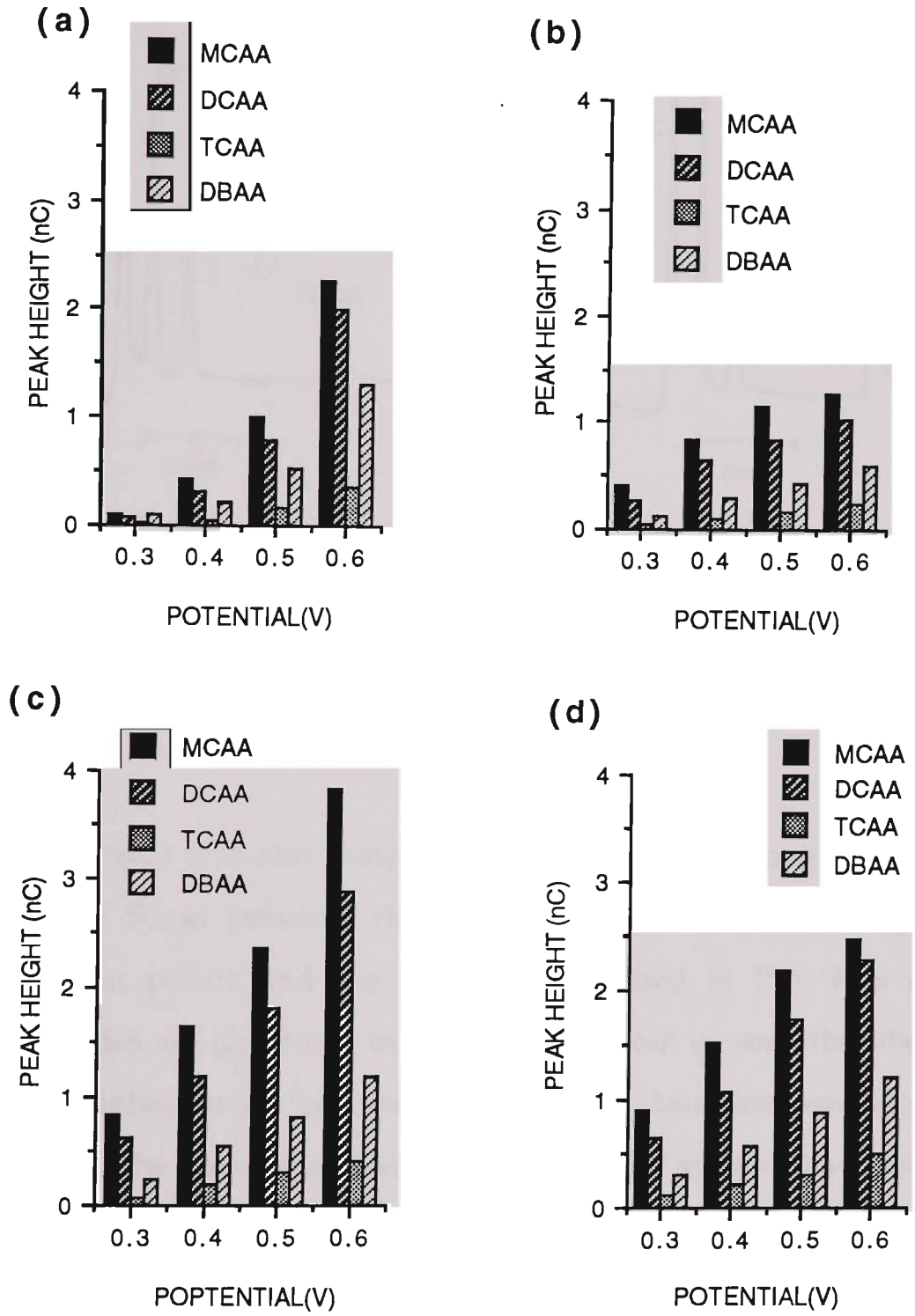

***Figure 5.24**: Effect of oxidation potential in pulsed integrated amperometric detection for haloacetic acids at (a) PPy/Cl, (b) PPy/DS, (c) PPy/SBA and (d) PPy/PTS. E_1 was varied as in x-axis, E_2=-0.8V, t_1=t_2=200ms, t_S=10-60mS. Chromatographic conditions as in Figure 5.14.*

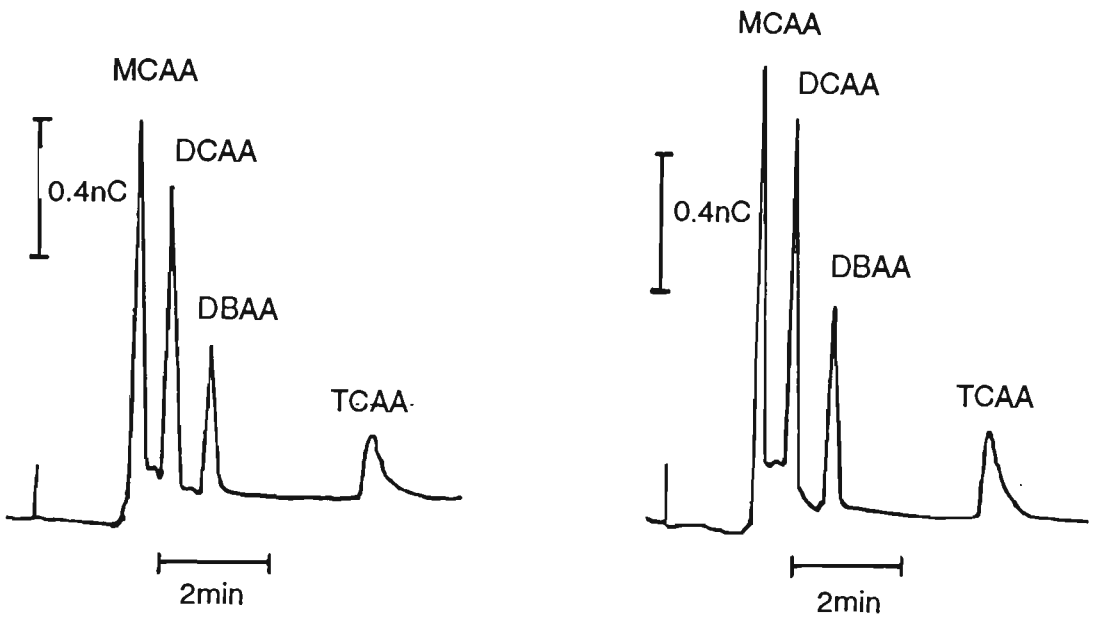

Figure 5.25: *Chromatograms obtained at PPy/DS (50μm). E_2=-0.8V, (a) E_1= 0.5 V and (b) E_1=0.6V, $t_1=t_2$=200ms, t_S=10-60ms. Chromatographic conditions as in Figure 5.14.*

The current was also sampled at different points along the positive pulse, for the 50μm polymer electrodes. The current was sampled at three different points and the responses obtained at PPy/PTS and PPy/DS electrodes are illustrated in Figure 5.26. It can be seen that the sensitivities were highest at the beginning of the pulse but decreased along the pulse width. The trend was similar for all polymer systems and potential pulses investigated. If one closely analyses the current decay at PPy/PTS, it can be seen that current decay was gradual. At PPy/DS electrode, however, the current decrease was initially steep (between first point and second) and followed by a slight decrease between the second point and third point. This difference in current decay profile also signifies the difference in the affinities of the polymers for the haloacetic acid. Clearly this type of information cannot be obtained by the conductivity method.

The selectivity factors were also calculated for different points but no significant differences were observed.

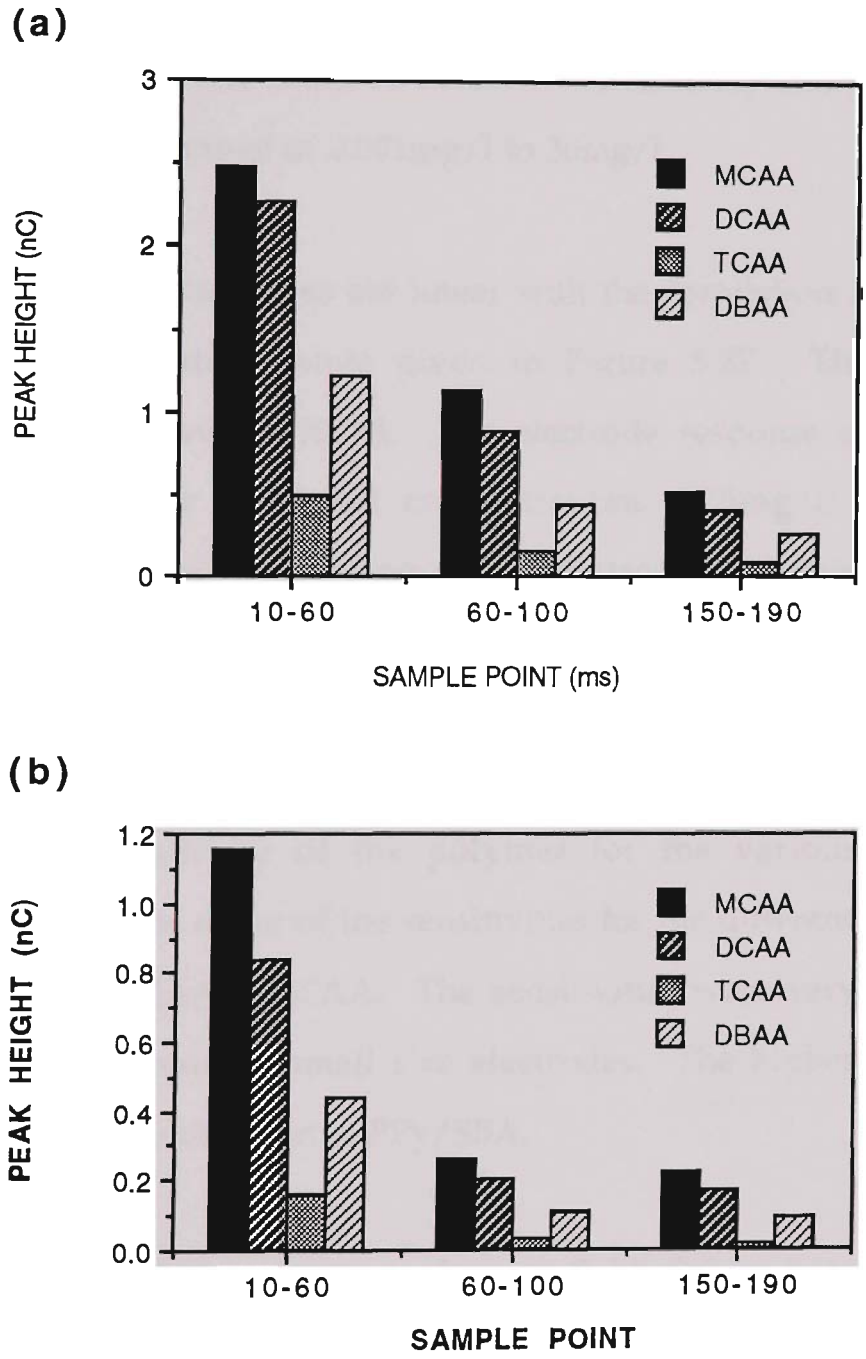

Figure 5.26: *Effect of sample point position on the responses obtained at (a) PPy/PTS, (b) PPy/DS. E_1=+0.5V, E_2=-0.4V, t_1=t_2=200ms, t_S=as in x-axis. Chromatographic conditions as in Figure 5.14.*

5.3.6.1 Calibration and Limits of Detection

The calibration curves were obtained for MCAA, DCAA, TCAA and DBAA for all four polymer electrodes during the analysis. A concentration dependent anodic current was obtained. By this approach , MCAA, DCAA, TCAA and DBAA could be detected conveniently and reproducibly over the concentration range of 0.001mg/l to 30mg/l.

The calibration curves are linear with the correlation coefficient > 0.992 for the concentration range given in Figure 5.27. This corresponds to a confidence level of 99.9%. The electrode response deviated significantly from linearity at higher concentrations (>35mg/l). This could be a consequence of overloading of the electrodes. The slopes (sensitivities) of calibration curves for MCAA, DCAA, TCAA and DBAA were calculated for each electrode by linear regression and are given in Table 5.4. The differences in these sensitivities are thought to reflect differences in the prevailing affinity of the polymer for the various analytes. For all electrodes, the order of the sensitivities for the different analytes is MCAA > DCAA > DBAA > TCAA. The sensitivities were very low due to the low level of current on small size electrodes. The highest sensitivities for all analytes were obtained at PPy/SBA.

The limits of detection are given in Table 5.5 and they correspond to the concentrations for which S/N =2 (50µl injections). The lowest LODs were obtained at PPy/SBA (0.001mg/l, 0.01mg/l, 0.1mg/l and 0.1mg/l for MCAA, DCAA, TCAA and DBAA respectively). The detection limits for these analytes are better than those obtained by conductivity detection (0.01mg/l, 0.1mg/l, 1.0mg/l and 0.5mg/l for MCAA, DCAA, TCAA and DBAA respectively).

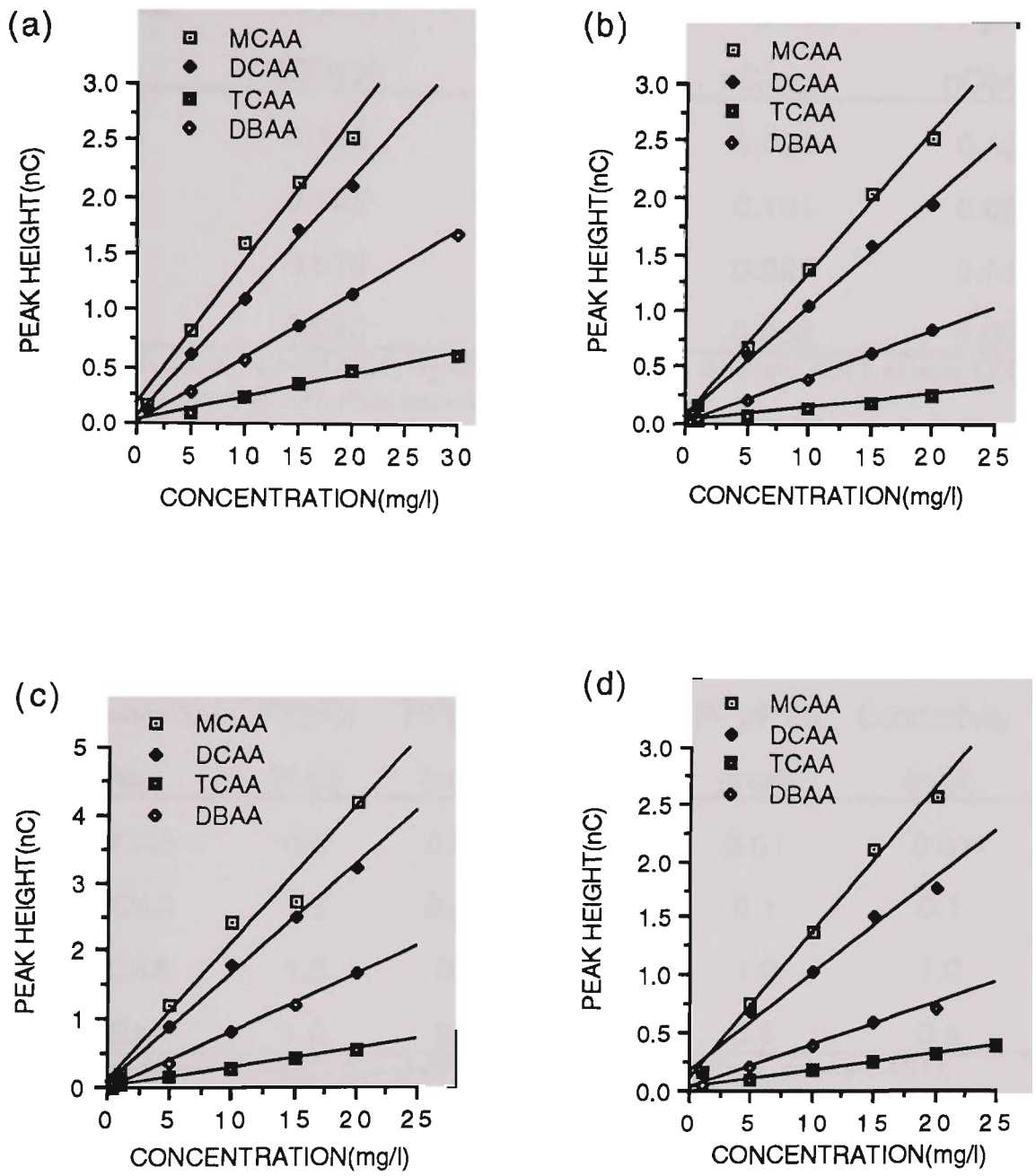

***Figure 5.27**: Calibration graphs for (a) PPy/Cl, (b) PPy/DS, (c) PPy/SBA and (d) PPy/PTS. E_1=+0.5V, E_2=-0.4V, $t_1=t_2$=200ms, t_s=10-60ms, Chromatographic conditions as in Figure 5.14.*

Table 5.4 *Sensitivities obtained for the detection of haloacetic acids at polymer electrodes*

Haloacetic acids	PPy/Cl nC/mg/l	PPy/DS nC/mg/l	PPy/SBA nC/mg/l	PPy/PTS nC/mg/l
MCAA	0.125	0.128	0.200	0.128
DCAA	0.105	0.098	0.161	0.084
TCAA	0.019	0.012	0.027	0.014
DBAA	0.056	0.041	0.083	0.036

Conditions; E_1=0.5V, E_2=-0.4V, t_1=t_2=200ms, t_s=10-60ms, column : AS11, eluent: 21.0 mM NaOH, suppressor: AMMS11. Flow rate=1ml/min

Table 5.5 *Detection limits obtained at polymer electrodes for haloacetic acids*

Haloacetic Acid	PPy/Cl (mg/l)	PPy/DS (mg/l)	PPy/SBA (mg/l)	PPy/PTS (mg/l)	Conductivity (mg/l)
MCAA	0.5	0.01	0.001	0.01	0.01
DCAA	0.5	0.01	0.01	0.1	0.1
TCAA	1.0	0.5	0.1	1.0	1.0
DBAA	1.0	0.1	0.1	0.5	0.5

Conditions; E_1=0.5V, E_2=-0.4V, t_1=t_2=200ms, t_s=10-60ms, column : AS11, eluent: 21.0 mM NaOH, suppressor: AMMS11. Flow rate=1ml/min

Table 5.6 compares the performance of the amperometric detection of haloacetic acids compared with conductivity, UV [337], and method 522 [334]. These values are higher than the values reported in US EPA method 552. The LOD for MCAA, however, is better than those obtained by conductivity and UV methods. The LOD for DCAA has also been improved when compared with the conductivity method.

Table 5.6 *Detection limits for haloacetic acids obtained by different methods*

Haloacetic Acid	PPy (μg/l)	Ion-exchange[a] (conductivity) (μg/l)	Ion-exclusion[b] (UV) (μg/l)	Method 552[c] (μg/l)
MCAA	1.00	8.00	70.00	0.10
DCAA	10.00	16.00	8.00	0.09
TCAA	100.00	80.00	5.10	0.06
DBAA	100.00	30.00	90.00	0.05

a and b: Reference 337
c: Reference 334

In all cases, the polymer electrodes were durable for 8-10 hours. The response magnitude, however, decreased in the initial stages of the analysis. This decrease was observed to be 30% during the first 30 minutes of analysis. Generally the same polymer film could be used for CV after FIA, with no evidence of chemical and mechanical deterioration. The electroactivity of the sensors monitored by cyclic voltammetry after analysis is given in Figure 5.28.

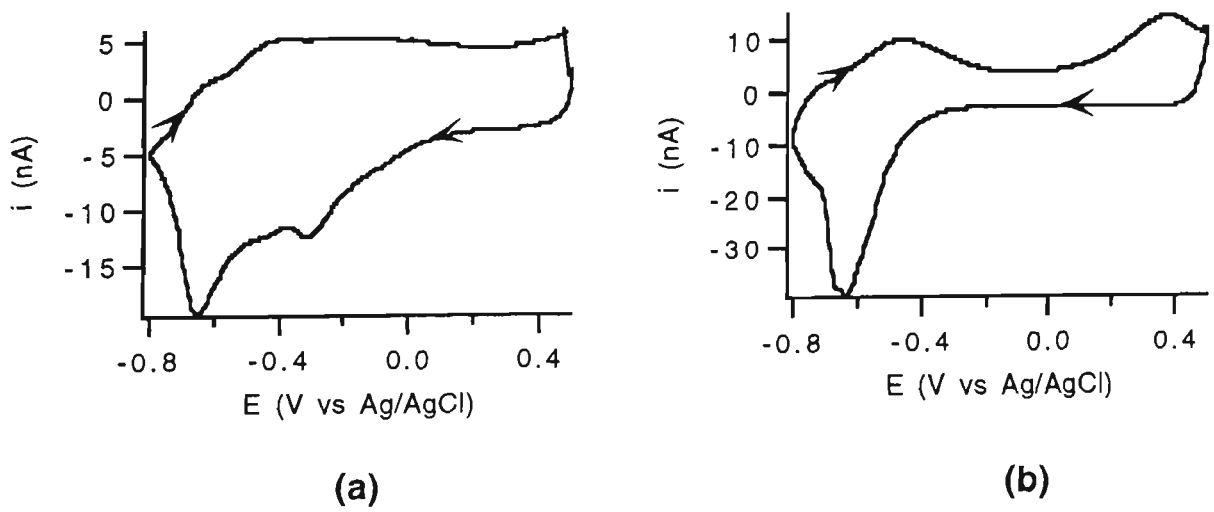

***Figure 5.28**: Cyclic voltammetry of (a) PPy/SBA and (b) PPy/DS in 0.1M $NaNO_3$. Scan rate=50mV/s.*

5.4 CONCLUSIONS

It has been shown in this Chapter that organic acids can be detected at conducting polymer electrodes. The electrochemistry of the polymer in analyte solutions shows slow diffusion of the anions and the current magnitude was different for different analytes. The cyclic voltammetric responses were also dependent on the nature of the polymer due to the incorporated counterion. The responses were better defined on PPy/SBA (50μm) electrodes compared to PPy/Cl (10μm or 50μm) electrodes. The current magnitude was also dependent on the polymer nature. The incorporation and expulsion of analyte anions was also confirmed by the mass changes during redox cycling.

The separation of the ions was achieved by anion chromatography within 8 minutes. Detection was not pursued with 10μm electrodes because they suffer from stability limitations, where polymers tended to be washed off after a few hours. The 50μm electrodes, however, were stable and were applied in the analysis. It is observed that selectivity could be obtained either by changing the electrochemical conditions or polymer nature. This suggests that the problem with coelution of analytes can be solved if such materials which show greater selectivities for analytes are applied.

As far as the mechanism of signal generation is concerned, it could be the combination of several factors. The currents obtained at the polymer modified electrodes are largely composed of currents arising from ion-exchange processes; as the response magnitude is dependent on the applied potentials. The applied potential dictates the extent of the ion-exchange process. The other factors include solution conductivity change as the analyte plug passes over the electrode, since the eluent used possess very

low conductivity (3.5μS). The electrode charging is also important but in the case of microelectrodes it could be considered to be negligible. The potential dependence of signal generation clearly dismisses the idea that the conductivity increase associated with the passage of the analyte is a major factor in the signal.

Excellent linear calibration curves were obtained for MCAA, DCAA, TCAA and DBAA at all the polymer modified electrodes investigated. The limit of detection has been improved for MCAA and DCAA as compared to conductivity and UV methods [337]. But these detection limits are higher than the EPA method 552 [334]. The method, however, can be improved by changing the polymer composition, choosing the one which would be more sensitive to the analytes.

Perhaps the most interesting aspect of these conducting polymer sensors is that selectivity was tuneable to a large degree by manipulation of the composition of the polymer as well as the potentials applied.

CHAPTER 6

GENERAL CONCLUSIONS

6.1 GENERAL CONCLUSIONS

The properties of conducting polymers like conductivity, electroactivity, facility to incorporate desired species, easy preparation of tailor made surfaces by monomer functionalisation and single-step electrochemical polymerisation on electrode substrates, make them suitable materials for electroanalytical applications. The feasibility and advantages of using conducting polymers as sensor has already been demonstrated by several workers [8,182,185,186].

These characteristic features of conducting electroactive polymers were addressed in this research project for the detection of amino acids and haloacetic acids inorder to develop a simpler, more sensitive and selective method compared to the existing ones. The electrode modification was carried out both by incorporating a range of counterions with different size and nature, or applying functionalised monomers to create a variety of electrochemical properties. These electrochemical properties are useful in improving the sensitivities and selectivities of the electroanalytical system.

It was observed that the polymerisation process was little affected by the nature of the counterion; as the growth potentials observed ranged between 0.55-0.65V. On the contrary, the electrochemical properties of the resulting polymer were influenced greatly by the nature and size of the anions incorporated. Three types of ion-exchange behaviour were observed during redox processes. The first type is the anion exchange property of polymer, such as PPy/Cl, due to the mobile small counterion (Cl^-). The second type involves both the anion and cation exchange properties of polymers that are incorporated with less mobile counterions (DS^-, PTS^-, SBA^- and $HBSA^-$). Finally, the third type is purely the cation exchange property of the polymer

synthesised with completely immobile counterions (PVS^-). This doping by cations during the reduction scan is termed as 'pseudo-cathodic doping' [115]. This property of the polymer films increases with the increase in the counterion size and decrease in the counterion mobility. Ideal behaviour of this type was observed in polyelectrolyte incorporated polymers.

The electrochemical properties were also influenced by the nature of the electrolyte solution. The size and charge of both anion and cation are important. Monovalent anions (Cl^-, NO_3^-) were incorporated and expelled easily during the redox process at PPy/CSA electrodes. The incorporation of divalent anions was not easily achieved resulting instead in monovalent cations being incorporated as charge compensating species. Similarly, divalent cation incorporation was not facilitated into the polymer electrode during redox processes.

The functionalised polymer PMPC was prepared at potentials above 1.0V, and a red colour polymer was obtained irrespective of counterion incorporated. PMPC has cation exchange groups permanently attached to the C3 position. During redox cycling, weak cation exchange properties were observed but mechanical instability of these polymers in aqueous solutions hinders their application.

Chiral polymers were prepared by electrosynthesising polypyrrole with (+) or (-) camphorsulfonate as the counterion, or PEP with perchlorate as the counterion. These polymers were characterised by EQCM. In the case of PPy/CSA, an equal polymer mass (34μg) was deposited irrespective of which hand of the counterion was applied. The rate of polymerisation for PPy/CSA remained constant during the polymerisation. The polymerisation process of PEP studied by EQCM showed that the

polymerisation efficiency was lower at the beginning of the polymerisation, probably due to the formation of some oligomers.

EQCM studies after polymerisation were also considered. The mass decrease and increase during respective reduction and oxidation at the PPy/CSA confirmed its anion exchange property, both in NO_3^- and in CSA^- solutions. The potential step experiment also showed mass decrease and mass increase with reduction and oxidation potentials respectively, showing anion exchange. The presence of a second reduction peak in the voltammogram was attributed to deeply trapped anions in the polymer matrix. This was confirmed by mass decrease in the corresponding region. Anion exchange property was also observed in PPEP during redox cycling and potential step characterisation. The presence of the substituent at the N atom of pyrrole had deteriorated the mechanical properties of the polymer, as it appeared powdery. The electrochemical stability also decreased during repetitive redox cycling and potential pulsing of the polymer in perchlorate solution. The CD spectra recorded for both PPy/CSA and PPEP did not show the presence of chain chirality.

The modified electrodes were then applied in the detection of amino acids. It was observed during stationary cell experiments (CV, NPV, CA) that zwitterions (alanine, serine) could not be incorporated into the polymers during CV. The acidic amino acids showed anion and cation exchange processes during redox cycling but the low current could be due to low solution conductivity or the larger size of the anions. Doping/dedoping processes were also observed for aspartic acid in NPV. In CA maximum current flow was obtained in aspartic acid. Arginine was also difficult to incorporate due to its large size and low solution conductivity. The high solution resistance of these amino acids causes iR drop problems. The

observations made during these analyses indicate that aspartic acid could easily be distinguished from the other amino acids investigated.

In FIA analysis of amino acids, typical FIA peaks were obtained for aspartic acid. The electrode fouling in amperometric detection was easily overcome by applying pulsed potentials where the polymer was periodically oxidised and reduced. The sensitivity was low for alanine and serine. This was probably because the hydrophobic and hydrogen bonding properties for alanine and serine respectively, as predicted for these amino acids due to the R-group, were not strong enough to produce strong signals. The responses for four amino acids, belonging to each group, are characteristic. Amino acid/polymer interaction can be characterised as neutral, anionic and cationic [279,280]. For aspartic acid, where adequate sensitivity was obtained, the correlation coefficient is 0.979 for linear calibration over the concentration range of 7.5×10^{-6}M to 6×10^{-5}M. This corresponds to a 99% confidence level. The limit of detection for aspartic acid was 7.5×10^{-6}M (1ppm). In stability studies, it was observed that over 12 hours the response decreased only by 25%.

The selectivity for each amino acid can be manipulated by changing the counterion incorporated. Therefore it can be concluded that each polymer electrode has different affinity for a particular amino acid. The maximum response was obtained for aspartic acid at PPy/SBA electrode. The responses were higher for arginine at PPy/DS electrode due to cation interactions. A pattern could be developed for each amino acid from the responses obtained for each amino acid at these polymer electrodes. The development of this type of pattern is important as the pattern gives more reliable selective detection of the analyte.

The signal generated as a function of applied potential does not just compose of current arising from doping/dedoping [29]. The possible factors that contribute to the signal are polymer conductivity [185], which is dependent on the potential applied and leads to a current due to doping/dedoping of the eluent ions, current due to doping/dedoping of analyte, current due to charging/discharging of the electrode, and pH dependence of the polymer conductivity. An important conclusion can be drawn from the observations made here that the nature of the analyte is the most important factor in signal generation; as the signals differ significantly for the amino acids belonging to different groups under similar experimental conditions.

The detection of amino acids was extended to conducting polymer modified microelectrodes (10μm) in order to improve selectivity and sensitivity of the system. The conducting polymers were deposited successfully on microelectrodes and the counterions which were used to prepare polymers on macroelectrodes were easily incorporated, except PVS. However, higher current densities and monomer concentrations along with 1 M Cl^- for PPy/Cl were required. Due to spherical diffusion on microelectrodes, fast mass transport to and from the electrode takes place. Therefore the radical cations produced at the microelectrodes do not get sufficient time to combine and deposit on the electrode surface. An increase in the pyrrole concentration was required to deposit the polymer. The polymer showed adequate redox characteristics and satisfactory stability. Well defined electrochemistry was observed at microelectrodes during redox cycling and chronoamperometry compared with macroelectrodes where both polymers were grown under similar experimental conditions. Fast mass transfer during redox processes and lower iR drop problems at microelectrodes promote electrochemical properties of the polymer film. The responses in

aspartic acid solution were more prominent at microelectrodes compared with macroelectrodes. For arginine, responses were only obtained at microelectrodes while no doping of arginine was obtained at macroelectrodes.

The microelectrode based detection of amino acids also indicated that not only was the polymer responsive to amino acids but also that the sensitivity was highest for arpartic acid, and that it had increased by more than 100% as compared with macroelectrodes. A pattern was developed for each amino acid by normalizing the responses obtained at different electrodes. The patterns for aspartic acid and arginine, however, had become more selective. It is also possible to distinguish between alanine and serine. Such pattern development is advantageous, especially in a situation where the sensor element is only partially selective to the analyte. These patterns provide greater confidence in the selectivity of detection of the analytes. Linear calibration was observed between 7.5×10^{-6}M and 1×10^{-4}M. The correlation coefficient of the calibration was 0.992 and 0.982 for aspartic and glutamic acids respectively. This corresponds to 99.9% confidence level. The lower slopes of the calibration curves compared with those obtained at the macroelectrode were due to the difference in the electrode sizes. The limits of detection are 3×10^{-6}M (0.4ppm) for both aspartic acid and glutamic acid. The LOD for aspartic acid was an improvement over that obtained with macroelectrodes. The stability of the microelectrodes, however, was not as good as that of the macroelectrodes. Sudden loss in the microelectrode response without any prior indication has posed difficulties in evaluating the sensor life time. In general, amino acid responses and sensitivities at these microelectrodes are superior to those obtained at macroelectrodes.

Conducting polymer modified electrodes were also applied for the detection of haloacetic acids. The electrochemistry of the polymer in analytes shows slow diffusion of the acid anions. The cyclic voltammetric responses were also dependent on the nature of the polymer, due to the incorporated counterion. The responses were better defined at PPy/SBA (50μm) electrodes compared to PPy/Cl (10μm or 50μm) electrodes. The incorporation and expulsion of analyte anions was also confirmed by the mass changes during redox cycling.

Subsequent to anion separation in sodium hydroxide eluent, the detection was performed in suppressed eluent because it was observed that the polymer electrodes were not electrochemically stable in alkaline eluent (21mM). All polymers, irrespective of the counterion incorporated, lost their electroactivity with repetitive cycling. In EC detection, polymers were responsive to all haloacetic acids analysed. Detection was not pursued with 10μm electrodes because they suffer from stability limitations; where polymers tended to be washed off after a few hours. The 50μm electrodes, however, were stable and were applied in the analysis. It was observed that the selectivity factor could be changed either by changing the electrochemical conditions or polymer nature. This suggests that the problem with coelution of analytes (MCAA and MBAA) can be solved if such materials, which show greater selectivities for analytes, are applied.

Similar to amino acid detection, the signal for haloacetic acids might be composed of several factors. The sensitivity and selectivity factors depended on the applied potential and this supports the idea that the ion-exchange process is the dominant factor contributing to the signal obtained. The ion-exchange process on each polymer electrode is dependent on the potential applied and polymer nature (due to counterion incorporated). The

contribution from the electrode charging can be considered negligible in the case of microelectrodes. The change in the solution conductivity also adds to the signal as the analyte plug passes over the electrode. The haloacetic acids can be detected over the concentration range 0.001mg/l to 30mg/l. Significant deviation from linearity was observed at concentrations higher than 35mg/l. The correlation coefficients for the calibration curves are >0.992 which corresponds to 99.9% confidence level. The highest sensitivities were obtained at PPy/SBA electrodes and the LOD for MCAA and DCAA are 1.00μg/l and 10μg/l respectively. These LODs for MCAA and DCAA have improved compared with conductivity and UV [337] detection methods.

The outcomes from this work have added substantially to the field of electroanalytical detection of organic acids at conducting polymers. A significant contribution has been made towards the general understanding of the variables which affect selectivities and sensitivities for the analytes. The most interesting aspect of these sensors is that selectivity was tunable to a large degree by manipulation of the composition of the polymer as well as the potentials applied. Prior to this work, conducting polymers and microelectrodes were not applied for detection of amino acids. Conducting polymer based sensors have been proven to be powerful tools for the improvement of electrochemical detection and their future is expected to continue; especially in the application of microarrays coated with conducting polymers in pattern recognition of amino acids.

REFERENCES

1. L. R. Faulkner, *Chem. Eng. News*, 62 (1984) 28.
2. R. W. Murray, A. G. Ewing and R. A. Durst, *Anal. Chem.*, 59 (1987) 379-A.
3. R. F. Lane and A. T. Hubbard, *J. Phys. Chem.*, 77 (1973) 1401 and 1411.
4. R. P. Baldwin and K. N. Thompson, *Talanta*, 38 (1991) 1.
5. G. Sittampalam and G. S. Wilson, *Anal. Chem.*, 55 (1983) 1608.
6. K. M. Korfhage, K. Ravichandran and R. P. Baldwin, *Anal. Chem.*, 56 (1984)1154.
7. J. E. Frew and H. A. O. Hill., *Anal. Chem.*, 59 (1987) 933A.
8. Y. Ikariyama and W. R. Heineman, *Anal. Chem.*, 58 (1986) 1803.
9. M. M. Malone, A. P. Doherty, M. R. Smyth and J. G. Vos, *Analyst*, 117 (1992) 1259.
10. A. Merz and A. J. Bard, *J. Am. Chem. Soc.*, 100 (1978) 3222.
11. M. R. Van De Mark and L. L. Miller, *J. Am. Chem. Soc.*, 100 (1978) 3225.
12. A. Merz, *Nachr. Chem. Techn. Lab.*, 30 (1982) 18.
13. R. W. Murry, *Annu. Rev. Mater. Sci.*, 14 (1984) 145.
14. M. Kaneko and D. Wohrle, *In Advances in Polymer Sciences*, Vol. 84, Springer-Verlag, Berlin, 1988, p141.
15. A. F. Diaz, K. K. Kanazawa and G. P. Gardini, *J. C. S. Chem. Comm.*, (1979) 635.
16. K. K. Kanazawa, A. F. Diaz, R. H. Geiss, W. D. Gill, J. F. Kwak, J. A. Logan, J. F. Rabolt and G. B. Street, *J. C. S. Chem. Comm.*, (1979) 854.
17. A. Diaz, J. M. V. Vallejo and A. M. Duran, *IBM J. Res. Develop.* 25 (1981) 42.
18. C. K. Chiang, C. R. Fincher, Y. W. Park. A. J. Heeger,

H. Shirakawa. E. J. Louis, S. C. Gau and A. G. MacDiarmid, *Phy. Rev. Lett.*, 39 (1977) 1098.

19. S. Roth and M. Filzmoser, *Adv. Mater.*, 2 (1990) 356.
20. S. Roth and H. Bleier, *Adv. in Physics*, 36 (1987) 385.
21. H. Shirakawa, E. J. Louis, A. G. MacDiarmid, C. K. Chiang and A. J. Heeger, *J. C. S. Chem. Commun.*, (1977) 578.
22. C. K. Chiang, Y. W. Park, A. J. Heeger, H. Shirakawa, E. J. Louis and A. G. MacDiarmid, *J. Chem. Phys.*, 69 (1978) 5098.
23. A. F. Diaz and J. I. Castillo, *J. C. S. Chem. Commun.*, (1980) 397.
24. D. M. Ivory, G. G. Miller, J. M. Sowa, L. W. Shacklette, R. R. Chance and R. H. Baughman, *J. Chem. Phys.*, 71 (1979) 1506.
25. G. Tourillon and F. Garnier, *J. Electroanal. Chem.*, 135 (1981) 173.
26. A. F. Diaz and J. A. Logan, *J. Electroanal. Chem.*, 111 (1980) 111.
27. G. E. Wnek, J. C. W. Chien, F. E. Karazs and C. P. Lillja, *Polymer*, 20 (1979) 1441.
28. M. Umana and J. Waller, *Anal. Chem.*, 58 (1986) 2979.
29. P. R. Teasdale and G. G. Wallace, *Analyst*, 118 (1993) 329.
30. H. Shinohara, T. Chiba and M. Aizawa, *Sens. Actuators*, 13 (1988) 79.
31. J. C. Cooper and E. A. H. Hall, *Biosens. Bioelectron.*, 7 (1992) 473.
32. E. M. Genies and C. Tsintavis, *J. Electroanal. Chem.*, 195 (1985) 109.
33. P. N. Bartlett and P. R. Birkin, *Synth. Met.*, 61 (1993)15.
34. H. Harada, T. Fuchigami and T. Nonaka, *J. Electroanal. Chem.*, 303 (1991) 139.
35. A. J. Downard and D. Pletcher, *J. Electroanal Chem.*, 206 (1986) 147
36. P. Bauerle, *Adv. Mater.*, 5 (1993) 879.
37. E. M. Genies, G. Bidan and A. F. Diaz, *J. Electroanal. Chem.*,

149 (1983) 101.

38. S. Asavapiriyanont, G. K. Chandler, G. A. Gunawardena and D. Pletcher, *J. Electroanal. Chem.*, 177 (1984) 229.

39. I. Rodriguez, M. L. Marcos and J. Gonzalez-Velasco, *Electrochim. Acta*, 32 (1987) 1181.

40. M. Takakubo, *Synth. Met.*, 16 (1986) 167.

41. R. A. Bull, Fu-Ren. F. Fan and A. J. Bard, *J. Electrochem. Soc.*, 129 (1982) 1009.

42. C. O. Too, S. A. Ashraf, H. Ge, K. J. Gilmore, S. G. Pyne and G. G. Wallace, *Polymer*, 34 (1993) 2684.

43. J. R. Reynolds, P. A. Poropatic and R. L. Toyooka, *Macromolecules*, 20 (1987) 958.

44. M. Salmon and G. Bidan, *J. Electrochem. Soc.*, 132 (1985) 1897.

45. T. F. Otero and C. Santamaria, *Synth. Met.*, 51 (1992) 313.

46. H. Eisazadeh, K. J. Gilmore, A. J. Hodgson, G. Spinks and G. G. Wallace, *Colloids and Surf.*, 103 (1995) 281.

47. A. Lopez, M. F. M. Viegas, G. Bidan and E. Vieil, *Synth. Met.*, 63 (1994) 73.

48. L. J. Buckley, D.K. Roylance and G. E. Wnek, *J. Polymer, Sci., Part B: Polym. Physics*, 25 (1987) 2179.

49. A. F. Diaz and J. Bargon, *in Handbook of Conducting Polymers*, Vol.1, T. A. Skotheim (Ed.), Marcel Dekker, New York, 1986, p82.

50. P. Hulser and F. Beck, *J. Appli. Electrochem.*, 20 (1990) 596.

51. F. Beck and P. Hulser, *J. Electranal. Chem.*, 289 (1990) 159.

52. P. Hulser and F. Beck, *J. Electrochem. Soc.*, 137 (1990) 2067.

53. K. Imanishi, M. Satoh, Y. Yasuda, R. Taushima and S. Aoki, *J. Electroanal. Chem.*, 242 (1988) 203.

54. J. L. Sauvajol, D. Chenouni, J. P. Lere-Porte, C. Chorro, B. Bouicala and J. Petrissans, *Synth. Met.*, 38 (1990) 1.

55. F. Tadjar, S. Ymmel, M. Janda, P. Duchek, P. Holy and I. Stibor, *Collect. Czech. Chem. Commun.*, 54 (1989) 1299.

56. J. M. Ko, H. W. Rhee, S. M. Park and C. Y. Kim, *J. Electrochem Soc.*, 137 (1990) 905.

57. F. T. A. Vork, B. C. A. M. Schuernans and E. Barenderecht, *Electrochim Acta*, 35 (1990) 567.

58. J. Roncali, F. Garnier and M. Lemaire, *Synth. Met.*, 15 (1986) 323.

59. J. Roncali and F. Garnier, *Macro. J. Chem.*, 10 (1986) 4.

60. M. Akisato, S. Tanaka and K. Kaeriyama, *Synth. Met.*, 14 (1986) 279.

61. A. J. Downard and D. Pletcher, *J. Electrochem. Chem.*, 206 (1986) 147.

62. A. J. Downard and D. Pletcher, *J. Electrochem. Chem.*, 206 (1986) 139.

63. M. Satoh, K. Kaneto, K. Yoshino, *Synth. Met.*, 14 (1986) 289.

64. M. Ogasawara, K. Funahashi, T. Demura, T. Hagiwara and K. Iwata, *Synth. Met.*, 14 (1986) 61.

65. S. C. Sharma, S. Krishnamoorthy, S. V. Naidu. C. I. Eom, S. Krichene and J. R. Reynolds, *Phys. Rev. B.*, 41 (1992) 5258.

66. L. S. Curtin, G. C. Komplin and W. J. Pietro., *J. Phys. Chem.*, 92 (1988) 12.

67. L. F. Warren and D. P. Anderson, *J. Electrochem. Soc.*, 134 (1987) 101.

68. D. S. Maddison and C. M. Jenden, *Polym. Int.*, 27 (1992) 231.

69. J. M. Ko, H. W. Rhee and C. Y. Kim, *Makromol. Chem. Macromol. Symp.*, 33 (1990) 353.

70. D. J. Walton, C. E. Hall and A. Chyla, *Analyst*, 117 (1992) 1305.

71. C. Zhong, K. Doblhofer and G. Weinberg, *Faraday Discuss. Chem. Soc.*, 88 (1989) 307.

72. K. Hyodo and M. Omae, *Electrochimica Acta*, 35 (1990) 1245.

73. G. Tourillon and F. Garnier, *J. Polym.Sci., 22* (1984) 33.

74. A. F. Diaz, J. I. Castillo, J. A. Logan and W. Y. Lee, *J. Electroanal. Chem.*, 129 (1981) 115.

75. A. F. Diaz, *Chem. Scr.*, 17 (1981) 145.

76. R. J. Waltman. J. Bargon and A. F. Diaz, *J. Phys. Chem.*, 87 (1983) 1459.

77. G. B. Street, T. C. Clarke, M. Krounbi, K. K. Kanazawa, V. Lee, P. Pfluger, J. C. Scott, and G. Weiser, *Mol.Cryst. Liq. Cryst.*, 83 (1982) 253.

78. G. B. Street, R. H. Geiss, S. E. Lindsey, A. Nazzal and P. Pfluger, *In Proceedings of the Conference on Electronic Extraction and Interaction Processes in Organic Molecular Aggregates*, P. Reineker, H. Haken, and H. C. Wolf, (Eds.), Springer, New York, 1983, p242.

79. C. K. Baker and J. R. Reynolds, *J. Electranal. Chem.*, 251 (1988) 307.

80. C. K. Baker and J. R. Reynolds, *Synth. Met.*, 28 (1989) C21.

81. T. Inoue and T. Yamase, *Bull.Chem. Soc. Jap.*, 56 (1983) 985.

82. G. Kossmehl and G. Chatzitheodorou, *Makromol. Chem. Rapid. Commun*, 2 (1982) 551.

83. G. Kossmehl and G. Chatzitheodorou, *Mol. Cryst. Liq. Cryst.*, 83 (1982) 291.

84. J. Heinze. K. Hinkelmann, M. Dietrich and J. Mortensen, *DECHEMA Monographie*, 102 (1986) 209.

85. J. Heinze. K. Hinkelmann and M. Land, *DECHEMA, Monographie*, 112 (1989) 75.

86. A. F. Diaz, A. Martinez, K. K. Kanazawa and M. Salmon, *J. Electroanal Chem.*, 130 (1980) 181.

87. G. B. Street, *In Handbook of Conducting Polymers*, Vol.1, T. A. Stotheim, (ed), Marcel Dekker, New York, 1986, p 265.

88. M. G. Kanatzidis, *Chem. Eng. News*, 60 (1990) 36.

89. G. Tourillon and F. Garnier, *J. Phys. Chem.*, 87 (1983) 2289.

90. T. C. Chung, J. H. Kaufman, A. J. Heeger and F. Wudl, *Phys. Rev.*, 30B (1984) 702.

91. W. Zhang and S. Dong, *Electrochim.Acta*, 38 (1993) 441.

92. J. Preza, I. Lundstrom and T. A. Skotheim, *J. Electro Chem. Soc.*, 129 (1982) 1685.

93. M. Salmon, A. F. Diaz, A. J. Logan, M. Krounbi and J. Bargon, *Mol. Cryst. Liq. Cryst.*, 83 (1982) 1297.

94. A. G. MacDirmaid, L. S. Yang, W. S. Huang, B. D. Humphrey, *Synth. Met.*, 18 (1987) 393.

95. A. F. Diaz and B. Hall, *IBM J. Res. Develop.*, 27 (1983) 342.

96. T. Iyoda, A. Ohtani, T. Shimidzu and K. Honda, *Chem. Lett.*, (1986) 687.

97. M. Salmon, A. F. Diaz, A. J. Logan, M. Krounbi and J. Bargon, *Mol. Cryst. Liq. Cryt.*, 83 (1982) 265.

98. S. Kuwabata, K. I. Okamoto, O. Ikeda and H. Yoneyama, *Synth. Met.*, 18 (1987) 101.

99. M. Nishizawa, T. Matsue and I. Uchida, *Anal. Chem.*, 64 (1992) 2642.

100. M. Marchesiello and E. M. Genies, *Electrochim.Acta*, 37 (1992) 1987

101. A. J. Hodgson, M. J. Spencer and G. G. Wallace, *React. Polym.* 18 (1992) 77.

102. O. A. Sadik and G. G. Wallace, *Anal. Chim. Acta*, 279 (1993) 209.

103. L. L. Miller, B. Zinger and Q. X. Zhou, *J. Am. Chem. Soc.*, 109 (1987) 2267.

104. R. A. Bull, F. R. Fan and A. J. Bard, *J. Electrochem. Soc.*, 130 (1983) 1636.

105. D. J. Belanger, J. Nadreau and G. J. Fortier, *J. Electroanal. Chem.*, 274 (1989) 143.

106. L. P. Couves and S. J. Porter, *Synth. Met.*, 28 (1989) 761.

107. S. B. Adelojou, S. J. Shaw and G. G. Wallace, *Anal. Chim. Acta*, 281 (1993) 611 and 621.

108. T. Shimidzu, React. *Polym.*, 6 (1987) 221.

109. D. T. Glatzhofer, J. Ulanski and G. Wegner, *Polymer*,

28 (1987) 449.

110. W. Wernet and G. Wegner, *Makromol. Chem.*, 188 (1987) 1465.

111. A. Kassim, H. Block, F. J. Devis and G. R. Mitchell, *J. Mater. Chem.*, 2 (1992) 987.

112. A. Kassim, F. J. Davis and G. R. Mitchell, *Synth. Met.*, 62 (1994) 41.

113 E. M. Genies and J. M. Pernaut, *Synth. Met.*, 10 (1984/85) 117.

114. J. Kaufman, K. K. Kanazawa and G. B. Street, *Phys. Rev. Lett.*, 53 (1984) 2461.

115. T. Shimidzu, A. Ohtani, T. Iyoda and K. Honda, *J. Electroanal. Chem.*, 224 (1987) 123.

116. R. E. Noftle and D. Pletcher, *J. Electroanal. Chem.*, 227 (1987) 229.

117. K. Naoi, M. M. Lien and W. H. Smyrl, *J. Electrochem. Soc.*, 35 (1991) 1971.

118. M. M. Lien, W. H. Smyrl and M. Morita, *J. Electroanal. Chem.*, 309 (1991) 333.

119. R. C. D. Peres, M. A. De Paoli and R. M. Torresi, *Synth. Met.*, 48 (1992) 259.

120. V. M. Schmidt and J. Heitbaum, *Electrochim. Acta*, 38 (1993) 349.

121. C. Zhong and K. Doblhofer, *Electrochimica Acta*, 35 (1990) 1971.

122. V. M. Schmidt, C. Barbero and R. Kotz, *J. Electroanal. Chem.*, 352 (1993) 301.

123. A. F. Diaz, J. Castillo,K. K. Kanazawa, J. A. Logan, M. Salmon and O. Frjardo, *J. Electroanal. Chem.*, 133 (1981) 233.

124. J. Hlavaty, V. Papez, L. Kavan and P. Krtil, *Synth. Met.*, 66 (1994) 165.

125. M. D. Imisides, P. R. Teasdale and G. G. Wallace, *Encyclopedia of Analytical Science*, Academic Press Limited, 1995, p 4621.

126. J. Bargon, S. Mohmand and R. J. Waltman, *IBM, J. Res. Dev.*,

27 (1983) 330.

127. A. Nazzal and G. B. Street, *J.C. S. Chem Commun.*, (1983) 84.

128. M. Salmon, M. E. Garbajal, J. C. Juarez, A. F. Diaz and M. C. Rock, *J. Electrochem Soc.*, 131 (1984) 1802

129. A. Deronzier, M. Essakalli and J. C. Moutet, *J. Electroanal. Chem.*, 244 (1988) 163.

130. A. Deronzier and M. Essakalli, *J. Phys Chem.*, 95 (1991) 1737.

131. H. D. Tabba and K. M. Smith, *J. Org. Chem.*, 49 (1984) 1870.

132. P. G. Pickup, *J. Electranal. Chem.*, 225 (1987) 273.

133. E. E. Havinga, L.W. van Horssen, W. ten Hoeve, H. Wynberg and E. W. Meijer, *Polym. Bulletin*, 18 (1987) 277.

134. N. Sundaresan, S. Basak, M. Pomerantz and J. R. Reynolds, *J. C. S. Chem. Commun.*, (1987) 621.

135. G. Baidan, B. Ehui and M. Lapkowski, *J. Phys. Part D: Appl. Phys.*, 21 (1988) 1043.

136. C. Zhong, W. Storck and K. Doblhofer, *Ber. Bunsenges. Phys. Chem.*, 94 (1990) 1149.

137. T. Komori and T Nonaka, *J. Am. Chem. Soc.*, 105 (1983) 5690.

138. S. Abe, T. Nonaka and T. Fuchigami, *J. Am. Chem. Soc.*, 105 (1983) 3630.

139. J. C. Moutet and E. Saint-Aman, F. Tran-Van, P. Angibeaud and J. P. Utille., *Adv. Mater.*, 4 (1992) 511.

140. D. Delabouglise and F. Garnier, *J. Chim. Phys.*, 89 (1992) 1131.

141. D. Delabouglise and F. Garnier, *Synth. Met.*, 39 (1990) 117.

142. M. Lemaire, D. Delabouglise, R. Garreau, A. Guy and J. Roncali, *J. C. S. Chem. Commun.*, (1988) 658.

143. D. Kotkar, V. Joshi and P. K. Ghosh, *J. C. S. Chem. Commun.*, (1988) 917.

144. M. Andersson, P. O. Ekeblad, T. Hjertberg, O. Wennerstorm and

O. Inganas, *Polym. Commun.* 32 (1991) 546.

145. R. L. Elsenbaumer, H. Eckhardt, Z. Iqbal, J. Toth and R. H. Baughman, *Mol. Cryst. Liq. Cryst.* 118 (1985) 111.

146. M. M. Bouman, E. E. Havinga, R. A. J. Janssen and E. W. Meijer, *Mol. Cryst. Liq. Cryst.*, 256 (1994) 439.

147. M. R. Majidi, L. A. P. Kane-Maguire and G. G. Wallace, *Polymer*, 35 (1994) 3113.

148. M. R. Majidi, L. A. P. Kane-Maguire and G. G. Wallace, *Polymer*, 36 (1995) 3597.

149. M. Gazard, *In Handbook of Conducting Polymers*, Vol.1, T. J. Skothelm, (Ed), Marcel Dekker, New York, (1986) pp 673.

150. S. W. Feldberg, *J. Am. Chem, Soc.*, 106 (1984) 4671.

151. J. Tanguy, N. Mermilliod, and M. Hoclet, *Synth. Met.*, 18 (1987) 7.

152. J. Tanguy, M. Slama, M. Hoclet and J. L. Baudouin, *Synth. Met.*, 28 (1989) C145.

153. W. J. Albery, Z. Chen, B. R. Horrocks, A. R. Mount , P. J. Wilson, D. Bloor, A. T. Monkman and C. M. Elliott, *Faraday Discuss. Chem. Soc.*, 88 (1989) 247.

154. B. J. Feldman, P. Burgmayer and R. W. Murray, *J. Am. Chem. Soc.*, 107 (1985) 872.

155. K. Naoi, M. M. Lien and W. H. Smyrl, *J. Electroanal. Chem.*, 272 (1989) 273.

156. T. Matencio, M.-A. De Paoli, R. C. D. Peres, R. M. Torresi and S. I. Cordoba de Torresi, *Synth Met.*, 72 (1995) 59.

157. J. H. Kaufman, K. K. Kanazawa and G. B. Street, *Phys. Rev. Letters*, 53 (1984) 2461.

158. C. Dusemund and G. Schwitzgebel, *Ber. Bunsenges. Phys. Chem.*, 95 (1991) 1543.

159. C. Dusemund and G. Schwitzgebel, *Synth. Met.* 55-57 (1993) 1396.

160. R. Bilger and J. Heinze, *Synth. Met.*, 41-43 (1991) 2893.

161. S. Basak, C. S. C. Bose and K. Rajeshwar, *Anal. Chem.*, 64 (1992) 1813.

162. J. R. Reynolds, N. S. Sundaresan, M. Pomerantz, S. Basak and C. Baker, *J. Electroanal. Chem.*, 250 (1988) 355.

163. D. Orata and D. A. Buttry, *J. Am. Chem. Soc.*, 109 (1987) 3574.

164. D. Orata and D. A. Buttry, *J. Electranal. Chem.*, 257 (1988) 71.

165. R. M. Torresi, S. I. Cordoba-Torresi, C. Gabrielli, M. Keddam and H. Takenouti, *Synth. Met.*, 61 (1993) 291.

166. F. Beck, P. Braun and M. Oberst, *Ber. Bunsenges. Phys. Chem.*, 91(1987) 967.

167. F. Beck, *Electrochim. Acta*, 33 (1988) 839

168. P. Novak, B. Rasch and W. Vielstich, *J. Electrochem. Soc.*, 138 (1991) 3300.

169. P. Novak and W. Vielstich, *J. Electrochem. Soc.*, 137 (1990) 1036.

170. P. Novak and W. Vielstich, *J. Electrochem. Soc.*, 137 (1990) 1681.

171. P. A. Christensen and A. Hamnett, *Electrochim. Acta*, 36 (1991) 1263.

172. 207 G. Mengoli, M. M. Musiani, M. Fleischman and D. Pletcher, *J. Appl. Electrochem.*, 14 (1984) 285.

173. Q. Renyuan, Q. Junjin and J. Bazhen, *Synth. Met.*, 14 (1986) 81.

174. V. V. Kras'ko, A. A. Yakovleva and Ya. M. Kolotyrkin, *Electrokhimiya*, 22 (1986) 1432.

175. T. Kobayashi, H. Yoneyama and H. Tamura, *J. Eletroanal. Chem.*, 177 (1984) 281.

176. T. Osaka, K. Naoi, S. Ogano and S. Nakamura, *J. Electrochem. Soc.*, 134 (1987) 2096.

177. R. A. Saraceno, J. G. Pack and A. G. Ewing, *J. Electroanal. Chem.*, 197 (1986) 265.

178. R. Noufi, D. Tench and L. F. Warren, *J. Electrochem. Soc.*,

127 (1980) 2310.

179. A. Ivaska, *Electroanalysis*, 3 (1991) 247.

180. Gerard Bidan, *Sens. Actuators B*, 6 (1992) 45.

181. A. Hulanicki, S. Glab and F. Ingman, *Pure and Appl. Chem.*, 63 (1991) 1247.

182. S. Dong, Z. Sun and Z. Lu, *Analyst*, 113 (1988) 1525.

183. Z. Lu, Z. Sun and S. Dong, *Electroanalysis*, 1 (1989) 271.

184. S. Dong, Z. Sun and Z. Lu, *J. C. S. Chem. Commun.*, (1988) 993.

185. Y. Ikariyama, C. Galiatsatos, W. R. Heineman and S. Yamauchi, *Sens. Acuators*. 12 (1987) 455.

186. J. Ye. and R. P. Baldwin, *Anal. Chem.*, 60 (1988) 1979.

187. E. Wang and A. Liu, *Anal. Chim. Acta*, 252 (1991) 53.

188. P. Ward and M. R. Smyth, *Talanta*, 40 (1993) 1131.

189. R. C. Martinez, F. B. Dommnz, M. Gonzalez and J. H. Mendez, R.C. Orellana, *Anal. Chim. Acta*, 279 (1993) 299.

190. O. A. Sadik and G. G. Wallace, *Electranalysis*, 5 (1993) 555.

191. R.John, *Ph.D Thesis, University of Wollongong.*

192. S. Sukeerthi and A. Q. Contractor, *Ind. J. Chem.*, 33 A (1994) 565.

193. C. Iwakura, Y. Kajiya, and H. Yoneyama, *J. C. S. Chem. Commun.*, (1988) 1019.

194. D. T. Hoa, T. N. Suresh Kumar, R. S. Srinivasa, R. Lal, N. S. Punekar and A. Q. Contractor, *Anal Chem.*, 64 (1992) 2645.

195. M. Gholamian, T. N. Suresh Kumar and A. Q. Contractor, *Proc. Ind. Acad. Sci.*, 97 (1986) 457.

196. T. Matsue, M. Nishizawa, T. Sawaguchi and I. Uchida, *J. C. S. Chem. Commun.*, (1991) 1029.

197. P. N. Bartlett and P. R. Birkin, *Anal. Chem.*, 65 (1993) 1118.

198. E. Tamiya, I. Karube, S. Hattori, M. Suzuki and K. Yokoyama., *Sens.Actuators*, 18 (1989) 297.

199. J. M Slater and E. J. Watt, *Anal.Procc*, 26 (1989) 397.

200. W. Schuhmann, R. Lammert, B. Uhe and H. L. Schmidt, *Sens.Actuators, B1* (1990) 537.

201. C. G. J. Koopal, M. C. Feiters, R. J. M. Nolte, B. de. Ruiter, R. B. M. Schasfoort, R. Czajka and H. Van. Kempen, *Synth. Met.*, 51 (1992) 397.

202. W. Schuhmann, *Sens.Actuators B*, 4 (1991) 41.

203. K. Ramanathan, N. S. Sundaresan and B. D. Malhotra, *Eletroanalysis*, 7 (1995) 579.

204. Q. Pei and R. Qian, *Synth. Met.*, 45 (1991) 35.

205. G. P. Kittelson, H. S. White and M. S. Wrighton, *J. Am. Chem. Soc.*, 106 (1984) 7389.

206. N. M. Ratcliffe, *Anal. Chim. Acta*, 239 (1990) 257.

207. J. Miasik, A. Hooper and B. Tofield, *J. Chem. Soc., Faraday Trans. I*, 82 (1986) 1117.

208. T. Hanawa, S. Kuwabata and H. Yoneyama, *J. Chem. Soc., Faraday Trans. I*, 84 (1988) 1587.

209. T. Hanawa and H. Yoneyama, *Bull. Chem. Soc. Jpn.*, 62 (1989) 1710.

210. T. Hanawa and H. Yoneyama, *Synth. Met.*, 30 (1989) 341.

211. P. N. Bartlett and S. K. Ling Chung, *Sens.Actuators*, 20 (1989) 287.

212. P. N. Bartlett, B. M. Archer and S. K. Ling Chung, *Sens. Actuators*, 19 (1989) 125.

213. Y. Katsumi, H. N. Singh, G. J. Rabe and W. F. Schmidt, *Polym.Commun.*, 26 (1985) 103.

214. J. N. Thackeray and M. S. Wrighton, *J. Phys. Chem.*, 90 (1986) 6674.

215. S. Chao and M. S. Wrighton, *J. Am. Chem. Soc.*, 109 (1987) 6627.

216. C. Budrowski and J. Przyluski, *Synth. Metal.*, 41-43 (1991) 597.

217. J. Przyluski and C. Budrowski, *Synth. Metal.*, 41-43 (1991) 1163.

218. P. T. Kissinger and W. R. Heineman, *J. Chem. Edu.*, 60 (1983) 702.

219. S. Ching, R. Dudek and E. Tabet, *J. Chem. Edu.*, 71 (1994) 602.

220. D. A. Buttry and M. D. Ward, *Chem. Rev.*, 92 (1992) 1355.

221. G. Sauerbrey, Z . *Phys.*, 155 (1959) 206.

222. K. K. Kanazawa and J. G. Gordon, *Anal. Chem.*, 57 (1985) 1770.

223. K. Stulik and V. Pacakova, *In Electroanalytical Measurements in Flowing Liquids*, E. Horwood Limited, Chichester Publishers, England, 1987.

224. T. Schalkhammer, E. Mann-Buxbaum and F. Pittner, *Sens.Actuators B*, 4 (1991) 273.

225. B. F. Y. Yon-Hin, M. Smolander, T. Crompton and C. R. Lowe, *Anal. Chem.*, 65 (1993) 2067.

226. Z. Gao and A. Ivaska, *Anal. Chim. Acta*, 284 (1993) 393.

227. J. Y. Lim, W. Paik and I. Yeo. *Synth. Met.*, 69 (1995) 451.

228. K. K. Kanazawa, A. F. Diaz, M. T. Krounbi and G. B. Street, *Synth. Met.*, 4 (1981) 119.

229. H. Ge, K. J. Gilmore, S. A. Ashraf, C. O. Too and G. G. Wallace. *Polymer*, 34 (1993) 2007.

230. H. Ge, S. A. Ashraf, K. J. Gilmore, C. O. Too and G. G. Wallace, *J. Electranal. Chem.*, 340 (1992) 41.

231. M. Iseki, K. Saito, M. Ikematsu, Y. Sugiyama, K. Kuhara and A. Mizukami, *J. Electroanal. Chem.*, 358 (1993) 221.

232. R. E. Lancaster and C. A. Vander Werf, *J. Org. Chem.*, 23 (1958) 1208.

233. R. A. Nicolaus and L. Mangoni, *Gazz. Chim. Ital.*, 85 (1955) 1378.

234. S. Bruckenstein and M. Shay, *Electrochim.Acta*, 30 (1985) 1295.

235. C. Gabrielli, M. Keddam and R. Torresi, *J. Electrochem. Soc.*, 138 (1991) 2657.

236. R. John and G. G. Wallace, *J. Electroanal. Chem.*, 354 (1993) 145.

237. T. Shimidzu, A. Ohtani and K. Honda, *J. Electroanal. Chem.*, 251 (1988) 323.

238. J. M. Barisci, P. Murray, C. J. Small and G. G. Wallace, *Electroanalysis*, 1996, in press.

239. R. Casas, A. Dicko, J. M. Ribo, N. Ferrer-Anglada, R. Bonnett, N. Hanly and D. Bloor, *Synth. Met.*, 39 (1990) 275.

240. K. Kaeriyama and H. Masuda, *Synth. Met.*, 41-43 (1991) 389.

241. V. Haase and F. Beck, *Electrochim. Acta*, 39 (1994) 1195.

242. A. F. Diaz and K. K. Kanazawa, *In Extended Linear Chain Compounds*, J. S. Miller, (Ed.), Plenum, New York, 1982, p147.

243. A. Deronzier, J. C. Moutet. *Acc. Chem. Res.*, 22 (1989) 249.

244. R. L. Petty, W. C. Michel, J. P. Snow and K. S. Johnson., *Anal. Chim. Acta*, 142 (1982) 299.

245. P. Lindroth and K. Mopper, *Anal.Chem.*,51 (1979) 1667.

246. D. P. Nikolelis, *Analyst*, 112 (1987) 763.

247. C. D. Stalikas, M. I. Karayannis and S. M. Tzouwara-Karayanni, *Analyst*, 118 (1993) 723.

248. S. Blackburn, *In Amino Acid determination; Methods and Techniques*, Edward Arnold Publishers, London, 1968.

249. *Instrumentation in Amino Acid Sequence Analysis*, R. N. Perham (Ed.), Academic Press, London, 1975.

250. K. T. Hsu and L. B. Currie., *J. Chromatogr.* 166 (1978) 555.

251. J. R. Benson and P. E. Hare, *Proc. Nat. Acad. Sci. USA.*, 72 (1975) 619.

252. N. Seller and L. Demisch, *In Handbook of Derivatives for Chromatography* , K. Blau and G. S. King, (Eds.), Heyden, London, 1977, Chapter 9.

253. N. Seller, *J. Chromatogr*, 143, (1977) 221.

254. J. Abecassis, C. David-Eteve and A. Soun, *J. Liq. Chromatogr.*, 8 (1985), 135.

255. G. Ogden and P. Foldi, *LC-GC.*, 5 (1987) 28.

256. D. C. Johnson, S. G. Weber, A. M. Bond, R. M. Wightman, R. E. Shoup and I. S. Krull, *Anal. Chim. Acta*, 180 (1986) 187.

257. P. T. Kissinger, *J. Chromatogr.* , 488 (1989) 31.

258. B. S. Hui and C. O. Huber, *Anal. Chim. Acta*, 134 (1982) 211.

259. J. A. Polta and D. C. Johnson, *J. Liq. Chromatogr.*, 6 (1983) 1727.

260. A. Liu and E. Wang, *Anal. Chim. Acta.*, 280 (1993) 223.

261. P. W. Alexander, P. R. Haddad, G. K. C. Low and C. Maitra, *J. Chromatogr.*, 209 (1981) 29.

262. C. R. Loscombe and G. B. Cox, *J. Chromatogr.*, 166 (1978) 403.

263. P. W. Alexander, and C. Maitra, *Anal. Chem.*, 53 (1981) 1590.

264. P. R. Haddad, P. W. Alexander and M. Troianowicz, *J. Chromatogr.*, 315 (1984) 261.

265. M. Fleischmann, K. Korinek and D. Pletcher, *J. C. S. Perkin, II*, (1972) 1396.

266. J. B. Kafil and C. O. Huber, *Anal. Chim. Acta*, 139 (1982) 347.

267. M. W. White, *J. Chromatogr.*, 262 (1983) 420.

268. J. A. Cox and E. Dabek-Zlotorzynska, *Electroanalysis*, 3(1991)239.

269. L. E. Welch, W. R. LaCourse, D. A. Mead, Jr. and D. C. Johnson, *Anal. Chem.*, 61 (1989) 555.

270. P. J. Vandeberg and D. C. Johnson, *Anal. Chem.*, 65 (1993) 2713.

271. M. D. Imisides, R. John, P.J. Riley and G. G. Wallace, *Electroanalysis*, 3 (1991) 879.

272. M. D. Imisides, G. G. Wallace and E. A. Wilke, Trans. *Anal. Chem.*, 7 (1988) 1543.

273. M. W. Espenscheid, A. R. Ghatak-Roy, R. B. Moore, R. M. Penner, M. N. Szentirmay and C. R. Martin, *J. Chem. Soc. Faraday Trans.*, 82 (1986) 1051.

274. S. Dong and Y. Wong, *Electroanalysis*, 1 (1989) 99.

275. Y. P. Lin and G. G. Wallace, *J. Electroanal. Chem.*, 247 (1988) 145.

276. P. R. Teasdale, M. J. Spencer and G. G. Wallace, *Electroanalysis*, 1 (1989) 541.

277. M. I. Imisides and G. G. Wallace, *J. Electroanal. Chem.*, 246 (1988) 181.

278. H. K. Yussoufi, A. Yassar, S. Baiteche, M. Hmyene and F. Garnier, *Synth. Met.* , 67 (1994) 251.

279. P. R. Teasdale and G. G. Wallace, *Polym. Int.*, 35(1994)197.

280. P. R. Teasdale, H. Ge, K. Gilmore and G. G. Wallace, *Polym. Int.*, 29 (1992) 299.

281. R. S. Deinhammer, M. D. Porter and K. Shimazu, *J. Electroanal. Chem.*, 387 (1995) 35.

282. Q. Pei and R. Qian, *Elecrochim. Acta*, 37 (1992) 1075.

283. E. M. Genies and A. A. Syed, *Synth. Met.*, 10 (1984) 21.

284. A. S. Fiorillo, C. Di Bartolomeo, A. Nannini and D. De Rossi, *Sens. Actuators B*, 7 (1992) 399.

285. H. Shinohara, M. Aizawa and H. Shirakawa, *J. C. S. Chem. Commun.*, (1986) 87.

286. M. Nishizawa, T. Matsue and I. Uchida, *Sens. Actuators B*, 13-14 (1993) 53.

287. J. Tamm, A. Hallik and A. Alumaa, *Synth. Met.*, 55-57 (1993) 1473.

288. R. M. Wightman., *Anal. Chem.*, 53 (1981) 1125A.

289. A. M. Bond, M. Fleischmann and J. Robinson , *J. Electroanal. Chem.*, 168 (1984) 299.

290. A. M. Bond, M.,Fleischmann and J. Robinson, *J. Electroanal. Chem.*, 172 (1984) 11.

291. *Microelectrodes*, J. Wang, Ed., VCH publishers, New York, 1990.

292. S. Pons, and M. Fleischmann, *Anal. Chem.*, 59 (1987) 1291A.

293. *Ultramicroelectrodes*, M. Fleischmann, S. Pons, D. R. Rolison, and P. O. Schmidt, Eds.,Datatech Systems, Morganton, NC, 1987.

294. *Microelectrodes: Theory and Applications*, M. I. Montenegro, M. A. Queiros and J. L. Daschbach (Eds), Kluwer Academic Press, Dordrech, 1991.

295. C. Amatore, *in Molecular Electrochemistry of Inorganic, Bioinorganic and Organometallic Compounds*, Vol. 385, A. J. L. Pombeiro, and J. McCleverty (Eds), NATO ASI Series C: Mathematical and Physical Sciences, Kluwer Academic Press, Dordrecht, 1993, p.625.

296. R. M. Wightman, and D. O. Wipf, *Electroanal. Chem.*, 15 (1989) 267.

297. J. Heinze, *Angew. Chem. Int. Ed. Engl.*, 105 (1993) 1327.

298. J. B. Cooper and A. M. Bond, *Anal. Chem.*, 65 (1993) 2724.

299. M. F. Bento, M. J. Medeiros, M. I. Montenegro, C. Beriot and D. Pletcher, *J. Electroanal. Chem.*, 345 (1993) 273.

300. K. B. Oldham, *J. Electroanal. Chem.* 337 (1992) 91.

301. M. Ciszkowska, Z. Stojek, S. E. Morris and J. G. Osteryoung, *Anal. Chem.*, 64 (1992) 2372.

302. D. K. Y. Wong and A. G. Ewing, *Anal. Chem.*, 62 (1990) 2697.

303. A. M. Bond, and F. G. Thomas, *Langmuir*, 4 (1988) 341.

304. G. Wikmark, J. Lejon, and L. Nyholm, *Water. Chem. Nucl. React. Syst.*, 6 (1992) 219.

305. L. Nyhlom and G. Wikmark, *Anal. Chim. Acta*, 273 (1993) 41.

306. L. Nyhlom and G. Wikmark, *Anal. Chim., Acta.* 257 (1992) 7.

307. R. R. De Vitre, M. L. Tercier and J. Buffle, *Anal. Proc.*, 28 (1991) 74.

308. R. O. Ansell, H. McAleer, A. McNaughtan and J. R. Pugh, *Anal. Proc.*, 28 (1991) 63.

309. J. S. Feinberg and W. J. Bowyer, *Microchem, J.*, 47 (1993) 72.

310. J. Wang and J. M. Zadeii, *J. Electroanal. Chem.*, 246 (1988) 297.

311. C. P. Andrieux, P. Andebert, P. Hapiot, M. Nechtschein and C. Odin, *J. Electroanal. Chem.*, 305 (1991) 153.

312. R. John and G. G. Wallace, *J. Electroanal. Chem.*, 306 (1991) 157.

313. L. M. Abrantes,J. C. Mesquita,M. Kalaji and L. M. Peter, *J. Electroanal. Chem.*, 307 (1991) 275.

314. M. Kalaji, L. M. Peter, L. M. Abrantes and J. C. Mesquita, *J. Electroanal. Chem.*, 274 (1989) 289.

315. O. A. Sadik and G. G. Wallace, *Electroanalysis*, 6 (1994) 860.

316. R. John and G. G. Wallace, *J. Electroanal. Chem.*, 283 (1990) 87.

317. W. L. Caudill, J. O. Howell and R. M. Wightman, *Anal. Chem.*, 54 (1982) 2532.

318. M. Ciszkowska and Z. Stojek, *J. Electroanal. Chem.*, 213 (1986) 189.

319. H. Ji, J. He, S. Dong and E. Wang, *J. Electroanal. Chem.*, 290 (1990) 93.

320. L. Loub, F. Opekar, V. Pacakova and K. Stulik, *Electroanalysis*, 4 (1992) 447.

321. W. H. Glaze and G. R. Peyton, *In Water Chlorination: Environmental Impact and Health Effects*, Vol.2, R. L. Jolley et al. (Eds.), Ann Arbor Science Publishers, Ann Arbor, Michigan, (1977) p 3.

322. P. C. Uden, J. W. Miller, *J. Am. Water Works Assoc.*, 75 (1983) 524.

323. J. M. Sendra and V. Todo, *J. Inst. Brew.*, 96 (1990) 85.

324. J. J. Rook in *Formation of Haloforms During Chlorination of Natural Waters. Water Treatment Exam.*,23 (1974) 234.

325. A. D. Reckhow and P.C. Singer, *J. Am. Water Works Assoc.*, 82 (1990) 173.

326. D. L. Norwood, G. P. Thompson, J. D. Johnson and R. F. Christman, *In Water Chlorination: Environmental Impact and Health Effects*, Vol. 5, R. L. Jolley, et al. (Eds.), Lews Publisher Inc., Chelsea, MI,

(1985) p1115.

327. S. W. Krasner, M. J. McGuire, J. G. Jacangelo, N. L. Patania, K. M. Reagan and E. M. Aeita, *J. Am. Water Works Assoc.* 81 (1989) 41.

328. R. J. Bull, I. M. Sanchez, M. A. Nelson, J. K. Larson and A. J. Lansing, *J. Toxicology*, 63 (1990) 341.

329. R. F. Christman, D. L. Norwood, D. S. Millington, J. D. Johnson and A. A. Stevens, *Environ. Sci. Technol.*, 17 (1983) 625.

330. D. L. Norwood, J. D. Johnson and R. F. Christman, *Water Chlorination: Environmental Impact and Health Effects*, Vol 4, R. L. Jolley et al., (Eds.) Ann Arbor Science Publishers, Ann Arbor, Michigan, (1983) p 191.

331. J. D. Johnson, R. F. Christman, D. L. Norwood, D. S. Millington, *Environ Health Perspect*, 46 (1982) 63.

332. EWB. De Leer, J. S. Sinninghe Damste, C. Erkelens, L. De Galan, *Environ Sci. Technol.*, 19 (1985) 512.

333. J. C. Ireland, L. A. Moore, H. Pourmoghaddas and A. A. Stevens, *Biomedical and Environmental Mass Spectrometry*, 17 (1988) 483.

334. US EPEA, 1990, Methods for the Determination of Organic Compounds in drinking Water. Supplement I. *Determination of Halo-Acetic Acids in Drinking Water by Liquid-. Liquid Extraction, Derivatiztion, and Gas Chromatography with electron Capture Detection* (Method # 552) Environmental Monitoring and Support Lab. Cincinati, Ohio.

335. S. Husain, R. Narsimha S. N. Alvi and R. N. Rao, *J. Chromatogr.*, 600 (1992) 316.

336. M. Houdeau, M. Thibert and M. Caude, *Analusis*, 5 (1977) 286.

337. L. M. Nair, R. Saari-Nordhaus and J. M. Anderson,Jr., *J. Chromatogr., A*, 671 (1994) 309.

338. G. G. McLeod, K. Jeffreys, J. M. R. MacAllister, J. Mundell, S. Affrossman and R. A. Pethrick, *J. Physics. Chem. Solids,* 48 (1987)921.

339. H. Munstedt, *Polymer*, 27 (1986) 899.

340. B. Sun, J. J. Jones , R. P. Burford, and M. Skyllas-Kazacos, *J. Mater. Sci.*, 24 (1989) 4024.

341. *Lauges'Hand book of Chemistry.*, Thirteenth Edition., J. A. Dean, (Ed.), Mc Graw-Hill Book Company. New York. 1972.

342. Haloacetic Acid Separation, 7anion+ Mixed HAC'S, Dionex Method.